OBSERVATIONS ON SEISMIC WAVES REFLECTED AT THE EARTH'S CORE BOUNDARY

Thesis by

Samuel T. Martner

In Partial Fulfillment of the Requirements

For the Degree of

Doctor of Philosophy

California Institute of Technology

Pasadena, California

1948

ACKNOWLEDGMENTS

The author wishes to extend his grateful acknowledgment to Dr. Beno Gutenberg for the supervision, help, and inspiration which contributed to the completion of the work leading to this report and for constructive criticism of the thesis during its composition and in final draft. Dr. Hugo Benioff was constantly willing and able to discuss the problems involving the seismic instruments and for this the writer is appreciative. Gratitude is also felt for Mr. Francis Lehner's excellent technical assistance on the measurement of instrumental constants.

ABSTRACT

On the seismograms of many earthquakes the waves reflected from the outer boundary of the earth's core oftentimes write traces which appear larger than the size of the shock warrants. A systematic study has been made of the displacement ratios of these core reflections to the direct body waves. Data accumulated during the course of this investigation tend to confirm the idea that the displacement ratios of the longitudinal waves reflected from the core to the longitudinal direct waves are greater than the presently accepted theory would indicate. Some possible causes of these differences are investigated, but reasonable changes in the assumptions do not result in an explanation of all of the discrepancy between the observed and theoretical data. Additional research projects are suggested that might help in answering some of the puzzling features of these phenomena.

TABLE OF CONTENTS

ILLUSTRATIONS

I. INTRODUCTION

This paper deals with the energy of seismic waves reflected from the core of the earth. As in all scientific problems, a study of this subject invites two different lines of approach: the theoretical consideration of the question based entirely upon inductive reasoning and a consideration of the results obtained by physical measurements of the actual phenomena involved. Theoretically, problems of energy transmission by seismic waves have been presented by many former workers in seismology; physical measurements of seismic wave amplitudes and energies, however, have previously been presented only for direct body waves, surface waves, and waves which have reflected from the surface or crustal layers of the earth. In this report, the results obtained by previous investigators of the theory will be presented, largely without derivation of pertinent formulae; and the writer will restrict himself to the quantitative physical measurements made during the course of recent research and to some of the implications of the results obtained.

The notations used in this paper are all in current use by various authors; but due to differences in notation, a brief resumé of the symbols is not out of order at this place. The longitudinal wave will be designated as P; the transverse wave as S. The letter c indicates a reflection from the core boundary. Thus PcP is the wave that travels from the epicenter of the earthquake to the core boundary as a longitudinal wave, is reflected there, and proceeds to the surface of the earth as a longitudinal wave. The symbol V will be used for velocity with a subscript to indicate the wave in question. A subscript o will be used to indicate that the quantity refers to its value at the surface of the earth, 1 will indicate that the quantity is to be evaluated in the mantle adjacent to the core boundary, and 2 will indicate that the quantity is to be evaluated in the

core adjacent to the core boundary. Thus, the symbol V_{P1} represents the velocity of longitudinal waves in the mantle just outside the core. Angles of incidence will be indicated by i. Amplitudes will be represented by A. Incident rays will be shown by a subscript e or i, reflected waves by the subscript r, and refracted waves by the subscript f. Thus the amplitude of a reflected transverse wave will be A_{rs}, and the sine of its angle of of incidence will be shown as sin i_{rs}. Density will be shown by the symbol ρ. Energy will be indicated by E. Thus the energy of the incident longitudinal wave will be shown as E_{ip}. Axes of reference, x, y, and z will be right hand with the z-axis in the vertical direction and the x-axis in the direction of the componant of the ray in the horizontal plane. Displacements will be designated as u, v, and w, in the directions x, y, and z, respectively. When maximum horizontal displacement is to be indicated, the symbol u will also be used, and its use will allow it to be distinguished from the horizontal displacement in the direction of wave propagation. u_{EW} and u_{NS} will be used to show the horizontal displacement in the east-west and the north-south direction, respectively. The symbol Δ will indicate epicentral distances in degrees of arc. h will be used for depths of focus. Other symbols will be designated and defined as occasion arises for their use. A resumé of notation can be found in Appendix A.

Certain assumptions have been made throughout the course of the investigations leading to this report. These assumptions make the results less precise than would be the case if all of the factors involved were definitely and conclusively known. In the following presentation, the assumptions will be enumerated and discussed. The systematic errors caused by these assumptions are largely reduced by using ratios wherever possible; however, random errors,due to many suppositions and probably varying physical phenomena at the focus or source of the seismic energy, are

introduced and tend to enlarge the scattering of recorded data. The essence, therefore, of the evaluation of the data obtained is, as in any other interpretative problem, a search for confirmation or condemnation of a given hypothesis, with due regard for the inherent errors in the data. The inherent errors in this case are probably larger than the precise physicist is used to dealing with. The reader is requested to keep in mind these thoughts while proceeding through the following discussion, as the methods used throughout are believed to result in accuracies at least of first order definiteness.

II. THEORY

The theory of the transmission of seismic waves has been discussed previously by many authors. The following discussion is a brief resume of those portions of the theory pertinent to the present discussion.

The true amplitude of a seismic wave for any point can be expressed by the following formula:

$$A_e = C\ T\ f\ \sqrt{\frac{\sin i_s}{\sin\Delta \cos i_o}\ \frac{di_o}{d\Delta}}\ e^{-\int \kappa dD} \qquad (1)$$

where:

A_e = incident amplitude

C = constant depending on the energy at the source of the earthquake, the radius of the earth, and the units used

T = period of the seismic waves

f = square root of the product of the ratios of transmitted or reflected energy, as the case may be, to the incident energy at each discontinuity of density and/or wave velocity along the path of the ray.

$e^{-\int \kappa dD}$ = absorption along the ray path D where the absorption factor is k

Δ = epicentral distance in degrees of arc

i_s = angle of incidence of the ray at the source

i_o = angle of incidence of the ray at the recording point

Details of the derivation of the above formula and the assumptions made can be found in Gutenberg 14/. The assumptions made in the derivation of this formula are: (1) the source of the energy is a point, (2) close to the focus, or source of the energy, energy is propagated spherically in equal amounts in all directions, (3) higher order terms in approximating infinitesimals are disregarded, and (4) energy flow in the direction of the wave front is negligible.

If it is desired to obtain the displacement of the ground at any point on the earth's surface, the incident amplitude (A_e) must be multi-

plied by a factor which is the ratio of the ground displacement to the incident amplitude:

$$u=A_e(u/A_e);\quad v=A_e(v/A_e);\quad \text{or}\quad w=A_e(w/A_e) \qquad (2)$$

where:

u/A_e, v/A_e, w/A_e = the ratio of the ground displacement in the u, v, and w directions, respectively, to the incident amplitude, depending only on Poisson's ratio and the angle of incidence for a given wave type.

Values of u/A_e, v/A_e, and w/A_e have been determined under varying assumptions of the value of Poisson's ratio at the surface (see 36/, 13/, 24/, and 18/. Gutenberg, in the last reference cited, has plotted these ratios for both transverse and longitudinal incident waves, for values of Poisson's ratio of 0.273, 0.250, 0.239, and 0.215. Throughout this report, where this ratio is required, these graphs will be used and a Poisson's ratio of 0.250 will be assumed. Using this value in lieu of the others mentioned can make no more than a 10 percent difference in the above ratios.

The various variables in equations (1) and (2) can be discussed further. The constant C is dependent on the energy released at the focus in the form of wave type in question, the radius of the earth, and the units used. The last two of these three factors remain constants at all times; the energy release, however, is different for each earthquake and is possibly different for different types of waves (longitudinal or transverse), although studies to date show that there is probably little variation in the latter 19/. The relationships of the angles of incidence in the formula are derived from the following equation, depending on Snell' law:

$$\frac{r_s \sin i_s}{V_s} = \frac{r_o \sin i_o}{V_o}$$

where:

r_s = distance from the center of the earth to the earthquake focus

r_o = radius of the earth

V_s = velocity of the wave in question at the focus

V_o = velocity of the wave in question at the earth's surface.

The quantity $di_o/d\Delta$ is obtained from a plot of i_o vs. Δ, which in turn can be readily determined from $\sin i_o = V_o/\overline{V}$, where $\overline{V}$ is the "apparent velocity" obtained from the observed traveltime curve of the phase in question and V_o is the velocity at the surface of the wave in question at the surface. This formula can be derived by simple geometry from a sketch of the wave front at the surface.

The absorption $e^{-\int k dD}$ is a relatively small factor. Gutenberg 19/, from a study of P, P'P', and P'P'P', found that the value of k=0.00012/km; and, as this equals the value previously found for G waves (very long surface waves), he concluded that " it seems, therefore, that for all those earthquake waves which are not much affected by crustal layers the absorption is about the same". Using this value of k and considering the fact that the largest difference in the path lengths of the direct waves and the waves reflected from the core boundary is at a zero epicentral distance, one can readily calculate the maximum reduction factor in the amplitude ratio of PcP/P or ScS/S:

$$\text{Absorption} = \sqrt{e^{-\int k dD}} = \sqrt{e^{-0.00012 \cdot 5840}} = \sqrt{0.496}$$

where:

k= 0.00012/km
D= 5840 km = two times the depth of the core boundary from the surface of the earth

This gives a maximum amplitude reduction factor for absorption of 0.704, i.e. the theoretical value of the ratio of the amplitude of PcP to the amplitude of P will be under maximum conditions reduced by 30 percent by

considering absorption in lieu of disregarding it. Of course, this percentage is theoretically reduced as the epicentral distance is increased; until, at $\Delta = 103^{\circ}$, P grazes the core and the absorption of both P and PcP are theoretically equal.

The factor f of equation (1) has been the subject of discussion by many previous workers. Knott 26/, in 1888, published the first paper from which the values of the ratios of reflected and transmitted energies to incident energies could be determined. Results of research by Zoeppritz 35/, which developed comparable formulae from consideration of amplitudes instead of energies, were published in 1919 after his death. Blut 4/, in 1932, further contributed to the theory by publishing equivalent formulae derived from a consideration of the absolute energy relationships. Macelwane 27/ presents a recapitulation of the development of the formulae of these three men, and the reader is referred to his discussion for further details, if the original publications are unavailable. Subsequent discussions and numerical computations of the factors contained in f have been published by Jeffreys 24/, Muskat 29/, Dix 10/, Joos and Teltow 25/, Muskat and Meres 30/, Ott 31/, Gutenberg 18/, and Dana 8/. Among these the last two papers are of particular importance in this report as they contain numerical data directly bearing on distant earthquakes, and the theoretical values referred to in this paper will be largely taken from these two articles.

A brief review of the methods employed by Zoeppritz in the derivation of his equations is presented below primarily to bring to mind the assumptions involved. By simple geometry, assuming plane waves (where each particle propagating the wave moves with harmonic vibrations) and neglecting any energy flow in the direction of the wave front, the following formulae for the instantaneous amplitude (Φ_{ip} for longitudinal waves and Φ_{is} for transverse waves) are derived:

$$\Phi_{ip} = A_{ip}\, e^{im\left(t - \frac{x \sin i_{ip} + z \cos i_{ip}}{V_{p1}}\right)}$$

$$\Phi_{is} = A_{is}\, e^{im\left(t - \frac{x \sin i_{is} + z \cos i_{is}}{V_{s1}}\right)}$$

where:

$$m = 2\pi/T$$

Again by simple geometric relationships, the following formulae can be derived for the reflected and transmitted wave amplitudes:

$$\Phi_{rp} = A_{rp}\, e^{im\left(t - \frac{x \sin i_{rp} - z \cos i_{rp}}{V_{p1}}\right)}$$

$$\Phi_{rs} = A_{rs}\, e^{im\left(t - \frac{x \sin i_{rs} - z \cos i_{rs}}{V_{s1}}\right)}$$

$$\Phi_{fp} = A_{fp}\, e^{im\left(t - \frac{x \sin i_{fp} + z \cos i_{fp}}{V_{p2}}\right)}$$

$$\Phi_{fs} = A_{fs}\, e^{im\left(t - \frac{x \sin i_{fs} + z \cos i_{fs}}{V_{s2}}\right)}$$

Using the fundamental equations of wave motion (where elastic processes only are considered and the body forces have been neglected):

$$\frac{\partial^2 \Theta}{\partial t^2} = \frac{\lambda + 2\mu}{\rho} \nabla^2 \Theta$$

$$\frac{\partial^2}{\partial t^2}(\omega_x, \omega_y, \omega_z) = \frac{\mu}{\rho} \nabla^2 (\omega_x, \omega_y, \omega_z)$$

where:

Θ = dilatation $= \frac{\partial u}{\partial x} + \frac{\partial v}{\partial y} + \frac{\partial w}{\partial z}$

$\omega_x, \omega_y, \omega_z$ = one-half the components of the curl, with respect to the axes indicated by subscripts

∇ = Laplacian operator $= \frac{\partial^2}{\partial x^2} + \frac{\partial^2}{\partial y^2} + \frac{\partial^2}{\partial z^2}$

λ, μ = Lamé's constants,

the components of the normal and tangential stresses can be derived. The following boundary conditions which must be satisfied can then be expressed in terms of displacements:

(1) Equality of the sums of the normal displacements on the two sides of the discontinuity

(2) Equality of the sums of the tangential displacements on the two sides of the discontinuity

(3) Equality of the sums of the normal stresses across the discontinuity

(4) Equality of the sums of the tangential stresses across the discontinuity.

These boundary conditions, of course, assume that the plane of the discontinuity is without slip. Assuming an incident longitudinal wave and using simple geometric relationships, the following formulae for the displacement components can be derived:

$$u_{ip} = \Phi_{ip} \sin i_{ip} \qquad w_{ip} = \Phi_{ip} \cos i_{ip}$$

$$u_{rp} = \Phi_{rp} \sin i_{ip} \qquad w_{rp} = -\Phi_{rp} \cos i_{ip}$$

$$u_{rs} = \Phi_{rs} \cos i_{rs} \qquad w_{rs} = \Phi_{rs} \sin i_{rs}$$

$$u_{fp} = \Phi_{fp} \sin i_{fp} \qquad w_{fp} = \Phi_{fp} \cos i_{fp}$$

$$u_{fs} = -\Phi_{fs} \cos i_{fs} \qquad w_{fs} = \Phi_{fs} \sin i_{fs}$$

Now, assuming plane waves, the following Zoeppritz equations for the case of an incident longitudinal wave can be obtained by substituting the equations for the displacement components and the equations for the instantaneous amplitudes into the boundary conditions:

$$A_{ip} \cos i_{ip} - A_{rp} \cos i_{ip} + A_{rs} \sin i_{rs} - A_{fp} \cos i_{fp} - A_{fs} \sin i_{fs} = 0$$

$$A_{ip} \sin i_{ip} + A_{rp} \sin i_{ip} + A_{rs} \cos i_{rs} - A_{fp} \sin i_{fp} + A_{fs} \cos i_{fs} = 0$$

$$-A_{ip} \cos 2i_{rs} - A_{rp} \cos 2i_{rs} + A_{rs} \left(\frac{V_{s1}}{V_{p1}}\right) \sin 2i_{rs} + A_{fp} \left(\frac{\rho_2}{\rho_1}\right)\left(\frac{V_{p2}}{V_{p1}}\right) \cos 2i_{fp} - A_{fs} \left(\frac{\rho_2}{\rho_1}\right) \frac{V_{s2}}{V_{p1}} \sin i_{fs} = 0$$

$$-A_{ip} \cos 2i_{ip} + A_{rp} \sin 2i_{ip} + A_{rs} \left(\frac{V_{p1}}{V_{s1}}\right) \cos 2i_{rs} + A_{fp} \left(\frac{\rho_2}{\rho_1}\right)\left(\frac{V_{s2}}{V_{s1}}\right)^2 \left(\frac{V_{p1}}{V_{p2}}\right) \sin 2i_{fp} - A_{fs} \left(\frac{\rho_2}{\rho_1}\right)\left(\frac{V_{s2}}{V_{s1}}\right)^2 \left(\frac{V_{p1}}{V_{p2}}\right) \cos i_{fs} = 0$$

Similarly, assuming an incident transverse wave, (with vibration of particles on the vertical plane, i.e. SV type) the following formulae can be written for the displacement components:

$$u_{is} = \Phi_{is} \cos i_{is} \qquad w_{is} = \Phi_{is} \sin i_{is}$$
$$u_{rp} = \Phi_{rp} \sin i_{rp} \qquad w_{rp} = -\Phi_{rp} \cos i_{rp}$$
$$u_{rs} = \Phi_{rs} \cos i_{is} \qquad w_{rs} = \Phi_{rs} \sin i_{is}$$
$$u_{fp} = \Phi_{fp} \sin i_{fp} \qquad w_{fp} = \Phi_{fp} \cos i_{fp}$$
$$u_{fs} = -\Phi_{fs} \cos i_{fs} \qquad w_{fs} = \Phi_{fs} \sin i_{fs}$$

and the Zoeppritz equations are:

$$-A_{is} \sin i_{is} - A_{rp} \cos i_{ip} + A_{rs} \sin i_{is} - A_{fp} \cos i_{fp} - A_{fs} \sin i_{fs} = 0$$

$$A_{is} \cos i_{is} - A_{rp} \sin i_{ip} + A_{rs} \cos i_{is} - A_{fp} \sin i_{fp} + A_{fs} \cos i_{fs} = 0$$

$$A_{is} \sin 2i_{is} - A_{rp}\left(\frac{V_{p1}}{V_{s1}}\right) \cos 2i_{is} + A_{rs} \sin 2i_{is} + A_{fp}\left(\frac{\rho_2}{\rho_1}\right)\left(\frac{V_{p2}}{V_{s1}}\right) \cos 2i_{fs} + A_{fs}\left(\frac{\rho_2}{\rho_1}\right)\left(\frac{V_{s2}}{V_{s1}}\right) \sin i_{fs} = 0$$

$$-A_{is} \cos 2i_{is} - A_{rp}\left(\frac{V_{s1}}{V_{p1}}\right) \sin 2i_{ip} + A_{rs} \cos 2i_{is} + A_{fp}\left(\frac{\rho_2}{\rho_1}\right)\left(\frac{V_{s2}^2}{V_{s1} V_{p2}}\right) \sin 2i_{fp} - A_{fs}\left(\frac{\rho_2}{\rho_1}\right)\left(\frac{V_{s2}}{V_{s1}}\right) \cos i_{fs} = 0$$

Assuming that the incident transverse wave is propagated by the vibration of particles in a horizontal plane (SH type), the normal strains equation and the normal stress equation disappears and the Zoeppritz equations become:

$$A_{is} + A_{rs} - A_{fs} = 0$$

$$A_{is} - A_{rs} - A_{fs}\left(\frac{\rho_2}{\rho_1}\right)\left(\frac{V_{s2}}{V_{s1}}\right)\frac{\cos i_{fs}}{\cos i_{is}} = 0$$

There are two special cases of reflection that are of particular interest in this report, i.e. the reflection of a longitudinal wave at the core boundary and the reflection of a transverse wave at the core boundary. In the case of the incident longitudinal wave against the core boundary, we will assume that the core acts as a liquid, inasmuch as the transmitted transverse wave through the core has not been observed. This assumption causes $V_{S2}=0$, sin $i_{fp}=0$, and the tangential strain equation disappears. Therefore, Zoeppritz' equations for an incident longitudinal wave become:

$$A_{ip} \cos i_{ip} - A_{rp} \cos i_{ip} + A_{rs} \sin i_{is} - A_{fp} \cos i_{fp} = 0$$

$$-A_{ip} \cos 2i_{is} - A_{rp} \cos 2i_{is} + A_{rs}\left(\frac{V_{s1}}{V_{p1}}\right) \sin 2i_{is} + A_{fp}\left(\frac{\rho_2}{\rho_1}\right)\left(\frac{V_{p2}}{V_{p1}}\right) = 0$$

$$-A_{ip} \sin 2i_{ip} + A_{rp} \sin 2i_{ip} + A_{rs}\left(\frac{V_{p1}}{V_{s1}}\right) \cos 2i_{is} = 0$$

In the case of the incident transverse wave (SV type) against the core boundary, Zoeppritz' equations similarly reduce to:

$$-A_{is}\sin i_{is} - A_{rp}\cos i_{ip} + A_{rs}\sin i_{is} - A_{fp}\cos i_{fp} = 0$$

$$A_{is}\sin 2i_{is} - A_{rp}\left(\frac{V_{p1}}{V_{s1}}\right)\cos 2i_{is} + A_{rs}\sin 2i_{is} + A_{fp}\left(\frac{\rho_2}{\rho_1}\right)\left(\frac{V_{p2}}{V_{p1}}\right) = 0$$

$$-A_{is}\cos 2i_{is} + A_{rp}\left(\frac{V_{s1}}{V_{p1}}\right)\sin 2i_{ip} + A_{rs}\cos 2i_{is} = 0$$

In the case of the incident transverse wave (SH type) against the core boundary, Zoeppritz' equations reduce to:

$$A_{is} = A_{rs}$$

From a consideration of the problem from an energy viewpoint, such as Knott or Blut used, the following check equation of energy can be derived (again assuming that the energy flow is perpendicular to the wave front):

(a) for an incident longitudinal wave,

$$1 = \frac{A_{rp}^2}{A_{ip}^2} + \frac{A_{rs}^2}{A_{ip}^2}\frac{\sin i_{rs}}{\sin i_{ip}} + \frac{A_{fp}^2}{A_{ip}^2}\left(\frac{\rho_2}{\rho_1}\right)\frac{\sin 2i_{fp}}{\sin 2i_{ip}}$$

(b) for an incident transverse wave (SV type),

$$1 = \frac{A_{rp}^2}{A_{is}^2}\frac{\sin 2i_{ip}}{\sin 2i_{is}} + \frac{A_{rs}^2}{A_{is}^2} + \frac{A_{fp}^2}{A_{is}^2}\left(\frac{\rho_2}{\rho_1}\right)\frac{\sin 2i_{fp}}{\sin 2i_{is}}$$

(c) for an incident transverse wave (SH type),

$$1 = \frac{A_{rs}^2}{A_{is}^2}$$

The energy ratios can also be expressed as:

(a) for an incident longitudinal wave,

$$\frac{E_{rp}}{E_{ip}} = \frac{A_{rp}^2}{A_{ip}^2}$$

$$\frac{E_{fp}}{E_{ip}} = \frac{A_{fp}^2}{A_{ip}^2}\left(\frac{\rho_2}{\rho_1}\right)\frac{\sin 2i_{fp}}{\sin 2i_{ip}}$$

$$\frac{E_{rs}}{E_{ip}} = \frac{A_{rs}^2}{A_{ip}^2}\frac{\sin i_{rs}}{\sin i_{is}}$$

(b) for an incident transverse wave (SV type):

$$\frac{E_{rp}}{E_{is}} = \frac{A_{rp}^2}{A_{is}^2}\frac{\sin 2i_{ip}}{\sin 2i_{is}}$$

$$\frac{E_{rs}}{E_{is}} = \frac{A_{rs}^2}{A_{is}^2}$$

$$\frac{E_{fp}}{E_{is}} = \frac{A_{fp}^2}{A_{is}^2}\left(\frac{\rho_2}{\rho_1}\right)\frac{\sin 2i_{fp}}{\sin 2i_{is}}$$

(c) for an incident transverse wave (SH type),

$$\frac{E_{fs}}{E_{is}} = \frac{A_{fs}^2}{A_{is}^2} = 1$$

The numerical computations for Ae, u, v, and w as shown in formulae (1) and (2) above have been presented by Dana 9/ for P, SV, SH, PcP, PcS, and ScS, and many other phases. His calculations are all based on the following assumptions:

$V_{po} = 5.5$ km/sec ; $V_{so} = 3.2$ km/sec

$V_{p1} = 13.7$ km/sec ; $V_{s1} = 7.25$ km/sec

$V_{p2} = 8.0$ km/sec

$\rho_2/\rho_1 = 10.1/5.4$

In his computations, the value of the constant C is taken to be equal to π, and the period T is taken as 1. The absorption K is assumed to be negligible; so the absorption term $e^{-\int K dD}$ is considered to be unity.

In addition to the evaluation of Ae, u, v, and w for the various phases, Dana also computed the ratios of u, v, and w for PcP/P, PcS/P, ScS(SV)/SV, ScS(SH)/SH, ScS(SH)/SV, ScP/SV, and various other combinations. As the value of C is a constant at least for the same type of wave (longitudinal or transverse) for the same earthquake if the energy is assumed to be propagated equally in all directions around the source, or focus, this factor cancels in deriving these ratios and its assumed value has no bearing on the ratios obtained.

Dana's assumption that the period is 1 sec gives the same results as though he had computed the ratio of u/Te, v/Te, and w/Te; so, in comparing observations with his computations, it is necessary to reduce the observations to ratios of u/Te, v/Te, or w/Te, or in effect to multiply the ratio of u's by the reciprocal of the ratio of the observed periods. In the reduction of the observational data obtained for this report, the value of

u/Te (or w/Te) was obtained for each phase which was measured, and the ratios of u/Te (or w/Te) for PcP/P, PcS/P, etc., were obtained by the division of these quantities.

On the graphs in the later parts of this report, the theoretical curves which are presented are plotted from the calculations of Dana, except where otherwise specifically indicated.

III. INSTRUMENTATION

INTRODUCTION

Prior to evaluating the results obtained by seismographs, in terms of either ground displacements or energy relationships; it is, of course, necessary to obtain the response characteristics of the various instruments used in the investigations.

For this report the instruments which were used were those in normal operation at the Seismological Laboratory at Pasadena, California. A list of these seismographs follows:

Inst. No.	Comp.	Type of Instrument	Design To	Design Tg	Normal Static Magnif.
I	N-S	Wood-Anderson Torsion	0.8 sec		2800
II	E-W	Wood-Anderson Torsion	0.8		2800
IIA	Z	Benioff Electro-Magnetic	1	90 sec	
IVA	N-S	Benioff Electro-Magnetic	1	90	
IVB	E-W	Benioff Electro-Magnetic	1	90	
V	E-W	Wood-Anderson Torsion	6		800
VA	N-S	Wood-Anderson Torsion	6		800
VI	N-S	Benioff Strain	0.016(ca)	70	
VIA	Z	Benioff Electro-Magnetic	1	0.23	
VIBN	N-S	Benioff Electro-Magnetic	1	0.2	
VIBE	E-W	Benioff Electro-Magnetic	1	0.2	

N-S	North-South	To	Pendulum free period
E-W	East-West	Tg	Galvanometer free period
Z	Vertical		

The theory of the response of these instruments has been reported, at least partially, in various publications, but the portions of the theory relevant to the present discussion will be briefly summarized in the follow-

ing pages.

Also the necessary tests for obtaining response characteristics were made during the course of this project and the results of these tests will be given in this chapter.

Wood-Anderson Torsion Seismograph

The theory of the Wood-Anderson torsion seismograph has been reported by Anderson and Wood 1/.

Assuming a continuous ground displacement of simple harmonic Form:

$$\xi = C \sin\omega t$$

where:

ξ = displacement of the earth particles

C = Maximum ground displacement

$\omega = 2\pi/Te$

Te = Period of the ground vibration,

we arrive at a solution of the differential equation of motion of the seismograph of the form reported by Galitzin 12/, Wiechert 34/, and many others:

$$V = A^*/C = V_o/U$$

where:

V = dynamic magnification
A* = maximum trace amplitude of the seismogram
V_o = static mangification
$U = (1+u_p^2)\sqrt{1-\mu^2 f(u_p)}$
$u_p = Te/To$
To = free period of the seismometer
$\mu^2 = (1-h^2) = 1-(\varepsilon/\omega_o)^2$
ε = damping constant of the differential equation of motion
$\omega_o = 2\pi/To$
$f(u_p) = [2u_p/(1+u_p^2)]^2$

To determine the maximum "amplitude" of the earth displacement, one multiplies the maximum trace amplitude (A*) of the seismogram times U for the earth period in question divided by the static magnification of the seismograph:

$$C = A^*U/V_o$$

Short Period Wood-Anderson Torsion Seismograph (Instruments I and II)

The short period Wood-Anderson seismographs (Instruments I and II) of the Pasadena Seismological Laboratory were tested on October 23, 1946; and, from a number of determinations, the following data were obtained:

	To	ρ
Instrument I	0.80±0.01	11.0±1.0
Instrument II	0.63±0.05	11.85±0.4

where:

To = pendulum free period

ρ = damping ratio

Galitzin's tables 11/ were used to obtain $\mu^2 = 0.63$ for Instrument I, and $\mu^2 = 0.62$ for Instrument II; and to obtain log U vs. u from u = 0.0 to 2.0 by steps of 0.1. A nomograph developed by Schmidt 33/ was used for the values of U vs. u from u = 2.2 to 5.2 by steps of 0.2. From these date Te vs. U/V_0 were obtained, for values of Te from 0.000 to 4.160 sec by steps of 0.080 sec for Instrument I, and from 0.000 to 3.276 sec by steps of 0.063 sec for Instrument II. These data are given in tables 1 and 2 and are shown graphically on graphs 1 and 2.

The theoretical response curves of these instruments, when adjusted to their normal conditions of To = 0.80 sec and h = 0.85, are shown in table 3 and graph 3.

Long Period Wood-Anderson Torsion Seismographs (Instruments V and VA)

The long period Wood-Anderson torsion seismographs (Instruments V and VA) of the Pasadena Seismological Laboratory were tested on October 23, 1946, and from a number of determinations the following data were obtained:

	To	ρ
Instrument V	6.36±0.01	32.4±3.6
Instrument VA	5.65±0.02	30.4±2.4

As Galitzin's tables do not contain log U vs. u for these values of free period, the necessary computations were made. For Instrument V: $\rho = 32.4$; $h = 0.742$; $\mu^2 = 0.45$; and for Instrument VA: $\rho = 30.4$; $h = 0.735$; $\mu^2 = 0.46$. Tables 4 and 5 give the results of computation of U for these instruments. Also shown is Te vs. U/V_o for both instruments, Te ranging from 00.00 to 25.44 sec for Instrument V and from 00.00 to 22.60 sec for Instrument VA. The data of Te vs. U/V_o for the two instruments are shown on graphs 4 and 5.

The theoretical response curves for these instruments, adjusted to their normal conditions of To = 6 sec and $h = 0.85$, are shown in table 3 and graph 6.

Benioff Electro-Magnetic Seismograph

The general theory of the Benioff Electro-magnetic seismograph has been presented by Benioff 2/. Assuming that the ground displacement is of continuous simple harmonic form, that is:

$$\xi = C \sin \omega t$$

$$\omega = 2\pi / Te$$

where:

ξ = displacement of the earth particles
Te = period of the earth wave
C = maximum "amplitude" of ground displacement,

and if the seismometer and galvanometer damping are adjusted to the critical value, then:

$$z = CBQ \sin (\omega t + \Delta)$$

where:

z = displacement of the recording light spot on the photographic paper
Q = frequency response characteristic
Δ = phase displacement of the galvanometer relative to the earth's displacement
B = magnification constant depending on distance of galvanometer lens to recording drum, steady state length and section of transducer air-gap, and reluctances of transducer, of shunt and of leakage of system.

The quantity Q is the most important quantity in the above formula if one wishes to compare maximum earth displacement, or energies, from different phases in the same earthquake, as it is the only instrumental variable involved, for the other quantity involving the instrument can be considered as a constant composed of terms relating only to the optical, mechanical, and electrical features of the instrument. This frequency response characteristic can be determined from the original differential equations of motion and the theory of the electro-magnetic transducer as:

$$Q = \frac{\omega^3}{(\omega_o^2 + \omega^2)\left[(\omega_g^2 + \omega^2 + 4\mathcal{E}_g^2\omega^2\right]^{1/2}}$$

where:

$\omega_o = 2\pi/To$
$\omega_g = 2\pi/Tg$
To = free period of pendulum
Tg = free period of galvanometer
$\mathcal{E}_g$ = damping constant in the damping term of the galvanometer differential equation of motion

With the assumption that we have critical damping of both pendulum and galvanometer (i.e. $\mathcal{E}_g = \omega_g$; $\epsilon = \omega_o$):

$$Q = \frac{\omega^3}{(\omega_o^2 + \omega^2)(\omega_g^2 + \omega^2)}$$

If we now let:

$$u_p = Te/To \quad \text{and}$$

$$u_g = Te/Tg$$

we can reduce Q to:

$$Q = \frac{To\ u_p}{2\pi(1 + u_p^2)(1 + u_g^2)}$$

now setting:

$$a = \frac{z}{C \sin(\omega t + \Delta)} \quad , \qquad \text{and}$$

$$k = B/2\pi$$

we obtain:

$$a = k\ \frac{To\ u_p}{(1 + u_p^2)(1 + u_g^2)} \quad ,$$

which is the well known equation of dynamic magnification developed by Galitzin 12/.

If one wishes to compare only the ratios of ground displacement of two different waves, as mentioned above, one may compare the ratios of a/k for each wave, as k contains only instrumental "constants" which will remain the same for a given instrument for the same earthquake.

However, if one wishes to compute actual ground displacements, the instrumental constants become important. The determination of B by electrical, magnetic, and optical analysis of the component parts of the seismometer and galvanometer systems is extremely difficult, if not impossible (for a theoretical discussion of the equations involved see Galitzin 12/, Benioff 2/, etc.). However, there are several other methods of determining this constant. The method used for this report was that of suddenly applying a small force to the pendulum of the seismometer (the well known dropped test weight method).

If the energy of a dropped test weight of mass m_o is transmitted to the pendulum at its center of percussion parallel to the free direction of motion of the pendulum, whose mass is M, then:

$$B = \frac{-z_w}{\beta U} \quad *$$

where:

z_w = trace amplitude on the seismogram at the time t

$\beta = m_o g/M$

g = acceleration of gravity

$$U = \frac{\{2+(\omega_o-\omega_g)t\}e^{-\omega_o t} - \{2-(\omega_o-\omega_g)t\}e^{-\omega_g t}}{(\omega_o-\omega_g)^2}$$

(see Appendix B for details of derivation)

When B is determined, the maximum amplitude of the ground motion (C) can be determined by measuring the maximum trace amplitude on the seismogram and multiplying by 1/a for the period of earth motion (Te) in question:

$$C = A^*/a$$

---

* This formula has not been published, to the writer's knowledge. Its derivation was accomplished by Dr. H. Benioff, California Institute of Technology, who forwarded it to the author.

where:

A^* = maximum trace amplitude on the seismogram

If the ground displacement is desired in microns (μ) and the trace amplitude is measured in millimeters (mm), the formula is:

$$C = (A^*/a) \times 1000$$

where:

C = maximum ground displacement (microns)
A^* = maximum trace amplitude on seismogram (millimeters)
a = dynamic magnification

Long Period Benioff Electro-Magnetic Seismographs (Instruments IIA, IVN, and IVE)

There are three long period Benioff electro-magnetic seismographs in routine operation at the Pasadena Seismological Laboratory. Instrument IIA is a vertical component pendulum of 1 sec free period electromagnetically coupled to a 90 sec galvanometer. Instruments IVN and IVE are horizontal component pendulums of the same period and coupled to the same type of galvanometers.

A theoretical response curve for these instruments has been calculated (see table 6), and k/a vs. Te and a/k vs. Te have been plotted on graph 7. A periodic damping has been assumed for both pendulum and galvanometer in these calculations.

A theoretical response curve to the dropping of the test weight has been computed using the formula of the step function response characteristic U:

$$U = \frac{\left\{2 + (\omega_o - \omega_g)t\right\} e^{-\omega_o t} - \left\{2 - (\omega_o - \omega_g)t\right\} e^{-\omega_g t}}{(\omega_o - \omega_g)^3}$$

Numerical calculations are shown in table 7, and a graphical presentation showing U vs. t has been prepared as graph 8.

The time at which maximum U, or maximum trace amplitude, is reached may be easily obtained by differentiating U with respect to t, and setting the result equal to zero, and solving for t:

$$\frac{dU}{dt} = \frac{e^{-\omega_o t}\left\{(\omega_o - \omega_g) - \omega_o\left[2 + (\omega_o - \omega_g)t\right]\right\} + e^{-\omega_g t}\left\{(\omega_o - \omega_g) + \omega_g\left[2 - (\omega_o - \omega_g)t\right]\right\}}{(\omega_o - \omega_g)^3} = 0$$

Inserting numerical constants:

$$\omega_o = 2\pi/To = 2\pi, \quad \text{and}$$
$$\omega_g = 2\pi/Tg = 2\pi/90,$$

and disregarding $e^{-\omega_o t}$ as infinitesimal with respect to $e^{-\omega_g t}$, we obtain:

$$t = \frac{\omega_o + \omega_g}{\omega_g (\omega_o - \omega_g)} = 14.48 \text{ sec.}$$

By differentiating twice and again inserting constants, one obtains the point of inflection of the curve at:

$$t = \frac{2}{(\omega_o - \omega_g)} = 0.322 \text{ sec.}$$

As an example of the method necessary to construct a response curve showing dynamic magnification (V) vs. period of the earth waves (Te) , or maximum earth amplitude divided by trace amplitude (C/A*) vs. Te, the following is cited. On February 6, 1947, tests were run on Instrument IVN which gave the following data:

Test weight on --- $z_\omega = 72.8\text{mm}_{(max)}$
Test weight off --- $z_\omega = 71.8\text{mm}_{(max)}$

Inserting this data into the formula:

$$V = a = A^*/C = BQ$$

where:

$$B = z_{\omega(max)} / \beta U_{(max)}$$

$\beta = m_o G/M = 0.000002 \times 9800 = 0.0196 \text{ mm/sec}^2$ (these Benioff instruments are so constructed that the mass of the test weight is 0.000002 of the mass of the pendulum)

$z_{\omega(max)} = 72 \text{ mm}$

$U_{(max)} = 0.133 \text{ sec}^3$

then:

$$B = \frac{72 \text{ mm}}{0.0196 \text{ mm/sec}^2 \times 0.133 \text{ sec}^3} = 27600/\text{sec}$$

Inserting the value of B into the equation of dynamic magnification:

$$V = BQ = \frac{27600}{\text{sec}} \left(\frac{a}{k}\right) \frac{\text{sec}}{2\pi} = 4393 \left(\frac{a}{k}\right)$$

Computing V vs. Te, or C/A* vs. Te, is merely a matter of multiplying the values of a/k, or k/a, respectively, by the factor 4393, which has been done in table 8. Values of a/k and k/a can be taken from the previously mentioned table 6. A graph showing V vs. Te and C/zA* vs. Te

has been prepared (see graph 9).

The point of maximum response can be easily obtained for these instruments by differentiating the formula for a/k with respect to Te, setting the result equal to zero, and solving for Te:

$$a/k = \frac{Te\ To^2\ Tg^2}{(To^2 + Te^2)(Tg^2 + Te^2)}$$

Since the maximum of a/k is the minimum of k/a:

$$\frac{d(k/a)}{dTe} = 3\ Te^4 + (To^2 + Tg^2)\ Te^2 - To^2\ Tg^2 = 0$$

Solving for To=1 sec and Tg=90 sec:

$$Te = 0.99975 \text{ sec.}$$

For this value of Te:

$$a/k = 0.49994$$

Short Period Benioff Electro-Magnetic Seismographs (Instruments VIA, VIBN, VIBE)

There are three short period Benioff electro-magnetic seismographs in routine operation at the Pasadena Seismological Laboratory. Instrument VIA utilizes the same pendulum as Instrument IIA, but the output of a second transducer is electro-magnetically coupled to a galvanometer with a free period of 0.23 sec. Instruments VIBN and VIBE utilize the outputs of the pendulums of Instruments IVN and IVE, respectively, but they are coupled into galvanometers of 0.2 sec free period.

Theoretical response curves, assuming aperiodic damping of pendulums and galvanometers, have been prepared (see tables 9 and 10). Graphs showing k/a vs. Te and a/k vs. Te for Instruments VIA and VIB have been prepared (see graphs 10 and 11).

Maximum response occurs at a point which may be determined by differentiating k/a with respect to Te, equating to zero, and solving for Te. Results show a maximum response for Instrument VIA at Te = 0.211 sec and gives a value of k/a = 9.13. For Instrument VIB this point is at Te = 0.187; k/a = 10.37.

Determination of the response coefficient (U) is similar to the method shown previously under the "Long Period Benioff Electro-Magnetic Seismograph". Response in this case, however, depends more upon the characteristics of the pendulum than was the case with the long period instruments. Calculation of U for instruments VIB are shown in table 11 and results graphically presented are shown in graphs 12 and 13.

To find the time at which maximum U occurs, the problem is again the same as in the case of the long period instruments except in this case $e^{-\omega t}$ cannot be disregarded and the differentiated equation is transcendental in form. For Instrument VIB (To = 1 sec; Tg = 0.2 sec), the equation

$dU/dt = 0$ reduces to:

$$8\pi t = \log_e \left[\frac{3 + 20\pi t}{3 + 4\pi t} \right]$$

By methods of successive approximations this may be solved, and gives a value of $t = 0.2384$ sec.

Benioff Strain Seismograph

The theory of the Benioff strain seismograph has been reported by Benioff 3/.

In this paper it is shown that if the ground displacement is of the form:

$$\xi = C \sin \omega t \quad ,$$

the equation of motion for the light spot on the recording drum is:

$$\frac{d^2z}{dt^2} + 2\epsilon \frac{dz}{dt} + \omega_g^2 z = V a \omega^2 \sin \omega t \quad ,$$

which is identical with the simple pendulum seismograph equation, the solution of which is:

$$z = V_o \; G \; C \sin (\omega t + \delta)$$

where:

Vo = static magnification

$$G = \frac{1}{\left[(u_g^2 - 1)^2 + 4 h^2 u^2\right]^{1/2}}$$

Long Period Benioff Strain Seismograph (Instrument VI)

There was one long period Benioff strain seismograph in routine operation at the Pasadena Seismological Laboratory during the period of time that the earthquakes occurred which were studied for this report. Since then an additional horizontal instrument has been installed.

As the galvanometers in use with these instruments have a free period of 70 sec, and are critically damped, one can readily obtain the value of G in the previously mentioned equation. Then by plotting:

$$V = A^*/C = V_0 G$$

one could obtain the dynamic magnification characteristics of Instrument VI.

However, as V_0 is practically impossible to determine accurately and is always a constant for a given instrument during the same earthquake, we may use G as a multiplying factor when trying to obtain the ratio of maximum earth displacements for various phases during the same earthquake, in the same way that a/k is used for the Benioff electro-magnetic instruments.

G and 1/G have been calculated and the results are shown in table 12 and graph 13.

IV. PROCEDURE

The methods employed during the measurements and the subsequent calculations will be briefly discussed in this chapter.

From a comprehensive file of earthquakes, which is maintained at the Seismological Laboratory at Pasadena, shocks were selected with epicentral distances from Pasadena greater than 20° and less than 90°, with magnitudes (as per Richter's magnitude scale 32/) of 7.0 or more, with shallow focus (depth in general 10 to 30 km), recorded during the years 1940 to 1945,inclusive. Not all earthquakes of this classification were used for this study; the ones excluded were those which had azimuths and distances of such values that they were adequately covered by data from other shocks. The shocks used for this report are listed in table 13.

The origin times, locations, and magnitudes of many of these shocks are presented by Gutenberg and Richter 23, p. 615-17/; these data for the rest of the shocks are taken from unpublished work of Dr. B. Gutenberg. The earthquakes are designated by a number which will be used for identification purposes. On table 14, the "quality" is the symbol originated by Gutenberg and Richter. It indicates the quality of the location as follows: A, epicenter probably within 1 degree of arc; B, within 2 degrees; C, within 3 degrees. "Pad" is a cross-index to Dr. Gutenberg's file of location, origin time, and magnitude computations.

Some earthquakes with a depth of focus of as much as 60 kilometers were used in this study, but the use of these shocks was restricted to those areas where shallower shocks were unavailable. In table 13 all shocks with foci slightly deeper than normal are noted as have a depth (h).

The trace amplitudes and trace periods of the P, PcP, PcS, S, and

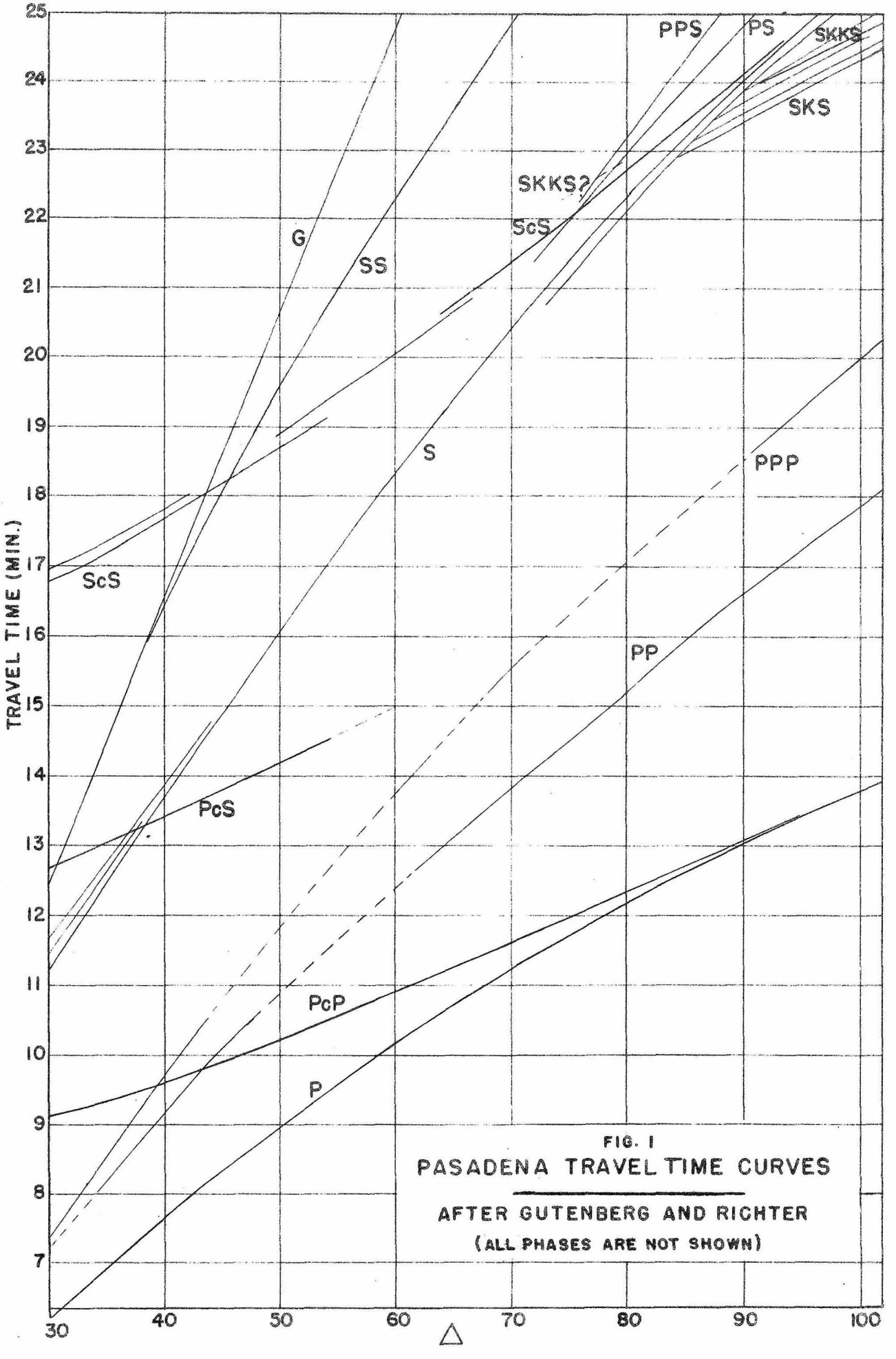

FIG. 1

PASADENA TRAVEL TIME CURVES

AFTER GUTENBERG AND RICHTER

(ALL PHASES ARE NOT SHOWN)

and ScS phases were measured on the seismograms of these shocks to the closest tenth of a millimeter. Depending upon the instrument in question, the speeds of the recording drums are such that a second of time is either 1 mm or 0.5 mm (strain---Instrument VI---0.25 mm); so that the maximum possible accuracy of period measurement is either 0.1 or 0.2 sec. Actually, for long period waves the accuracy is not this high, especially when the amplitude is not large, as there is often indecision on the part of the measurer as to the true point of maximum amplitude or the true location of the zero line. Some variation is usually to be noted between individual oscillations in the same wave train, with the period generally increasing as one proceeds toward the tail of the wave train. However, in almost all cases several period measurements can be made and an average reading can be obtained. Maximum amplitudes were measured; and, in most cases the maximum occurred in the second or third oscillation of the wave train instead of at the first oscillation recorded for the particular phase. The results of these measurements are shown in table 14.

Graphs 14 to 19, inclusive, were then used to obtain the factor R, which is $\frac{Ae/A^*}{Te}$ for the torsion instruments, $\frac{k/a}{Te}$ for the electro-magnetic instruments, and $\frac{1/G}{Te}$ for the strain. Multiplying this factor with the observed trace amplitudes A* results in the value RA* (Ae/Te for the torsion instruments, $\frac{(k/a)A^*}{Te}$ for the electro-magnetic instruments, and $\frac{A^*/G}{Te}$ for the strain). The last two quantities above, namely $\frac{(k/a)A^*}{Te}$ and $\frac{A^*/G}{Te}$, vary directly as Ae/Te, if records taken with the same instrument are compared. As the various instruments have only one direction of freedom of movement, oriented N-S, E-W, or vertical, the quantity RA* varies directly as u_{NS}/Te, u_{EW}/Te, or w/Te, as the case may be, again assuming records from the same instrument are compared. From these data the values of $\frac{u_{NS}PcP/Te}{u_{NS}P/Te}$, $\frac{w\ ScS/Te}{w\ S/Te}$, etc., are obtained by division. The results of these computations

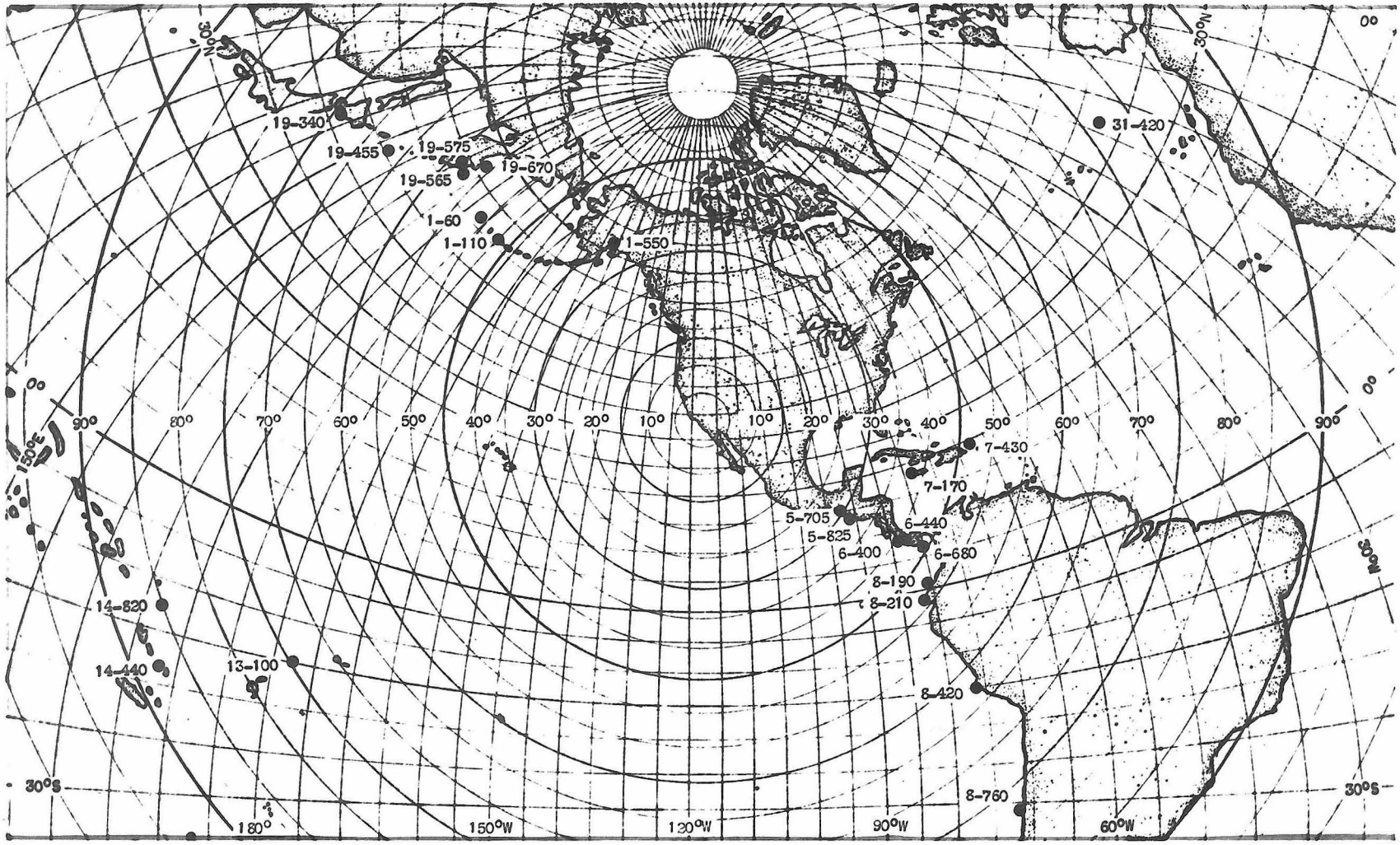

Figure 2 --- DISTRIBUTION OF EARTHQUAKES. Base map is a stereographic projection with Pasadena at the center (des. and del. by C.F. Richter, E.C. Nichols, and J.M. Nordquist)

are shown in table 14. In this table new symbols are introduced for convenience in designating the following quantities:

$$\frac{u_{NS} \text{ (or } u_{EW}\text{, or w) PcP/Te}}{u_{NS} \text{ (or } u_{EW}\text{, or w) P /Te}} = S1$$

$$\frac{u_{NS} \text{ (or } u_{EW}\text{, or w) PcS/Te}}{u_{NS} \text{ (or } u_{EW}\text{, or w) P /Te}} = S2$$

$$\frac{u_{NS} \text{ (or } u_{EW}\text{, or w) ScS/Te}}{u_{NS} \text{ (or } u_{EW}\text{, or w) S /Te}} = S3$$

$$\frac{u_{NS} \text{ (or } u_{EW}\text{, or w) ScP/Te}}{u_{NS} \text{ (or } u_{EW}\text{, or w) S /Te}} = S4$$

In general it was assumed that the dominating period carried the greatest amount of energy. However, in all cases of doubt, where there were more than one pronounced period registered, both, or in some cases several, periods and their respective amplitudes were measured. In such instances the set of values which showed upon computation the greatest energy was used in subsequent calculations. This rule was not strictly adhered to, however. For example, in shock number 19-565, S showed two well-developed periods, one of 24.0 sec with a trace amplitude of 3.1 and one of 6.0 sec with a trace amplitude of 1.3. The values computed for RA* for these two dominant periods were 3.33 and 1.33, respectively. However, ScS for this same shock was recorded on the same instrument with only one dominant period of 8.0 sec. When the ratio of $\frac{u_{EW} \text{ ScS/Te}}{u_{EW} \text{ S /Te}}$ was graphed in this instance, the 8.0 sec wave of ScS was compared with the 6.0 sec period wave of S instead of with its 24.0 sec wave. With such a difference in the two frequencies, it was assumed that this procedure would give more exact results.

The results obtained by the methods outlined above have been graphed for clearer visualization. In these graphs, the symbols u and w have been used in lieu of the terms u/Te and w/Te. As stated previously, the u and w computed by Dana 9/ were in reality these quantities. Graphs 20 to 25,

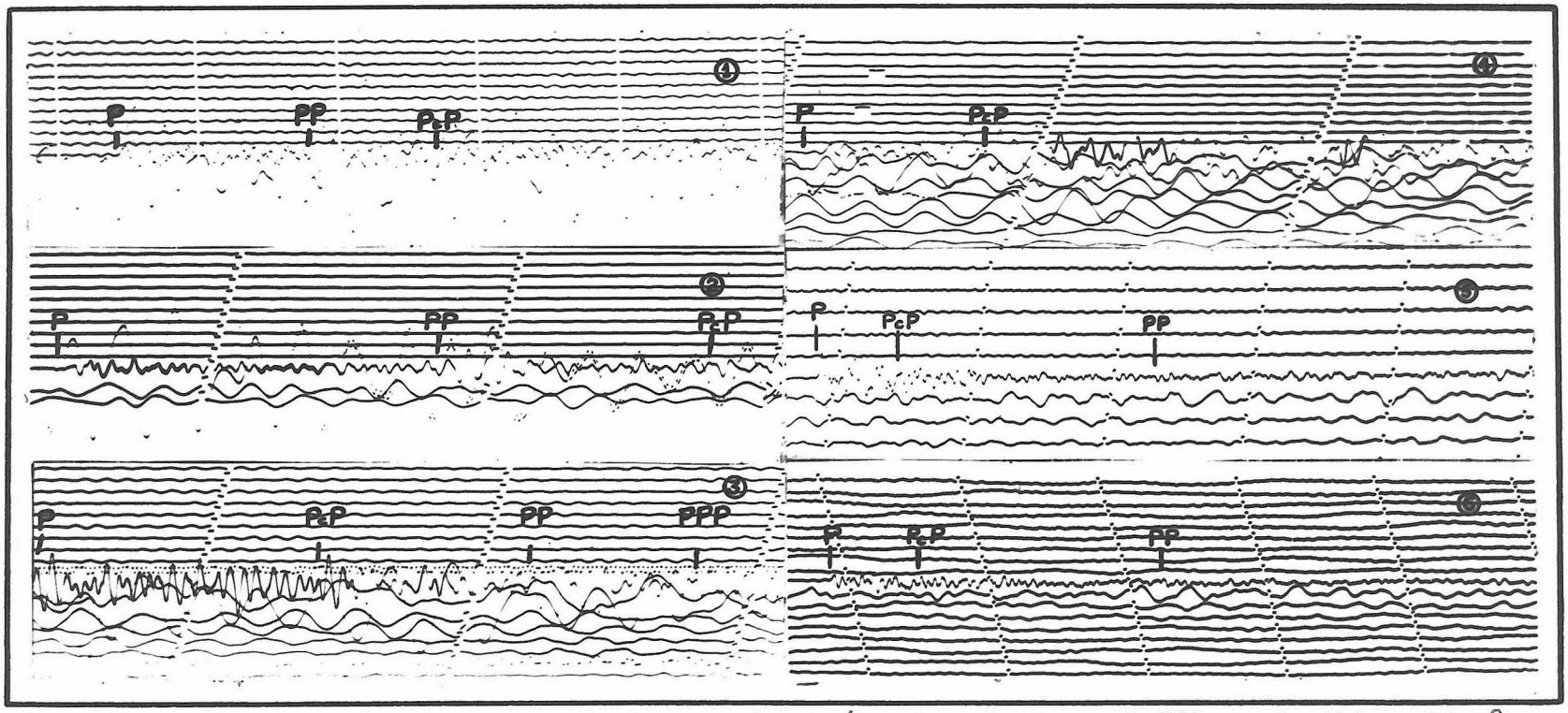

Figure 3 --- Examples of seismograms showing P and PcP (No. 1 - Shock no. 1-550, Inst. IVA, Δ=34.6°; No. 2 - Shock no. 1-550, Inst V, Δ=34.6°; No. 3 - Shock no. 7-430, Inst. V, Δ=47.5°; No. 4 - Shock no. 8-420, Inst V, Δ=63°; No. 5 - Shock no. 19-455, Inst. IIA, Δ=65.8°; No. 6 - Shock no. 19-455, Inst. IVB, Δ=65.8°).

inclusive, are as follows:

Graph 20 --- $\frac{u_{EW}PcP}{u_{EW}P}$ and $\frac{u_{NS}PcP}{u_{NS}P}$ as a function of $\triangle$

Graph 21 --- $\frac{w\ PcP}{w\ P}$ as a function of $\triangle$

Graph 22 --- $\frac{u_{EW}ScS}{u_{EW}S}$ and $\frac{u_{NS}ScS}{u_{NS}S}$ as a function of $\triangle$

Graph 23 --- $\frac{w\ ScS}{w\ S}$ as a function of $\triangle$

Graph 24 --- $\frac{u_{EW}PcS}{u_{EW}P}$, $\frac{u_{NS}PcS}{u_{NS}P}$, $\frac{u_{EW}ScP}{u_{EW}S}$, and $\frac{u_{NS}ScP}{u_{NS}S}$ as a function of $\triangle$

Graph 25 --- $\frac{w\ PcS}{w\ P}$ and $\frac{w\ ScP}{w\ S}$ as a function of $\triangle$

In practice it is impossible to distinguish definitely between the phases PcS and ScP for shallow earthquakes. Therefore, graphs 24 and 25 were computed with the supposition that the phase arriving at the proper time was, in the case of $\frac{u(\text{or } w)PcS}{u(\text{or } w)P}$, PcS; and, in the case of $\frac{u(\text{or } w)ScP}{u(\text{or } w)S}$, ScP, even though the two numerators are identical. However, assuming that the longitudinal and transverse waves receive equal amounts of energy at the source, the theoretical values of $u_{EW}PcS$ and $u_{NS}PcS$ are approximately three times those of $u_{EW}ScP$ and $u_{NS}ScP$, and theoretically w ScP is about 10 to 15 times w PcS (see page 39 for a further discussion). Therefore, since most of the energy is represented in the ratios $\frac{u_{EW}PcS}{u_{EW}P}$, $\frac{u_{NS}PcS}{u_{NS}P}$, and $\frac{w\ ScP}{w\ S}$, the other ratios represented in graphs 24 and 25 are of little interest.

Several points of interest regarding the general reliability of the data presented in graphs 20 to 25, inclusive, should be brought to light prior to a careful study of these charts.

The accurate recognition of the various phases in question is, of course, one of the most important problems which the seismogram interpreter must face. The P wave is always the first arrival (see fig. 1) in the range of distances in which we are interested, and there is little doubt

about its true identification. There are several epicentral distances, on the other hand, at which PcP may be regarded with more scepticism. At 40 to 45 degrees, PcP and PP (the longitudinal wave which is reflected once at the surface of the earth about halfway between the focus and the recording station) arrive within a few seconds of each other. However, the writer found little trouble, in most cases, in distinguishing between these two phases. A much greater difficulty is encountered at distances greater than about 70 degrees. In this range PcP arrives a few seconds after P. Sometimes, it is intimately associated with the P train and is so "overridden" by the P train that interpretation is not good, especially in the larger distances of this range. Another factor contributing to the doubtful interpretation of PcP at these distances is the possible presence of pP (the wave which is reflected at the surface of the earth near the epicenter and then proceeds to the recording station.) If the shock occurs at the surface of the earth, pP is, of course, non-existent; however, if there is depth of focus, pP should be present, and the pP -P time interval increases with an increase in the depth of focus. Therefore, even though the earthquakes with which we are interested are known to be surface shocks, they may have enough depth of focus to produce a pP, which will record on the seismogram a few seconds after P. The same reasoning applies to the phase sP. In this range of distances greater than about 70 degrees, doubt arises whether one is measuring pP, sP, or PcP. Sometimes, the recognition of PcP is fairly certain; sometimes it is extremely doubtful.

At distances less than about 39 degrees, the identification of PcS (or ScP) is questionable, especially if its period is as long as the period of S, which arrives at about the same time or earlier.

Aside from the complication mentioned in the last paragraph, S is

readily distinguished except at distances greater than about 84 degrees. In this range, S is preceded by SKS (the wave which travels to the core boundary as a transverse wave, through the core as a longitudinal wave, and thence to the recording station as a transverse wave).

There are several ranges of distance where the recognition of ScS on the seismogram may become dubious. At less than 40 degrees it is usually so intimately mixed with the short period surface waves that no interpretation is possible. At distances less than about 47 degrees, distinguishing ScS from SS may be difficult. At distances greater than 65 degrees there is the possibility of interference by SKS (see Gutenberg 15/). From 70 to 80 degrees, PS and PPS arrive within a few seconds of ScS, and identification is not positive. At distances greater than 80 degrees interference similar to that of pP, sP, and PcP exists; in this case it is pS, sS, and ScS that may be hard to distinguish.

Another source of interpretation difficulty arises from the type of routine recording employed. The light beam from the galvanometer falls on a continuously rotating drum, around which the photographic paper is wrapped. This drum rotates at the rate of one revolution every 15 minutes (or 30 minutes, depending on the instrument) and travels at right angles to the direction of rotation at the rate of 2.5 (or 5.0 mm) per revolution. This causes the recorded trace to be proximate to itself every 15 (or 30) minutes. Therefore, oftentimes in a large earthquake the trace of the large surface waves, which arrive for an hour or more after the beginning of the shock, override the recording of the earlier phases so badly that the record is a scrambled, intricate muddle of lines that cannot be interpreted. In such cases table 14 has been marked by the symbol "ov". Drifting of the zero line may also cause an overriding effect which prevents interpretation; but such trouble is rarely found on any of the instruments except the strain

seismograph.

The reliability of the various instruments deserves mention at this point. The torsion instruments may be expected to maintain their stability over a longer period, i.e. their simple mechanical and optical system probably changes properties less than the more complicated mechanical and electro-magnetic system of the Benioff type instruments. A study of graphs 14 to 19, inclusive, discloses some interesting facts concerning variations which might arise due to small errors in the measurement of trace periods. Both the short-period torsions and the short-period Benioffs have a large change in magnification x period per change in period in the range of frequencies in which we are interested. The long-period torsions have much less change, and the long-period Benioffs have a practically flat response over this range. The conclusions that may be drawn from these facts are (1) the long-period torsions are probably the most reliable instruments for computing actual ground displacements because of their better stability and fairly low magnification x period gradient, and (2) the long-period Benioffs and the long-period torsions are the most reliable instruments for computing <u>ratios</u> of ground displacements for the same earthquake, the former because of their almost flat magnification x period gradient and the latter because of their fair magnification x period gradient and their simpler systems, which have no galvanometers or electrical circuits to cause deviation. These facts should be borne in mind during subsequent discussions of the results.

V. RESULTS

The data shown in graphs 20 to 25, inclusive, can now be discussed in greater detail. All of the data shows the wide scatter that is to be expected in a study of this sort. The use of displacement ratios instead of absolute values of displacement, which disposes of the necessity of considering the absolute energy released during a given earthquake, still requires the assumption that the energy is propagated equally in all directions from the focus. The direction and type of movement at the focus, i.e. the tectonic factors involved, make it improbable that such an assumption is true. This may account for much of the scatter, but it seems reasonable to assume that such effects would be more or less of a random nature if data were presented from a variety of shocks at various distances and azimuths as is the situation in this study (see fig. 2). Therefore, even if these effects are present, a statistical mean curve could still be applied to the data.

Another cause of scatter is the group of assumptions made with regard to the instrumentation and seismogram interpretation. It is unlikely, however, that these assumptions would account for more than a factor of 2 or 3 in the results, especially when it is considered that, in lieu of actual displacements, ratios of displacements of waves that are sometimes of identical period and most of the time very close to the same period are being evaluated. Two graphs have been prepared which show the consistency between the long-period Benioff and the long-period Wood-A nderson instruments. Graph 26 shows the ratios of the ground displacements computed from Instrument IVB to the ground displacements computed from Instrument V for both the P and PcP phases. Graph 27 shows the ratios of the ground displacements divided by the trace periods for the same instruments and phases. The expected scatter in the results is apparent. The graphs suggest several

other points of interest. The graph of the ratios of the ground displacements shows a much wider scatter than the graph showing the ratios of the ground displacements divided by the periods. This implies that the registrations of the seismographs are more reliable for receipt of energy for various parts of the spectrum than for the recording of ground amplitudes; i.e. the energy content of a given portion of the spectrum, while varying from the energy content of another part of the spectrum, will not vary as much as the ground amplitude resulting from the application of that energy. As the ratios of instrument IVB/V are greater at shorter epicentral distances, four more graphs (graphs 28 to 31, inclusive) were prepared, showing ratios of ground displacement and $\frac{\text{ground displacement}}{\text{period}}$ as a function of the trace periods recorded by these instruments. A study of these graphs contributes nothing towards the solution of this problem. Appearances indicate that period measurements on one of these instruments can be viewed with scepticism.

The u ratios of PcP/P (graph 20) show observed values of approximately 10 times the theoretical values. The w ratios of PcP/P are not nearly so inconsistent, being, in general, only 2 to 5 times greater than the theoretical curve. The u and w ratios of ScS/S (graphs 22 and 23) are fairly consistent with the theoretical computations, i.e. they seem to group themselves fairly within the limits of probable error. The interpretation of the PcS/P and the ScP/S data (graphs 24 and 25) is less conclusive. A condition which does not appear on these graphs is that the actual horizontal displacement (u) of PcS should theoretically be about three times that of ScP and the vertical displacement (w) of ScP should theoretically be about 10 to 15 times that of PcS, if the value of C in equation (1) on page 4 is the same for both an initial longitudinal and initial transverse wave at the source (see Dana 9, p.30,table2/).

Gutenberg 19, p.61/ found that the value of C* for S waves is very close to the value of C for P waves. Therefore, it may tentatively be assumed that a preponderance of the displacement in the vertical direction is probably due to the ScP phase; and, more uncertainly, most of the horizontal displacement is due to the presence of the PcS phase. The data tend to confirm this idea, as the w ratios of ScP/S are more in accord with the theoretical values than are the w rations of PcS/P; and the u ratios of PcS/P are, in general, only twice their theoretical values, while there is a much greater disparity between the u ratios of ScP/S and their theoretical values. The method of approach used in this research gives no insight into the conformance or non-conformance of the u ratios of ScP/S or the w ratios of PcS/P, and the graphs showing these ratios are of little interest, as mentioned previously. In general, therefore, it can be said that the displacement ratios of ScS/S and ScP/S seem not unreasonable in the light of the present theory, the horizontal displacement ratios of PcS/P and the vertical displacement ratios of PcP/P are not unprobable, and the horizontal displacement ratios of PcP/P seem definitely greater than the theory indicates.

Explanation of the discrepancies between the observed and the theoretical horizontal displacement ratios of PcP/P could fall into two general classifications: (1) the theoretical values of the displacements of PcP

---

* Gutenberg's C is not the same as the C used in this paper, although it is a measure of the percentage of the total energy of the earthquake carried by the wave in question. If we designate the value of C given by Gutenberg as C_1, and call the C of Dana and this paper C_2, it is readily shown that:

$$\log_{10} C_2 = (0.9\ M + 0.7) - C_1$$

where:

M = magnitude of earthquake.

Therefore, for a given earthquake (where M is a constant) if C_1 is found to be equal for different phases, C_2 must be equal for those phases.

might be smaller than is actually the case, or (2) the theoretical values of the displacements of P might be greater than is actually true. In an effort to clarify this situation, the magnitudes of the various eqrthquakes were computed by means of a formula developed by Gutenberg 19, p.66,form. (18)/. This formula contains an empirical constant and was originally derived for use with body waves. The computations are shown in table 15 and the results are graphed on graph 32. To obtain these magnitudes, which are logarithmically proportional to the square roots of energies, an evaluation must be made of the magnification of the instruments used. For the values shown in table 15, instruments/IIA, IVA, and IVB (long-period Benioffs) were used, and the magnification constant of the / instruments was set at Q = 4393, a value determined for instrument IVA as explained previously in the chapter on instrumentation. Even if this constant is wrong by a factor of 2, the magnitude is changed by only 0.3. The "true" magnitudes (i.e. those computed from the records of many stations recording and reporting displacements due to the shock in question) minus the magnitudes as computed from Gutenberg's formula for body waves using the displacement values obtained for PcP and P in this study are plotted as ordinates on graph 32; the "true" magnitudes are shown as abscissas. All seismic stations have a certain "ground factor" which, in many cases, causes the trace amplitudes of the incoming waves to appear larger or smaller than their true amplitudes would indicate. The "ground factor" at Pasadena, obtained over many years of amplitude study, is approximately -0.2 on the magnitude scale (i.e. Pasadena shows a smaller amplitude than an average station should with no "ground factor"). On the graph this phenomenon has been included in computing M_2. Any phase giving the "true observed" magnitude should, therefore, show a cluster of points about the zero axis. A glance at graph 32 reveals that the values determined from

V (long-period Wood-Anderson) and

Benioff

the P phase of the earthquakes used for this study are close to their theoretical values, whereas the magnitudes determined from the vertical component of ground displacement of PcP are slightly too high and the magnitudes determined from the horizontal components of ground displacement of PcP are approximately 1.0 magnitude too large. This gives a strong indication, if the empirical constant of Gutenberg's formula is correct, that the PcP phase, and not the P phase, varies from the theoretical expectations and has about 10 times the amplitude (or about 70 times the energy) that the theory indicates. That the empirical constant of Gutenberg's formula is correct is verified by the fact that magnitudes computed from PP conform to those obtained from P.

The above results invited a closer scrutiny of the factors involved in the theoretical determination of the displacements of PcP. To aid in this analysis the various factors of formula (1) on page 4 were graphed. Graph 34 shows the percentage of the displacement ratio loss due to u (or w)/Ae, f, and $\sqrt{\frac{\tan i_o}{\sin \Delta} \frac{di_o}{d\Delta}}$ for PcP/P at various epicentral distances. Since the absorption term was not calculated into the theoretical curves presented on graphs 20 to 25, it has not been included on this graph, although it varies from about 0.70 at $\Delta = 0^o$ to 1.00 at $\Delta = 103^o$, as mentioned previously. The effect of absorption, if included on graphs 20 to 25, would be to further enlarge the differences between the observed and theoretical displacement ratios of PcP/P, since the path of PcP is always longer than the path of P. A study of graph 34 reveals that none of these factors contributes less than about 40 percent of the reduction in the displacement ratios of PcP/P at an epicentral distance of from 50° to 60°. Therefore, if it is supposed that any one of these factors is set equal to unity, it would have a maximum effect of making the theoretical displacement ratios only about two and one-half times their value, in this

range of distances, under the present assumptions. Setting these factors equal to unity is, of course, an absurdity. If f is set equal to unity, it would mean that, at the reflection at the core boundary, all of the energy of an incident longitudinal wave would be reflected as a longitudinal wave. The existence of PcS and P' (the wave which passes through the core as a longitudinal wave after refraction from a longitudinal wave at the core boundary) disputes this possibility. If $\sqrt{\frac{\tan i_o}{\sin \Delta} \frac{di_o}{d\Delta}}$ were set equal to unity, it would mean that there is less energy spread per unit distance in the PcP wave than in the P wave and that no spreading takes place due to the convexity of the reflecting core surface. Setting u/AeΛ as unity could be possible but would dispute the theory of reflection at a free surface under the conditions of small angles of incidence.

As a further study of possible changes in the theoretical displacements of PcP, it was thought desirable to see in more detail what influence changes in the physical constants on either side of the core boundary would have on the factor f. The velocity of longitudinal waves (V_{p1}) and the velocity of shear waves (V_{s1}) in the mantle just outside the core boundary of 13.7 km/sec and 7.25 km/sec, respectively, is established within close limits of error by many years of meticulous research by many workers (a resume is given in Macelwane 28, pp. 265-74/; see also Gutenberg and Richter 22, pp. 134-5/). These are the velocities used by Dana in his calculations. Although a large amount of work has also been done on the velocity of longitudinal waves within the core (see Macelwane 28, pp. 274-80/; Gutenberg and Richter 21/), the possible error in the results of this work is greater. Dana used in his calculations the value of 8.0 km/sec for the velocity of longitudinal waves just inside the core boundary (V_{p2}). The assumption that the core does not transmit shear waves, based upon the fact that no such waves have ever

been recognized on seismograms, may be in error. However, if it is assumed that shear waves are transmitted into the core, the amount of reflected energy would decrease, causing still further reduction in the theoretical displacement values, a condition opposed to the desired correction. The ratio of the densities on either side of the core boundary is still more doubtful than the velocities of seismic waves in this region of the earth's interior. Dana used the values of 10.1 gm/cm^3 for the density just within the core boundary and 5.4 gm/cm^3 just outside the core. These data were taken from a table reprinted after Bullen 5,6/. However, Bullen, in his revised work assigns the values 9.69 gm/cm^3 and 5.56 gm/cm^3, respectively. In investigating f, the values for the mantle just outside the core boundary were left unchanged, but V_{p2} and ρ_2/ρ_1 were varied to see what the effect on the factor f would be. An upper limit of 9 km/sec and a lower limit of 7 km/sec were set on V_{p2} as the extreme possibilities for this element. A value of V_{p2} beyond these two limits is considered highly improbable. For ρ_2/ρ_1 extreme limits of 2.0 and 1.0 were set. Anything beyond these limits would involve density distributions in the core that are considered impossible. Therefore, three various values of ρ_2/ρ_1 were chosen (2.0, 1.5, and 1.0) and two values of V_{p2} were chosen (7.0 km/sec and 9.0 km/sec); then the values of f for an incident and reflected longitudinal wave ($\sqrt{E_{rp}/E_{ip}}$) were computed using these six conditions (see table 16). The graphical presentation of these data and the values obtained by Dana (V_{p2}= 8 km/sec; ρ_2/ρ_1= 10.1/5.4) are shown in graph 35. The value of $\sqrt{E_{rp}/E_{ip}}$ is always positive, and it has been graphed above and below the zero line only to avoid confusion in interpretation. The points where the curves cross the zero line are changes in phase (from compression to dilatation) of the reflected wave at the reflecting surface. As can be seen from the

graph, the maximum conditions of V_{p2}= 9 km/sec and ρ_2/ρ_1 = 2.0 would result in an increase in f, and thus an increase in u (or w), of only about 16 percent.

One other phenomenon concerning the core boundary should be mentioned at this time. This is the spread of the reflected seismic energy due to the convexity of the core's surface, which makes the reflecting surface act as a convex mirror instead of as a plane mirror. This spread is theoretically taken account of in the $di_o/d\Delta$ term of equation (1) on page 4 (see the derivation of this formula in 14/ for details.)

That the angle of incidence at the core may vary somewhat from the computed values without seriously affecting the value of f can be readily seen by inspecting graph 35. Since the angle of incidence at the core (i_c) is a function of the epicentral distance (Δ) and since the curve of $\sqrt{E_{rp}/E_{ip}}$ is relatively flat, a small change in the angle of incidence would not affect the theoretical value of f materially.

One of the assumptions made in the theory is that there is no first order discontinuity between the bottom of the crust and the core boundary. This assumption is based upon good observational data (see Gutenberg and Richter 20/.

There are certain conditions near the surface of the earth that are worthy of discussion. As previously mentioned, there is the possibility that the energy might not leave the focus of the earthquake equally in all directions. To increase the theoretical displacement ratios of PcP/P , the assumption would have to be made that, in general, more energy be propagated downward than horizontally at the source. If this were true, at large epicentral distances where the angles of incidence of P and PcP become about the same (see graph 36) there would be a large decrease in the

displacement ratios. One might argue that PcP, in some unexplained fashion, leaves the focus in a different azimuthal direction than does *P*. Table 17 shows the variations between the true azimuths from Pasadena to the epicenters of the shocks and the azimuths calculated from the E-W and N-S displacements shown by instruments IVA and IVB (long-period Benioffs). The greatest variation is 22^{o} and the differences group themselves nicely about their true values. These data are considered to be quite confirmatory for azimuthal studies of this sort.

The values of the wave velocities (V_{po} and V_{so}) and the dependent angles of incidence (i_o) at the surface of the earth are involved in the theoretical calculations. In Dana's calculations, used for the theoretical curves of this report, the longitudinal wave at the surface (V_{po}) was assigned a value of 5.5 km/sec. This is very close to the value determined for the "granitic" layer under Pasadena 16, 17/. However, the crustal layers may be too thin with respect to the wave lengths of P and PcP at large epicentral distances to affect the angles of incidence. If the period of a seismic wave is, for example, 3 seconds, the wave length in a medium with a velocity of 5.5 km/sec is 16 1/2 km, which is comparable with the 18 km thickness of the "granitic" layer near Pasadena. Below the "granitic" layer are two "basaltic" layers, totaling some 19 km thick near Pasadena, which have velocities for longitudinal waves of 6.0 and 6.9 km/sec. Below this is the outer boundary of the mantle, with a velocity of 8.0 km/sec. Due to the prevalence of periods of P and PcP of several seconds, it is doubtful how the angles of incidence of these phases correspond to the various velocities in the crust.

In an attempt to investigate this situation, the angles of incidence (i_{po}) of P and PcP were computed from the observed displacements of instruments IIA, IVA, and IVB (long-period Benioffs). Table 17 shows these

computed values for P, which were calculated using the following formulae:

$$\tan \bar{i} = \frac{\sqrt{u_{NS}^2 + u_{EW}^2}}{w}$$

$$\bar{i} = 2\, i_{so}$$

$$\sin i_{po} = (V_{po}/V_{so}) \sin i_{so}$$

where:

$\bar{i}$ = "apparent" angle of incidence at the surface of the earth
i_{so} = angle of incidence for transverse waves at the surface
i_{po} = angle of incidence for longitudinal waves at the surface

The conversion from $\bar{i}$ to i_{po} which is shown in the last two formulae above was accomplished by a conversion table showing $\bar{i} - i_{po}$ for various values of i_{po} prepared by Gutenberg 14, p.48, tab.4/. This chart is reproduced graphically as graph 39. These computed values of i_{po} are compared with the theoretical values of the angles of incidence (i_{pot}), which were obtained from Dana 7, p. 110/. Dana, as previously mentioned, used a value of V_{po} of 5.5 km/sec. $i_{po} - i_{pot}$ has been plotted as a function of epicentral distance on graph 37. The i_{po} values of PcP were computed in the same way as those of P, and the i_{pot} values of PcP were also taken from Dana 7, p. 37/ for a value of V_{po} of 5.5 km/sec. The values of $i_{po} - i_{pot}$ for PcP have been plotted as a function of epicentral distance on graph 38.

To investigate the effects of the crustal layers on the angles of incidence, $i_{po} - i_{pot}$ was computed, assuming V_{po} as 8.0 km/sec, and the results were also plotted on graphs 37 and 38. For this problem, i_{pot} for P was computed by using the following formula (see Gutenberg 14, p.191/:

$$\sin i_{pot} = V_{po}\, (dt/d\Delta) = V_o/\bar{V}_\Delta$$

where:

V_o = velocity of longitudinal waves at the surface = 8.0 km/sec

$\bar{V}_\Delta$ = "apparent" velocity as computed from the travel-time curve.

The values of $\bar{V}_\Delta$ were taken from Dana 7, p.108/. The values of i_{pot} for PcP for a value of V_{po} = 8.0 km/sec were computed by the following formula:

$$\frac{r_o \sin i_{pot}}{V_{po}} = \frac{r_c \sin i_{pc}}{V_{pl}}$$

where:

r_o = radius of the earth = 6366 km

r_c = radius of the core = 3446 km

i_{pc} = angle of incidence at the core (taken from Gutenberg and Richter 22, p.103/)

These values of i_{pot} are shown in graph 36.

The plots of P in graph 37 show the scatter that is expected from this method of obtaining the angles of incidence, but they are grouped fairly well around the zero line. However, the plots of PcP in graph 38 show a peculiar arrangement that shows little difference at about $= 65^o$ but an increasing difference with a decrease in epicentral distance. This deviation of the observed angles of incidence of PcP from their theoretical values is at present unexplained. The use of $V_{po} = 8.0$ km/sec instead of $V_{po} = 5.5$ km/sec makes little difference in a consideration of the observed values of i_o and their theoretical values.

The use of $V_{po} = 8.0$ km/sec in lieu of $V_{po} = 5.5$ km/sec does make a considerable difference, however, in the theoretical displacement ratios of PcP/P because of the $\sqrt{\frac{\tan i_o \, di_o}{\sin \Delta \, d\Delta}}$ term. u and w have been computed for various epicentral distances using this larger value of V_{po}, and the results are tabulated in table 20 and shown on graph 40. A study of the graph reveals that the theoretical displacement ratios are increaded by 1 1/2 to 2 times when $V_{po} = 8.0$ km/sec instead of $V_{po} = 5.5$ km/sec. This correction, while in the right direction for diminishing the difference between the observed and theoretical values, is far short in magnitude for explaining the full variation of the horizontal displacement ratios of PcP/P.

VI. CONCLUSIONS

A study of the ratios of the observed ground displacements produced by seismic waves reflected from the earth's core to those produced by direct body waves has led to results that strongly indicate that the horizontal displacement ratios of PcP/P are definitely larger than that which is expected from the presently accepted theory; the vertical displacement ratios of PcP/P and the horizontal displacement ratios of PcS/P are slightly greater, but not unreasonably so; and the horizontal displacement ratios of ScS/S and the vertical displacement ratios of ScS/S and ScP/S are reasonably in accordance with what is to be expected.

Two results of further investigation indicate that the causes for the discrepancies mentioned above seem to involve the PcP phase and not the P phase. Magnitudes of the earthquakes investigated, when computed from the ground displacements produced by PcP, are definitely greater than the sizes of the earthquakes warrant; whereas, the magnitudes determined from P are consistent with expectations. These were computed by Gutenberg's formula 19, p.66, form.(18)/ for determining magnitude from body waves. The empirical constant contained in this formula has been derived from a study of surface waves; and, as the ground displacements of both P and PP have given consistent results in many previous calculations, the constant is undoubtedly correct within close limits of error. The other inconsistency is the result of observations of the incident directions of the PcP waves at the earth's surface. The angles of incidence of the PcP waves are not in accordance with their theoretical values; whereas the P waves are reasonably conformable.

An investigation of the theoretical formula for the displacement due to seismic waves reveals that no single factor can be changed sufficiently to account for the observed horizontal displacement ratios of PcP/P. A

reasonable change in the physical constants for the earth's core produces only about 16 percent change in these displacement ratios. An assumption that the energy is, in general, propagated from the focus in an unequal manner, such that the PcP wave would receive more than the amount it would obtain with equal distribution, does not seem to be in accord with the observed displacement ratios. The assumption that the angle of incidence at the Mohorovičić discontinuity (the discontinuity at the bottom of the earth's crust) is to be used (since the thickness of the crustal layers is comparable with the wave length) would account for about 15 or 20 percent of the discrepancy of the horizontal displacement ratios of PcP/P and would improve the fit of the other phases. The angles of incidence of PcP computed from the observed data agree with the values computed from the ray theory neither on this assumption nor on the assumption that the seismic waves' angles of incidence are affected by the crustal layers; their peculiar behavior is, as yet, not definitely explained.

A number of assumptions have been made in deriving the instrumental constants and frequency response characteristics. The errors which are introduced in this way are considered to be small with respect to the variation of the ground displacement ratios from their theoretical values.

In general, the recognized, recorded wave train of PcP is shorter than that of P. This suggests two possible sources of error. The energy of PcP may be contained in a shorter time span than the energy of P; although, if such be true, the writer has no explanation for the mechanism causing the phenomenon. Its effect would tend to increase the ground displacement of P$_{\sim}$cP. However, since a continuous ground motion of simple harmonic form has been assumed in deriving the instrumental responses and a definite time of beginning of motion is the actual physical case, it is possible that a later oscillation in the P train has been measured than in the

case of the PcP wave. Theoretically, the result of such measurement would be to decrease the observed ground displacement ratio of PcP/P. However, neither of these effects explain the disagreement of the angles of incidence of PcP.

In the derivation of the formulae for the reflection coefficients at the core boundary, the assumption of plane waves is a simplification which may not be justified. If a more complex analysis of the problem would lead to the result that the reflected compressional wave contains a transverse component in addition to its longitudinal motion, this would serve to explain the apparent greater angle of incidence computed from the observed amplitudes of PcP. Additional theoretical investigation is required to solve the problem.

VII. SUGGESTIONS FOR ADDITIONAL STUDY

Several projects that might yield results that would clarify the situation concerning the return of seismic energy after reflection or refraction at the core boundary will be mentioned in this paragraph. A study of the PcP, ScS, PcS, and ScP phases from deep focus earthquakes would add considerable data. The use of deep focus earthquakes presents several advantages over the use of surface shocks, namely: (1) The interference or overriding by surface waves is non-existent, (2) PcS and ScP can be distinguished readily because they arrive at different times, and (3) at distances over 70 degrees, pP and sP would not interfere with the recognition of PcP, nor would sS interfere with ScS. New theoretical values similar to Dana's would have to be calculated. Another approach would be to study the phases which are transmitted through the core, such as P', P'P', SKS, PKS, PKKP, SKKS, etc. Dana has calculated the theoretical displacement values for these phases for surface shocks.

Appendix A

SYMBOLS USED IN THIS REPORT

Wave designation and transmission and reflection theory

A =Maximum amplitude

c =Reflection at the core boundary

E =Energy

e or i =Incident (subscript)

f =Square root of the product of the ratios of transmitted or reflected energy, as the case may be, to the incident energy at each discontimuity of density and/or wave velocity along the path of the ray

f =Refracted (subscript)

h =Depth of focus

i =Angle of incidence

i_{po} =Angle of incidence of longitudinal waves at the surface (calculated from observations)

i_{pot} =Angle of incidence of longitudinal waves at the surface (calculated from the ray theory and travel-time curves)

$\bar{i}$ ="Apparent" angle of incidence

i or e =Incident (subscript)

K =Wave through the earth's core

M =Magnitude

P =Direct longitudinal body wave

p =Longitudinal wave (subscript)

pP =The wave which travels from the earthquake focus as a longitudinal wave, reflects from the earth's surface near the epicenter, and thence travels as a longitudinal wave to the recording station.

PP =The longitudinal wave reflected once at the earth's surface about halfway between the focus and the recording station.

P' =The wave which travels through the mantle as a longitudinal wave, refracts into the earth's core, travels through the earth's core, refracts into the mantle, and travels as a longitudinal wave to the recording station.

P'P' =The wave which travels as a P', reflects at the surface of the earth,

and thence proceeds to the recording station as P'.

r =Reflected (subscript)

S =Direct transverse body wave

s =Transverse wave (subscript)

SV =Transverse wave, with vibration of particles in the vertical plane containing the ray path.

SH =Transverse wave, with vibration of particles in a horizontal direction.

SKS =The wave which travels through the mantle as a transverse wave, refracts into the earth's core, travels through the core, refracts into the mantle, and travels to the recording station as a transverse wave.

sP =The wave which travels from the focus as a transverse wave, reflects from the earth's surface near the epicenter, and thence travels to the recording station as a longitudinal wave.

T =Period

t =Time

Te =Period of the ground motion

u =Displacement, horizontal, in the plane of wave propagation; also maximum horizontal displacement; also u/Te

u_{NS} =Component of the horizontal displacement in the north-south direction

u_{EW} =Component of the horizontal displacement in the east-west direction

V =Wave velocity

$\overline{V}_{\Delta}$ ="Apparent" wave velocity

v =Displacement, horizontal, at right angles to the plane of wave propagation.

w =Displacement, vertical; also w/Te

x,y,z =Coordinate axes (z=vertical, x=horizontal in the plane of wave propagation)

o =Evaluated at the surface of the earth (subscript)

1 =Evaluated in the mantle adjacent to the core boundary (subscript)

2 =Evaluated in the core adjacent to the core boundary (subscript)

Δ =Epicentral distance in degrees of arc

Θ =Dilatation $= \frac{\partial u}{\partial x} + \frac{\partial v}{\partial y} + \frac{\partial w}{\partial z}$

λ, μ =Lames constants

ρ =Density

Φ =Instantaneous amplitude

$\omega_x, \omega_y, \omega_z$=One-half the components of the curl, with respect to the axes indicated by the subscripts.

Instruments

Ae =Maximum ground amplitude

A* =Maximum trace amplitude

a =Galitzin's dynamic magnification symbol for electro-magnetic instruments

B =Magnification constant

C =Maximum ground displacement

G $=V/V_o$ (strain seismograph)

g =Acceleration of gravity

h $= \varepsilon/\omega_o$ =damping constant

k =Galitzin's constant for electro-magnetic seismographs =B/2

M =Mass of pendulum or inertial reactor of seismometer

m_o =Mass of test weight

Q =Frequency response characteristic

R =A general symbol used to indicate $\frac{Ae/A^*}{Te}$ for the torsion seismographs, $\frac{k/a}{Te}$ for the electro-magnetic seismographs, and $\frac{1/G}{Te}$ for the strain seismograph

T =Period

Te =Period of ground motion

To =Free period of pendulum or inertial reactor of seismometer

Tg =Free period of galvanometer

t =Time

u =Te/To

u_p =Te/To

u_g =Te/Tg

U $=(1+u^2)\sqrt{1-\mu^2 f(u)}$; where $f(u)=[2u/(1+u^2)]^2$ (for Wood-Anderson seismographs

U =Step function response characteristic of electro-magnetic seismograph

V =Dynamic magnification

V_o =Static magnification

z =Trace amplitude of the seismogram at time t

Δ =Phase displacement of the galvanometer relative to the ground displacement.

ε =Damping constant of the differential equation of motion of the seismometer

ε_g =Damping constant of the differential equation of motion of the galvanometer

Λ $=\log_{10}\rho$

μ^2 $=(1-h^2)=1-(\epsilon/\omega_o)^2$ = damping constant

ξ =Displacement of the ground particles; ground displacement

ρ =Damping ratio

ω $=2\pi/Te$ = angular frequency of ground motion

ω_o $=2\pi/To$ = angular frequency of pendulum or inertial reactor of seismometer

ω_g $=2\pi/Tg$ = angular frequency of galvanometer

Appendix B

Theoretical response to the dropping of a test weight

$$M\frac{d^2x}{dt^2} + 2M\epsilon\frac{dx}{dt} + M\omega_o^2 x = -m_o g$$

$$\frac{d^2x}{dt} + 2\epsilon\frac{dx}{dt} + \omega_o^2 x = -m_o g/M$$

where: M = pendalum mass
m_o = mass of test weight
g = acceleration of gravity
ϵ = damping constant
ω_o = frequency of pendalum (nat.)

if: seismometer damping is critical:

$$\frac{d^2x}{dt^2} + 2\omega_o\frac{dx}{dt} + \omega_o^2 x = -m_o g/M = -\beta \qquad \text{where: } \beta \equiv m_o g/M$$

the steady state solution of this is:

$$x = e^{-\omega_o t}(C_1 + C_2 t) - \frac{\beta}{\omega_o^2} \quad ; \quad \frac{dx}{dt} = -\omega_o e^{-\omega_o t}(C_1 + C_2 t) + e^{-\omega_o t} C_2$$

when: $t = 0$; $\frac{dx}{dt} = 0$; $x = 0$

$$C_1 = \frac{\beta}{\omega_o^2} \quad ; \quad C_2 = \frac{\beta}{\omega_o^2}$$

and:

$$\frac{dx}{dt} = -\omega_o e^{-\omega_o t}\left[\frac{\beta}{\omega_o^2} + \frac{\beta t}{\omega_o}\right] + e^{-\omega_o t}\left[\frac{\beta}{\omega_o}\right] = -\beta t e^{-\omega_o t}$$

Since: the output of the seismometer transducer,

$$E = \frac{\eta\phi_o}{2x_o}\frac{dx}{dt}\ \text{e.m.u.} = \frac{-\eta\phi_o}{2x_o}\beta t e^{-\omega_o t}$$

where: ϕ_o = flux
η = no. of turns of coil
x_o = static air gap length

We can apply this electro-motive force to the terminals of the galvanometer and the equation of motion of the galvanometer becomes:

$$\frac{d^2\theta}{dt^2} + 2\epsilon_g\frac{d\theta}{dt} + \omega_g^2\theta = \frac{DE}{rm}$$

where: θ = angular deflection of galvanometer
ϵ_g = damping constant " "
D = electro-dynamic " " "
r = sum of galvanometer resistances
m = moment of inertia of galvanometer suspension.

Introducing the value of E:

$$\frac{d^2\theta}{dt^2} + 2\epsilon_g\frac{d\theta}{dt} + \omega_g^2\theta = \frac{-\eta\phi_o D}{2x_o rm}\beta t e^{-\omega_o t} = F\beta t e^{-\omega_o t}$$

where F is defined by $F \equiv -\frac{\eta\phi_o D}{2x_o rm}$

The steady state solution of this is (when the seismometer damping is critical, i.e. $\epsilon_g = \omega_g$):

$$\theta = e^{-\omega_g t}\left[C_3 + C_4 t + F\beta\left\{t\int e^{\omega_g t} t e^{-\omega_o t}\,dt - \int t^2 e^{\omega_g t} e^{-\omega_o t}\,dt\right\}\right]$$

Integrating where shown and reducing:

$$\theta = e^{-\omega_g t}\left[C_3 + C_4 t + F\beta e^{(\omega_g-\omega_o)t}\left\{\frac{t}{(\omega_g-\omega_o)^2} - \frac{2}{(\omega_g-\omega_o)^3}\right\}\right]$$

$$\frac{d\theta}{dt} = -\omega_g e^{-\omega_g t}\left[C_3 + C_4 t + F\beta e^{(\omega_g-\omega_o)t}\left(\frac{t}{(\omega_g-\omega_o)^2} - \frac{2}{(\omega_g-\omega_o)^3}\right)\right]$$
$$+ e^{-\omega_g t}\left[C_4 + F\beta(\omega_g-\omega_o)e^{(\omega_g-\omega_o)t}\left(\frac{t}{(\omega_g-\omega_o)^2} - \frac{2}{(\omega_g-\omega_o)^3}\right) + F\beta\left(\frac{e^{(\omega_g-\omega_o)t}}{(\omega_g-\omega_o)^2}\right)\right]$$

when $t=0$; $\theta=0$; $\frac{d\theta}{dt}=0$

$$C_3 = \frac{2F\beta}{(\omega_g-\omega_o)^3}$$

$$C_4 = \frac{F\beta}{(\omega_g-\omega_o)^2}$$

Inserting constants and simplifying:

$$\theta = F\beta\left[\frac{\{2+(\omega_o-\omega_g)t\}e^{-\omega_o t} - \{2-(\omega_o-\omega_g)t\}e^{-\omega_g t}\}}{(\omega_o-\omega_g)^3}\right]$$

Letting the quantity in brackets be U:

$$\theta = F\beta U$$

$$z_w = 2LF\beta U$$

where: z_w = trace amplitude, on recording drum at time t, under influence of dropping test weight at time = $t_o = 0$

L = distance from galvanometer lens to recording drum.

Letting:

$$B \equiv -2LF$$

$$z_w = -B\beta U$$

$$B = \frac{z_w}{\beta U}$$

where: B = constant of amplification

$\beta = mg/M$

$$U = \frac{\{2+(\omega_o-\omega_g)t\}e^{-\omega_o t} - \{2-(\omega_o-\omega_g)t\}e^{-\omega_g t}}{(\omega_o-\omega_g)^3}$$

Appendix C

Graphs

Graph 1 --- Magnification Curve, Mechanical Seismograph
Instrument I

T_0=0.80; ρ=11.1; h=0.608; μ=0.63

Ae = amplitude of ground motion (microns)
A* = trace amplitude (mm)
V = dynamic magnification
V_0 = static magnification
Te = period of ground motion (sec)

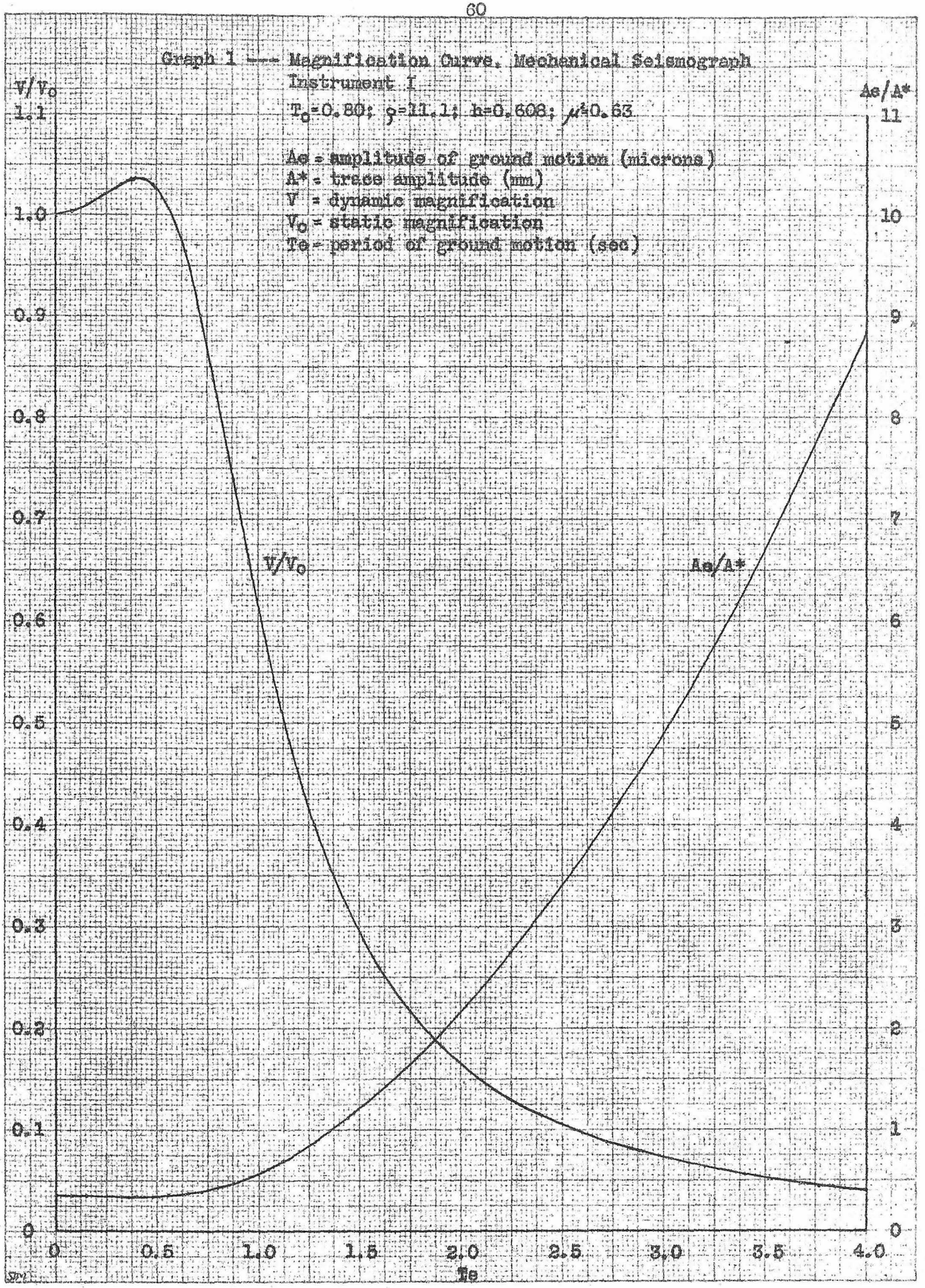

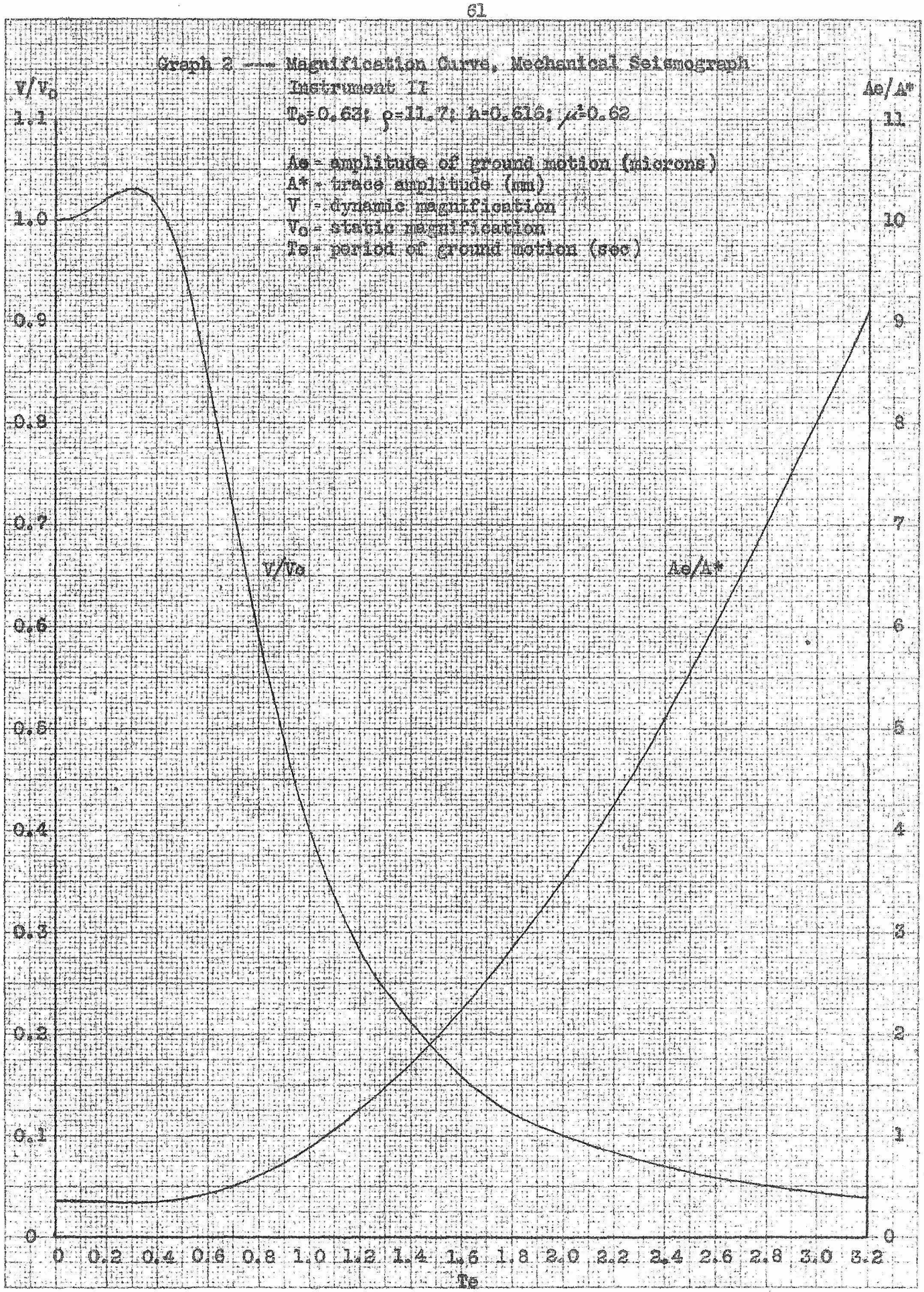
Graph 2 --- Magnification Curve, Mechanical Seismograph
Instrument II
T_0=0.63; ρ=11.7; h=0.616; μ^2=0.62
Ae = amplitude of ground motion (microns)
A* = trace amplitude (mm)
V = dynamic magnification
V_0 = static magnification
Te = period of ground motion (sec)
V/V_0
Ae/A*
V/Vo
Ae/A*
1.1
1.0
0.9
0.8
0.7
0.6
0.5
0.4
0.3
0.2
0.1
0
11
10
9
8
7
6
5
4
3
2
1
0
0 0.2 0.4 0.6 0.8 1.0 1.2 1.4 1.6 1.8 2.0 2.2 2.4 2.6 2.8 3.0 3.2
Te

Graph 3 --- Magnification Curve, Mechanical Seismograph
Theoretical adjustment; short-period Wood-Anderson
T_o=0.80; h=0.85; μ=0.28

Ae = amplitude of ground motion (microns)
A* = trace amplitude (mm)
V = dynamic magnification
V_o = static magnification
To = period of ground motion (sec)

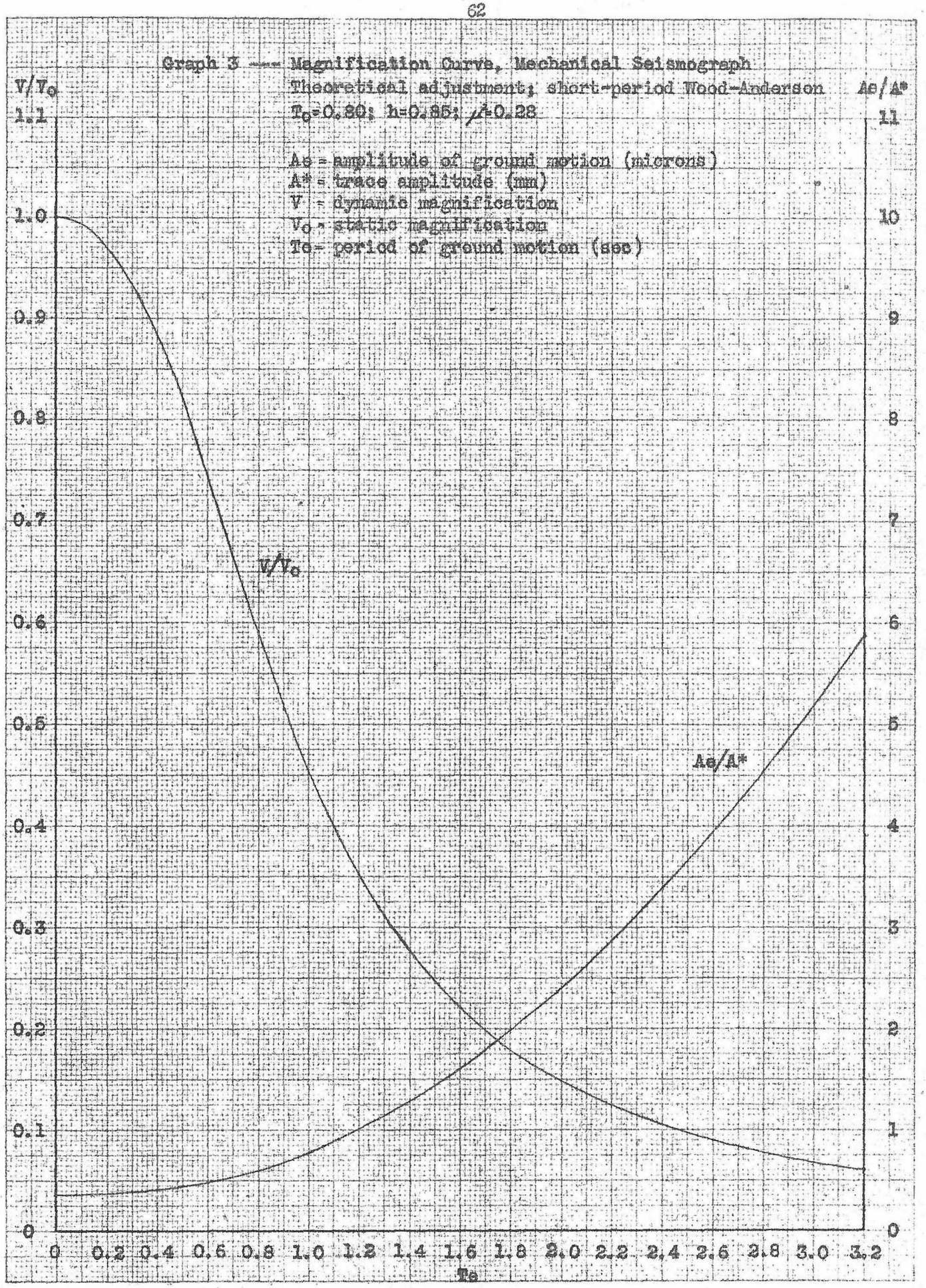

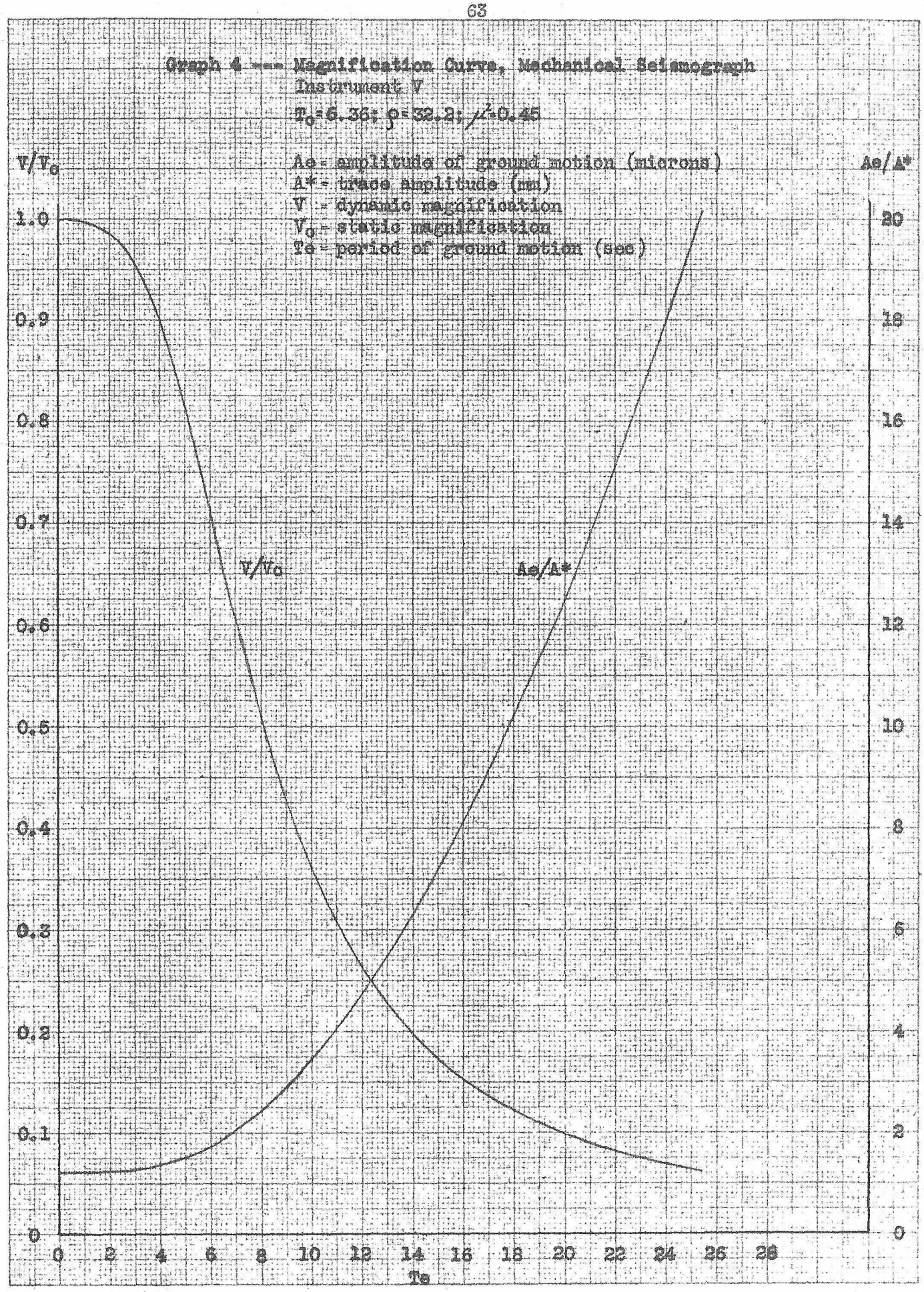
Graph 4 --- Magnification Curve, Mechanical Seismograph
Instrument: V
T_0=6.36; ρ=32.2; μ^2=0.45
Ae = amplitude of ground motion (microns)
A* = trace amplitude (mm)
V = dynamic magnification
V_0 = static magnification
Te = period of ground motion (sec)
V/V0
Ae/A*
V/V0
Ae/A*
1.0
0.9
0.8
0.7
0.6
0.5
0.4
0.3
0.2
0.1
0
20
18
16
14
12
10
8
6
4
2
0
0 2 4 6 8 10 12 14 16 18 20 22 24 26 28
Te

Graph 5 --- Magnification Curve, Mechanical Seismograph
Instrument VA
$T_0 = 5.65$; $\rho = 30.1$; $\mu = 0.46$

Ae = amplitude of ground motion (microns)
A* = trace amplitude (mm)
V = dynamic magnification
V_0 = static magnification
Te = period of ground motion (sec)

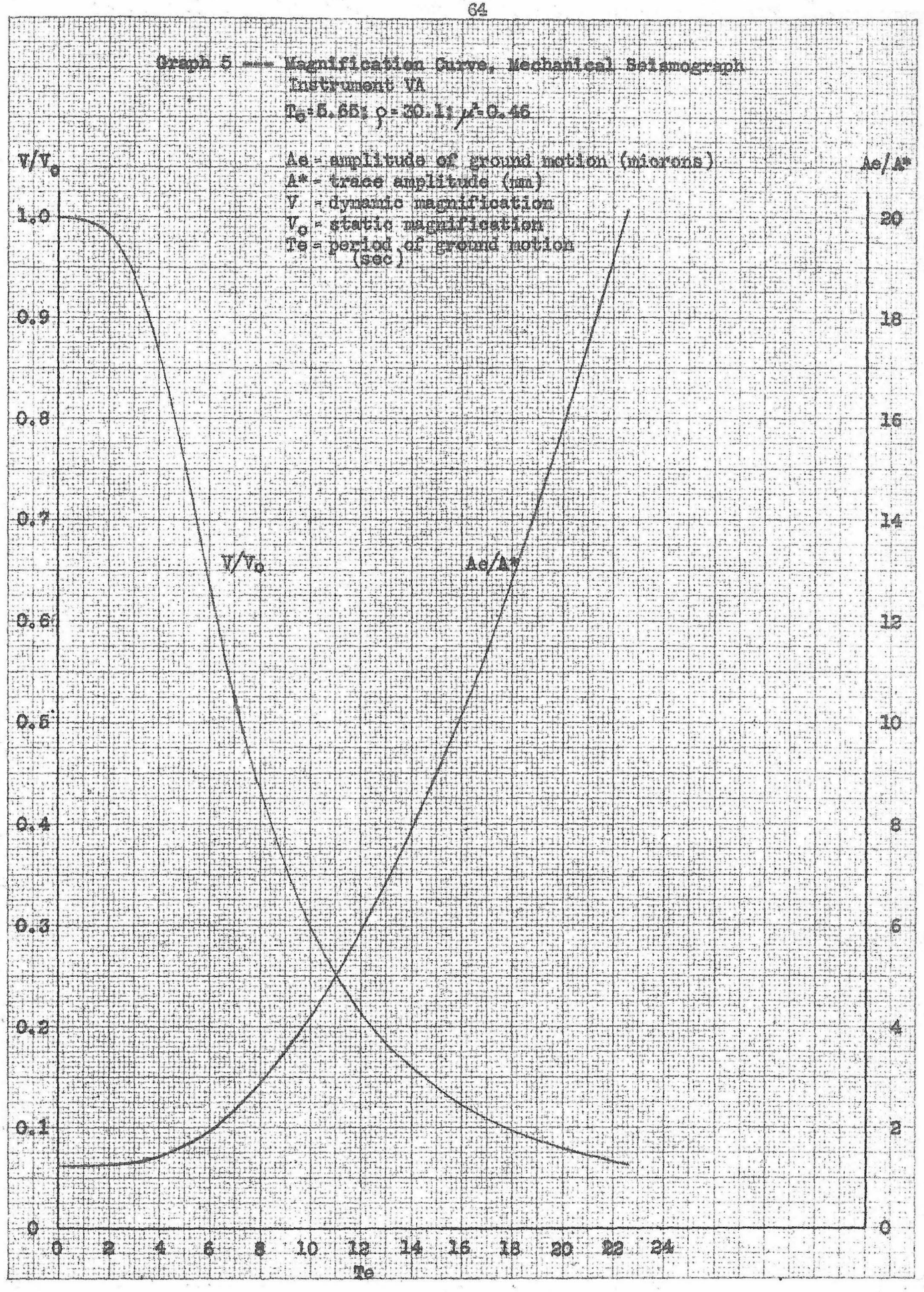

Graph 6 --- Magnification Curve, Mechanical Seismograph
Theoretical adjustment; long-period Wood-Anderson
T_0=6.0; h=0.85; μ^2=0.28

Ae = amplitude of ground motion (microns)
A* = trace amplitude (mm)
V = dynamic magnification
V_0 = static magnification
Te = period of ground motion (sec)

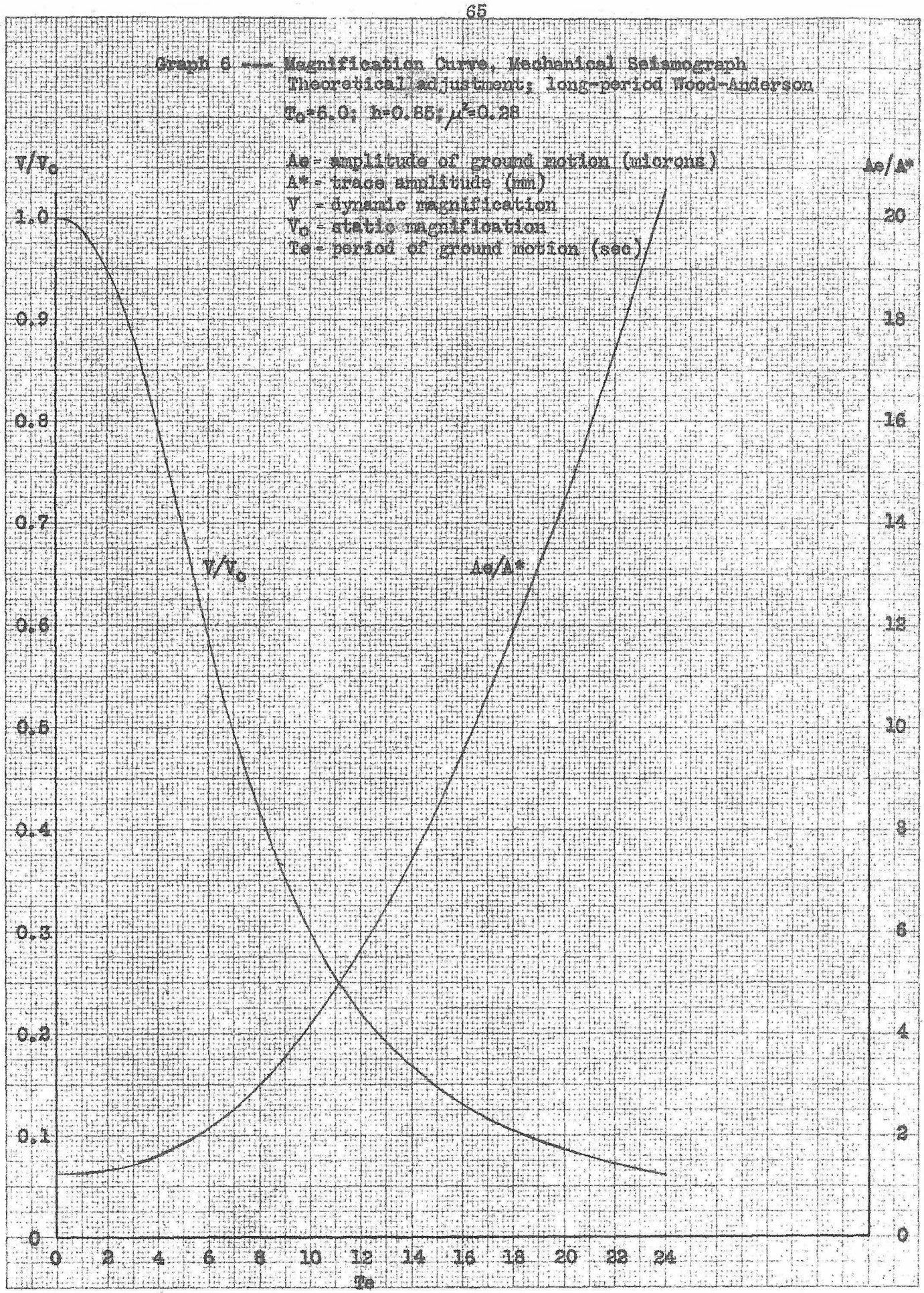

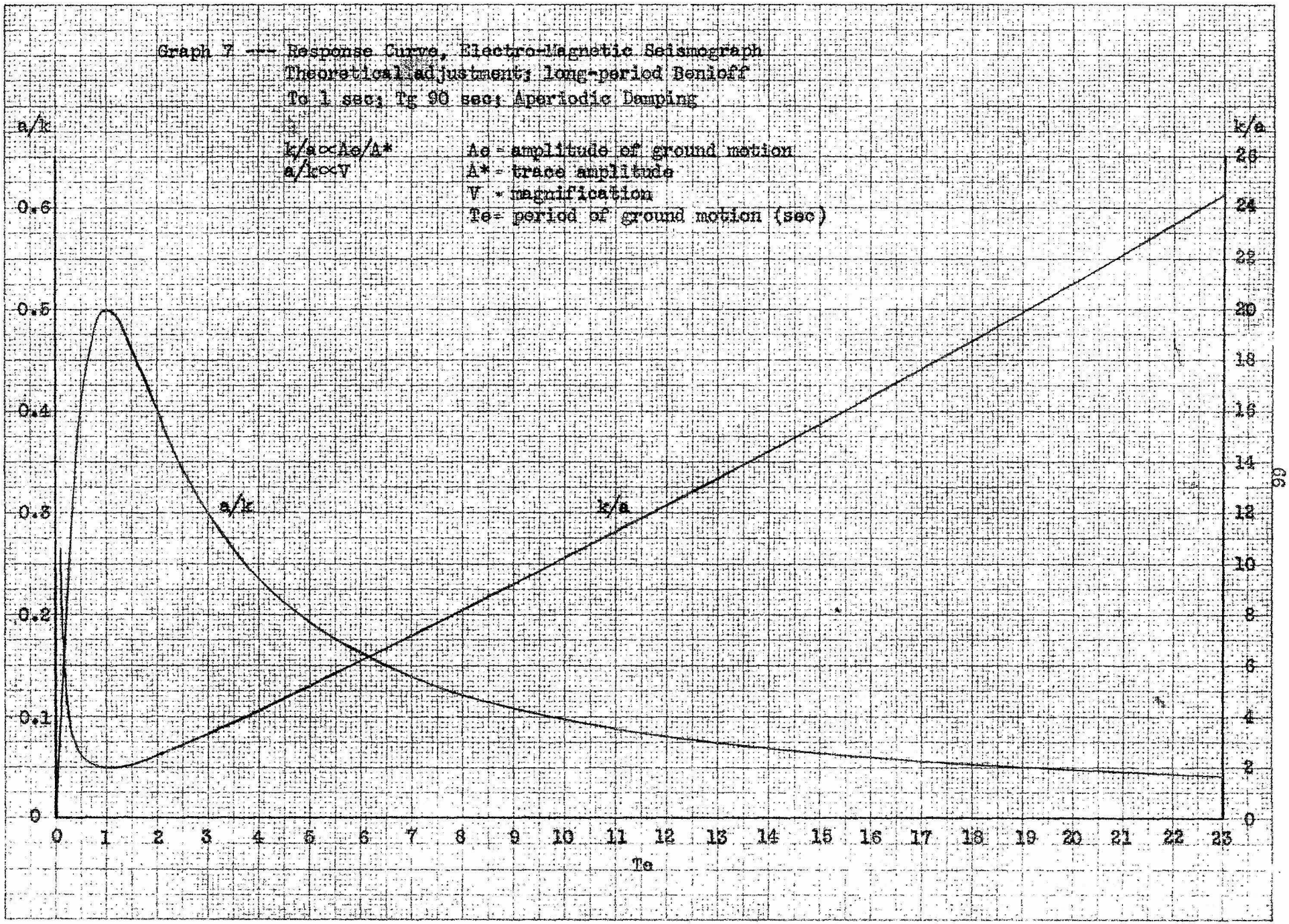
Graph 7 --- Response Curve, Electro-Magnetic Seismograph
Theoretical adjustment; long-period Benioff
To 1 sec; Tg 90 sec; Aperiodic Damping
a/k
k/a
k/a<Ae/A*
a/k<V
Ae = amplitude of ground motion
A* = trace amplitude
V = magnification
Te= period of ground motion (sec)
0.6
0.5
0.4
0.3
0.2
0.1
0
a/k
k/a
0 1 2 3 4 5 6 7 8 9 10 11 12 13 14 15 16 17 18 19 20 21 22 23
Te
26
24
22
20
18
16
14
12
10
8
6
4
2
0

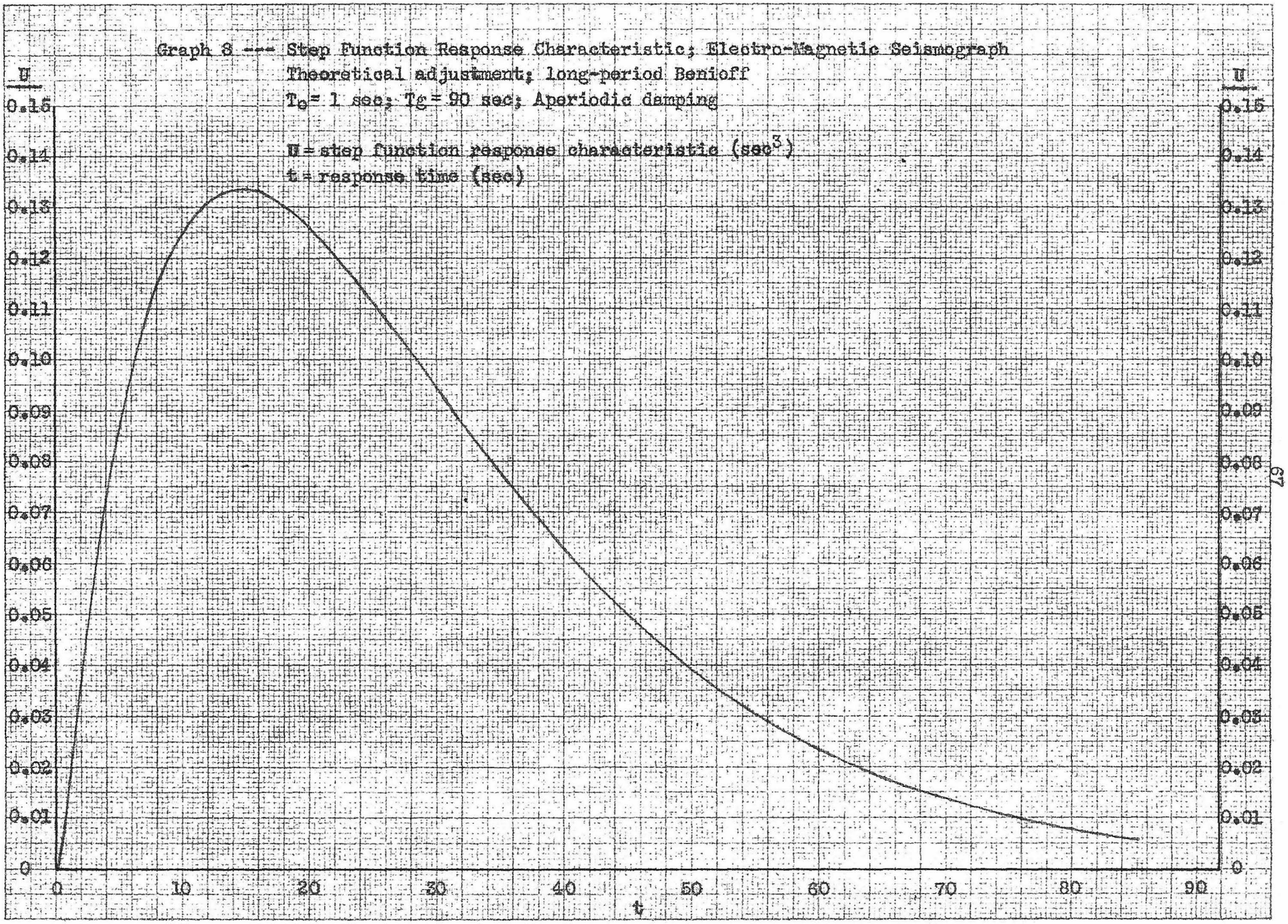
Graph 8 --- Step Function Response Characteristic; Electro-Magnetic Seismograph
Theoretical adjustment; long-period Benioff
T_0 = 1 sec; Tg = 90 sec; Aperiodic damping
U = step function response characteristic (sec^3)
t = response time (sec)
U
0.15
0.14
0.13
0.12
0.11
0.10
0.09
0.08
0.07
0.06
0.05
0.04
0.03
0.02
0.01
0
0
10
20
30
40
50
60
70
80
90
t

Graph 9 --- Magnification Curve; Electro-Magnetic Seismograph
Instrument IVA
T_o = 1 sec; T_g = 90 sec; Critically damped

Ao = amplitude of ground motion (microns)
A* = trace amplitude (mm)
V = magnification
Te = period of ground motion (sec)

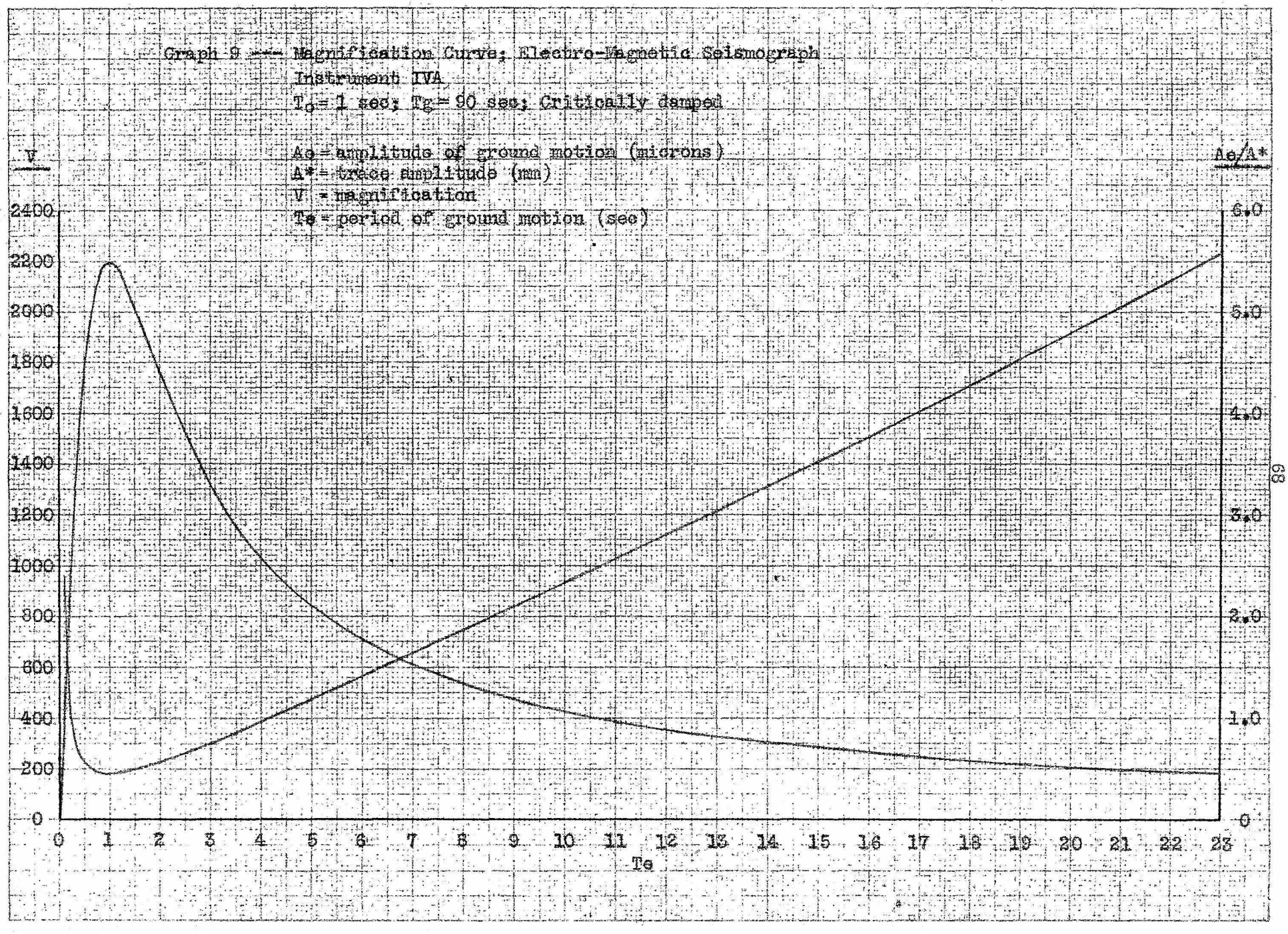

Graph 10 ---- Response Curve; Electro-Magnetic Seismograph
Theoretical adjustment; Instrument VIA
To = 1 sec; Tg=0.25 sec; Aperiodic damping

$k/a \propto Ae/A^*$
$a/k \propto V$

Ae = amplitude of ground motion
A* = trace amplitude
V = magnification
Te = period of ground motion (sec)

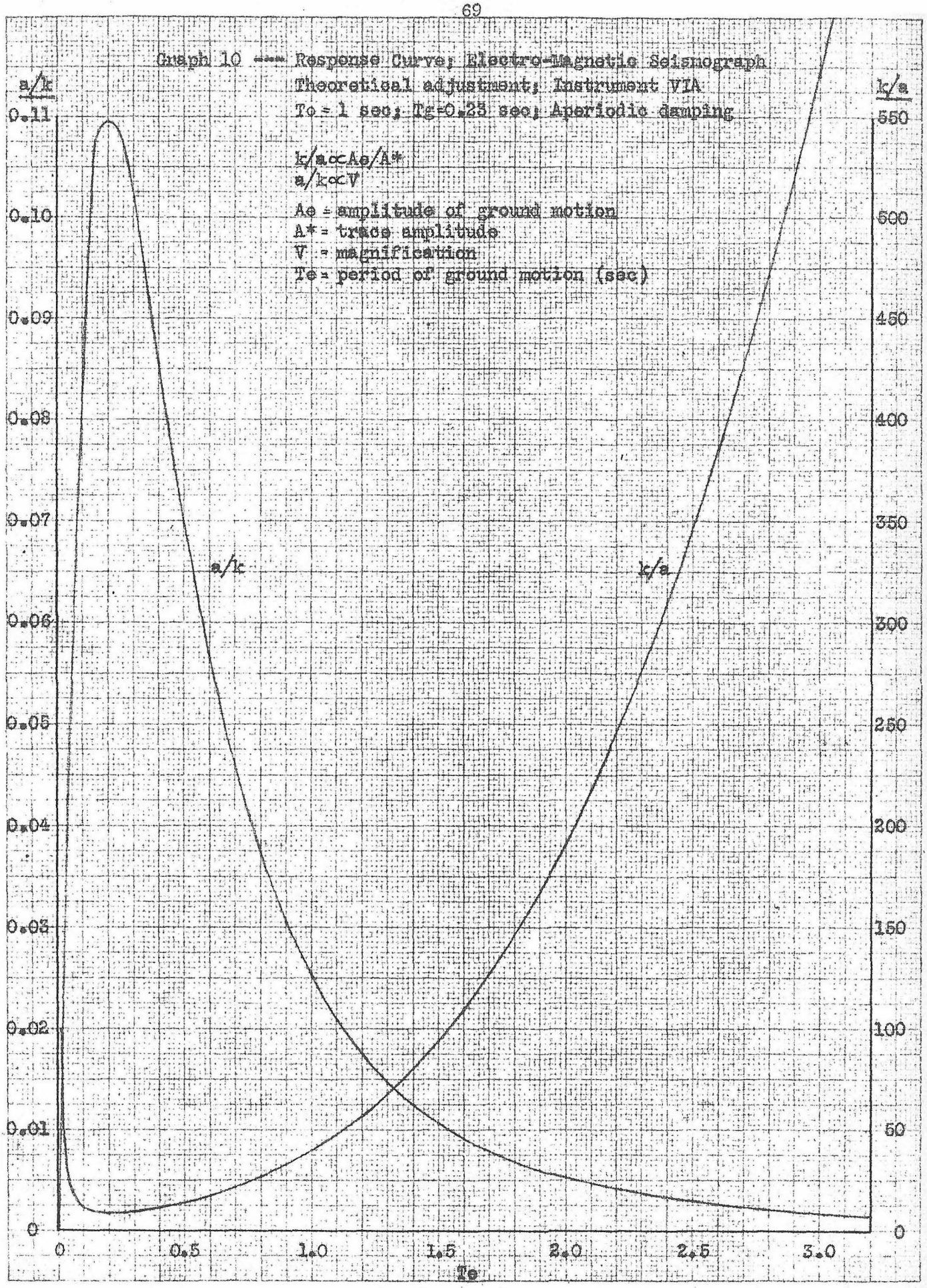

Graph 11 --- Response Curve; Electro-Magnetic Seismograph
Theoretical adjustment; Instrument VIB
To = 1 sec; Tg = 0.2 sec; Aperiodic damping

$k/a \propto Ae/A^*$
$a/k \propto V$

Ae = amplitude of ground motion
A* = trace amplitude
V = magnification
Te = period of ground motion (sec)

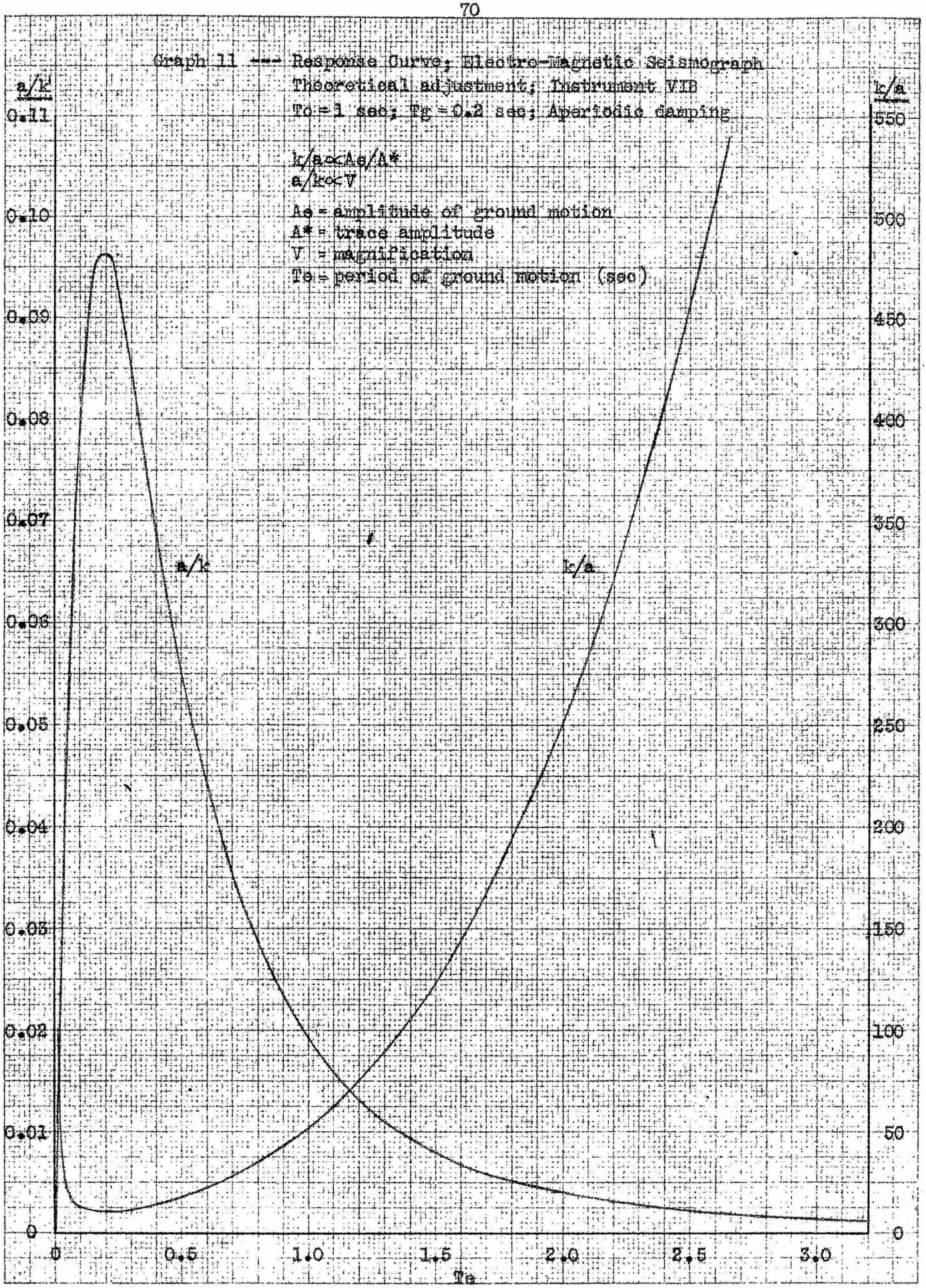

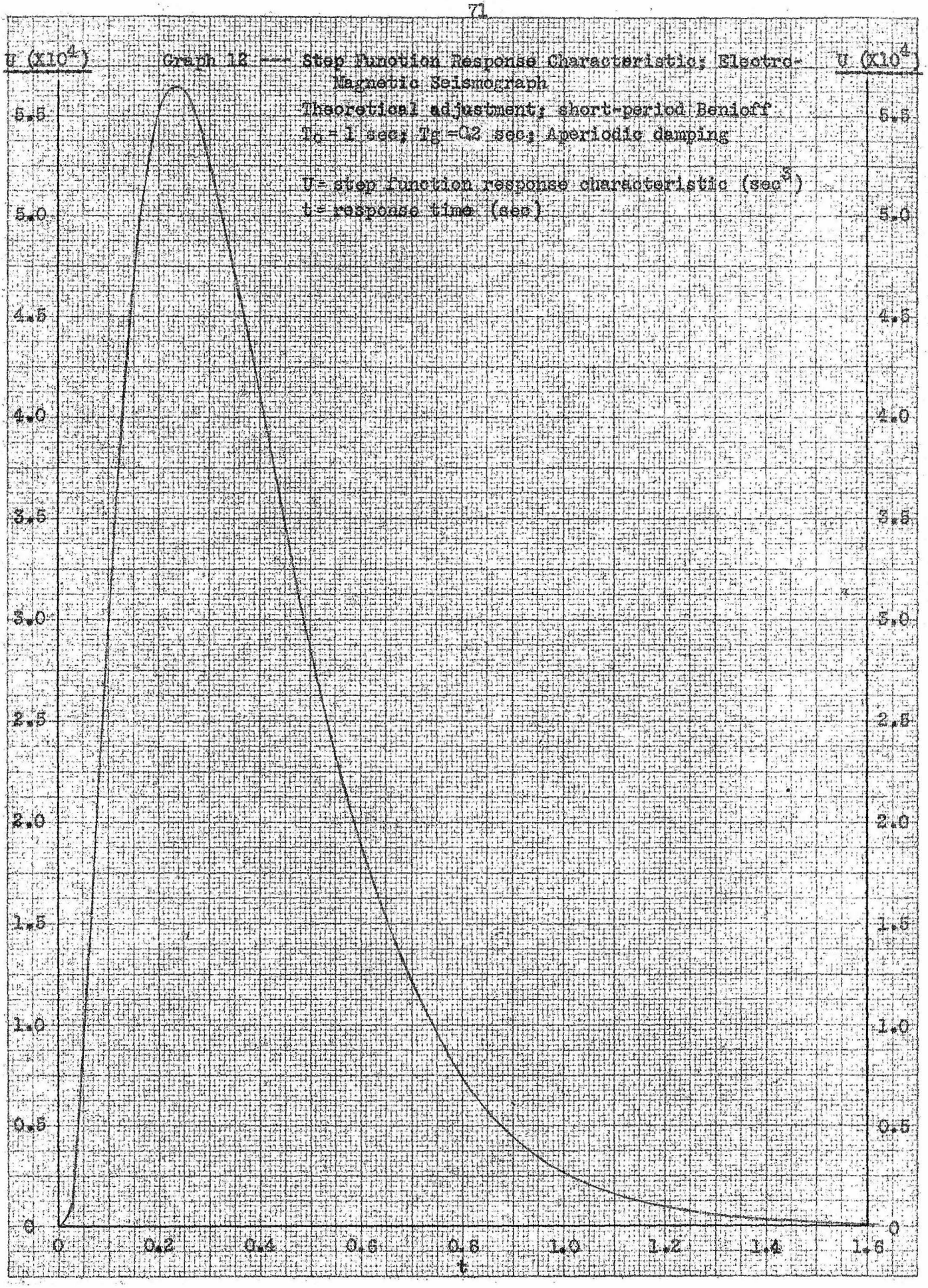
U (X10⁴)
Graph 12 --- Step Function Response Characteristic; Electro-Magnetic Seismograph
Theoretical adjustment; short-period Benioff
T₀ = 1 sec; Tg = 0.2 sec; Aperiodic damping
U= step function response characteristic (sec⁻³)
t= response time (sec)
U (X10⁴)
5.5
5.0
4.5
4.0
3.5
3.0
2.5
2.0
1.5
1.0
0.5
0
0
0.2
0.4
0.6
0.8
1.0
1.2
1.4
1.6
t

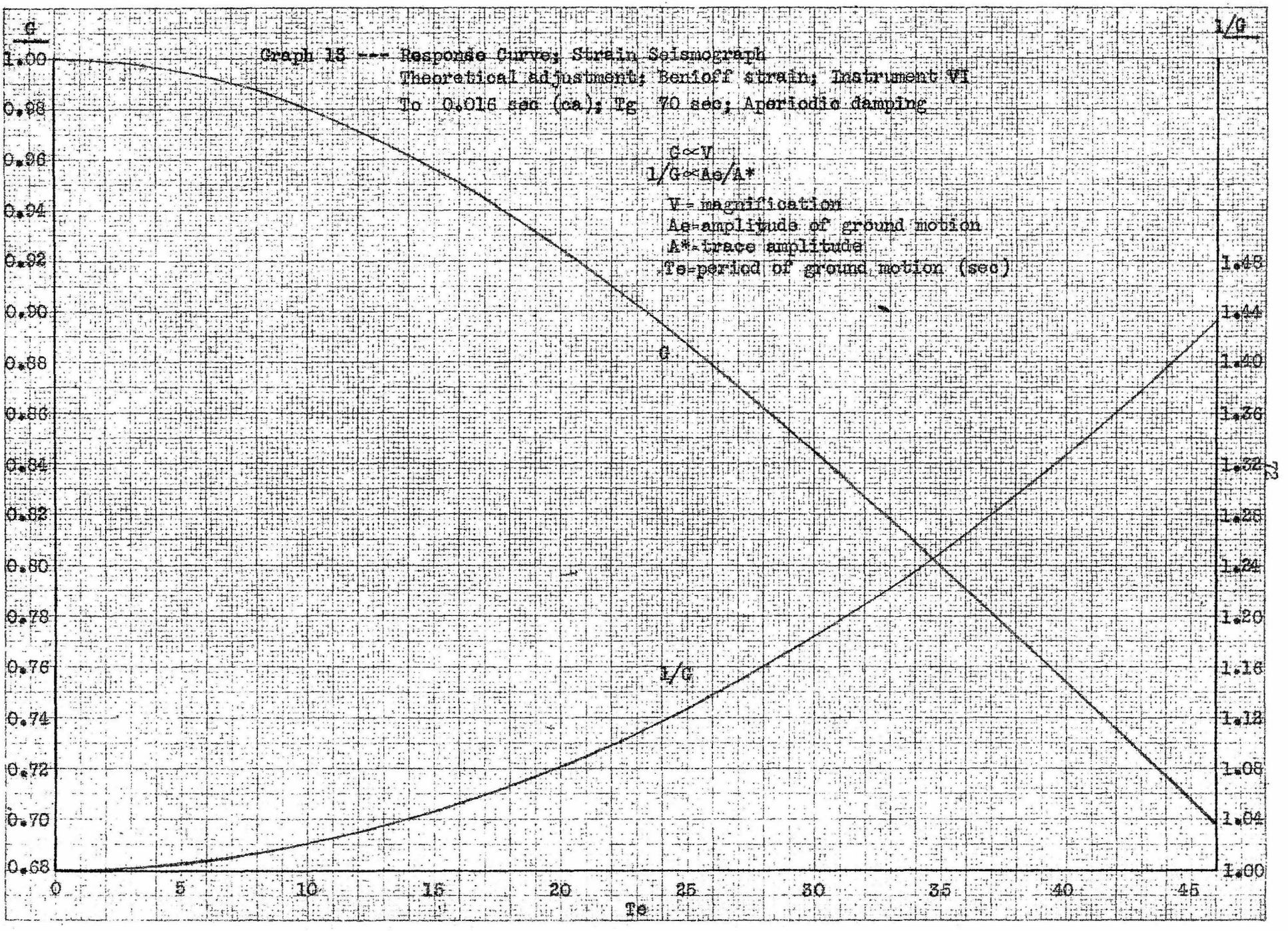
G
1/G
Graph 15 --- Response Curve; Strain Seismograph
Theoretical adjustment; Benioff strain; Instrument VI
To 0.0116 sec (ca); Tg 70 sec; Aperiodic damping
G∝V
1/G∝As/A*
V - magnification
As-amplitude of ground motion
A*-trace amplitude
Ts-period of ground motion (sec)
G
1/G
1.00
0.98
0.96
0.94
0.92
0.90
0.88
0.86
0.84
0.82
0.80
0.78
0.76
0.74
0.72
0.70
0.68
1.48
1.44
1.40
1.36
1.32
1.28
1.24
1.20
1.16
1.12
1.08
1.04
1.00
0
5
10
15
20
25
30
35
40
45
Ts

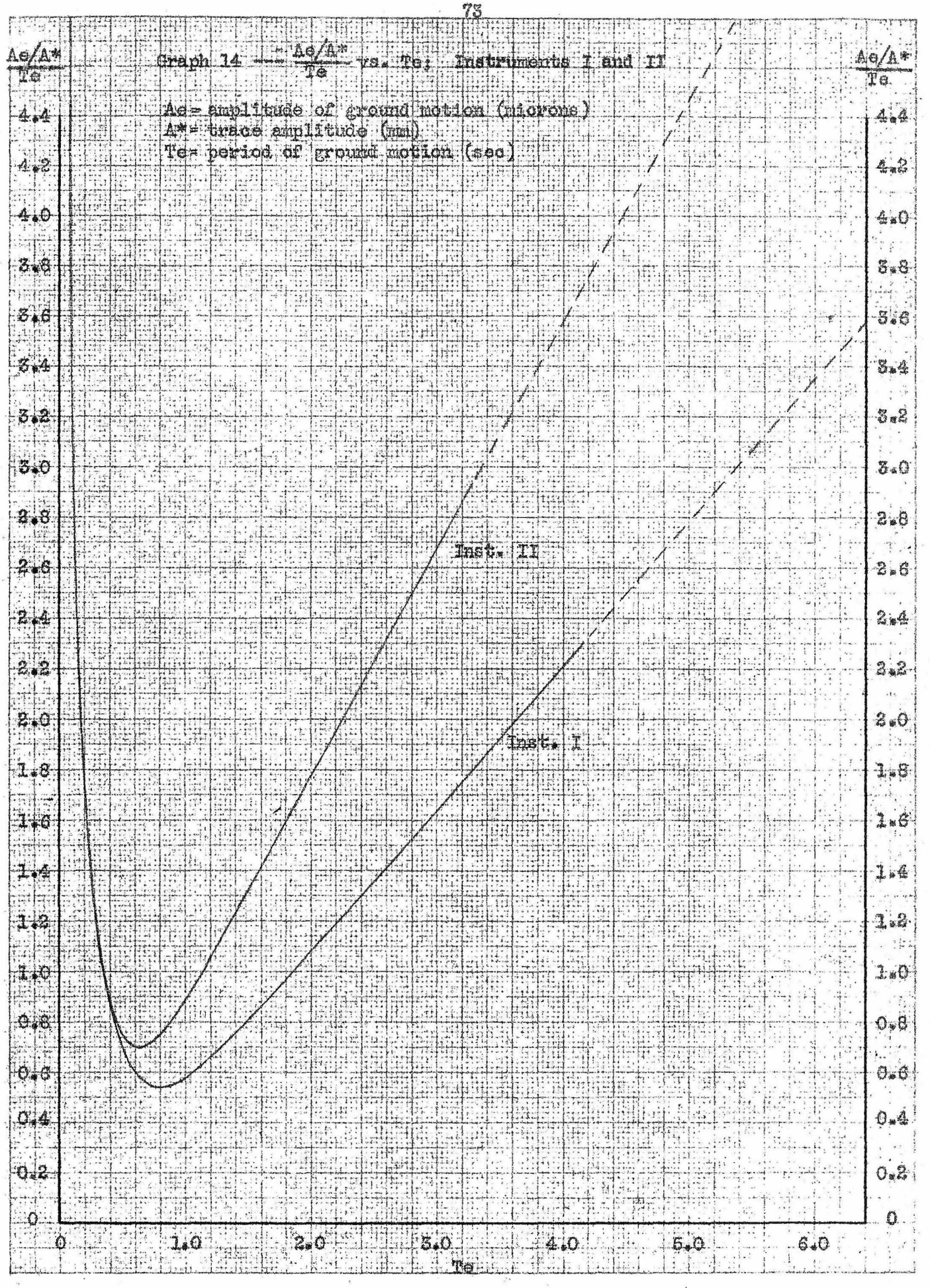
Graph 14 — $\frac{Ae/A^*}{Te}$ vs. Te; Instruments I and II
Ae = amplitude of ground motion (microns)
A* = trace amplitude (mm)
Te = period of ground motion (sec)
Inst. II
Inst. I
Te
0
1.0
2.0
3.0
4.0
5.0
6.0
0.2
0.4
0.6
0.8
1.2
1.4
1.6
1.8
2.2
2.4
2.6
2.8
3.2
3.4
3.6
3.8
4.2
4.4

Graph 15 --- $\frac{Ae/A^*}{Te}$ vs. Te; Instruments V and VA

Ae = amplitude of ground motion (microns)
A* = trace amplitude (mm)
Te = period of ground motion (sec.)

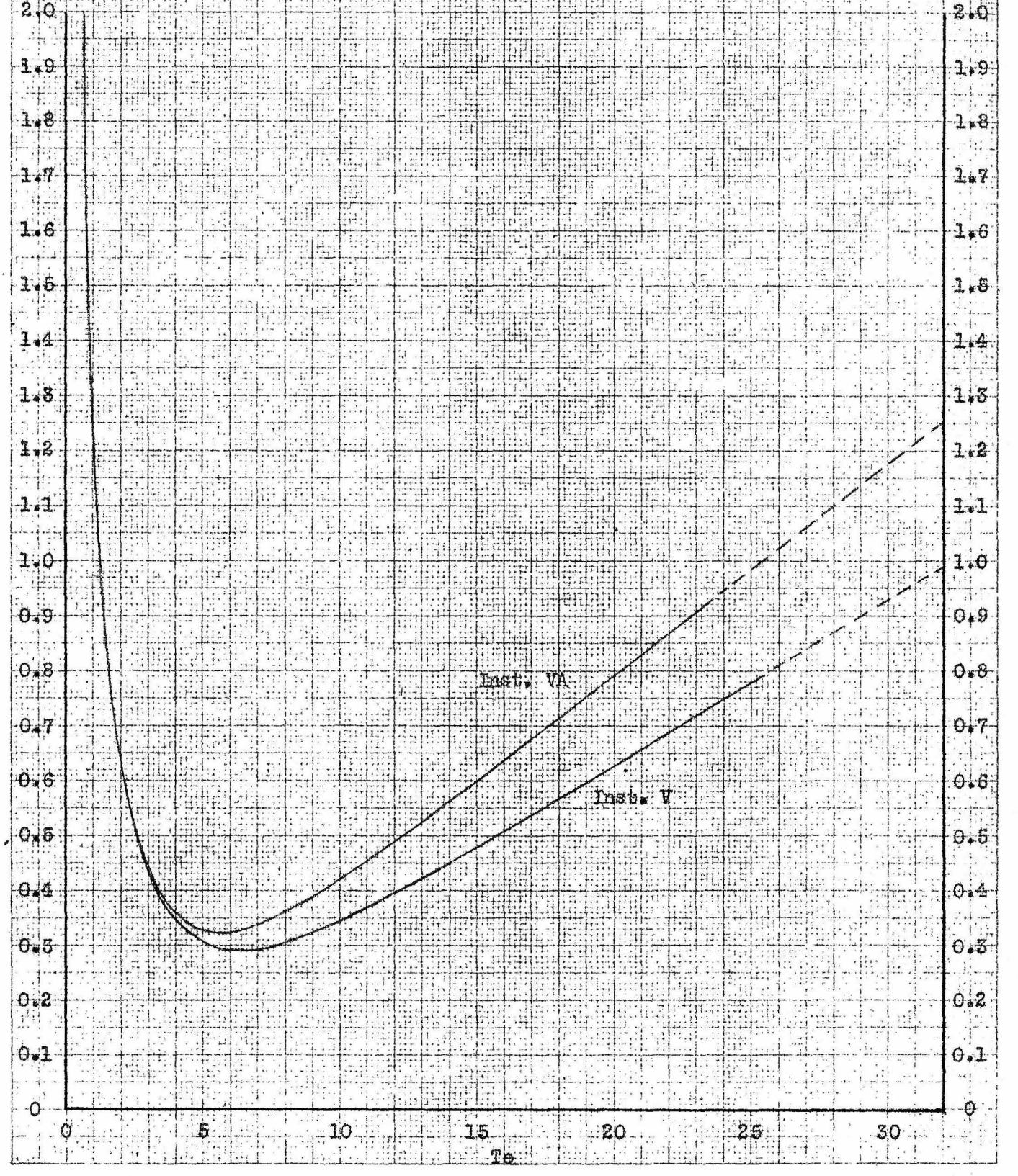

Graph 16 --- $\frac{k/a}{Te}$ vs. Te; Instruments IIA, IVA, and IVB

$k/a \propto Ae/A^*$

Ae = amplitude of ground motion
A* = trace amplitude
Te = period of ground motion (sec.)

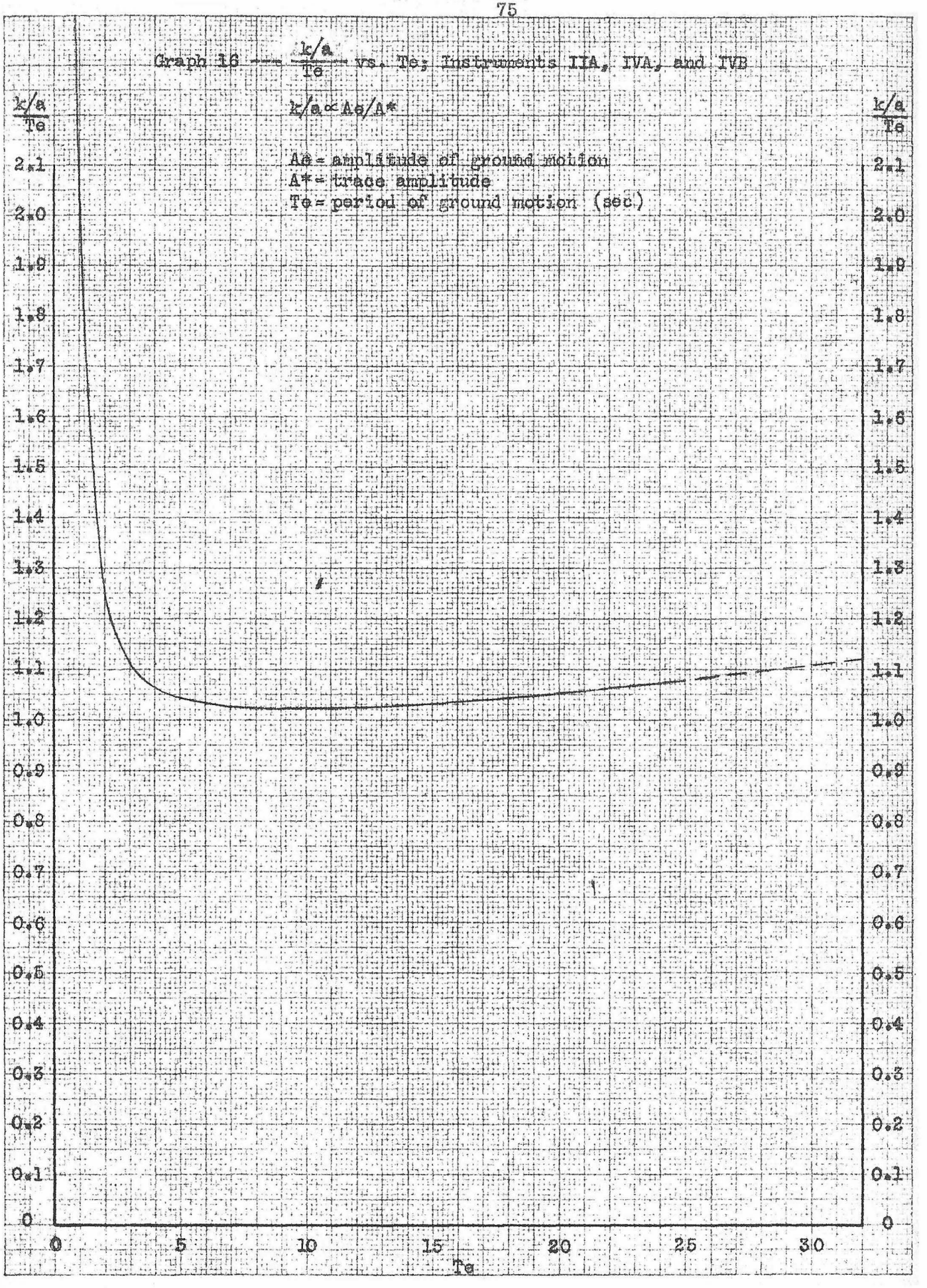

Graph 17 --- $\frac{Ae/A^*}{Te}$ vs. Te; Instrument IVA

Ae = amplitude of ground motion (microns)
A* = trace amplitude (mm)
Te = period of ground motion (sec)

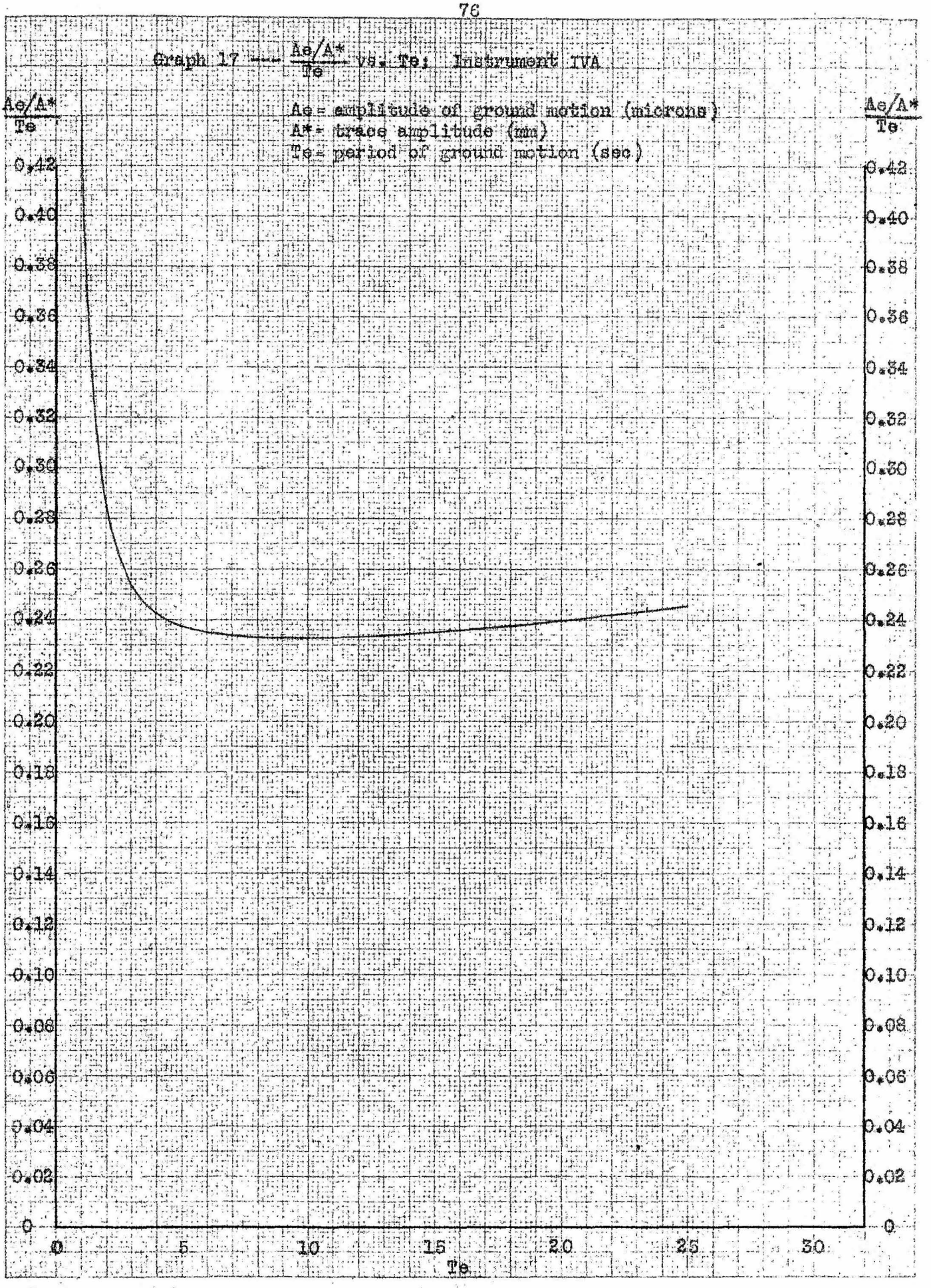

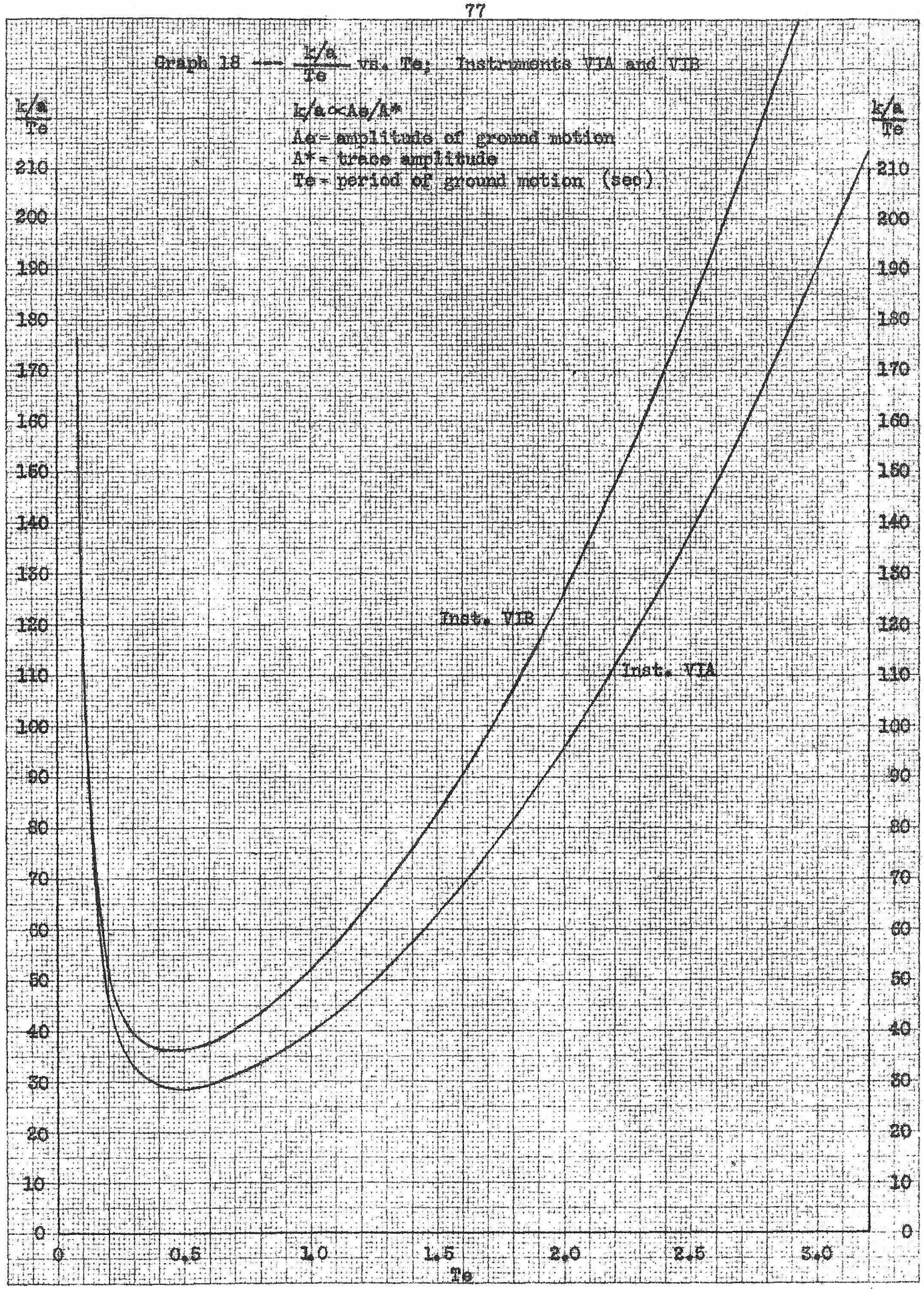
Graph 18 --- k/a / Te vs. Te; Instruments VIA and VIB
k/a < Ae/A*
Ae = amplitude of ground motion
A* = trace amplitude
Te = period of ground motion (sec)
k/a / Te
Inst. VIB
Inst. VIA
Te
0
0.5
1.0
1.5
2.0
2.5
3.0
10
20
30
40
50
60
70
80
90
100
110
120
130
140
150
160
170
180
190
200
210

Graph 19 ---- $\frac{1}{G \cdot Te}$ vs. Te; Instrument VI

$1/G \propto Ae/A^*$

Ae = amplitude of ground motion
A* = trace amplitude
Te = period of ground motion (sec)

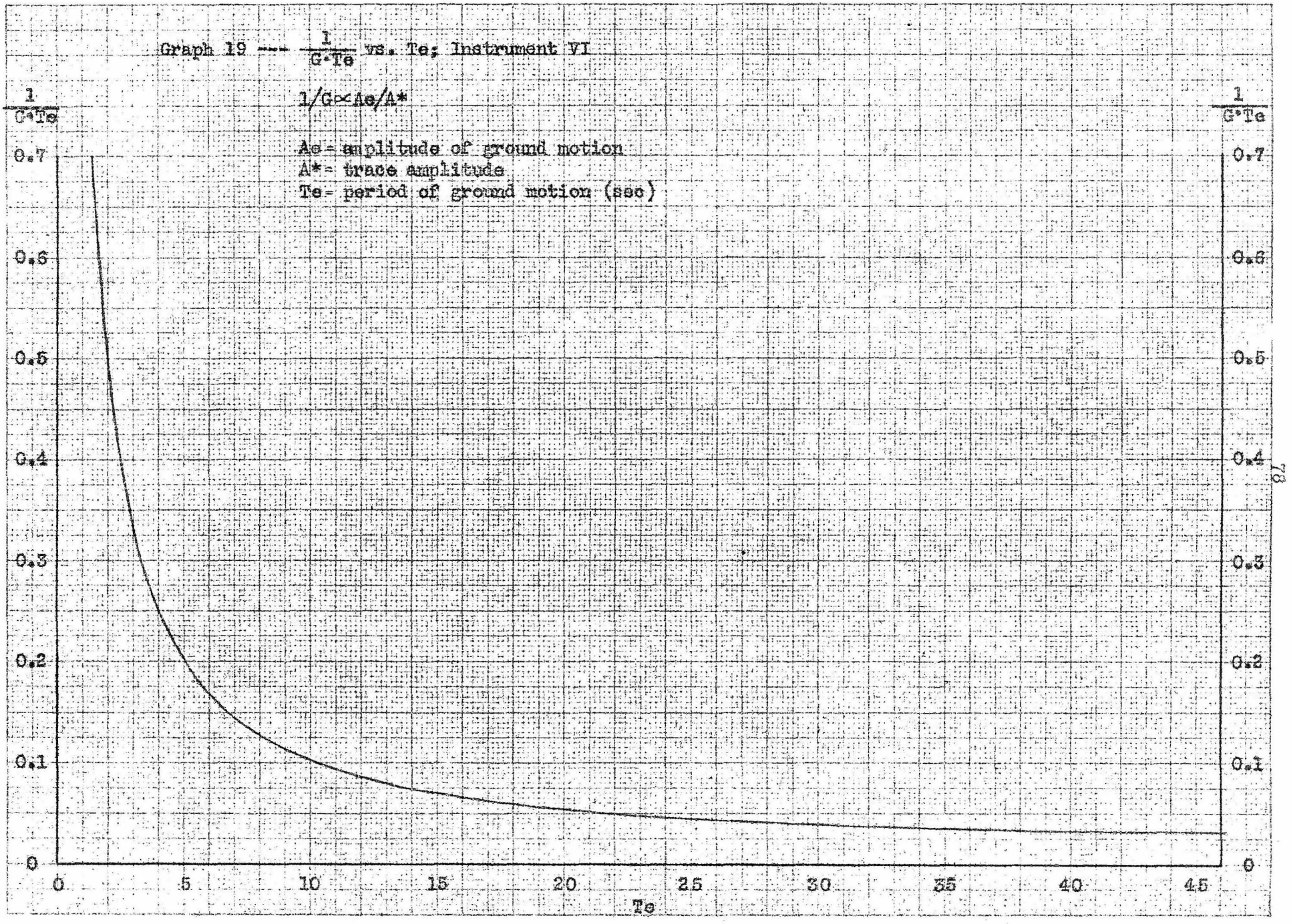

$\frac{U_{EW\,P\&P}}{U_{EW\,P}}$ & $\frac{U_{NS\,P\&P}}{U_{NS\,P}}$

N-S	E-W	Inst.
▽	□	I, II
○	◎	IVA, B
■	●	V, VA
×	+	VIB

Theoretical Ratio

10 9 8 7 6 5 4 3 2 1 .9 .8 .7 .6 .5 .4 .3 .2 .1 .09 .08 .07 .06 .05 .04 .03 .02 .01

3 10 20 30 40 50 60 70 80 90 100 110

△

Graph 21

$\frac{W_{P_0P}}{W_P}$

Inst.
○ II A
× VI A

Theoretical Ratio

10 9 8 7 6 5 4 3 2 1 .9 .8 .7 .6 .5 .4 .3 .2 .1 .09 .08 .07 .06 .05 .04 .03 .02 .01

0 10 20 30 40 50 60 70 80 90 100 110

△

Graph 22

$\frac{U_{EW\,ScS}}{U_{EW\,S}}$ & $\frac{U_{NS\,ScS}}{U_{NS\,S}}$

N-S	E-W	Inst.
▽	□	I, II
○	◎	IVA, B
■	●	V, VA
×	+	VIB

Theoretical Ratio $ScS_{(SV)}/SV$
$ScS_{(SH)}/SH$

10 9 8 7 6 5 4 3 2 1 .9 .8 .7 .6 .5 .4 .3 .2 .1 .09 .08 .07 .06 .05 .04 .03 .02 .01

0 10 20 30 40 50 60 70 80 90 100 110

△

Graph 23

$\frac{W's.s}{W's}$

Inst.
○ II A
× VI A

Theoretical Ratio

10
9
8
7
6
5
4
3
2
1
,9
,8
,7
,6
,5
,4
,3
,2
,1
,09
,08
,07
,06
,05
,04
,03
,02
,01

0 10 20 30 40 50 60 70 80 90 100 110

△

Graph 24

$\frac{U_{EW}P_cS}{U_{EW}P}$ & $\frac{U_{NS}P_cS}{U_{NS}P}$

$\frac{U_{EW}S_cP}{U_{EW}S}$ & $\frac{U_{NS}S_cP}{U_{NS}S}$

N-S	E-W	Inst.
▽	□	I, II
⊙	◉	IVA, B
■	●	V, VA
×	+	VIB

Theoretical Ratio

Theoretical Ratio

10 9 8 7 6 5 4 3 2 1 .9 .8 .7 .6 .5 .4 .3 .2 .1 .09 .08 .07 .06 .05 .04 .03 .02 .01

20 30 40 50 60 70 20 50 40 50 60 70

△ △

Graph 25

$\frac{W P_c S}{W_p}$

$\frac{W S_d P}{W S}$

	Inst
○	IIA
×	VIA

Theoretical Ratio

Theoretical Ratio

10 9 8 7 6 5 4 3 2 1 .9 .8 .7 .6 .5 .4 .3 .2 .1 .09 .08 .07 .06 .05 .04 .03 .02 .01

20 30 40 50 60 70 20 30 40 50 60 70

△ △

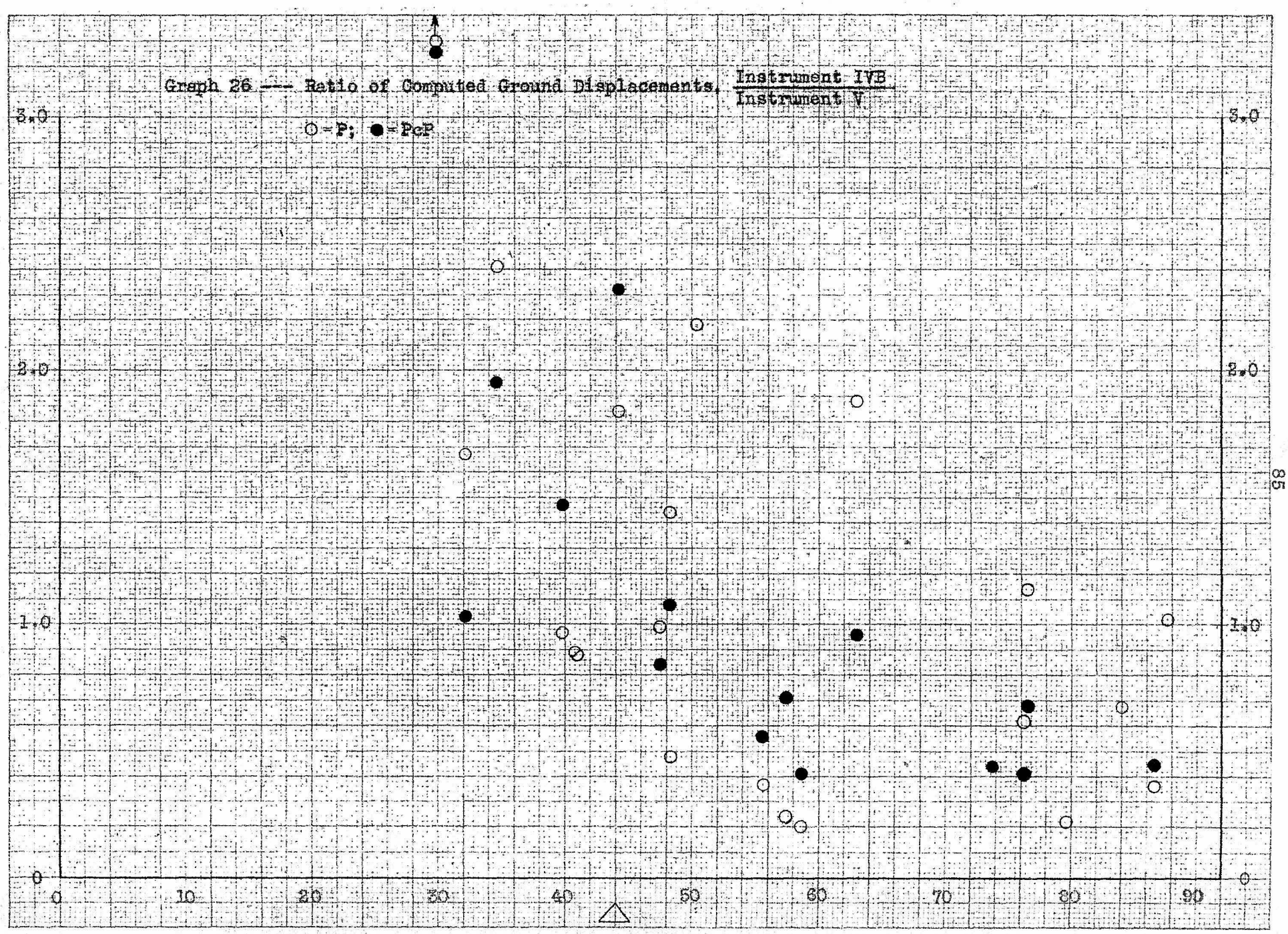
Graph 26 --- Ratio of Computed Ground Displacements, Instrument IVB / Instrument V
○ = P; ● = PcP
3.0
2.0
1.0
0
0
10
20
30
40
50
60
70
80
90

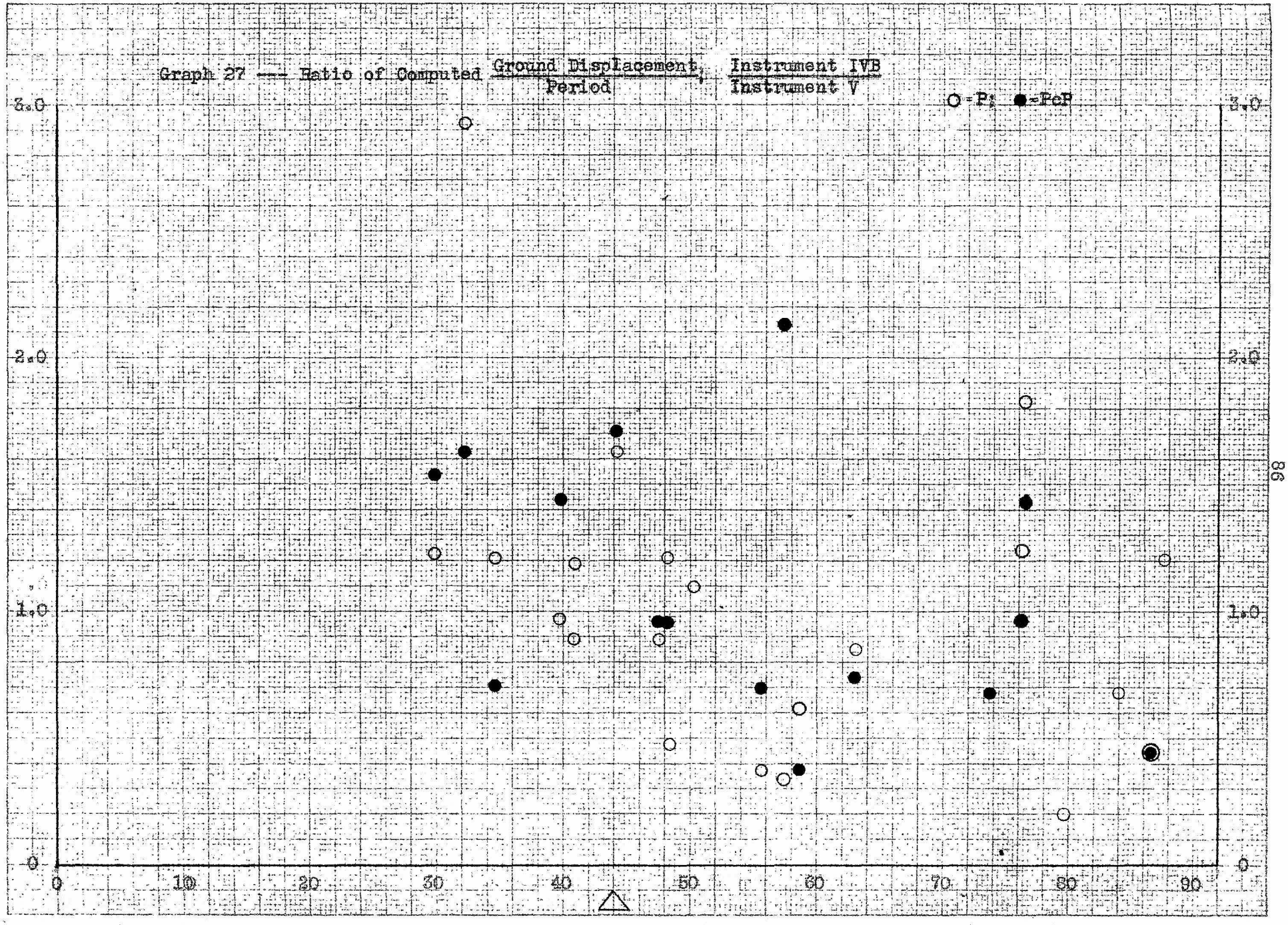
Graph 27 --- Ratio of Computed Ground Displacement, Instrument IVB / Period, Instrument V
○=P; ●=PcP
3.0
2.0
1.0
0
0
10
20
30
40
50
60
70
80
90

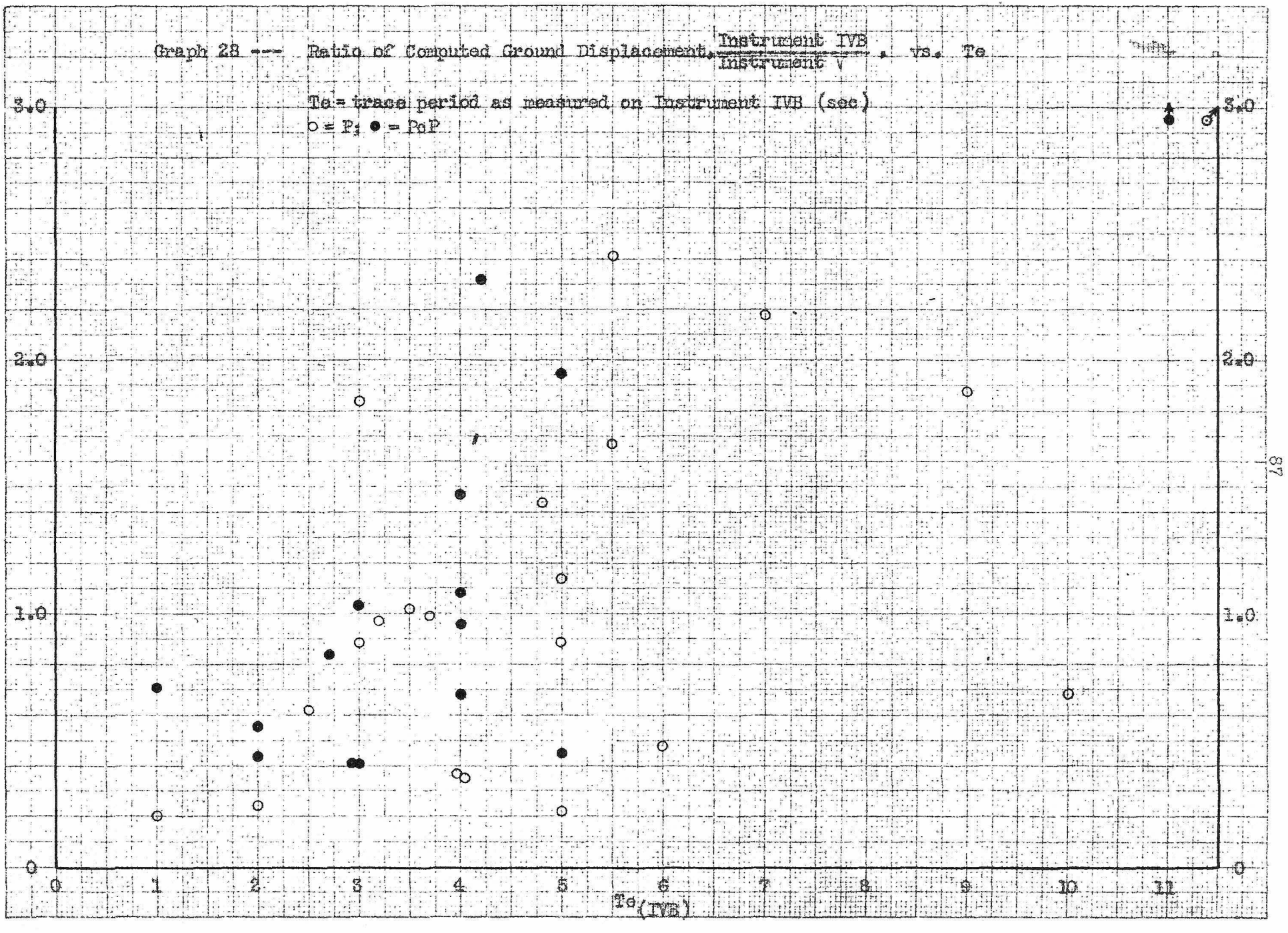
Graph 28 --- Ratio of Computed Ground Displacement, Instrument IVB / Instrument V , vs. Te
Te = trace period as measured on Instrument IVB (sec)
○ = P; ● = PoP
3.0
2.0
1.0
0
0
1
2
3
4
5
6
7
8
9
10
11
Te (IVB)

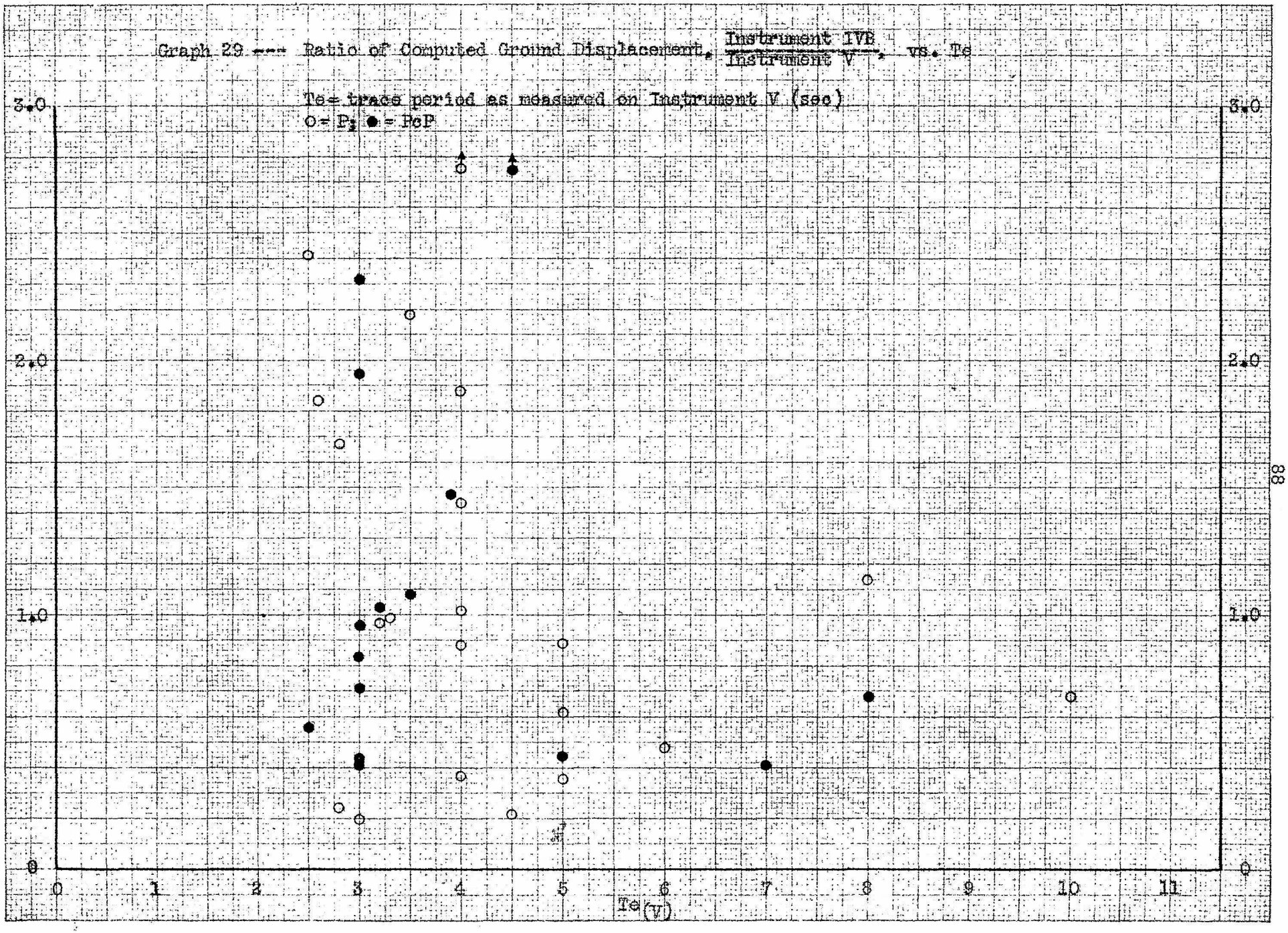
Graph 29 --- Ratio of Computed Ground Displacement, Instrument IVE / Instrument V, vs. Te
Te = trace period as measured on Instrument V (sec)
○ = P, ● = PcP
3.0
2.0
1.0
0
0
1
2
3
4
5
6
7
8
9
10
11
Te (V)

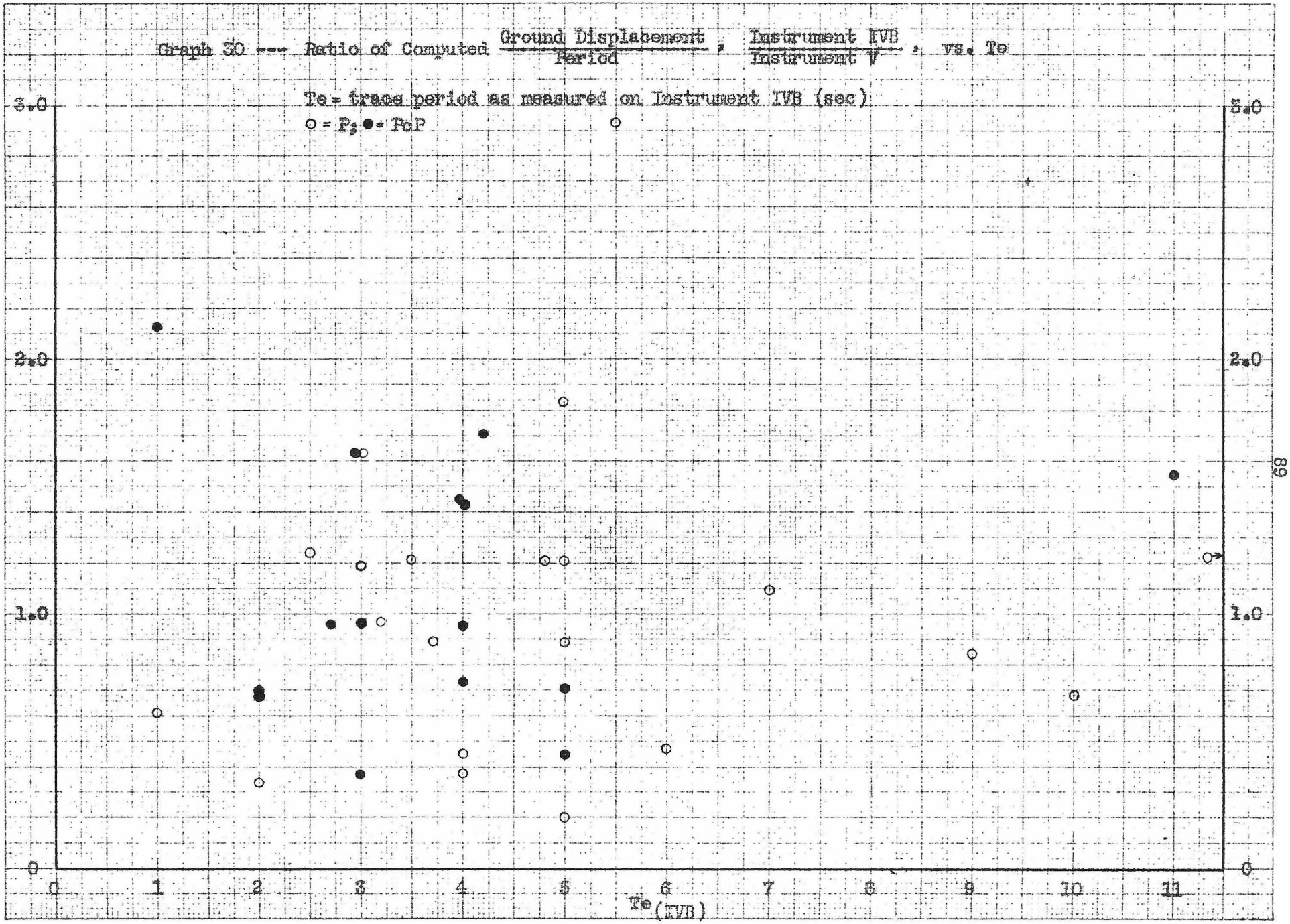
Graph 30 --- Ratio of Computed Ground Displacement / Period , Instrument IVB / Instrument V , vs. Te
Te = trace period as measured on Instrument IVB (sec)
○ = P, ● = PcP
3.0
2.0
1.0
0
0
1
2
3
4
5
6
7
8
9
10
11
Te (IVB)

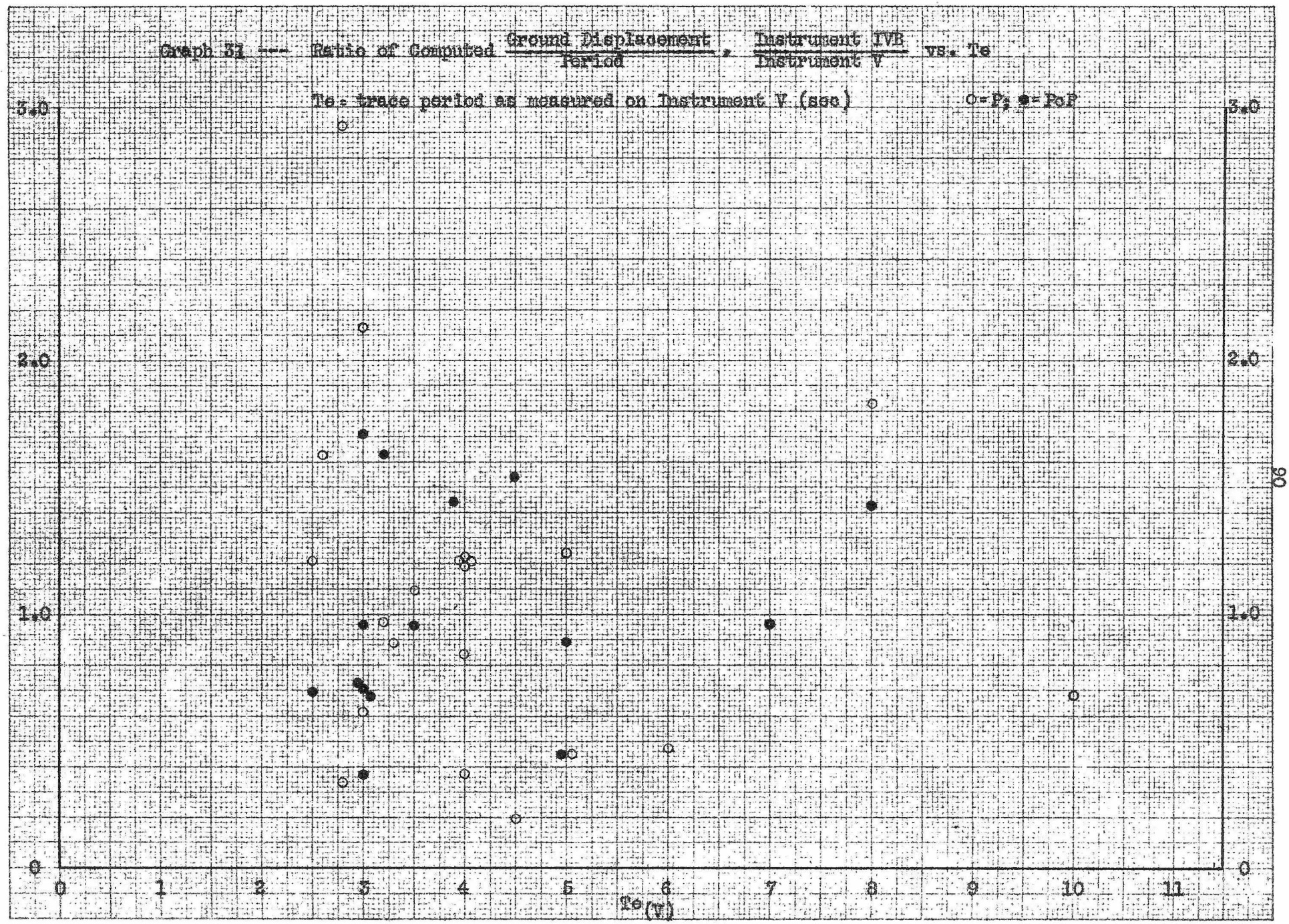
Graph 51 --- Ratio of Computed Ground Displacement / Period , Instrument IVB / Instrument V vs. Te
Te = trace period as measured on Instrument V (sec)
○=P; ●=PoP
3.0
2.0
1.0
0
0
1
2
3
4
5
6
7
8
9
10
11
Te(V)

Graph 52

MAGNITUDE DETERMINATION FROM P AND PcP

M_1 = MAGNITUDE COMPUTED FROM REPORTS OF MANY STATIONS

M_2 = MAGNITUDE COMPUTED FROM P AND PcP

HOR. COMP.: ○ = P, ● = PcP ; VERT. COMP.: ⊖ = P, ◐ = PcP.

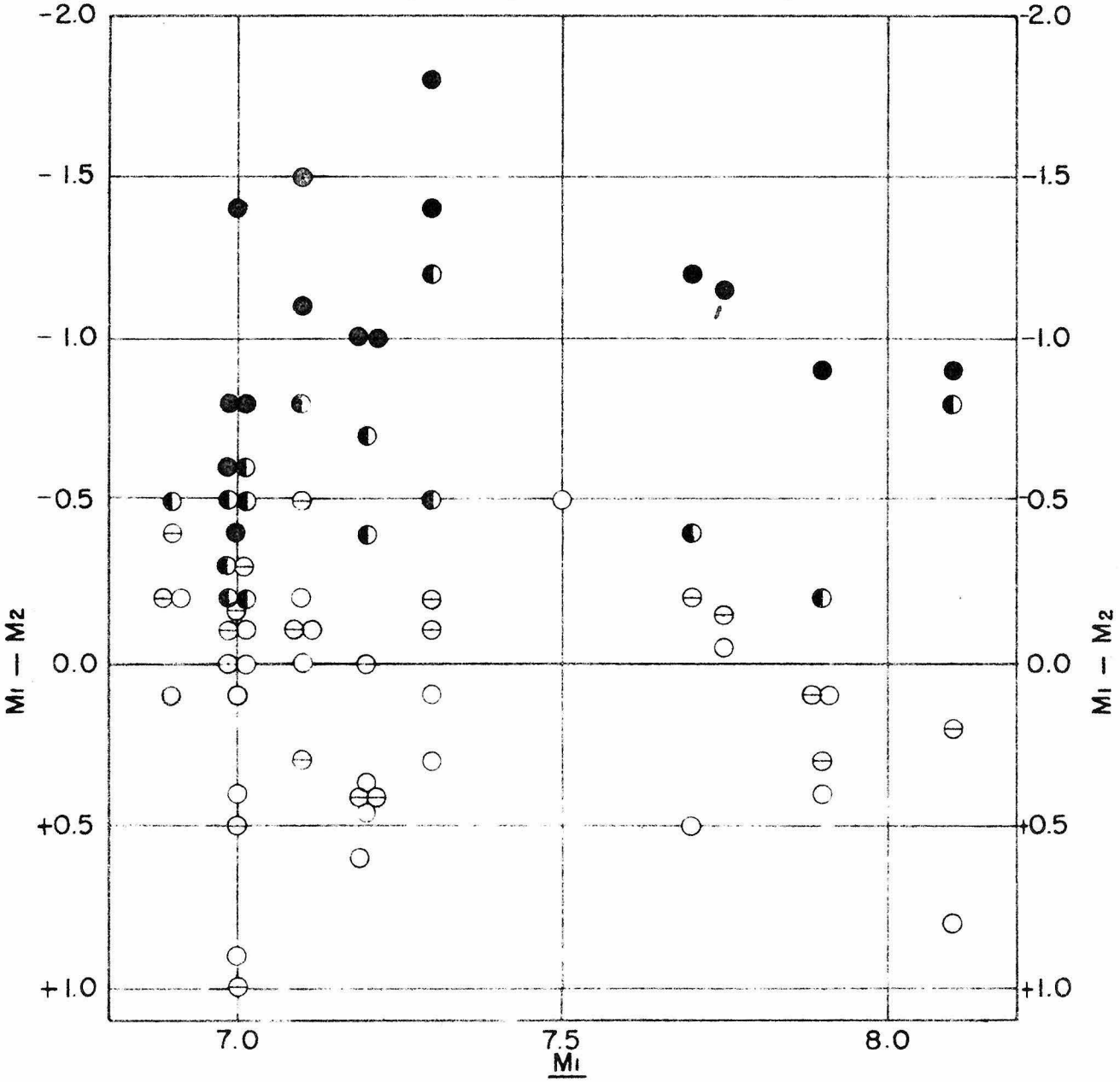

$M_2 = A + 0.1(M_2 - 7) - \lg T + \lg u$ (OR $\lg w$) ± "STATION CORRECTION"

WHERE

$A = 6.3 - \lg U$ (OR $\lg W$)

NOTE: PASADENA "STATION CORRECTION" OF −0.2 HAS BEEN USED IN THE ABOVE GRAPH

Graph 33

A VS. Δ (FOR PGP)
A = 63 − lg U (OR lg W)
A(U)
A(W)
A
Δ
9.8
9.6
9.4
9.2
9.0
8.8
8.6
8.4
8.2
8.0
7.8
7.6
7.4
7.2
7.0
0
10
20
30
40
50
60
70
80
90
100
57PM

Graph 34

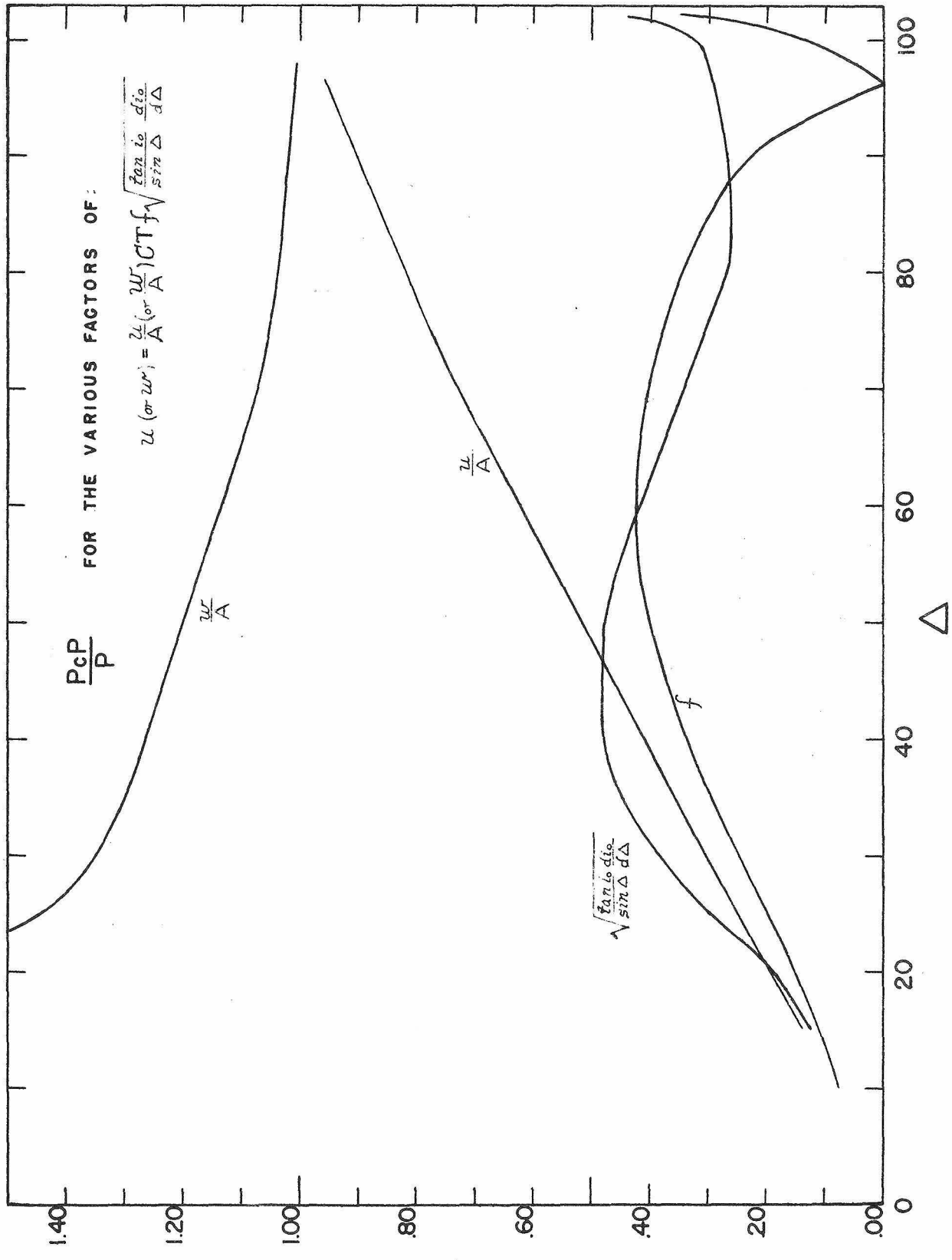
PcP/P
FOR THE VARIOUS FACTORS OF:
u (or w) = u/A (or w/A) CT f √(tan i₀ / sin Δ) di₀/dΔ
w/A
u/A
f
√(tan i₀ / sin Δ) di₀/dΔ
Δ
0
20
40
60
80
100
.00
.20
.40
.60
.80
1.00
1.20
1.40

Graph 35

$\sqrt{\frac{E_{rp}}{E_{ip}}}$ vs. Δ at the boundary of the core; waves incident from above
$\sqrt{\frac{E_{rp}}{E_{ip}}}$
Δ
Curve
V_{p_2}
ρ_2/ρ_1
α 6 km/sec 2
β 6.8 3/2
γ 6.9 1
δ 7 2
ε 7.1 3/2
ζ 7.2 1
η 8 10.1/5.4
1.0
0.9
0.8
0.7
0.6
0.5
0.4
0.3
0.2
0.1
0.0
0.1
0.2
0.3
0.4
0.5
0
10
20
30
40
50
60
70
80
90
100

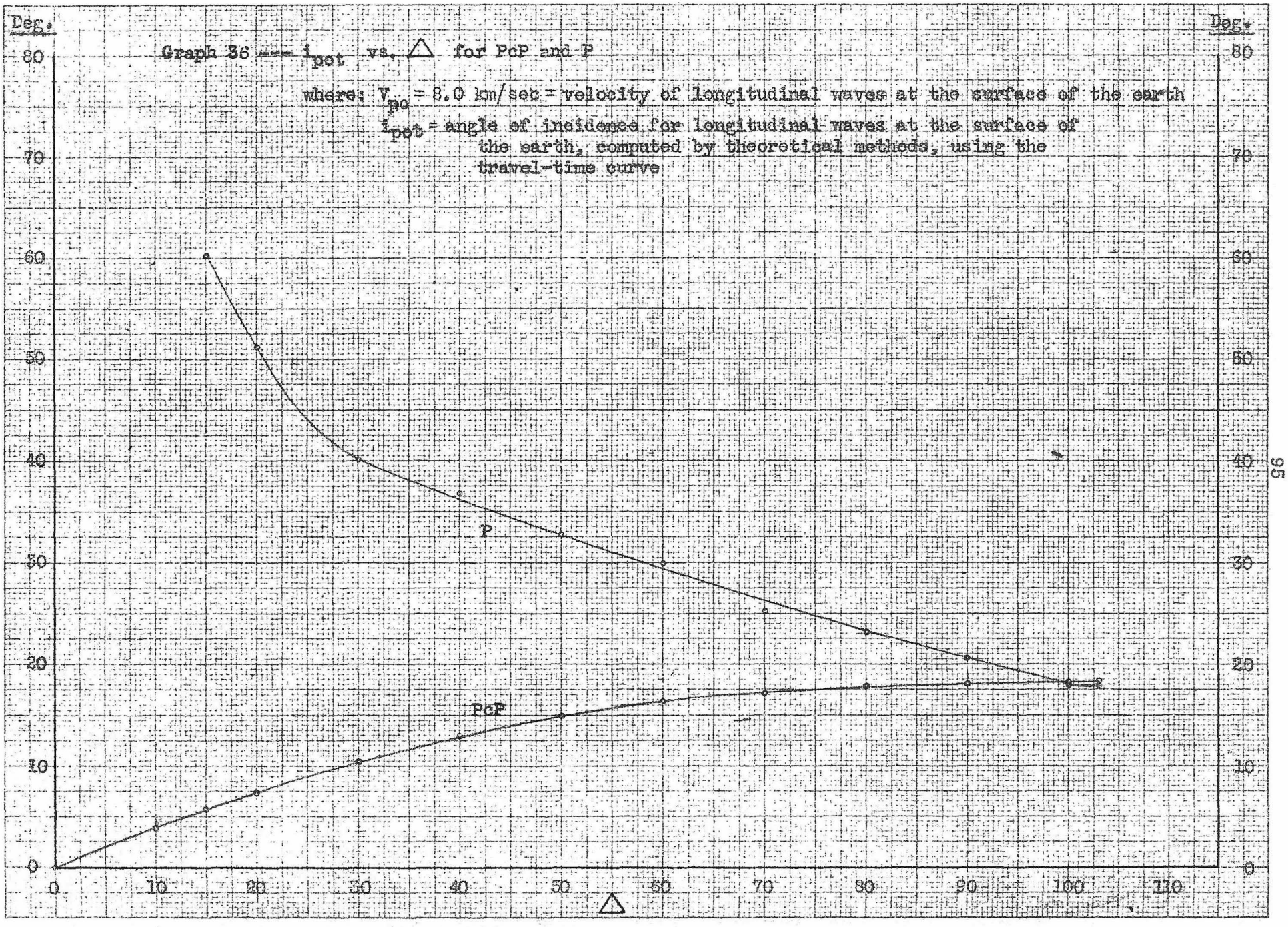
Deg.
Deg.
Graph 36 --- i_{pot} vs. △ for PcP and P
where: V_{po} = 8.0 km/sec = velocity of longitudinal waves at the surface of the earth
i_{pot} = angle of incidence for longitudinal waves at the surface of the earth, computed by theoretical methods, using the travel-time curve
80
70
60
50
40
30
20
10
0
P
PcP
0
10
20
30
40
50
60
70
80
90
100
110
△

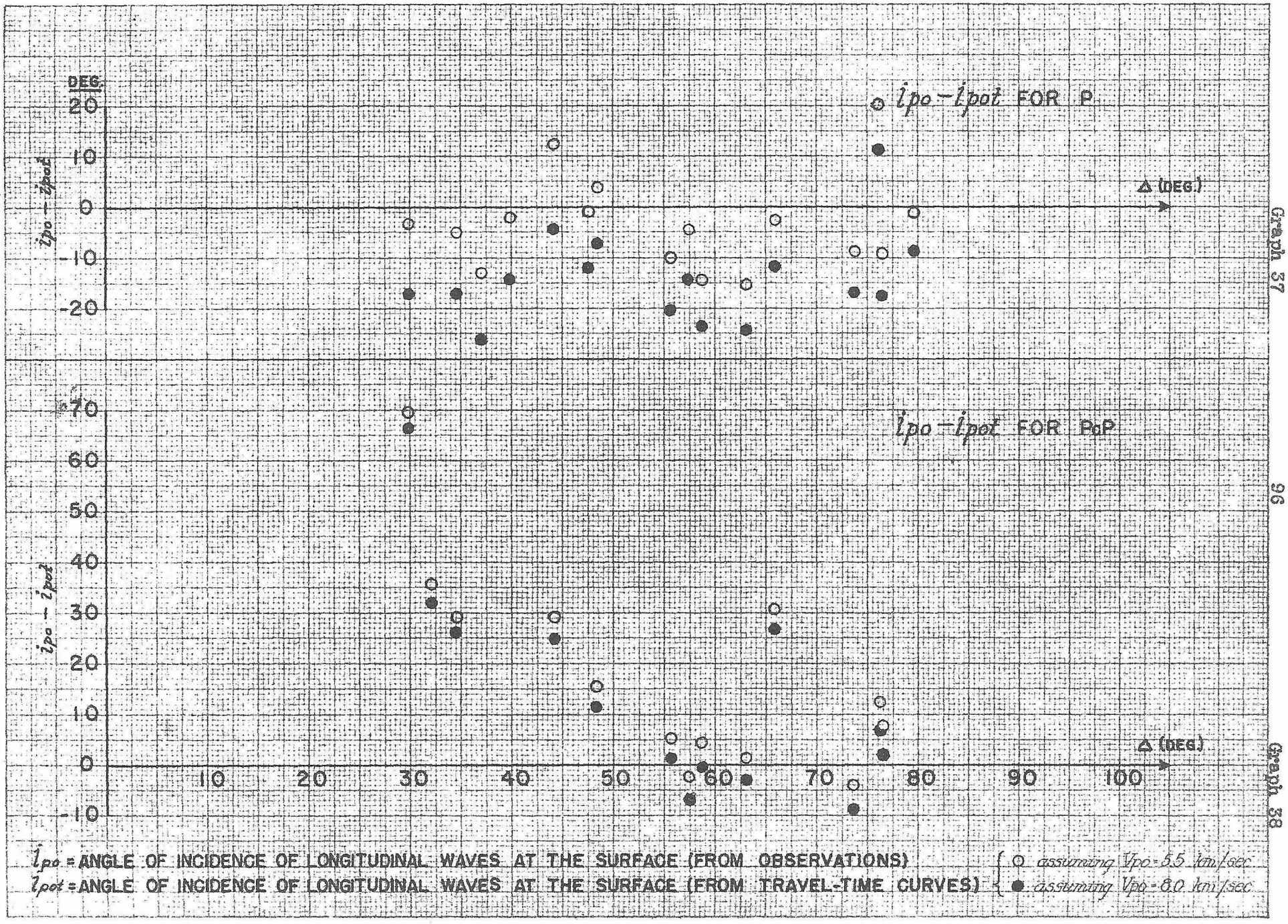
DEG.
20
10
0
-10
-20
$i_{po} - i_{pot}$
$i_{po} - i_{pot}$ FOR P
Δ (DEG.)
Graph 37
70
60
50
40
30
20
10
0
-10
$i_{po} - i_{pot}$
$i_{po} - i_{pot}$ FOR PcP
Δ (DEG.)
10
20
30
40
50
60
70
80
90
100
Graph 38
96
i_{po} = ANGLE OF INCIDENCE OF LONGITUDINAL WAVES AT THE SURFACE (FROM OBSERVATIONS)
i_{pot} = ANGLE OF INCIDENCE OF LONGITUDINAL WAVES AT THE SURFACE (FROM TRAVEL-TIME CURVES)
○ assuming V_{po} = 5.5 km/sec
● assuming V_{po} = 8.0 km/sec

Graph 39

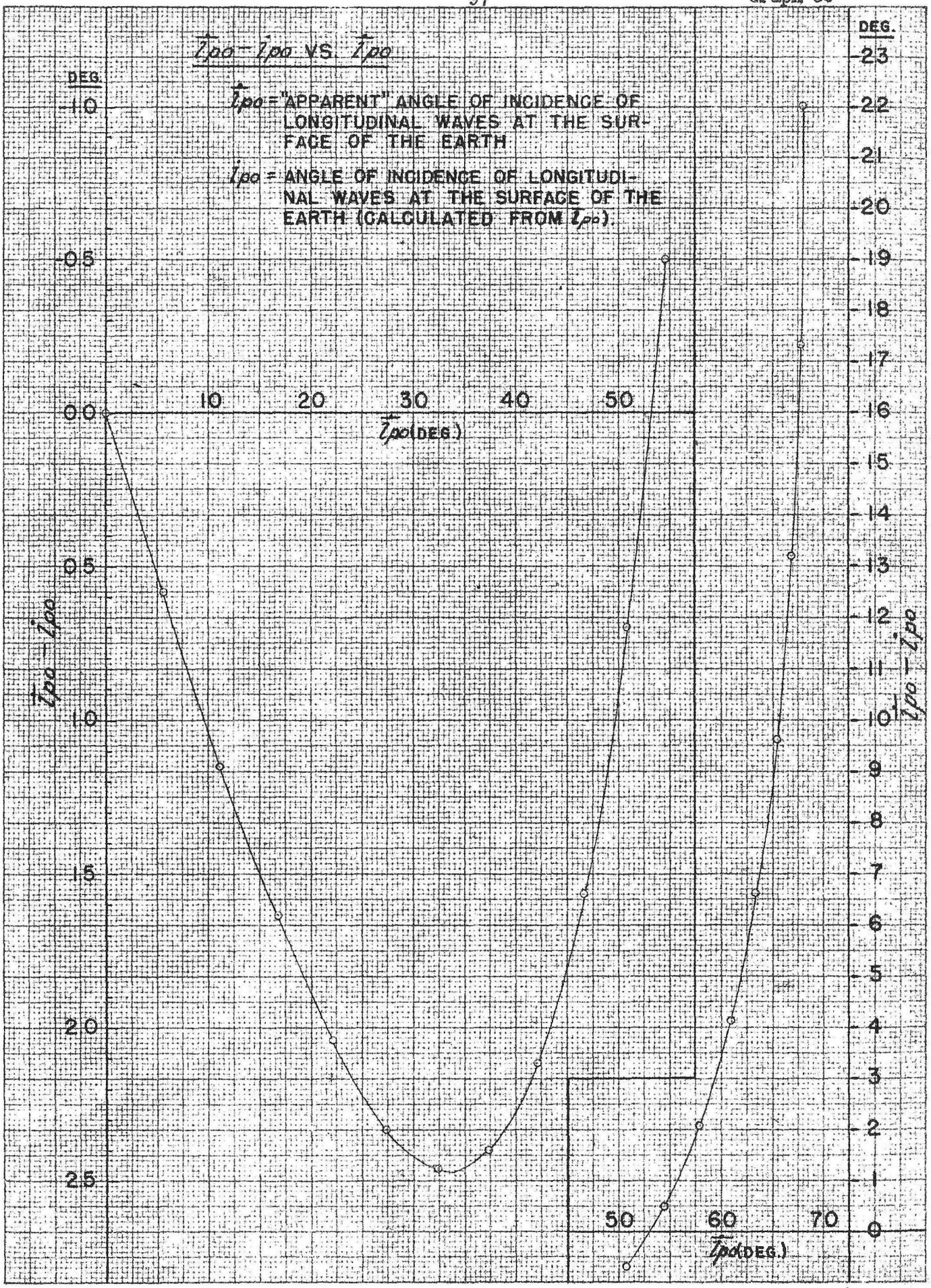
$\bar{i}_{po} - i_{po}$ VS. $\bar{i}_{po}$
$\bar{i}_{po}$ = "APPARENT" ANGLE OF INCIDENCE OF LONGITUDINAL WAVES AT THE SURFACE OF THE EARTH
i_{po} = ANGLE OF INCIDENCE OF LONGITUDINAL WAVES AT THE SURFACE OF THE EARTH (CALCULATED FROM $\bar{i}_{po}$).
DEG.
1.0
0.5
0.0
0.5
1.0
1.5
2.0
2.5
10
20
30
40
50
60
70
$\bar{i}_{po}$ (DEG.)
$\bar{i}_{po} - i_{po}$
DEG.
23
22
21
20
19
18
17
16
15
14
13
12
11
10
9
8
7
6
5
4
3
2
1
0

Graph 40

THEORETICAL RATIO — $\frac{u_{PcP}}{u_P}$ & $\frac{w_{PcP}}{w_P}$

ASSUMING V_{po}=5.5 KM/SEC AND V_{po}=8.0 KM/SEC

V_{po}= VELOCITY OF LONGITUDINAL WAVES AT THE SURFACE OF THE EARTH

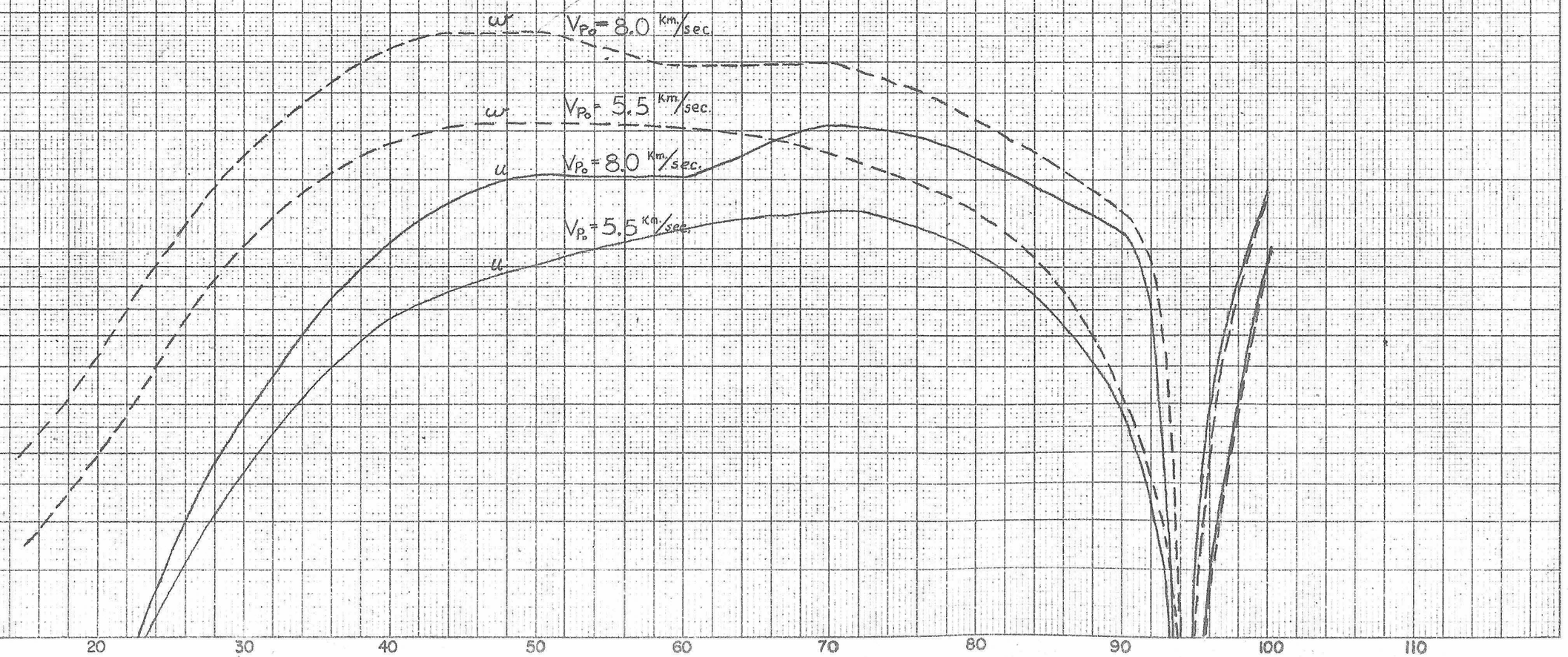

Appendix D

Tables

Table 1---Instrument I---Determination of response characteristic

$\rho = 11.1$; $\mu^2 = 0.63$; $h = 0.608$; To = 0.8; Vo = 2800

u	log U	U	1/U	Te	U/Vo
0.0	0.0000	1.0000	1.0000	0.000	0.35714
0.1	$\bar{1}$.9989	0.9975	1.0025	0.08	.35625
0.2	$\bar{1}$.9958	.9904	1.010	0.16	.35371
0.3	$\bar{1}$.9914	.9804	1.020	0.24	.35014
0.4	$\bar{1}$.9871	.9708	1.030	0.32	.34671
0.5	$\bar{1}$.9848	.9656	1.036	0.40	.34486
0.6	$\bar{1}$.9871	0.9708	1.030	0.48	0.34671
0.7	$\bar{1}$.9968	.9928	1.007	0.56	.35457
0.8	0.0161	1.0378	0.964	0.64	.37064
0.9	.0458	1.1113	.900	0.72	.39689
1.0	.0851	1.2165	.822	0.80	.43446
1.1	0.1318	1.3557	0.738	0.88	0.48418
1.2	.1832	1.5247	.656	0.96	.54454
1.3	.2369	1.7255	.580	1.04	.61625
1.4	.2912	1.9565	.511	1.12	.69875
1.5	.3448	2.212	.452	1.20	.79000
1.6	0.3970	2.495	0.401	1.28	0.89107
1.7	.4474	2.802	.357	1.36	1.00071
1.8	.4959	3.133	.319	1.44	1.11893
1.9	.5424	3.487	.287	1.52	1.24536
2.0	.5869	3.863	.259	1.60	1.37964
2.2		4.545	0.22	1.76	1.62321
2.4		5.555	.18	1.92	1.98393
2.6		6.667	.15	2.08	2.38107
2.8		7.692	.13	2.24	2.74714
3.0		8.772	.114	2.40	3.13286
3.2		10.000	0.100	2.56	3.57143
3.4		11.364	.088	2.72	4.05892
3.6		12.658	.079	2.88	4.52071
3.8		14.085	.071	3.04	5.03036
4.0		15.625	.064	3.20	5.58036
4.2		17.241	0.058	3.36	6.15750
4.4		19.231	.052	3.52	6.86821
4.6		21.277	.047	3.68	7.59893
4.8		22.727	.044	3.84	8.11678
5.0		24.752	.0404	4.00	8.84000
5.2		26.810	0.0373	4.16	9.57500

Table 2 --- Instrument II --- Determination of response characteristic

ρ=11.7; μ^2=0.62; h=0.616; T_o=0.63; V_o=2800

u	log U	U	1/U	Te	U/V_o
0.0	0.0000	1.0000	1.000	0.000	0.35714
0.1	$\bar{1}$.9990	.9977	.002	0.063	.35652
0.2	.9961	.9911	.009	0.126	.35396
0.3	.9922	.9822	.018	0.189	.35079
0.4	.9886	.9741	.027	0.252	.34789
0.5	.9871	.9707	.030	0.315	.34668
0.6	$\bar{1}$.9904	0.9781	1.022	0.378	0.34932
0.7	0.0011	1.0025	0.9975	0.441	.35804
0.8	.0212	.0500	.9524	0.504	.37500
0.9	.0514	.126	.8861	0.567	.40214
1.0	.0909	.233	.8110	0.630	.44036
1.1	0.1375	1.373	0.7283	0.693	0.48036
1.2	.1885	.544	.6477	0.756	.55143
1.3	.2418	.745	.5731	0.819	.62521
1.4	.2956	.974	.5066	0.882	.70500
1.5	.3487	2.232	.4480	0.945	.79714
1.6	0.4005	2.515	0.3976	1.008	0.89821
1.7	.4506	.822	.3544	1.071	1.00786
1.8	.4987	3.153	.3172	1.134	.12607
1.9	.5449	.507	.2851	1.197	.25250
2.0	.5892	.883	.2575	1.260	.38679
2.2			0.22	1.386	1.62521
2.4			.18	1.512	.98595
2.6			.15	1.638	2.38107
2.8			.13	1.764	.74714
3.0			.107	1.890	3.33779
3.2			0.100	2.016	3.57143
3.4			.088	2.142	4.05392
3.6			.079	2.268	4.52071
3.8			.070	2.394	5.10214
4.0			.063	2.520	5.66[illegible]95
4.2			0.057	2.646	6.26571
4.4			.052	2.772	6.86821
4.6			.047	2.898	7.59893
4.8			.044	3.024	8.11678
5.0			.0404	3.150	8.84000
5.2			0.0373	3.276	9.57500

Table 3 --- Instruments I, II, V, and VA --- Determination of response characteristic; theoretical adjustment

Insturments I and II ---μ^2=0.28; h=0.85; To=0.8; V_o=2800
Instruments V and VA ---μ^2=0.28; h=0.85; To=6.0; V_o=800

u	log $(1+u_p^2)$	log f(u)	log $\sqrt{1-\mu^2 f(u)}$	log U	U	1/U	Inst. I and II Te	V	U/V_o	Inst. V and VA Te	V	U/Vo
0.0	0.0000			0.0000	1.000	1.000	0.00	2800		0.0	800	1.250
0.2	.0170	T.1701	T.9908	.0078	.019	0.981	0.16	2747	0.36393	1.2	785	1.274
0.4	.0645	.6773	.9697	.0342	.081	.925	0.32	2590	.38607	2.4	740	1.351
0.6	.1335	.8913	.9466	.0801	.202	.832	0.48	2330	.42929	3.6	666	1.503
0.8	.2148	.9786	.9527	.1475	.405	.712	0.64	1994	.50179	4.8	570	1.781
1.0	.3010	0.0000	.9287	.2297	.697	.589	0.80	1649	.60607	6.0	471	2.121
1.2	0.3874	T.9856	T.9314	0.3188	2.084	0.480	0.96	1344	0.74429	7.2	384	2.605
1.4	.4713	.9517	.9374	.4087	.563	.390	1.12	1092	.91536	8.4	312	3.204
1.6	.5514	.9074	.9443	.4957	3.151	.319	1.28	893	1.11821	9.6	255	3.914
1.8	.6274	.8579	.9510	.5784	.788	.264	1.44	739	.35286	10.8	211	4.745
2.0	.6990	.8062	.9571	.6561	4.530	.221	1.60	619	.61736	12.0	177	5.663
2.2	0.7664	T.7541	T.9624	0.7288	5.356	0.187	1.76	524	1.91286	13.2	150	6.695
2.4	.8299	.7026	.9669	.7968	6.263	.160	1.92	448	2.23679	14.4	128	7.829
2.6	.8899	.6523	.9708	.8607	7.256	.138	2.08	386	.59143	15.6	110	9.070
2.8	.9465	.6055	.9741	.9206	8.329	.120	2.24	336	.97464	16.8	96	10.411
3.0	1.0000	.5563	.9769	.9769	9.482	.105	2.40	294	3.38643	18.0	84	11.853
3.2	1.0508	T.5108	T.9793	1.0301	10.72	0.093	2.56	260	3.82857	19.2	74	13.40
3.4	.0990	.4670	.9814	.0804	12.03	.083	2.72	230	4.29643	20.4	64	15.04
3.6	.1449	.4249	.9832	.1281	13.43	.074	2.88	207	.79643	21.6	59	16.79
3.8	.1886	.3843	.9847	.1753	14.90	.067	3.04	188	5.32143	22.8	54	18.63
4.0	.2304	.3453	.9861	.2165	16.46	.061	3.20	171	.87857	24.0	49	20.58

Table 4 --- Instrument V --- Determination of response characteristic

ρ=32.2; μ^2=0.45; h=0.742; To=6.36; Vo=800

u	log $(1+u_p^2)$	log f(u)	log $\sqrt{1-\mu^2 f(u)}$	log U	U	1/U	Te	U/Vo
0.0	0.0000			0.0000	1.000	1.000	0.000	1.25000
0.1	.0043	$\bar{2}$.5934	$\bar{1}$.9961	.0004	.001	0.999	0.636	.25125
0.2	.0170	$\bar{1}$.1701	.9850	.0020	.005	.995	1.272	.25625
0.3	.0374	.4814	.9682	.0056	.013	.987	1.908	.26625
0.4	.0645	.6775	.9477	.0122	.028	.973	2.544	.28500
0.5	.0969	.8062	.9262	.0231	.054	.949	3.180	.31750
0.6	0.1335	$\bar{1}$.8913	$\bar{1}$.9064	0.0399	1.096	0.912	3.816	1.37000
0.7	.1732	.9459	.8901	.0633	.157	.864	4.452	.44625
0.8	.2148	.9786	.8786	.0934	.240	.806	5.088	.55000
0.9	.2577	.9952	.8721	.1298	.348	.742	5.724	.68500
1.0	.3010	0.0000	.8702	.1712	.484	.674	6.360	.85500
1.1	0.3444	$\bar{1}$.9961	$\bar{1}$.8718	0.2162	1.645	0.608	6.996	2.05625
1.2	.3874	.9956	.8759	.2653	.833	.546	7.632	.29125
1.3	.4298	.9704	.8816	.3114	2.048	.488	8.268	.56000
1.4	.4713	.9517	.8881	.3594	.288	.437	8.904	.86000
1.5	.5119	.9305	.8950	.4069	.552	.392	9.540	3.19000
1.6	0.5514	$\bar{1}$.9074	$\bar{1}$.9018	0.4532	2.839	0.352	10.176	3.54875
1.7	.5899	.8831	.9085	.4984	3.151	.317	10.812	.93875
1.8	.6274	.8579	.9148	.5422	.485	.287	11.448	4.35625
1.9	.6657	.8322	.9207	.5844	.840	.260	12.084	.80000
2.0	.6990	.8062	.9262	.6252	4.219	.237	12.720	5.27875
2.2	0.7664	$\bar{1}$.7541	$\bar{1}$.9359	0.7023	5.038	0.198	13.992	6.29750
2.4	.8299	.7026	.9441	.7740	.943	.166	15.264	7.42875
2.6	.8899	.6523	.9510	.8409	6.932	.144	16.536	8.66500
2.8	.9465	.6035	.9568	.9033	8.004	.125	17.808	10.00500
3.0	1.0000	.5563	.9616	.9616	9.153	.109	19.080	11.44125
3.2	1.0508	$\bar{1}$.5108	$\bar{1}$.9656	1.0166	10.39	0.096	20.352	12.9875
3.4	.0990	.4670	.9693	.0685	11.70	.085	21.624	14.6250
3.6	.1449	.4249	.9723	.1172	13.10	.076	22.896	16.3750
3.8	.1886	.3843	.9749	.1635	14.57	.069	24.168	18.2125
4.0	.2304	.3453	.9772	.2076	16.13	.062	25.440	20.1625

Table 5 --- Instrument VA --- Determination of response characteristic

ρ=30.1; μ^2=0.46; h=0.755; To=5.65; Vo=800

u	log $(1+u^2)$	log f(u)	log $\sqrt{1-\mu^2 f(u)}$	log U	U	1/U	Te	U/Vo
0.0				0.0000	1.000	1.000	0.000	1.25000
0.1			$\bar{1}$.9960	.0003	.001	.999	0.565	.25125
0.2			.9847	.0017	.004	.996	1.130	.25500
0.3			.9675	.0049	.012	.988	1.695	.26500
0.4			.9464	.0109	.026	.975	2.260	.28250
0.5			.9245	.0212	.050	.952	2.825	.31250
0.6			$\bar{1}$.9037	0.0372	1.089	0.918	3.390	1.36125
0.7			.8869	.0601	.148	.871	3.955	.43500
0.8			.8749	.0897	.229	.814	4.520	.53625
0.9			.8682	.1259	.336	.748	5.085	.67250
1.0			.8662	.1672	.470	.630	5.650	.83750
1.1			$\bar{1}$.8673	0.2117	1.628	0.614	6.215	2.03500
1.2			.8721	.2595	.819	.550	6.780	.27375
1.3			.8781	.3079	2.032	.492	7.345	.54000
1.4			.8848	.3561	.271	.440	7.910	.83875
1.5			.8920	.4039	.534	.395	8.475	3.16750
1.6	See Table 4	See Table 4	$\bar{1}$.8991	0.4505	2.821	0.354	9.040	3.52625
1.7			.9060	.4959	3.132	.319	9.605	.91500
1.8			.9125	.5399	.466	.289	10.170	4.33250
1.9			.9186	.5775	.779	.265	10.735	.72375
2.0			.9243	.6233	4.201	.238	11.300	5.25125
2.2			$\bar{1}$.9343	0.7007	5.020	0.199	12.430	6.27500
2.4			.9427	.7726	.924	.109	13.560	7.40500
2.6			.9498	.8397	6.913	.145	14.690	8.64125
2.8			.9557	.9022	7.984	.125	15.820	9.98000
3.0			.9607	.9607	9.135	.109	16.950	11.41375
3.2			$\bar{1}$.9649	1.0157	10.37	0.096	18.080	12.9625
3.4			.9686	.0676	11.68	.086	19.210	14.6000
3.6			.9717	.1166	13.08	.076	20.340	16.3500
3.8			.9744	.1650	14.55	.069	21.470	18.1875
4.0			.9767	.2071	16.11	.062	22.600	20.1375

Table 6 --- Instruments IIA, IVA, and IVB --- Determination of response characteristic; theoretical adjustment

T_o=1 sec; T_g=90 sec; Aperiodic damping

T_θ	u_p	u_g	$1+u_p^2$	$1+u_g^2$	a/k	k/a
0.1	0.1	0.001111	1.01	$1.0^5$12345	0.09901	10.10001
0.2	0.2	.002222	1.04	$1.0^5$49383	.19251	5.20003
0.4	0.4	.004444	1.16	$1.0^4$19753	.36035	2.77506
0.6	0.6	.006666	1.36	$1.0^4$44444	.44116	2.26677
0.8	0.8	.008888	1.64	$1.0^4$79012	.43777	2.05016
1	1	0.011111	2	1.00012345	0.4999	2.0004
2	2	.022222	5	.00049383	.3998	2.5013
3	3	.033333	10	.00111111	.2997	3.3367
4	4	.044444	17	.0019753	.2348	4.2589
5	5	.055555	26	.0030864	.1917	5.2165
			37			
6	6	0.066666	37	1.0044444	0.1614	6.1958
7	7	.077777	50	.0060495	.1392	7.1839
8	8	.088888	65	.0079012	.1221	8.1900
9	9	.099999	82	.0100000	.1087	9.1996
10	10	.111111	101	.0123456	.0973	10.2250
			122			
11	11	0.122222	122	1.0149383	0.0888	11.2613
12	12	.133333	145	.0177778	.0818	12.3031
13	13	.144444	170	.0208642	.0749	13.3511
14	14	.155555	197	.0241975	.0694	14.4002
15	15	.166666	226	.0277778	.0646	15.4739
16	16	0.177777	257	1.0316049	0.0603	16.5838
17	17	.188888	290	.0356790	.0566	17.6678
18	18	.199999	325	.0400000	.0533	18.7617
19	19	.211111	362	.0445679	.0502	19.9203
20	20	.222222	401	.0493827	.0475	21.0526
21	21	0.233333	442	1.0544444	0.0451	22.1730
22	22	.244444	485	.0597531	.0428	23.3645
23	23	.255555	530	.0650864	.0408	24.5098
24	24	.266666	577	.0711111	.0388	25.7732
25	25	.277777	626	.0771605	.0371	26.9542
50	50	.555555	2501	1.3086419	0.0150	66.6667

Formula used: $a/k = \frac{T_\theta}{(1+u_p^2)(1+u_g^2)}$

where: $u_p = T_\theta/T_o$; $u_g = T_\theta/T_g$

Table 7 --- Instruments IIA, IVA, and IVB --- Determination of step-function response characteristic, theoretical adjustment

T_o=1 sec; T_g=90 sec; Aperiodic damping

t	$2+(\omega_o-\omega_g)t$	$2-(\omega_o-\omega_g)t$	$\omega_o t$	$e^{-\omega_o t}$	$\omega_g t$	$e^{-\omega_g t}$	U
1.0027	8.23	-4.23	6.3	0.001836	0.07	0.93239	0.01651
2.0054	14.46	10.46	12.6	.003814	.14	.86936	.03791
3.0080	20.69	16.69	18.9		.21	.81058	.05640
4.0107	26.92	22.92	25.2		.28	.75578	.07222
5.0134	33.15	29.15	31.5		.35	.70469	.08564
6.0161	39.38	35.38	37.8		.42	.65705	.09691
7.0187	43.61	41.61	44.1		.49	.61263	.10627
8.0214	49.84	47.84			.56	.57121	.11392
9.0241		54.07			.63	.53259	.12005
10.0268		60.30			.70	.49659	.12483
11.0294		66.53			0.77	0.46301	0.12842
12.0321		72.76			.84	.43171	.13095
13.0348		78.99			.91	.40252	.13255
14.0375		85.22			.98	.37531	.13334
15.0401		91.45			1.05	.34994	.13341
16.0428		97.68			1.12	.32628	.13287
17.0455		103.91			1.19	.30422	.13179
18.0482		110.14			1.26	.28365	.13024
19.0508		116.37			1.33	.26448	.12831
20.0535		122.60			1.40	.24660	.12604
25.0669		153.75			1.75	0.17577	0.11138
30.0803		184.90			2.10	.12246	.09439
35.0937		216.05			2.45	.08529	.07772
40.1070		247.20			2.80	.06081	.06267
45.1204		278.35			3.15	.04235	.04973
50.1338		309.50			3.50	.03020	.03896
55.1472		340.65			3.85	0.02128	0.03022
60.1606		371.80			4.20	.01500	.02324
65.1739		402.95			4.55	.01057	.01775
70.1873		434.10			4.90	.00745	.01348
75.2007		465.25			5.25	.00525	.01018
80.2141		496.40			5.60	.00370	.00765
85.2275		527.55			5.95	.00261	.00573

Formula used: $$U = \frac{\left[\{2+(\omega_o-\omega_g)t\}e^{-\omega_o t} - \{2-(\omega_o-\omega_g)t\}e^{-\omega_g t}\right]}{(\omega_o-\omega_g)^3}$$

Table 8 --- Instrument IVA --- Determination of magnification curve

T_e	a/k	A^*/A_e	A/A^*(X1000)	$\frac{A_e/A^*}{T_e}$(X1000)
0.1	0.09901	435.0	2.29927	22.9927
0.2	.19231	844.8	1.18379	5.9190
0.4	.36035	1583.0	0.63174	1.5794
0.6	.44116	1938.0	.51603	0.8601
0.8	.48777	2142.8	.46672	.5834
1	0.4999	2196.1	0.45539	0.45539
2	.3998	1756.3	.56942	.28471
3	.2997	1316.6	.75960	.25320
4	.2348	1031.5	.96954	.24239
5	.1917	842.1	1.18754	.23751
6	.1614	709.0	1.41047	.23508
7	.1392	611.5	1.63541	.23363
8	.1221	536.4	1.86445	.23306
9	.1087	477.5	2.09429	.23270
10	.0978	429.6	2.32772	.23277
11	0.0888	390.1	2.56363	0.23306
12	.0813	357.2	2.80012	.23334
13	.0749	329.0	3.03938	.23380
14	.0694	304.9	3.28025	.23430
15	.0646	283.8	3.52400	.23493
16	.0603	264.9	3.77530	.23596
17	.0566	248.6	4.02207	.23659
18	.0533	234.1	4.27110	.23728
19	.0502	220.5	4.53486	.23868
20	.0475	208.7	4.79262	.23963
21	0.0451	198.1	5.04768	0.24037
22	.0429	188.0	5.31893	.24177
23	.0408	179.2	5.57966	.24259
24	.0388	170.4	5.86727	.24447
25	.0371	163.0	6.13612	.24544
50	0.0150	65.9	15.17667	0.30353

Formula used: $A^*/A_e = (a/k) \times 4393$

Table 9 --- Determination of response characteristic --- Instrument VIA

T_o=1.0 sec; T_g=0.23 sec; Aperiodic damping

T_e	u_p^2	u_g^2	$(1+u_p^2)$	$(1+u_g^2)$	k/a	a/k
0.01	0.0001	0.001890	1.0001	1.00189	100.1991	0.00998
.02	.0004	.007561	1.0004	1.00756	50.3982	.01984
.04	.0016	.030246	1.0016	1.03025	25.7974	.03876
.06	.0036	.068053	1.0036	1.06805	17.8650	.05597
.08	.0064	.120983	1.0064	1.12098	14.1020	.07091
0.1	0.01	0.189036	1.01	1.18904	12.0093	0.08327
.2	.04	.756144	1.04	1.75614	9.1319	.10951
.3	.09	1.701323	1.09	2.70132	9.8148	.10189
.4	.16	3.024575	1.16	4.02458	11.6713	.08568
.5	.25	4.725898	1.25	5.72590	14.3148	.06986
.6	.36	6.805293	1.36	7.80529	17.6920	.05652
.7	.49	9.262760	1.49	10.26276	21.8450	.04577
.8	.64	12.098299	1.64	13.09830	26.8515	.03724
.9	.81	15.311909	1.81	16.31191	32.8051	.03048
1.0	1.00	18.903592	2.00	19.90359	39.8072	.02512
1.1	1.21	22.873346	2.21	23.87335	47.9637	0.02085
1.2	1.44	27.221172	2.44	28.22117	57.3831	.01743
1.3	1.69	31.947070	2.69	32.94707	68.1751	.01467
1.4	1.96	37.051040	2.96	38.05104	80.4508	.01243
1.5	2.25	42.533081	3.25	43.53308	94.3217	.01060
1.6	2.56	48.393195	3.56	49.39320	109.8999	.00920
1.7	2.89	54.631380	3.39	55.63138	127.2977	.00786
1.8	3.24	61.247637	4.24	62.24764	146.6278	.00682
1.9	3.61	68.241966	4.61	69.24197	168.0204	.00595
2.0	4.00	75.614367	5.00	76.61437	191.5359	.00522
2.2	4.84	91.49338	5.84	92.49338	245.5279	0.00407
2.4	5.76	108.88469	6.76	109.88469	309.5085	.00323
2.6	6.76	127.78828	7.76	128.78828	384.3835	.00260
2.8	7.84	148.20416	8.84	149.20416	471.0589	.00212
3.0	9.00	170.13233	10.00	171.13233	570.4411	.001753
3.2	10.24	193.57278	11.24	193.57278	685.4369	0.001463
3.4	11.56	218.52552	12.56	219.52552	810.9531	.001233
3.6	12.96	244.99055	13.96	245.99055	953.8967	.001048
3.8	14.44	272.96786	15.44	273.96786	1113.1747	.000898
4.0	16.00	302.45747	17.00	303.45747	1289.6943	.000775
5.0	25.00	472.58980	26.00	473.58980	2462.667	0.000406
6.0	36.00	680.52930	37.00	681.52930	4202.764	.000238
7.0	49.00	926.27599	50.00	927.27599	6623.399	.000151
8.0	64.00	1209.82987	65.00	1210.82987	9837.993	.000102

Formula used: $a/k = \frac{T_o u_p}{(1+u_p^2)(1+u_g^2)}$

where: $u_p = T_e/T_o$; $u_g = T_e/T_g$

Table 10 --- Instrument VIB --- Determination of response characteristic

T_o=1.6 sec; T_g=0.2 sec; Aperiodic damping

T_e	u_p^2	u_g^2	$(1+u_p^2)$	$(1+u_g^2)$	k/a	a/k
0.01	0.0001	0.0025	1.0001	1.0025	100.260	0.009974
.02	.0004	.0100	1.0004	1.0100	52.020	.019223
.04	.0016	.0400	1.0016	1.0400	25.292	.039538
.06	.0036	.0900	1.0036	1.0900	18.232	.054849
.08	.0064	.1600	1.0064	1.1600	13.968	.071592
0.1	0.01	0.25	1.01	1.25	12.625	0.079208
.2	.04	1.00	1.04	2.00	10.400	.096154
.3	.09	2.25	1.09	3.25	11.308	.084688
.4	.16	4.00	1.16	5.00	14.500	.068966
.5	.25	6.25	1.25	7.25	18.125	.055172
.6	.36	9.00	1.36	10.00	22.667	.044117
.7	.49	12.25	1.49	13.25	28.204	.035456
.8	.64	16.00	1.64	17.00	34.850	.028694
.9	.81	20.25	1.81	21.25	42.736	.023399
1.0	1.00	25.00	2.00	26.00	52.000	.019231
1.1	1.21	30.25	2.21	31.25	62.784	0.015928
1.2	1.44	36.00	2.44	37.00	75.233	.013292
1.3	1.69	42.25	2.69	43.25	89.494	.011174
1.4	1.96	49.00	2.96	50.00	105.714	.009459
1.5	2.25	56.25	3.25	57.25	124.042	.008062
1.6	2.56	64.00	3.56	65.00	144.625	.006914
1.7	2.89	72.25	3.89	73.25	167.613	.005966
1.8	3.24	81.00	4.24	82.00	193.156	.005177
1.9	3.61	90.25	4.61	91.25	221.401	.004517
2.0	4.00	100.00	5.00	101.00	252.500	.003960
2.2	4.84	121.00	5.84	122.00	323.855	0.003088
2.4	5.76	144.00	6.76	145.00	408.417	.002448
2.6	6.76	169.00	7.76	170.00	507.385	.001971
2.8	7.84	196.00	8.84	197.00	621.957	.001608
3.0	9.00	225.00	10.00	226.00	753.333	.001327
3.2	10.24	256.00	11.24	257.00	902.713	0.001108
3.4	11.56	289.00	12.56	290.00	1071.294	.000933
3.6	12.96	324.00	13.96	325.00	1260.278	.000793
3.8	14.44	361.00	15.44	362.00	1470.363	.000680
4.0	16.00	400.00	17.00	401.00	1704.250	.000587
5.0	25.00	625.00	26.00	626.00	3255.200	0.000307
6.0	36.00	900.00	37.00	901.00	5556.17	.000180
7.0	49.00	1225.00	50.00	1226.00	8757.14	.000114
8.0	64.00	1600.00	65.00	1601.00	13008.13	.0000769

For formula used see table9.

Table 11 --- Instrument VIB --- Determination of step-function response characteristic; theoretical adjustment

T_o=1 sec; T_g=0.2 sec; Aperiodic damping

t	$2+(\omega_o-\omega_g)t$	$2+(\omega_o-\omega_g)t$	$\omega_o t$	$e^{-\omega_o t}$	$\omega_g t$	$e^{-\omega_g t}$	U
0.0159	+ 1.6	+ 2.4	0.1	0.904837	0.5	0.606531	$0.0^5 4995$
.0318	1.2	2.8	.2	.818731	1.0	.367879	$.0^4 2997$
.0477	0.8	3.2	.3	.740818	1.5	.223130	$.0^4 7645$
.0637	0.4	3.6	.4	.670320	2.0	.135335	$.0^3 13800$
.0796	0.0	4.0	.5	.606531	2.5	.082085	$.0^3 20683$
.0955	- 0.4	4.4	.6	.548812	3.0	.049787	$.0^3 27627$
.1114	0.8	4.8	.7	.496585	3.5	.030197	$.0^3 34155$
.1273	1.2	5.2	.8	.449329	4.0	.018316	$.0^3 39964$
.1432	1.6	5.6	.9	.406570	4.5	.011109	$.0^3 44895$
0.1592	- 2.0	+ 6.0	1.0	0.367879	5.0	0.006738	$0.0^3 48893$
.1751	2.4	6.4	1.1	.332871	5.5	.004087	$.0^3 51971$
.1910	2.8	6.8	1.2	.301194	6.0	.002479	$.0^3 54185$
.2069	3.2	7.2	1.3	.272532	6.5	.001503	$.0^3 55616$
.2228	3.6	7.6	1.4	.246597	7.0	$.0^3 9119$	$.0^3 56357$
.2387	4.0	8.0	1.5	.223130	7.5	$.0^3 553$	$.0^3 56499$
.2546	4.4	8.4	1.6	.201897	8.0	$.0^3 3355$	$.0^3 56135$
.2706	4.8	8.8	1.7	.182684	8.5	$.0^3 203$	$.0^5 55348$
.2865	5.2	9.2	1.8	.165299	9.0	$.0^3 1234$	$.0^3 54216$
0.3820	- 7.6	+ 11.6	2.4	0.090718	12.0	$.0^5 61$	$0.0^3 43434$
.4775	10.0	14.0	3.0	.049787	15.0	$.0^6 3059$	$.0^3 31361$
.5730	12.4	16.4	3.6	.027324	18.0	$.0^7 1523$	$.0^3 21342$
.6685	14.8	18.8	4.2	.014996	21.0	$.0^8 206$	$.0^3 13980$
.7639	17.2	21.2	4.8	.008230	24.0	$.0^{10} 3775$	$.0^4 3916$
.8594	19.6	23.6	5.4	.004517	27.0	$.0^{11} 1880$	$.0^4 5577$
.9549	22.0	26.0	6.0	.002479	30.0	$.0^{13} 9358$	$.0^4 3435$
1.0504	24.4	28.4	6.6	.001360	33.0	$.0^{14} 2320$	$.0^4 2091$
1.1459	- 26.8	+ 30.8	7.2	$0.0^3 7466$			$0.0^4 1260$
1.2414	29.2	33.2	7.8	$.0^3 4097$			$.0^5 753$
1.3369	31.6	35.6	8.4	$.0^3 2249$			$.0^5 447$
1.4324	34.0	38.0	9.0	$.0^3 1234$			$.0^5 265$
1.5279	36.4	40.4	9.6	$.0^4 677$			$.0^5 155$
1.6234	38.8	42.8	10.2	$.0^4 372$			$.0^6 907$
1.7189	41.2	45.2	10.8	$.0^4 204$			$.0^6 529$
1.8144	43.6	47.6	11.4	$.0^4 112$			$.0^6 314$
1.9099	46.0	50.0	12.0	$.0^5 614$			$.0^6 178$

0.0^3 indicates the number of zeros before the first significant figure in the decimal place

See table 7 for the formula used

Table 12 --- Instrument VI --- Determination of response curve

T_o=0.016 sec (ca); T_g=70 sec; Aperiodic damping

u	log 1/G	1/G	G	T_e	u	log 1/G	1/G	G	T_e
0.01	0.0000	1.0000	1.0000	0.7	0.41	0.0675	1.1682	0.8560	28.7
.02	.0002	1.0005	0.9995	1.4	.42	.0706	1.1765	.8500	29.4
.03	.0004	1.0010	.9990	2.1	.43	.0737	1.1850	.8439	30.1
.04	.0007	1.0016	.9984	2.8	.44	.0769	1.1937	.8377	30.8
.05	.0011	1.0025	.9975	3.5	.45	.0801	1.203	.8312	31.5
.06	.0016	1.0037	.9963	4.2	.46	.0834	1.212	.8251	32.2
.07	.0021	1.0049	.9951	4.9	.47	.0867	1.221	.8190	32.9
.08	.0028	1.0065	.9935	5.6	.48	.0900	1.230	.8130	33.6
.09	.0035	1.0081	.9920	6.3	.49	.0935	1.240	.8065	34.3
.10	.0043	1.0100	.9901	7.0	.50	.0969	1.250	.8000	35.0
0.11	0.0052	1.0120	0.9881	7.7	0.51	0.1004	1.260	0.7937	35.7
.12	.0062	1.0144	.9858	8.4	.52	.1039	1.270	.7874	36.4
.13	.0073	1.0170	.9833	9.1	.53	.1075	1.281	.7806	37.1
.14	.0084	1.0195	.9809	9.8	.54	.1111	1.292	.7740	37.8
.15	.0097	1.0226	.9779	10.5	.55	.1148	1.303	.7675	38.5
.16	.0110	1.0257	.9749	11.2	.56	.1185	1.314	.7610	39.2
.17	.0124	1.0290	.9718	11.9	.57	.1222	1.325	.7547	39.9
.18	.0138	1.0323	.9687	12.6	.58	.1259	1.336	.7485	40.6
.19	.0154	1.0361	.9652	13.3	.59	.1297	1.348	.7418	41.3
.20	.0170	1.0400	.9615	14.0	.60	.1335	1.360	.7353	42.0
0.21	0.0187	1.0440	0.9579	14.7	0.61	0.1374	1.372	0.7289	42.7
.22	.0205	1.0483	.9539	15.4	.62	.1413	1.385	.7220	43.4
.23	.0224	1.0529	.9498	16.1	.63	.1452	1.397	.7158	44.1
.24	.0243	1.0575	.9456	16.8	.64	.1491	1.410	.7092	44.8
.25	.0263	1.0624	.9413	17.5	.65	.1531	1.423	.7027	45.5
.26	.0284	1.0676	.9367	18.2	.66	.1570	1.436	.6964	46.2
.27	.0306	1.0730	.9320	18.9	.67	.1610	1.449	.6901	46.9
.28	.0328	1.0785	.9272	19.6	.68	.1651	1.463	.6835	47.6
.29	.0351	1.0842	.9223	20.3	.69	.1691	1.476	.6775	48.3
.30	.0374	1.0899	.9175	21.0	.70	.1732	1.490	.6711	49.0
0.31	0.0399	1.0962	0.9122	21.7	0.71	0.1773	1.504	0.6649	49.7
.32	.0423	1.1023	.9072	22.4	.72	.1814	1.518	.6588	50.4
.33	.0449	1.1089	.9018	23.1	.73	.1855	1.533	.6523	51.1
.34	.0475	1.1156	.8964	23.8					
.35	.0502	1.1225	.8909	24.5	0.80	0.2148	1.640	0.6098	56.0
.36	.0529	1.1295	.8853	25.2					
.37	.0557	1.1368	.8797	25.9	0.90	0.2577	1.810	0.5525	63.0
.38	.0586	1.1445	.8737	26.6					
.39	.0615	1.1521	.8680	27.3	1.00	0.3010	2.000	0.5000	70.0
.40	.0645	1.1601	.8620	28.0					

Table 13---List of earthquakes used for this report

No.	Region	Date(GCT)	Time (GCT)	Mag.	Location
1-60	Alaska	Apr. 16, 1940	06:07:43	7.1	53N 173½E
1-110	Alaska	Dec. 12, 1944	04:17:10	7.0	51½N 179½W
1-550	Alaska	Nov. 3, 1943	14:32:17	7.3	61-3/4N 151W
5-705	Mexico	June 28, 1944	07:58:54	7.0	15N 92½W
5-825	Mexico	May 2, 1943	23:36:59	7.7	14N 91W h=50±km
6-400	Cent.America	Dec. 6, 1941	21:24:40	6.9	8½N 84W
6-440	Cent.America	Dec. 5, 1941	20:46:58	7.5	8½N 83W
6-680	Cent.America	May 2, 1943	17:18:09	7.0	6½N 80W
7-170	Caribbean	Apr. 7, 1941	23:29:17	7.1	17-3/4N 78½W
7-430	Caribbean	July 29, 1943	03:02:16	7-3/4	19¾N 67½W
8-190	So.America	Aug. 23, 1944	23:40:01	6.9	½N 80½W
8-210	So.America	May 14, 1942	02:13:18	7.9	3/4S 81½W
8-420	So.America	Aug. 24, 1942	22:50:27	8.1	15S 76W
8-760	So.America	Apr. 6, 1943	16:07:15	7.9	30-3/4S 72W h=60±km
13-100	Fiji Islands	Oct. 21, 1943	23:08:13	7.0	15S 177½W
14-440	New Hebrides	Dec. 10, 1944	16:24:58	7.3	18S 168E h=60 km
14-820	New Hebrides	Nov. 16, 1944	12:10:58	7.3	12½S 167E
19-340	Japan	Feb. 18, 1945	10:08:07	7.0	42N 143E h=60 km
19-455	Kurile Is.	Oct. 26, 1942	21:09:13	7.2	45½N 151½E h=60 km
19-565	Kamchatka	Aug. 23, 1942	06:35:21	7.0	53N 163½E h=60 km
19-575	Kamchatka	Sep. 23, 1944	12:13:20	7.2	54N 160E h=40 km
19-670	Kamchatka	Apr. 15, 1945	02:35:22	7.0	57N 164E
31-420	E.Atlantic Oc.	Nov. 25, 1941	18:03:55	8.3	37½N 18½W
5-330	Mexico	Apr. 15, 1941	19:09:56	7.6	18N 103W *
5-345	Mexico	Feb. 26, 1943	09:20:45	7.5	17-3/4N 101½W *

* These shocks are at epicentral distances of 20.2° and 23°, respectively, and are too close for this study as PcP is lost in the S group.

Table 13 (cont'd)

No.	Region	Date (GCT)	Time (GCT)	Mag.	Location
8-330	So.America	May 24, 1940	16:38:57	8.0	10½S 77W **
32-455	Atlantic Oc.	Nov. 28, 1942	10:38:45	7.1	7½N 36W ***
1-61	Alaska	Apr. 16, 1940	06:43:07	7.2	52N 173½E ****

** This shock occurred while the records were being changed and relationships are not clear.

*** This shock wrote too small a record at Pasadena for the purposes of this report.

**** This shock overwritten by shock no. 1-60.

Table 14 --- Measurements of trace amplitudes and trace periods of P, PcP, PcS, S, and ScS, and the calculations of the ratios of the square roots of the energies for PcP/P, PcS/P, ScS/S, and ScP/S.

Abbreviations used in the following table

A^* = trace amplitude
T_e = trace period
A_e = amplitude of ground motion
R = $\frac{A_e/A^*}{T_e}$ for the torsion seismographs, $\frac{k/a}{T_e}$ for the electromagnetic seismographs, and $\frac{l/G}{T_e}$ for the strain seismograph

S_1 = $\frac{u_{EW}PcP}{u_{EW}P}$, $\frac{u_{NS}PcP}{u_{NS}P}$, or $\frac{w\ PcP}{w\ P}$

S_2 = $\frac{u_{EW}PcS}{u_{EW}P}$, $\frac{u_{NS}PcS}{u_{NS}P}$, or $\frac{w\ PcS}{w\ P}$

S_3 = $\frac{u_{EW}ScS}{u_{EW}S}$, $\frac{u_{NS}ScS}{u_{NS}S}$, or $\frac{w\ ScS}{w\ S}$

S_4 = $\frac{u_{EW}ScP}{u_{EW}S}$, $\frac{u_{NS}ScP}{u_{NS}S}$, or $\frac{w\ ScP}{w\ S}$

np = not perceptible enough for a clear reading
ni = no instrument in operation
nra = no record available in the files
ov = trace overridden so badly by other waves or by instrument drift as to make recognition or measurement impossible
tr = small amount of motion shows on record, but not enough for a reasonable reading

SHOCK NO.	REGION	DATE (G.C.T.)	ORIGIN TIME	MAG.	LOCATION	Δ
1-60	Alaska	4-16-40	06:07:43	7.1	52N173½E	50.3

QUAL.	PAD	h	AZIMUTH
A	61:133	-	312½

PHASE	P										
INST.	A*	Te	R	RA*	A*	Te	R	RA*			
I											
IVA	1.7	7.5	1.02	1.73							
VA	ni										
VI											
VIBN											
II											
IVB	2.5	7.0	1.02	2.55							
V	1.4	3.5	0.38	0.53							
VIBE	0.8	1.0	52	41.6							
IIA	2.3	2.0	1.25	2.88							
VIA	5.0	1.0	40	200							

PHASE	PcS										
INST.	A*	Te	R	RA*	A*	Te	R	RA*	S_2	S_4	
I											
IVA	1.4	8.0	1.02	1.43					0.826	0.274	
VA											
VI											
VIBN											
II											
IVB	2.2	12.0?	1.025	2.255					0.886	0.257	
V											
VIBE											
IIA	6.2	9.4	1.02	6.33					1.82	1.53	
VIA	2.0	2.0	96	192					0.96	0.316	

PHASE	S				ScS					
INST.	A*	Te	R	RA*	A*	Te	R	RA*	S_3	
I										
IVA	5.1	12.0	1.035	5.23	5.2	24.0	1.07	5.56	1.06	
VA	ni									
VI	0.4	8.0	0.128	0.051	1.1	9.0	0.114	0.126	2.45	
VIBN										
II										
IVB	8.5	16.0	1.035	8.79	5.7	16.0	1.035		0.671	
V	4.6	5.5	3.0	13.8						
VIBE	0.9	3.6	340 ±	306						
IIA	4.0	16.0	1.035	4.14	3.5	11.0	1.025	3.62	0.875	
VIA	1.6	4.3	380 ±	608	0.8	4.5	422	338	0.555	

SHOCK NO.	REGION	DATE (G.C.T.)	ORIGIN TIME	MAG.	LOCATION	Δ
1-110	Alaska	12-12-44	04:17:10	7.0	51½N179½E	46.4

QUAL.	PAD		AZIMUTH
B	74:606	50+	312

PHASE	P				PcP						
INST.	A*	Te	R	RA*	A*	Te	R	RA*	S_1		
I											
IVA											
VA											
VI											
VIBN											
II											
IVB											
V											
VIBE											
IIA	1.8	8.0	1.02	1.90	1.8	8.0	1.02	1.90	1.0		
VIA	1.7	1.5	63	-							

PHASE	PcS										
INST.	A*	Te	R	RA*	A*	Te	R	RA*	S_2	S_4	
I											
IVA											
VA											
VI											
VIBN											
II											
IVB											
V											
VIBE											
IIA	2.0	7.6	1.02	2.04					1.06	0.565	
VIA											

PHASE	S				ScS						
INST.	A*	Te	R	RA*	A*	Te	R	RA*	S_3		
I											
IVA	2.0	7.0	1.03	2.06	2.0	12.0	1.025	2.05	1.005		
VA											
VI											
VIBN											
II											
IVB	2.5	10.0	1.02	2.55							
V	2.3	7.0	0.34	0.78							
VIBE	0.7	7.0									
IIA	3.5	13.6	1.03	3.61	1.8	8.4	1.02	1.84	0.664		
VIA											

SHOCK NO	REGION	DATE (G.C.T.)	ORIGIN TIME	MAG.	LOCATION	Δ
1-550	Alaska	11-3-43	14:32:17	7.3	613/4N151W	34.6

QUAL.	PAD	h	AZIMUTH
A	71:498	-	334

PHASE	P				PcP				S_1		
INST.	A*	Te	R	RA*	A*	Te	R	RA*			
I	tr										
IVA	5.0	5.0	1.04	5.20	4.0	5.3	1.04	4.16	0.800		
VA	ni				ni						
VI	tr										
VIBN	13.3	1.0	52	692	4.8	3.0	251	1200	1.74		
II	tr										
IVB	5.2	5.0	1.04	5.41	2.5	5.0	1.04	2.60	0.480		
V	2.0	2.5	0.51	1.02	2.0	3.0	0.42	0.84	0.823		
VIBE	11.5	1.0	52	598	4.3	3.0	251	1079	1.80		
IIA	21.8	4.0	1.06	23.1	5.5	5.3	1.04	5.72	0.248		
VIA	29.8	1.3	52	1550	9.5	2.0	96	912	0.588		

PHASE	PcS								S_2	S_4	
INST.	A*	Te	R	RA*	A*	Te	R	RA*			
I											
IVA	12.5	13.0	1.03	12.9					2.48	1.26	
VA	ni										
VI	lost in S										
VIBN	2.3	8.0	1626	3740					5.41	1.15	
II											
IVB	11.8	14.0	1.03	12.2					2.25	0.686	
V	1.5	4.8	3.1	4.65					4.56	0.674	
VIBE	2.5	3.0	251	628					1.05	0.616	
IIA	27.4	12.0	1.025	28.1					1.22	1.95	
VIA	Not clear										

PHASE	S				ScS				S_3		
INST.	A*	Te	R	RA*	A*	Te	R	RA*			
I											
IVA	10.0	9.5	1.02	10.2		lost					
VA	ni										
VI	7.0	20.0	0.054								
VIBN	5.0	5.0	651	3255		in					
II											
IVB	17.2	14.0	1.03	17.7		surface					
V	2.3	5.5	3.0	6.90							
VIBE	2.4	4.0	426	1020							
						waves					
IIA	14.0	12.0	1.025	14.4							
VIA	2.5	3.0	190	475							

SHOCK NO.	REGION	DATE (G.C.T.)	ORIGIN TIME	MAG.	LOCATION	△
5-705	Mexico	6-28-44	23:36:59	7.0	15N92½W	29.8

QUAL.	PAD	h	AZIMUTH
B	68-395	50 ±	122½

PHASE	P				PcP				S_1
INST.	A*	Te	R	RA*	A*	Te	R	RA*	
I	np				np				
IVA	3.1	14.0	1.03	3.19	1.8	11.0	1.02	1.84	0.577
VA	ni				ni				
VI	np				np				
VIBN	2.3	0.8	43.5	100	doubtful				
II	np								
IVB	4.8	14.0	1.03	4.94	2.8	11.0	1.02	2.86	0.579
V	2.7	4.0	0.34	0.919	1.3	4.5	0.325	0.423	0.460
VIBE	2.0	0.8	43.5	87	doubtful				
IIA	12.0	14.0	1.03	12.4	2.3	7.0	1.025	2.36	0.190
VIA	2.8	2.0	95.5	268	2.0	1.3	52.5	105	0.392

PHASE	PcS								
INST.	A*	Te	R	RA*	A*	Te	R	RA*	
I									
IVA									
VA		lost							
VI									
VIBN									
		in							
II									
IVB		S							
V									
VIBE									
IIA									
VIA									

PHASE	S				ScS				S_2
INST.	A*	Te	R	RA*	A*	Te	R	RA*	
I	np								
IVA	11.5	12.0	1.025	11.8	in long waves				
VA	ni				ni				
VI									
VIBN	1.2	7.2	-	-	doubtful				
II	np								
IVB	10.5	10.0	1.02	10.7	in long waves				
V	3.9	11.5	0.38	1.48	" " "				
VIBE	1.4	3.8	387	542	doubtful				
IIA	14.5	23.0	1.065	15.4	doubtful				
VIA	-								

SHOCK NO.	REGION	DATE (G.C.T.)	ORIGIN TIME	MAG.	LOCATION	△
5-825	Mexico	8-6-42	23:36:59	7.7	14N91W	32.1

QUAL.	PAD	h	AZIMUTH
B	68:395	50^{t}	123

PHASE	P				PcP				S_1		
INST.	A*	Te	R	RA*	A*	Te	R	RA*			
I	0.4	1.1	0.615	0.246	-						
IVA	4.0	2.5	1.162	4.65	5.0	3.0	1.112	5.56	1.195		
VA	ni										
VI	ni										
VIBN	11.5	1.0	52.0	598	lost in aftershock ov.						
IVA	2.5	10.0	1.023	2.56	2.8	12.0	1.025	2.87	1.121		Addl.rdg.
II	0.3	1.1	0.970	0.291	-						
IVB	5.5	2.8	1.130	6.21	4.5	3.0	1.112	5.00	0.806		
V	2.8	2.8	0.455	1.274	3.3	3.2	0.410	1.352	1.061		
VIBE	8.5	1.0	52.0	612	lost in aftershock ov.						
IVB	2.5	9.0	1.022	2.55	-						Addl.rdg.
IIA	33.0	2.0	1.251	41.3	9.0	2.0	1.251	11.27	0.273		
VIA	23.5	1.0	39.81	936	11.0	1.5*	62.88	692	0.739		
IIA	18.0	8.0	1.024	18.42	8.5	10.0	1.023	8.70	0.472		Addl.rdg.

PHASE	PcS										
INST.	A*	Te	R	RA*	A*	Te	R	RA*			
I											
IVA											
VA		lost									
VI											
VIBN											
		in									
II											
IVB											
V											
VIBE		S									
IIA											
VIA											

PHASE	S				ScS						
INST.	A*	Te	R	RA*	A*	Te	R	RA*			
I	2.3	8.0									
IVA	> 65	13.0**									
VA	ni										
VI	ni					lost					
VIBN	10.5	6.0									
II	1.5	5.0				in					
IVB	110	13.0									
V	23.6	15.0									
VIBE	17.4	4.5				L					
II	1.8	8.0									Addl.rdg.
IIA	74.5	27									
VIA	11.0	5.5									

*May be larger ---Superimposed trace; **off record

SHOCK NO.	REGION	DATE (G.C.T.)	ORIGIN TIME	MAG.	LOCATION	△
6-400	Cent.America	12-6-41	21:24:40	6.9	8½N84W	40.8

QUAL.	PAD	h	AZIMUTH
A	68:370		127

PHASE	P				PcP				S_1		
INST.	A*	Te	R	RA*	A*	Te	R	RA*			
I											
IVA	2.6	4.0	1.065	2.77	lost	in PP					
VA	ni				ni						
VI	ov.				ov.						
VIBN	3.6	1.5	82.7	298	1.3	1.0	52.0	67.6	0.227		
II											
IVB	3.5	5.0	1.043	3.65	lost	in PP					
V	3.0	5.0	0.31	0.930	tr ---	but in PP					
VIBE	2.0	4.0	426	852	2.4	1.0	52	125	0.147		
IIA	10.0	5.0	1.043	10.43	lost	in PP					
VIA	8.5	4.0	322	2740	4.3	1.4	57.5	247	0.090		

PHASE	PcS								S_2	S_4	
INST.	A*	Te	R	RA*	A*	Te	R	RA*			
I											
IVA	0.4	4.0	1.065	0.426					0.154	0.415	
VA	ni										
VI	ov										
VIBN	0.5	4.5	530±	265					0.889	0.081	
II											
IVB	1.9	7.0	1.026	1.95					0.534	0.107	
V	1.2	6.5	0.29	0.348					0.374	0.105	
VIBE	0.5	6.0	926	463					0.544	0.122	
IIA	1.7	7.0	1.026	1.74					0.167	0.240	
VIA	np										

PHASE	S				ScS				S_3		
INST.	A*	Te	R	RA*	A*	Te	R	RA*			
I											
IVA	10.0	13.0	1.027	10.27	lost	in L					
VA	ni				ni						
VI	ov				ov						
VIBN	2.0	6.0	926	1852	lost	in L					
VIBN	1.3	10.0	2526	3280							Addl.rdg.
V	8.5	12.0	0.39	3.32							Addl.rdg.
II											
IVB	17.7	14.0	1.029	18.2	lost	in L					
V	8.7	7.5	0.30	2.61	lost	in L					
VIBE	2.0	6.0	926	1852	lost	in L					
VIBE	1.5	10.0	2526	3790							Addl.rdg.
IIA	7.1	9.5	1.022	7.26	3.4	8.0	1.024	3.48	0.480		
VIA	1.3	9.0			np						

SHOCK NO.	REGION	DATE (G.C.T.)	ORIGIN TIME	MAG.	LOCATION	△
6-440	Cent. America	12-5-41	20:46:58	7.5	8½N83W	40.9

QUAL.	PAD	h	AZIMUTH
A	68:370		126

PHASE	P				PcP				S_1		
INST.	A*	Te	R	RA*	A*	Te	R	RA*			
I	0.9	1.0	0.575		<0.3	?					
IVA	11.4	2.0	1.25	14.3	?						
VA	ni				ni						
VI	ov				ov						
VIBN	25.2	1.2	62.7	1580	in PP?						
I	1.0	2.0	1.085								Addl.rdg.
II	0.7	3.0			<0.3	?					
IVB	22.7	3.0	1.11	25.2	?						
V	14.2	4.0	0.34	4.83	3.8	5.0*	0.31	1.18	0.244		
VIBE	38	1.2	62.7		in PP?						
IIA	ov				ov						
VIA	>50	1.8	81.5	>4075	5.9	0.8*	33.6	198	<0.049		

PHASE	PcS								S_2	S_4	
INST.	A*	Te	R	RA*	A*	Te	R	RA*			
I	0.3	10	?								
IVA	?										
VA	ni										
VI	ov										
VIBN	1.1	9	?								
II	<0.1	?									
IVB	7.9	10.0	1.023	8.08					0.321		
V	5.7	8.0	0.305	1.74					0.360	0.268	
VIBE	no clear wave motion										
IIA	ov										
VIA	0.6	10.0**	2526	1516					0.372	0.187	

PHASE	S				ScS				S_3		
INST.	A*	Te	R	RA*	A*	Te	R	RA*			
I	1.5	12.0			in L. waves						
IVA	18.5	14.0	1.03	19.1	in L. waves						
VA	ni				ni						
VI	ov				ov						
VIBN	5.0	12	?		?						
II	0.5	12.0			in L. Waves						
IVB	?				in L. waves						
V	16.6	12.0	0.39	6.48	8.6	8.5	0.31	2.66	0.410		
VIBE	2.5	12	-		?						
IIA	off record				?						
VIA	6.6	8.0	-		?						
VIA	3.8	11.5	-								Addl.rdg.

* May be part of PP; ** Small period superimposed

SHOCK NO.	REGION	DATE (G.C.T.)	ORIGIN TIME	MAG.	LOCATION	△
6-680	Cent. America	5-2-43	17:18:09	7.1	6½N80W	44.2

QUAL.	PAD	h	AZIMUTH
B	71:470	60±	119½

PHASE	P				PcP*				S_1		
INST.	A*	Te	R	RA*	A*	Te	R	RA*			
I	0.15	1.5	0.805	0.121	np						
IVA	2.0	3.0	1.112	2.224	2.4	3.5	1.080	2.592	1.165		
VA	ni				ni						
VI	ni				ni						
VIBN	9.7	1.6	90.39	877	3.0	1.5	82.69	248	0.283		
II	0.3	1.5	1.320	0.396	np						
IVB	5.0	3.0	1.112	5.560	3.3	4.2	1.068	3.524	0.634		
V	1.6	2.6	0.486	0.778	1.1	3.0	0.426	0.469	0.603		
VIBE	9.8	1.5	82.69	810	3.0	1.4	75.51	227	0.279		
IIA	13.5	2.2	1.205	16.27	6.0	3.0	1.112	6.672	0.410		
VIA	20.9	2.0	95.77	2002	6.0	1.8	81.46	489	0.244		

PHASE	PcS								S_2	S_4	
INST.	A*	Te	R	RA*	A*	Te	R	RA*			
I	0.15	7.0	3.91	0.586					4.85		
IVA	2.4	8.0	1.024	2.46					1.105		
VA	ni										
VI	ni										
VIBN	1.3	4.0	426	554					0.632	0.763	
II	0.05	0.5	0.740	0.0370					0.0934		
IVB	2.2	5.5	1.036	2.28					0.410	0.113	
V	0.7	4.0	0.344	0.241					0.309	0.412	
VIBE	0.9	3.5	330	297					0.366	0.317	
IIA	4.1	7.0	1.026	4.20					0.258	0.685	
VIA	2.0	4.5	397	794					0.397	0.827	

PHASE	S				ScS				S_3		
INST.	A*	Te	R	RA*	A*	Te	R	RA*			
I	0.25	5			np						
IVA	6.5	9.0	1.022	6.643	Period?---Large kick						
VA	ni				ni						
VI	ni				ni						
VIBN	2.2	3.5	330	727	1.0	6.0	926	926	1.273		
IVB	21.5	23	1.066	22.9							Addl.rdg.
II	0.1	5?									
IVB	19.5	6.0	1.033	20.14	7.0	8.0	1.024	7.168	0.356		
V	1.7	4.0	0.344	0.585	0.3	4.0	0.344	0.103	0.176		
VIBE	2.2	4.0	426	937	1.2	6.0	926	1111	1.186		
V	2.5	20	0.626	1.565							Addl.rdg.
IIA	6.0	8.0	1.024	6.144	4.5	9.0	1.022	4.599	0.749		
VIA	2.4	4.5	400	960	Unreadable						

* PcP followed closely by PP

SHOCK NO	REGION	DATE (G.C.T.)	ORIGIN TIME	MAG.	LOCATION	Δ
7-170	Caribbean	4-7-41	23:29:17	7.1	173/4N78½W	39.8

QUAL.	PAD	h	AZIMUTH
A	56:53		104.5

PHASE	P				PcP				S1		
INST.	A*	Te	R	RA*	A*	Te	R	RA*			
I	0.2	2.2	1.19	0.238	0.3	2.5	1.36	0.408	1.715		
IVA	2.2	2.2	1.207	2.655	4.3	2.7	1.137	4.89	1.840		
VA	ni				ni						
VI	ni				ni						
VIBN	9.0	1.8	107.3	966	4.7	2.5	182.2	857	0.887		
II	0.3	3.5	3.13	0.939	0.3	3.3?	2.94	0.883	0.940		
IVB	4.3	3.2	1.097	4.72	6.5	4.0	1.065	6.92	1.467		
V	2.7	3.2	0.410	1.107	3.1	3.9*	0.353	1.094	0.988		
VIBE	9.3	2.8	222.1	2065	5.9	3.5	331.5	1956	0.947		
IIA	8.1	4.2	1.058	8.58	large but indefinite						
VIA	30±	2.5	138.0		9.7	2.5	138.0		0.323		

PHASE	PcS								S_2	S_4	
INST.	A*	Te	R	RA*	A*	Te	R	RA*			
I	in time marks										
IVA	1.7	7.0	1.0263	1.744					0.657	0.319	
VA	ni										
VI	ni										
VIBN	1.8	3.5	322	580					0.607	0.651	
II	np										
IVB	3.3	7±	1.026	3.38					0.716	0.153	
V	2.1	7.5	0.299	0.628					0.567	0.224	
VIBE	too small and irregular										
IIA	3.9	6.5	1.03	4.02					0.469	0.345	
VIA	-										

PHASE	S				ScS						
INST.	A*	Te	R	RA*	A*	Te	R	RA*			
I	0.2	4.0	2.21	0.442							
IVA	5.3	15.0	1.032	5.47							
VA	ni										
VI	ni					Lost					
VIBN	2.7	3.5	330	891							
VIBN	2.2	4.0	426	937							Addl. rdg.
						after					
II	0.3	5.0	4.29	0.129							
IVB	21.0	20	1.053	22.1							
V	8.4	9.5	0.334	2.81		L					
VIBE	2.3	6.0	926	2130							
IIA	11.4	10.0	1.023	11.67							
VIA	2.4	9½	?								

* doubtful --- in large waves of PP

SHOCK NO.	REGION	DATE (G.C.T.)	ORIGIN TIME	MAG.	LOCATION	Δ
7-430	Caribbean	7-29-43	03:02:16	7.75	19½N67½W	47.5

QUAL.	PAD	h	AZIMUTH
A	71:463		95

PHASE	P				PcP				S1		
INST.	A*	Te	R	RA*	A*	Te	R	RA*			
I											
IVA	6.4	3.5	1.08	6.91	3.6	3.0	1.112	4.00	0.579		
VA	ni										
VI	ni										
VIBN	26	1.0	52.0	1352	14.7	1.0	52.0	765	0.566		
II	0.6	3.2	2.86	1.716	0.7	3.0	2.675	1.873	1.092		
IVB	8.9	3.7	1.073	9.56	9.1	2.7	1.138	10.36	1.083		
V	6.1	3.3	0.401	2.45	5.8	3.0	0.423	2.46	1.003		
VIBE	21.7	1.0	52.0	1128	17.8	1.2	62.69	1117	0.990		
IIA	29.2	3.0	1.112	32.5	Indistinct but large						
VIA	38.5	1.0	39.81	1532	21	1.4	57.47	1206	0.788		

PHASE	PcS								S_2	S_4	
INST.	A*	Te	R	RA*	A*	Te	R	RA*			
I											
IVA	3.0±	10	1.0225	3.0675					0.444	0.107	
VA	ni										
VI	ni										
VIBN	in small local quake										
II	<0.1										
IVB	lost by ov.										
V	1.3	2.5	0.508	0.661					0.270	0.661	
VIBE	lost in local quake										
IIA	lost										
VIA	lost in local quake										

PHASE	S				ScS				S_3		
INST.	A*	Te	R	RA*	A*	Te	R	RA*			
I	0.9	7.0			0.3	7 or 8			0.333		
IVA	27.9	8.0	1.0238	28.6	lost in S						
VA	ni										
VI	ni										
VIBN	7.4	6.0			lost in S						
II	0.2	8.0**			0.1	8.0?			0.500		
IVB	lost	by ov.			ov.						
V	2.7	3.8	0.371	1.00	1.8	4.5*	0.324	0.583	0.583		
VIBE	3.5	3.7			lost in S						
IIA	ov.				ov.						
VIA	4.5	3.0			3.0	3.0			0.667		

* doubtful ** response one-sided

SHOCK NO.	REGION	DATE (G.C.T.)	ORIGIN TIME	MAG.	LOCATION	Δ
8-190	No. South America	10-23-44	23:40:01	6.9	½N80½W	48.3

QUAL.	PAD	h	AZIMUTH
A	74:598		126

PHASE	P				PcP				S_1		
INST.	A*	Te	R	RA*	A*	Te	R	RA*			
I											
IVA	0.8	6	1.03	0.824	np						
VA	ni				ni						
VI	1.5	3.0	0.333		np						
VIBN	2.3	0.8	43.6	100	1.1	1.8	107.3	118	1.18		
II											
IVB	1.0	6.0	1.03	1.03	np						
V	1.7	6.0	0.29	0.493	np						
VIBE	2.4	1.7	98.6	236	0.9	1.8	107.3	96.6	0.409		
IIA	5.0	10.0	1.02	5.10	2.0	5.0	1.04	2.08	0.408		
VIA	4.2	1.5	62.9	264	0.8	1.5	62.9	50.3	0.191		

PHASE	PcS								S_2	S_4	
INST.	A*	Te	R	RA*	A*	Te	R	RA*			
I											
IVA	tr?										
VA	ni										
VI											
VIBN	np										
II											
IVB	tr?										
V	np										
VIBE	np										
IIA	1.3	14.0	1.03	1.34					0.263	0.504	
VIA	np										

PHASE	S				ScS				S_3		
INST.	A*	Te	R	RA*	A*	Te	R	RA*			
I											
IVA	5.0	20	1.05	5.10	0.7	20	1.05	0.735	0.144		
VA	ni										
VI	3.0	30.0	0.039								
VIBN	0.6	6.0			0.03	6.0			0.05		
II											
IVB	2.3	20	1.05	2.42	0.8	20	1.05	0.840	0.347		
V	1.6	12.0	0.395	0.632	1.4	15	0.48	0.672	1.06		
VIBE	0.3	6.0			0.05	6.0			0.167		
IIA	2.6	12.0	1.025	2.66	1.8	10.0	1.02	1.84	0.692		
VIA	0.3	6.0			0.05	7.5	-				

SHOCK NO.	REGION	DATE (G.C.T.)	ORIGIN TIME	MAG.	LOCATION	Δ
8-210	So.America	5-14-42	02:13:18	7.9	3/45S81½W	48.3

QUAL.	PAD	h	AZIMUTH
B	68:381		129

PHASE	P				PcP				S_1		
INST.	A*	Te	R	RA*	A*	Te	R	RA*			
I	0.6	3.0	1.635	0.981	0.6	3.0	1.635	0.981	1.00		
IVA	6.1	4.4	1.053	6.43	4.9	3.0	1.112	5.55	0.864		
VA	ni				ni						
VI	ni				ni						
VIBN	11.7	2.0	126.3	1478	9.5	3.0	251.1	2380	1.612		
II	0.6	3.5	3.13	1.88	0.35	2.5	2.23	0.781	0.415		
IVB	10.5	4.8	1.047	10.99	6.0	4.0	1.065	6.38	0.581		
V	6.0	4.0	0.344	2.06	4.0	3.5	0.380	1.52	0.737		
VIBE	not well recorded				not well recorded						
IIA	21.1	5.0	1.043	22.0	11.0	4.0*	1.065	11.72	0.532		
VIA	25.2	1.8	81.46	2050	14.2	2.0	95.77	1360	0.663		

PHASE	PcS								S_2	S_4	
INST.	A*	Te	R	RA*	A*	Te	R	RA*			
I	np	?									
IVA	3.5	8.0*	1.024	3.59					0.559	0.0437	
VA	ni										
VI	ni										
VIBN	not well recorded										
II	not distinguishable										
IVB	5.0	6.0*	1.033	5.165					0.470	0.0781	
V	1.4	3.8	0.360	0.504					0.244	0.0927	
VIBE	not well recorded										
IIA	ov - doubtful										
VIA	4.0	2.0	95.77	383					0.187		

PHASE	S				ScS				S_3		
INST.	A*	Te	R	RA*	A*	Te	R	RA*			
I	0.7	7.0			0.6	7.0			0.858		
IVA	72½	34	1.135	82.3	9	12.0	1.025	9.23	0.112		
VA	ni										
VI	ni										
VIBN	3.7	6.0	700	2590	3.0	6.5	800±	2400	0.926		
II	0.2	11	9.81	1.96	0.3	8	7.13	2.14	1.092		
IVB	57½	36	1.150	66.1	23.0	26	1.083	24.9	0.376		
V	5.0	6.0	0.292	1.461	5.0	8.0	0.305	1.525	1.044		
VIBE	3.3	6.0	926	3150	3.3	7.0	1251	4130	1.301		
V	5.5	32	0.990	5.44					0.280		Addl.rdg.
IIA	23.5	28			not distinguishable						
VIA	too long period				too long period						

* doubtful

SHOCK NO.	REGION	DATE (G.C.T.)	ORIGIN TIME	MAG.	LOCATION	Δ
8-420	So. America	8-24-42	22:50:27	8.1	15S76W	63

QUAL.	PAD	h	AZIMUTH
B	69:396	60±	134

PHASE	P				PcP				S_1		
INST.	A*	Te	R	RA*	A*	Te	R	RA*			
I	0.1	1.4	0.75	0.075	0.6	1.4	0.75	0.45	6.00		
IVA	2.7	8.0	1.023	2.76	7.0	4.0	1.063	7.44	2.70		
VA	ni										
VI	ni										
VIBN	5.0	1.4	75.5	377	20.0	1.5	82.7	1653	4.39		
IVA	0.8	2.0	1.25	1.00							Addl. rdg.
II	0.1	1.5	1.32	0.132	?						
IVB	2.5	9.0	1.022	2.56	6.5	4.0	1.065	6.92	2.70		
V	2.0	4.0	0.344	0.688	5.0	3.0	0.427	2.135	3.10		
VIBE	4.7	1.4	75.5	355	17.4	1.4	75.5	1312	3.70		
IVB	1.0	2.0	1.251	1.251							Addl. rdg.
IIA	16.2	2.0	1.251	20.3	35.4	4.0	1.065	37.7	1.86		
VIA	24.0	1.6	68.7	1649	61.5	1.7	74.9	4610	2.80		

PHASE	PcS										
INST.	A*	Te	R	RA*	A*	Te	R	RA*			
I	np										
IVA	np										
VA	ni										
VI	ni										
VIBN	np										
II	np										
IVB	np										
V	trace?									1	
VIBE	np										
IIA	present but unmeasureable										
VIA	np										

PHASE	S				ScS				S_3		
INST.	A*	Te	R	RA*	A*	Te	R	RA*			
I	0.75	5.5	3.06	2.29	0.45	7?	3.91	1.76	0.768		
IVA	7.5	5.5	1.038	7.79	lost	in S					
VA	ni										
VI	ni										
VIBN	7.0	5.5	775	5420	lost	in S					
II	0.15?	6.0?	> 5	>0.75	np						
IVB	13.5	6.5	1.029	13.89	lost	in S					
V	7.0	22	0.688	4.82	lost	in S					
VIBE	2.6	6.0	926	2400	lost	in S					
IIA	?				?						
VIA	2.5	5.0	493	1232	?						

SHOCK NO.	REGION	DATE (G.C.T.)	ORIGIN TIME	MAG.	LOCATION	△
8-760	So. America	4-6-43	16:07:15	7.9	303/4S72W	79.6

QUAL.	PAD	h	AZIMUTH
B	69;431	60±	141

PHASE	P				PcP				S1		
INST.	A*	Te	R	RA*	A*	Te	R	RA*			
I	0.6	4.0	2.210	1.326	lost	in P					
IVA	4.5	4.0	1.065	4.793	?						
VA	ni				ni						
VI	ni				ni						
VIBN	12.6	0.9	47.5	598.5	11.5	0.9	47.5	546.3	0.913		
II	0.3	4.0	3.57	1.071	?						
IVB	5.3	5.0	1.043	5.528	?						
V	2.0	4.5	0.323	0.646	3.75	3.5	0.379	14.21	2.200		
VIBE	4.2	2.0	126.25	530	8.5	0.5	36.3	309	0.582		
IIA	22.0	5.1	1.042	22.92	lost	in P					
VIA	32.8	0.75	32.3	1059	29.5	0.8	33.6	991	0.936		

PHASE											
INST.	A*	Te	R	RA*	A*	Te	R	RA*			
I											
IVA											
VA											
VI											
VIBN											
II											
IVB											
V											
VIBE											
IIA											
VIA											

PHASE	S				ScS				S_3		
INST.	A*	Te	R	RA*	A*	Te	R	RA*			
I	0.9	6.2	3.454	3.109	0.3	10	4.5±	1.35	0.434		
IVA	ov.				ov.						
VA	ni				ni						
VI	ni				ni						
VIBN	5.5	6.0	926	5093	2.4	6.0	926	2222	0.436		
II	0.25	5.0	4.460	1.115	0.3	9.0	?				
IVB	ov.				ov.						
V	1.9	4.5	3.23	6.137	3.35	7.0	2.94	9.849	1.605		
VIBE	3.8	4.8	601	2284	4.2	7.0	1251	5254	2.300		
IIA	ov.				ov.						
VIA	3.5	6.5	820	2870	?						

SHOCK NO.	REGION	DATE (G.C.T.)	ORIGIN TIME	MAG.	LOCATION	Δ
13-100	Fiji	10-21-43	23:08:13	7.0	15S177½W	76.5

QUAL.	PAD	h	AZIMUTH
B	71:494		239

PHASE	P				PcP				S1
INST.	A*	Te	R	RA*	A*	Te	R	RA*	
I	tr				tr				
IVA	0.3	5.5	1.036	0.311	0.25	4.0	1.065	0.266	0.855
VA	ni				ni				
VI	poor record				poor record				
VIBN	1.5	1.0	52.0	78.0	indefinite --- microseisms				
II	tr				tr				
IVB	0.7	5.0	1.043	0.731	0.9	4.0	1.065	0.958	1.311
V	0.3	8.0	0.304	0.0912	0.5	8.0	0.304	0.1521	1.667
VIBE	1.1	1.1	57.08	62.8	0.8	2.0	126.3	101.1	1.61
IIA	3.8	7.5	1.025	3.89	1.5	6.5	1.029	1.542	0.396
VIA	2.8	1.1	43.6	122.1	3.7	1.0*	39.8	147.2	1.218

PHASE									
INST.	A*	Te	R	RA*	A*	Te	R	RA*	
I									
IVA									
VA									
VI									
VIBN									
II									
IVB									
V									
VIBE									
IIA									
VIA									

PHASE	S				ScS				
INST.	A*	Te	R	RA*	A*	Te	R	RA*	
I	tr				tr				
IVA	?				lost in S				
VA	ni				ni				
VI	poor record				poor record				
VIBN	lost in microseisms								
II	tr				tr				
IVB					lost in S				
V					lost in S				
VIBE	lost in microseisms								
IIA					lost in S				
VIA	not above microseism level								

* very indefinite that this is PcP

SHOCK NO.	REGION	DATE (G.C.T.)	ORIGIN TIME	MAG	LOCATION	Δ
14-440	New Hebrides	12-10-44	16:24:58	7.3	18S168E	86.6

QUAL.	PAD	h	AZIMUTH
B	74:605	50±	246

PHASE	P				PcP*				S_1
INST.	A*	Te	R	RA*	A*	Te	R	RA*	
I									
IVA	0.4	6.0	1.03	0.412	0.4	5.0	1.043	0.417	1.01
VA	ni								
VI	ov								
VIBN	1.4	0.9	47.5	66.5	1.1	1.0	52	57.2	0.860
II									
IVB	0.4	4.0	1.065	0.426	0.7	5.0	1.043	0.730	1.71
V	0.7	5.0	0.31	0.217	1.2	5.0	0.31	0.372	1.71
VIBE	1.4	1.0	52	72.9	1.2	1.0	52	62.4	0.856
IIA	6.1	6.0	1.03	6.29	5.0	8.0	1.024	5.12	0.814
VIA	6.6	1.0	39.8	263	6.0	1.0	39.8	239	0.910

PHASE									
INST.	A*	Te	R	RA*	A*	Te	R	RA*	
I									
IVA									
VA									
VI									
VIBN									
II									
IVB									
V									
VIBE									
IIA									
VIA									

PHASE	S				ScS				S_3
INST.	A*	Te	R	RA*	A*	Te	R	RA*	
I									
IVA	0.8	6.0	1.03	0.824	1.0	8.0	1.024	1.024	1.24
VA	ni								
VI	ov								
VIBN	0.1	5.5	-		0.05	6?	-		
II									
IVB	2.5	6.0	1.03	2.58	2.1	5.0**	1.043	2.19	0.849
V	3.6	6.0	0.29	0.725	3.5	6.0**	0.29	1.02	1.41
VIBE	1.0	5.5	-		0.5	6.0	-		
IIA	2.3	20	1.05	2.42	Lost in S				
VIA	-				-				

*May be pP in part; ** 1/2 cycle shift from S

SHOCK NO.	REGION	DATE (G.C.T.)	ORIGIN TIME	MAG.	LOCATION	Δ
14-820	New Hebrides	11-16-44	12:10:58	7.3	12½S167E	84.0

QUAL.	PAD	h	AZIMUTH
B	74-600		245

PHASE / INST.	P A*	P Te	P R	P RA*	PcP A*	PcP Te	PcP R	PcP RA*	S_1
I									
IVA	0.3	8.0	1.024	0.307	indisting. from P				
VA	ni				ni				
VI	not clear				not clear				
VIBN									
II									
IVB	0.4	10.0	1.0225	0.409	indisting. from P				
V	0.6	10.0	0.342	0.274	indisting. from P				
VIBE									
IIA	4.2	10.0	1.0225		indisting. from P				
VIA	0.6	2.0	95.77	57.4	1.1	1.2	47.82	52.6	0.918

PHASE / INST.	A*	Te	R	RA*	A*	Te	R	RA*	
I									
IVA									
VA									
VI									
VIBN									
II									
IVB									
V									
VIBE									
IIA									
VIA									

PHASE / INST.	S A*	S Te	S R	S RA*	ScS* A*	ScS* Te	ScS* R	ScS* RA*	S_3
I									
IVA	2.0	26.0	1.08	2.16	2.7	19.0	1.05	2.84	1.31
VA	ni				ni				
VI	0.3	11.0	0.094	0.028	1.1	20.0	0.054	0.059	2.10
VIBN									
II									
IVB	2.2	24.0	1.07	2.36	3.5	18.0	1.04	3.64	1.54
V	1.5	22.0	0.69	1.03	3.5	18.0	0.57	2.00	1.94
VIBE									
IIA	1.8	36	1.15‡	2.07	7.5	18	1.04	7.8	3.77
VIA									

* May be partly S motion

SHOCK NO.	REGION	DATE (G.C.T.)	ORIGIN TIME	MAG.	LOCATION	Δ
19-340	Japan	2-18-45	10:08:07	7.0	42N143E	73.7

QUAL.	PAD	h	AZIMUTH
B	88-12	50±	310

PHASE	P				PcP*				S_1
INST.	A*	Te	R	RA*	A*	Te	R	RA*	
I									
IVA	0.1	1.0	2.00	0.20	0.3	1.8	1.30±	0.39	1.95
VA	ni				ni				
VI	nra				nra				
VIBN	0.2	1.0	52.0	10.4	0.4	1.5	82.69	33.1	3.18
II									
IVB	0.05	1.0	2.00	0.10	0.2	2.0	1.251	0.250	2.50
V	np				0.3	3.0	0.425	0.128	-
VIBE	0.3	1.0	52.0	15.6	0.3	1.2	62.69	18.8	1.20
IIA	0.4	3.2	1.096	0.438	1.8	2.4	1.176	2.12	4.84
VIA	0.8	1.4	57.47	46.0	2.6	2.0	95.8	248	5.39

PHASE											
INST.	A*	Te	R	RA*	A*	Te	R	RA*			
I											
IVA											
VA											
VI											
VIBN											
II											
IVB											
V											
VIBE											
IIA											
VIA											

PHASE	S				ScS**				S_3		
INST.	A*	Te	R	RA*	A*	Te	R	RA*			
I											
IVA	0.7	6.0	1.033	0.724	0.8	8.0	1.024	0.820	1.13		
VA	ni				ni						
VI	nra				nra						
VIBN	2.0	3.0	251	502	trace						
II	0.1	5.0	4.5±	0.45	np						
IVB	1.5	6.0	1.033	1.55	0.6	8.0	1.024	0.615	0.397		
V	2.0	5.0	0.305	0.610	0.6	10.0	0.340	0.204	0.335		
VIBE	0.8	5.0	651	521	0.2	3.0	251	50.2	0.0964		
IIA	1.3	3.5	1.08	1.40	1.3	10.0	1.023	1.33	0.95		
VIA	not recorded well				?						

*follows pP by only 4 sec. **May be PPS

SHOCK NO.	REGION	DATE (G.C.T.)	ORIGIN TIME	MAG.	LOCATION	△
19-455	No. Japan	10-26-42	21:09:13	7.2	45½N151½E	65.8

QUAL.	PAD	h	AZIMUTH
B	69:403	60	312

PHASE	P				PcP				S_1		
INST.	A*	Te	R	RA*	A*	Te	R	RA*			
I	0.05	3.0	1.63	0.082	tr						
IVA	0.8	3.0	1.112	0.890	0.8	2.5	1.160	0.893	1.003		
VA	ni										
VI	ni										
VIBN	1.8	3.0	251	452	2.5	1.5	82.7	207	0.458		
II	0.05	3.0	2.68	0.134	tr						
IVB	1.4	3.4	1.086	1.520	1.8	3.0	1.112	2.01	1.32		
V	nra										
VIBE	1.0	3.0	251	251	3.5	1.5	82.7	289	1.15		
VIBE	2.3	1.0	52.0	120							Addl. rdg.
IIA	6.3	2.5	1.160	7.31	2.2	2.5	1.160	2.55	0.348		
VIA	8.6	2.5	139	1194	8.9	1.3	52.4	466	0.426		
VIA					4.4	2.5	139	612	0.559		Addl. rdg.

PHASE	PcS								S_2	S_4	
INST.	A*	Te	R	RA*	A*	Te	R	RA*			
I	np										
IVA	<0.2	?									
VA	ni										
VI	ni										
VIBN	<0.2										
II	np										
IVB	0.5	5.0	1.043	0.521					0.343	0.062	
V	nra										
VIBE	<0.2										
IIA	1.1	5.5	1.036	1.139					0.156	0.242	
VIA	ov by microseisms										

PHASE	S				ScS				S_3		
INST.	A*	Te	R	RA*	A*	Te	R	RA*			
I	0.1	5.0	2.77	0.277	np						
IVA	2.1	5.5	1.036	2.17	2.0**	7.0	1.026	2.05	0.991		
VA	ni										
VI	ni										
VIBN	1.7	3.5	333	566	< 0.5	doubtful					
II	0.35	5.0	4.46	1.56	np						
IVB	8.1	6.0	1.033	8.37	2.8*	5.5	1.036	2.90	0.346		
V	nra										
VIBE	5.5	3.5	333	1832	<0.3	doubtful					
IIA	4.5	5.0	1.043	4.69	1.6	7.5	1.025	1.64	0.350		
VIA	3.4	5.0	493	168	np	?					

** ca 12 sec late ; * ca 20 sec late

SHOCK NO.	REGION	DATE (G.C.T.)	ORIGIN TIME	MAG.	LOCATION	Δ
19-565	Japan	8-23-42	06:35:21	7.0	53N163½E	57.4

QUAL.	PAD	h +
B	90:75	60-

AZIMUTH 317

PHASE	P				PcP				S1		
INST.	A*	Te	R	RA*	A*	Te	R	RA*			
I	0.15	1.0	0.575	0.0863	0.03	1.3	0.705	0.0217	0.245		
IVA	1.0	2.5	1.165	1.165	0.1*	1.2	1.8±	0.18	0.155		
VA	ni				ni						
VI	badly scrambled record										
VIBN	3.7	1.3	68.8	254	1.0	1.3	68.8	69	0.270		
IVA	0.4	10.0	1.023	0.409							Addl. rdg.
II	0.15	1.0	0.890	0.134	0.05	1.0	0.890	0.0445	0.333		
IVB	0.7	2.0	1.251	0.876	0.4*	1.0	2.00	0.80	0.913		
V	1.3	2.8	0.456	0.593	0.2	3.0	0.428	0.0857	0.145		
VIBE	5.0	1.0	52.0	260	2.8	1.3	68.8	193	0.741		
IVB	0.2	9.0	1.022	0.204							Addl. rdg.
IIA	3.7	2.5	1.165	4.31	1.3	3.2	1.096	1.424	0.330		
VIA	20.6	1.1	43.6	898	6.2	1.3	52.4	325	0.362		

PHASE	PcS								S_2	S_4	
INST.	A*	Te	R	RA*	A*	Te	R	RA*			
I	small tr										
IVA	0.15	3.5	1.080	0.162					0.0926	0.0876	
VA	ni										
VI	scrambled record										
VIBN	not above microseisms										
II	np										
IVB	0.15	3.5	1.080	0.162					0.185	0.122	
V	0.15	3.5	0.380	0.0570					0.0961	0.214	
VIBE	0.25	1.4	75.5	18.87					0.0726	0.0818	
IIA	0.8	9.0	1.022	0.818					0.190	0.434	
VIA	1.3	2.0	95.8	124.6					0.139		

PHASE	S				ScS				S_3		
INST.	A*	Te	R	RA*	A*	Te	R	RA*			
I	tr				small tr						
IVA	1.7	27	1.089	1.849	0.3	19	1.048	0.314	0.170		
VA	ni				ni						
VI	scrambled				scrambled						
VIBN	0.25	5.5	776	194	0.25	4.0	426	107	0.549		
II	tr				tr						
IVB	1.3	6.0	1.033	1.33	0.6	8.0	1.024	0.614	0.462		
V	0.7	3.5	0.380	0.266	0.3	7.0	0.294	0.0883	0.332		
VIBE	0.7	3.5	330	231	0.25	3.5?	330	82.5	0.357		
IVB	3.1	24.0	1.074	3.33					0.185		Addl.rdg.
IIA	1.8	19	1.048	1.886	0.7	8.5	1.023	0.716	0.380		
VIA	not above microseism level										

* may be larger (in minute mark and under glass)

SHOCK NO.	REGION	DATE (G.C.T.)	ORIGIN TIME	MAG.	LOCATION	Δ
19-575	Kamchatcka	9-23-44	12:13:20	7.2	54N160E	58.6

QUAL.	PAD	h	AZIMUTH
B	74:589	40+	317

PHASE	P				PcP				S_1		
INST.	A*	Te	R	RA*	A*	Te	R	RA*			
I											
IVA	0.3	1.0	2.004	0.601	1.0	2.0	1.251	1.25	2.08		
VA	ni				ni						
VI	np				np						
VIBN	1.9	1.0	52.0	98.8	1.9	1.3*	68.8	131	1.33		
II											
IVB	0.4	1.0	2.004	0.802	1.4	3.0	1.112	1.56	1.95		
V	0.7	3.0	0.425	0.297	2.0	3.0	0.425	0.95	2.86		
VIBE	3.4	1.0	52.0	177	3.4	1.0	52.0	177	1.00		
V	0.4	2.5	0.51	0.204							Addl. rdg.
IIA	3.2	2.2	1.21±	3.87	5.0	3.0	1.112	5.56	1.44		
VIA	8.5	1.2	47.8	406	4.9	1.3	52.4	257	0.633		

PHASE	PcS								S_2	S_4	
INST.	A*	Te	R	RA*	A*	Te	R	RA*			
I											
IVA	0.7	10.0	1.023	0.717					1.90	0.234	
VA	ni										
VI	0.3	9.0	0.114	0.034						0.244	
VIBN	np										
II											
IVB	0.9	6.0	1.033	0.931					1.16	0.604	
V	1.2	5.0	0.31	0.372					0.877	0.367	
VIBE	0.4	6.0	926	370					2.09	2.10	
IIA	2.8	9.0	1.022	2.86					0.740	0.354	
VIA	0.2*	5.0	493	98.6					0.243?		

PHASE	S				ScS				S_3		
INST.	A*	Te	R	RA*	A*	Te	R	RA*			
I											
IVA	2.9	20.0	1.053	3.06	1.0	5.0	1.043	1.04	0.340		
VA	ni										
VI	2.8	22.0	0.050	0.140	0.45	6.0	0.168	0.756	5.40		
VIBN	0.5	3.0	251.1	126	0.4	3.0	251.1	100.3	0.796		
IVB	3.1	22.0	1.062	3.29							Addl. Rdg.
II											
IVB	1.5	6.5	1.028	1.54	1.0	5.0	1.043	1.04	0.675		
V	3.5	6.0	0.29	1.014	1.7	4.5	0.325	0.553	0.545		
VIBE	0.7	3.0	251.1	176	0.3	4.5	626±	188	1.07		
V	2.0	25.0	0.78	1.56							Addl. rdg.
IIA	7.6	22.0	1.062	8.08	3.7	6.5	1.029	3.80	0.470		
VIA	np				bare trace						

* very indefinite

SHOCK NO.	REGION	DATE (G.C.T.)	ORIGIN TIME	MAG.	LOCATION	Δ
19-670	Kamchatka	4-15-45	02:35:22	7.0	57N164E	55.6

QUAL.	PAD	h	AZIMUTH
B	88:16		320

PHASE	P				PcP				S_1		
INST.	A*	Te	R	RA*	A*	Te	R	RA*			
I	0.05	1.2	0.658	0.0329	0.2	1.4	0.75	0.150	4.56		?
IVA	0.7	4.0	1.065	0.746	0.6	1.5	1.5	0.90	1.21		
VA	ni				ni						
VI	np				np						
VIBN	2.6	1.0	52.0	135	2.5	1.2	62.5	156	1.16		
II	0.1	0.9	0.81	0.081	0.1	1.0	0.89	0.089	1.10		
IVB	0.8	4.0	1.065	0.851	0.5	2.0	1.25	0.625	0.73		
V	1.5	4.0	0.345	0.518	0.4	2.5	0.51	0.204	0.39		
VIBE	2.5	1.0	52.0	130	2.4	1.2	62.5	150	1.15		
IIA	6.4	3.0	1.11	7.10	2.2	2.0	1.25	2.76	0.39		
VIA	11.0	1.2	47.5	523	5.5	1.4	57.5	316	0.604		

PHASE	PcS								S_2	S_4	
INST.	A*	Te	R	RA*	A*	Te	R	RA*			
I											
IVA	Not clear										
VA	ni										
VI	1.8	18									
VIBN	not clear										
II											
IVB	not clear										
V	not clear										
VIBE	0.3	1.0	52.0	16.0					0.12	0.0762	?
IIA	2.2	4.5	1.05	2.31					0.33	0.350	
VIA	1.3	1.6	68.5	89.0					0.170	0.520	

PHASE	S				ScS				S_3		
INST.	A*	Te	R	RA*	A*	Te	R	RA*			
I											
IVA	7.5	14.0	1.03	7.72	1.0	5.0	1.04	1.04	0.13		
VA	ni				ni						
VI	4.5	24.0	0.046		not clear						
VIBN	0.4	4.5	526	210	0.4	5.0	651	260	1.238		
II											
IVB	3.0	6.0	1.03	3.09	2.4	7.0	1.025	2.46	0.80		
V	3.8	6.0	0.29	1.10	2.4	7.0	0.295	1.23	1.13		
VIBE	1.1	3.9	?		0.5	7.0	?				
IIA	6.4	15.0	1.03	6.60	1.9	8.0	1.025	1.95	0.30		
VIA	0.9	3.0	190	171	np						

SHOCK NO	REGION	DATE (G.C.T.)	ORIGIN TIME	MAG.	LOCATION	Δ
31-420	Atlantic Ocean	11-25-41	18:03:55	8.3	37½N18½W	76.2

QUAL.	PAD	h	AZIMUTH
A	57:b,c		32

PHASE	P				PcP				S1		
INST.	A*	Te	R	RA*	A*	Te	R	RA*			
I	0.25	2.5	1.36	0.340	0.25	1.3	0.705	0.176	0.518		
IVA	2.0	2.0	1.251	2.50	8.0	2.5	1.162	9.30	2.32		
VA	ni				ni						
VI	tr				tr						
VIBN	3.2	1.0	52.0	166	7.0	0.8	43.56	305	1.83		
II	0.15	0.8	0.745	0.112	0.15	1.0	0.890	0.133	1.09		
IVB	2.6	2.5	1.162	3.02	8.5	3.0	1.112	9.46	2.86		
V	1.8	5.0	0.308	0.555	7.6	7.0	0.294	2.24	4.03		
VIBE	3.8	1.0	52.0	198	5.4	1.1	57.08	308	1.56		
IIA	10.3	5.0	1.043	10.76	36.5	4.0	1.065	38.8	3.62		
VIA	15.2	1.0	39.81	605	21.3	0.6	29.49	628	1.038		

PHASE											
INST.	A*	Te	R	RA*	A*	Te	R	RA*			
I											
IVA											
VA											
VI											
VIBN											
II											
IVB											
V											
VIBE											
IIA											
VIA											

PHASE	S				ScS						
INST.	A*	Te	R	RA*	A*	Te	R	RA*			
I	0.4	11.5	?		0.7	7.5	?				
IVA	ov.				ov.						
VA	ni				ni						
VI	23	88	?		lost in S						
VIBN											
II	small; long period				small; long period						
IVB	ov				ov						
V	ov										
VIBE											
IIA	ov.										
VIA	not above microseisms										

Table 15 --- Magnitude determination from P and PcP

Shock No.	Horizontal Component of P								Vertical Component of P				
	$\left(\frac{A_e}{T_e}\right)_N$	$\left(\frac{A_e}{T_e}\right)_E$	u/T_e	$\log\left(\frac{u}{T_e}\right)$	A(U)*	M_2	M_1	M_1-M_2	$\left(\frac{w}{T_e}\right)$	$\log\left(\frac{w}{T_e}\right)$	A(W)*	M_2	M_1-M_2
1-110							7.0		0.433	-0.36	6.8	6.3	+0.7
1-60	0.395	0.56	0.68	-0.17	7.1	6.9	7.1	+0.2	0.657	-0.18	6.8	6.6	+0.5
1-550	1.19	1.13	1.57	+0.20	6.8	7.0	7.3	+0.3	5.27	+0.72	6.6	7.3	0.0
5-705	0.728	1.03	1.26	+0.10	6.8	6.9	7.0	+0.1	2.83	+0.45	6.6	7.1	-0.1
5-825	1.06	1.35	1.72	+0.24	6.8	7.0	7.7	+0.7	9.42	*0.97	6.6	7.7	0.0
6-400	0.632	0.88	1.09	+0.04	6.9	6.9	6.9	0.0	2.38	+0.38	6.7	7.1	-0.2
6-440	3.26	5.29	6.21	+0.79	6.9	7.8	7.5	-0.3					
6-190	0.188	0.365	0.41	-0.39	7.0	6.6	6.9	+0.3	1.163	+0.07	6.8	6.9	0.0
14-280	0.0730	0.113	0.13	-0.89	7.5	6.6	7.2	+0.6	0.399	-0.40	7.0	6.6	+0.6
14-440	0.094	0.157	0.18	-0.74	7.5	6.8	7.3	+0.5	1.432	+0.16	7.0	7.2	+0.1
19-340	0.046	0.023	0.05	-1.30	7.3	5.9	7.0	+1.1	0.100	-1.00	6.9	5.8	+1.2
19-575	0.137	0.304	0.33	-0.48	7.1	6.6	7.2	+0.6	0.883	-0.15	6.8	6.6	+0.6
19-670	0.170	0.356	0.39	-0.41	7.1	6.7	7.0	+0.3	1.619	+0.21	6.8	7.0	0.0
8-420	0.650	0.636	0.895	-0.05	7.2	7.1	8.1	+1.0	4.63	+0.67	6.9	7.7	+0.4
19-455	0.203	0.174	0.277	-0.57	7.1	6.4	7.2	+0.8	1.667	+0.22	6.8	7.0	+0.2
6-680	0.507	1.024	1.14	+0.06	7.0	7.1	7.1	0.0	3.71	+0.57	6.8	7.4	-0.3
8-210	1.466	2.40	2.81	+0.45	7.0	7.6	7.9	+0.3	5.02	+0.70	6.8	7.6	+0.3
7-430	1.577	2.32	2.80	+0.45	7.0	7.6	7.75	+0.15	7.41	+0.87	6.8	7.8	-0.05
7-170	0.605	1.092	1.25	+0.10	6.9	7.0	7.1	+0.1	1.96	+0.29	6.7	7.0	+0.1
8-760	1.092	0.953	1.45	+0.16	7.1	7.3	7.9	+0.6	5.23	+0.72	6.7	7.4	+0.5
13-100	0.0710	0.129	0.15	-0.83	7.3	6.4	7.0	+0.6	0.888	-0.05	7.0	6.9	+0.1
19-565	0.266	0.396	0.48	-0.32	7.1	6.8	7.0	+0.2	0.984	-0.01	6.8	6.8	+0.2

Formula used: $M_2 = A + 0.1\ (M_2 - 7) - \log T + \log u$ (or w)

* from Gutenberg 19, p. 65, table 4/

Table 15 (cont'd) --- Magnitude determination from P and PcP

Shock No.	Horizontal Component of PcP								Vertical Component of PcP				
	$\frac{A_e}{T_e}$ N	$\frac{A_e}{T_e}$ E	u/T_e	$\log \frac{u}{T_e}$	A(U)*	M_2	M_1	M_1-M_2	$\frac{w}{T_e}$	$\log \frac{w}{T_e}$	A(W)*	M_2	M_1-M_2
1-550	0.950	0.72	1.19	+0.08	8.2	8.5	7.3	-1.2	1.304	+0.12	7.4	7.6	-0.3
5-705	0.420	0.54	0.69	-0.16	8.3	8.2	7.0	-1.2	0.539	-0.27	7.4	7.1	-0.1
5-825	1.27	1.25	1.78	+0.25	8.2	8.7	7.7	-1.0	2.57	+0.41	7.4	7.9	-0.2
8-190									0.574	-0.24	7.4	7.2	-0.3
14-440	0.951	0.27	0.99	0.00	8.7	8.9	7.3	-1.6	1.167	+0.07	8.1	8.3	-1.0
19-340	0.089	0.116	0.14	-0.85	8.4	7.6	7.0	-0.6	0.484	-0.32	7.7	7.4	-0.4
19-575	0.265	0.65	0.71	-0.15	8.1	8.0	7.2	-0.8	1.269	+0.10	7.5	7.7	-0.5
19-670	0.205	0.173	0.27	-0.57	8.1	7.6	7.0	-0.6	0.629	-0.20	7.5	7.3	-0.3
8-420	1.70	1.86	2.42	+0.38	8.2	8.8	8.1	-0.7	8.60	+0.93	7.6	8.7	-0.6
19-455	0.204	0.459	0.50	-0.30	8.2	8.0	7.2	-0.8	0.581	-0.24	7.6	7.4	-0.2
6-680	0.591	0.637	0.87	-0.16	8.1	8.0	7.1	-0.9	1.521	+0.18	7.4	7.7	-0.6
8-210	1.27	1.49	1.96	+0.29	8.1	8.6	7.9	-0.7	2.68	+0.43	7.4	7.9	0.0
7-430	0.913	2.41	2.58	+0.41	8.1	8.7	7.75	-0.95					
7-170	1.11	1.34	1.74	+0.24	8.1	8.4	7.1	-1.3					
13-100	0.0607	0.0865	0.106	-0.98	8.4	7.4	7.0	-0.4	0.352	-0.45	7.8	7.3	-0.3
19-565	0.0411	0.1342	0.140	-0.85	8.1	7.2	7.0	-0.2	0.325	-0.49	7.5	7.0	0.0
1-110									0.433	-0.36	7.4	7.0	0.0

*from graph 33

Table 15a --- Determination of $A_{(U)}$ and $A_{(W)}$ for PcP

Δ	u_{PcP}*	$\frac{u}{CT}$*	$\log\left(\frac{u}{CT}\right)$	$A_{(U)wa}$	w_{PcP}*	$\frac{w}{CT}$*	$\log\left(\frac{w}{CT}\right)$	$A_{(W)wa}$
0.00°	0.00000	0.00000			0.0744	0.0237	-1.6253	7.9
4.60	.00179	.00057	-3.2441	9.5	.0892	.0284	-1.5467	7.8
7.00	.00459	.00146	-2.8356	9.1	.1020	.0325	-1.4881	7.8
8.00	.00583	.00186	-2.7305	9.0	.1060	.0337	-1.4724	7.8
16.60	.01417	.00451	-2.3458	8.6	.1990	.0633	-1.1986	7.5
25.40	.0351	.0112	-1.9508	8.3	.2897	.0922	-1.0353	7.3
34.60	.0601	.0191	-1.7190	8.0	.3710	.118	-0.9245	7.2
45.40	.0780	.0248	-1.6055	7.9	.4040	.129	-0.8894	7.2
57.20	.0783	.0249	-1.6038	7.9	.3490	.111	-0.9547	7.3
71.40	.0489	.0156	-1.8069	8.1	.1985	.0632	-1.1993	7.5
88.00	.01895	.00603	-2.2197	8.5	.0739	.0235	-1.6289	7.9
95.00	.00161	.000512	-3.2907	9.6	.00601	.00191	-2.7190	9.0
103.00	.0579	.0184	-1.7352	8.0	.2122	.0675	-1.1707	7.5

Δ	D (km) approx	kD	e^{-kD}	$\sqrt{e^{-kD}}$	$LOG\sqrt{e^{-kD}}$	$A_{(U)}$	$A_{(W)}$
0.00°	5800	0.696	0.4967	0.7048	-0.1518		
4.60	5800	.696	.4967	.7048	.1518	9.7	8.0
7.00	5900	.708	.4924	.7017	.1538	9.3	7.9
8.00	5900	.708	.4924	.7017	.1538	9.2	7.9
16.60	6000	.720	.4869	.6978	.1563	8.8	7.7
25.40	6200	.720	.4869	.6978	.1563	8.4	7.5
34.60	6500	.756	.4695	.6852	.1642	8.2	7.4
45.40	6900	.828	.4367	.6608	.1799	8.1	7.4
57.20	7400	.898	.4072	.6381	.1951	8.1	7.5
71.40	8200	.984	.3737	.6113	.2137	8.3	7.7
88.00	9100	1.092	.3356	.5793	.2371	8.8	8.2
95.00	9500	1.140	.3198	.5655	.2476	9.8	9.3
103.00	10000	1.200	.3012	.5488	.2606	8.3	7.7

k assumed to be 0.00012/km.; $A_{(U)wa}$ means $A_{(U)}$ without absorption included

* from Dana 7/

The formula on p. 141 (Mertner) should be in the following form

$$\sqrt{E_{rp}/E_{ip}} = \frac{-\frac{V_{p1}}{V_{s1}}\frac{V_{p2}}{V_{p1}}\frac{\rho_2}{\rho_1}\cos i_{ip}\cos 2i_{rs} - \frac{V_{p1}}{V_{s1}}\cos^2 2i_{rs}\cos i_{fp} - \frac{\rho_2}{\rho_1}\frac{V_{p2}}{V_{p1}}\sin 2i_{ip}\sin i_{rs} + \frac{V_{s1}}{V_{p1}}\sin 2i_{ip}\sin 2i_{rs}\cos i_{fp}}{+\frac{V_{p1}}{V_{s1}} \ldots\ldots \quad + \quad + \quad +}$$

Table 16 --- Results of computation of $\sqrt{E_{rp}/E_{ip}}$ at the core boundary, assuming incident longitudinal wave from above

i_{ip}		Col. A*	Col. B*	Col. C*	Col. D*	Col. E*	Col. F*
0°	0.00°	-0.324	0.011	-0.132	-0.207	0.136	-0.007
10	8.24	-0.292	0.037	-0.103	-0.176	0.161	0.021
20	16.42	-0.226	0.087	-0.047	-0.112	0.208	0.075
30	25.40	-0.120	0.169	0.046	-0.009	0.285	0.163
40	34.48	0.000	0.280	0.147	0.106	0.371	0.262
50	45.00	0.092	0.328	0.227	0.196	0.436	0.337
60	56.64	0.179	0.396	0.300	0.280	0.495	0.407
70	71.40	0.162	0.369	0.280	0.266	0.480	0.391
80	91.5	-0.052	0.164	0.069	0.059	0.297	0.195
83	97.4	-0.204	0.010	-0.087	-0.095	0.150	0.043
84	99.0	-0.271	-0.061	-0.157	-0.165	0.080	-0.028
85	99.8	-0.348	-0.146	-0.239	-0.246	0.006	-0.113
89	102.0	-0.574	-0.735	-0.777	-0.780	-0.663	-0.719
90	103.0						

* Assumptions:

	$\lambda/2$	V_{p1}	V_{p2}
Col. A	1	15.7 km/sec	7.0 km/sec
" B	1/2	" "	7.0 "
" C	2/3	" "	7.0 "
" D	1	" "	9.0 "
" E	1/2	" "	9.0 "
" F	2/3	" "	9.0 "

Formula used:

$$\sqrt{E_{rp}/E_{ip}} = \frac{\frac{V_{p2}}{V_{p1}}\frac{\rho_2}{\rho_1}\cos i_{ip}\cos 2i_{rs} - \frac{V_{p1}}{V_{s1}}\cos^2 2i_{rs}\cos i_{fp} + \frac{\rho_2}{\rho_1}\frac{V_{p2}}{V_{p1}}\sin 2i_{ip}\sin i_{rs} + \frac{V_{s1}}{V_{p1}}\sin 2i_{ip}\sin 2i_{rs}\cos i_{fp}}{\frac{V_{p2}}{V_{p1}}\frac{\rho_2}{\rho_1}\cos i_{ip}\cos 2i_{rs} + \frac{V_{p1}}{V_{s1}}\cos^2 2i_{rs}\cos i_{fp} + \frac{\rho_2}{\rho_1}\frac{V_{p2}}{V_{p1}}\sin 2i_{ip}\sin i_{rs} + \frac{V_{s1}}{V_{p1}}\sin 2i_{ip}\sin 2i_{rs}\cos i_{fp}}$$

Table 17 --- Determination of azimuth from PcP

Shock No.	$\frac{(A_o)_E}{(A_o)_N}$	θ *	Az (true)	diff.**
1-350	0.591	30.6°	334°	- 4.6
5-705	1.559	57.3	122 1/2	+ 0.2
5-825	0.898	41.9	123	+15.1
19-340	0.712	35.5	310	+14.5
19-575	1.871	61.9	317	-18.9
19-670	0.926	42.8	320	- 2.8
8-420	0.929	49.9	134	- 3.9
19-455	2.704	69.7	312	-21.7
6-680	1.633	58.5	119 1/2	+ 2.0
8-210	1.174	49.6	129	+ 1.4
7-430	2.55	68.6	95	+16.4
7-170	2.10	64.6	104 1/2	+10.9

*computed angle from North or South

** θ is $\begin{pmatrix} + = \text{clockwise} \\ - = \text{counter-clockwise} \end{pmatrix}$ from Az (true)

Table 18 --- Determination of $i_{pc}-i_{pot}$ for P

△	Shock No.	$\left[\frac{kA^*/a}{T}\right]_H$	$[kA^*/a]_N$	$\left[\frac{kA^*/a}{T}\right]_E$	$[kA^*/a]_E$	$[kA^*/a]_H$ [1]	$\left[\frac{kA^*/a}{T}\right]_Z$	$[kA^*/a]_Z$	$\bar{i}$ [2]	i_{pc}	Assum. $V_{pc}=5.5$ i_{pot} [3]	Assum. $V_{pc}=5.5$ $i_{pc}-i_{pot}$	Assum. $V_{pc}=8.0$ i_{pot}	Assum. $V_{pc}=8.0$ $i_{pc}-i_{pot}$
34.6°	1-550	5.20	26.0	5.41	27.05	37.5	23.1	92.4	22.1°	20.1°	25.1°	- 5.0°	38.3°	-17.2
29.8	5-705	3.19	44.6	4.94	69.1	82.1	12.4	178.6	25.3	23.1	26.4	- 3.3	40.3	-17.2
32.1	5-825	4.65	11.63	6.21	17.39	20.9	41.3	82.6	14.2	12.8	25.8	-13.0	39.3	-26.5
73.7	19-340	0.20	0.20	0.10	0.10	0.224	0.438	1.40	9.1	8.2	17.1	- 8.9	25.2	-17.0
58.6	19-575	0.601	0.601	0.802	0.802	1.002	3.87	8.52	6.7	6.0	20.2	-14.2	29.9	-23.9
55.6	19-670	0.746	2.98	0.851	3.40	4.52	7.10	21.3	12.0	10.8	20.8	-10.0	30.9	-20.1
63.0	8-420	1.00	2.00	1.25	2.50	3.20	20.3	40.6	4.5	4.0	19.3	-15.3	28.5	-24.5
65.8	19-455	0.890	2.67	1.52	5.17	5.82	7.31	18.3	17.6	15.9	18.7	- 2.8	27.6	-11.7
44.2	6-680	2.224	6.67	5.56	16.68	18.0	16.27	35.8	32.8	30.3	18.2	+12.1	34.6	- 4.5
48.3	8-210	6.43	28.3	10.99	52.8	59.9	22.0	110.0	28.5	26.1	22.3	+ 3.8	33.2	- 7.1
47.5	7-430	6.91	24.2	9.56	35.4	42.9	32.5	97.5	23.7	21.5	22.5	- 1.0	33.5	-12.0
39.8	7-170	2.655	5.84	4.72	15.1	16.2	8.58	36.0	24.2	22.0	24.1	- 2.1	36.3	-14.3
79.6	8-760	4.79	19.1	5.53	27.7	33.6	22.9	110.9	16.1	14.5	15.8	- 1.3	23.4	- 8.9
76.5	13-100	0.311	1.71	0.731	3.76	4.13	3.89	29.2	8.0	7.2	16.5	- 9.3	24.4	-17.2
57.4	19-565	1.165	2.91	0.876	1.75	3.40	4.31	10.79	17.5	15.8	20.4	- 4.6	30.3	-14.5
76.2	31-420	2.50	1.25	3.02	1.21	1.74	10.76	2.15	39.0	36.7	16.6	+20.1	24.5	+12.2

1/ $[kA^*/a]_H = \sqrt{(kA^*/a)_N^2 + (kA^*/a)_E^2}$

2/ $\tan \bar{i} = \frac{[kA^*/a]_H}{[kA^*/a]_Z}$

3/ from Dana 7/

Table 19 --- Determination of $i_{po}-i_{pot}$ for PcP

Δ	Shock No.	$\left[\frac{kA^*/a}{T}\right]_N$	$[kA^*/a]_N$	$\left[\frac{kA^*/a}{T}\right]_E$	$[kA^*/a]_E$	$[kA^*/a]_H$	$\left[\frac{kA^*/a}{T}\right]_Z$	$[kA^*/a]_Z$	$\frac{1}{i}$ [2]	i_{po}	Assum. $V_{po}=5.5$ i_{pot} [3]	Assum. $V_{po}=5.5$ $i_{po}-i_{pot}$	Assum. $V_{po}=8.0$ i_{pot}	Assum. $V_{po}=8.0$ $i_{po}-i_{pot}$
34.6°	1-550	4.16	22.0	2.60	13.0	25.6	5.72	30.3	40.2°	37.9°	8.5°	+29.4°	11.7°	+26.2°
29.8	5-705	1.84	20.2	2.86	31.5	37.4	2.36	16.5	66.2	77.9	8.0	+69.9	10.5	+67.4
32.1	5-825	5.56	16.7	5.00	15.0	22.4	11.27	22.5	44.9	43.1	8.2	+34.9	11.1	+32.0
73.7	19-340	0.39	0.703	0.25	0.50	0.863	2.12	5.08	9.6	8.6	12.6	- 4.0	17.4	- 8.8
58.6	19-575	1.25	2.50	1.56	4.68	5.31	5.56	16.68	17.6	15.9	11.4	+ 4.5	16.1	- 0.2
55.6	19-670	0.90	1.35	0.625	1.25	1.84	2.76	5.52	18.6	16.8	11.4	+ 5.4	15.7	+ 1.1
63.0	8-420	7.44	29.8	6.92	27.7	40.7	37.7	150.8	15.1	13.6	12.0	+ 1.6	16.6	- 3.0
65.8	19-455	0.893	2.23	2.01	6.03	6.44	2.55	6.37	45.3	43.5	12.6	+30.9	16.8	+26.7
44.2	6-680	2.59	9.07	3.52	14.81	17.4	6.67	20.02	41.0	38.8	9.6	+29.2	13.8	+25.0
48.3	8-210	5.55	16.6	0.781	19.5	25.6	11.72	46.8	28.7	26.3	10.7	+15.6	14.6	+11.7
76.5	13-100	0.266	1.064	0.958	3.83	3.98	1.45	10.02	21.6	19.6	11.9	+ 7.7	17.6	+ 2.0
57.4	19-565	0.18	0.216	0.80	0.80	0.820	1.42	4.56	10.2	9.2	11.4	- 2.2	16.0	- 6.8
76.2	31-420	9.30	3.72	9.46	3.15	4.87	38.8	9.70	26.7	24.4	11.9	+12.5	17.5	+ 6.9

For footnotes --- see table 18

Table 20 --- Determination of u PcP/u P and w PcP/w P, assuming V_{po}=8.0 km/sec

i_c	f	Δ	$\bar{V}$ km/sec	i_o	$di_o/d\Delta \sqrt{\frac{\tan i_o}{\sin\Delta}\frac{di_o}{d\Delta}}$	A	u/A	u	w/A	w	u PcP / uPP	w PcP / w P
For P:												
		15°	8.81	65°14'	2.96	4.98	15.65	1.77	27.7	0.84	13.15	0.00130	0.0307
		20	10.28	51 06	2.48	2.955	9.28	1.67	15.5	1.09	10.12	.00587	.0535
		30	12.43	40 04	0.508	1.46	4.59	1.46	6.70	1.45	6.65	.0288	.1291
		40	13.39	36 41	.374	0.657	2.06	1.32	2.72	1.52	3.13	.1026	.324
		50	14.80	32 43	.362	.551	1.73	1.21	2.09	1.62	2.80	.155	.356
		60	16.02	29 58	.323	.464	1.46	1.14	1.66	1.67	2.44	.153	.291
		70	18.81	25 10	.310	.405	1.27	0.96	1.22	1.77	2.25	.206	.299
		80	20.35	23 09	.292	.356	1.12	.88	0.987	1.82	2.04	.170	.216
		90	22.82	20 31½	.262	.313	0.983	.81	.796	1.84	1.81	.1104	.1254
		100	25.90	17 59½	.165	.233	.732	.71	.520	1.88	1.38	.094	.0907
		103	25.95	17 57½	.026	.093	.292	.71	.207	1.88	0.549	1.778	1.670
For PcP:												
12°07'	0.077	10		3 48	0.369	0.608	0.147	0.15	0.022	1.99	0.293		
18 04	.109	15		5 37	.354	.597	.204	.24	.049	1.98	.404		
23 53	.150	20		7 21	.338	.584	.275	.33	.091	1.97	.542		
35 14	.249	30		10 31	.308	.560	.438	.44	.193	1.96	.859		
45 14	.339	40		12 58½	.238	.494	.526	.53	.279	1.93	1.016		
54 23	.402	50		14 53½	.165	.414	.523	.62	.324	1.91	.998		
62 30	.423	60		16 17½	.114	.345	.374	.68	.254	1.90	.711		
69 14	.408	70		17 11	.0735	.277	.355	.71	.252	1.89	.672		
74 48	.345	80		17 46	.0438	.215	.233	.72	.168	1.89	.440		
79 25	.233	90		18 06	.0262	.166	.121	.73	.088	1.88	.227		
85 34	.136	100		18 22	.0231	.156	.0666	.74	.049	1.88	.125		
90 00	1.000	103		18 26	.0231	.156	.490	.75	.368	1.87	.917		

BIBLIOGRAPHY

1/ Anderson, J.A., and Wood, H.O.: Description and theory of the torsion seismometer, Seis. Soc. Am., Bull., vol. 15(1925), pp.1-72.

2/ Benioff, Hugo: A new vertical seismograph, Seis. Soc. Am., Bull., vol. 22(1932), pp. 155-169.

3/ ------: A linear strain seismograph, Seis. Soc. Am., Bull., vol. 25 (1935), pp. 283-309.

4/ Blut, H.: Ein Beitrag zur Theorie der Reflexion und Brechung elastischer Wellen an Unstetigkeitsflächen, Zeit. Geophysik, vol. 8 (1932), pp. 130-144, 305-322.

5/ Bullen, K.E.: The variation of density and the ellipticities of strata of equal density within the earth, Mon. Notices, Royal Astron. Soc., Geophy. Suppl., vol. 3(1936), pp. 395-401.

6/ -----: Note on the density and pressure inside the earth, Royal Soc. New Zealand, Trans., vol. 67(1937), pp. 122-124.

7/ Dana, S.W.: Amplitudes of seismic waves reflected and refracted at the earth's core, unpublished thesis, Calif. Inst. of Technology, Pasadena, California (1944).

8/ -----: The partition of energy among seismic waves reflected and refracted at the earth's core, Seis. Soc. Am., Bull., vol. 34 (1944), pp. 189-197.

9/ -----: The amplitudes of seismic waves reflected and refracted at the earth's core, Seis. Soc. Am , Bull. 35(1945), pp. 27-35.

10/ Dix, C.H.: Refraction and reflection of seismic waves, Geophysics, vol. 4(1939), pp. 81-101, 238-241.

11/ Galitzin, Fürst B.: Seismometrische Tabellen, Imper. Acad. Sci., St. P etersburg, Comptes-rendus des seances de la commission seismique permanente, T.4, Livr.I.(1911).

12/ -----: Vorlesungen über Seismometrie, Imper. Acad. Sci., St. Petersburg (1912), pp. 286-347, 348-382.

13/ Geiger, L. and Gutenberg, B.: Ueber Erdbebenwellen VI, Nacr. Gesell. d. Wiss. Göttingen, math.-phys. Kl. (1912), pp. 623-675.

14/ Gutenberg, B.: Theorie der Erdbebenwellen, Handbuch der Geophysik, vol. 4(1932).

15/ -----: On focal points of SKS, Seis. Soc. Am., Bull., vol. 28(1938), pp. 197-200.

16/ -----: Travel times of principal P and S phases over small distances in southern California, Seis. Soc. Am., Bull., vol.34(1944) pp. 13-32.

17/ Gutenberg, B.: Reflected and minor phases in records of near-by earthquakes in southern California, Seis. Soc. Am., Bull., vol. 34(1944), pp. 137-160.

18/ -----: Energy ratio of reflected and refracted seismic waves, Seis. Soc. Am., Bull., vol. 34(1944), pp. 85-102

19/ -----: Amplitudes of P, PP, and S and magnitudes of shallow earthquakes, Seis. Soc. Am., Bull., vol. 35(1945), pp. 57-69.

20/ ----- and Richter, C.F.: On seismic waves (second paper), Gerl. Beitr. Geophys., vol. 45(1935), pp. 280-360.

21/ ----- --- -----: P' and the earth's core, Mon. Notices, Royal Astron. Soc., Geophys. Suppl., vol. 4(1938), pp. 363-372.

22/ ----- --- -----: On seismic waves (fourth paper), Gerl. Beitr. Geophys., vol. 54(1939), pp. 94-136.

23/ ----- --- -----: Seismicity of the earth(supplementary paper), Geol. Soc. Am., Bull., vol. 56(1945), pp. 603-668.

24/ Jeffreys, H.: The reflexion and refraction of elastic waves, Mon. notices, Royal Astron. Soc., Geophys. Suppl., vol. 1(1926), pp. 321-334.

25/ Joos, G. and Teltow, J.: Zur Deutung der Knallwellenausbreitung an der Trennschicht zweier Medien, Physikal. Zeit., vol. 40 (1939), pp. 289-293.

26/ Knott, C.G.: Reflexions and refractions of elastic waves, with seismological implications, Philosophical Magazine, S. 5, vol. 48 (1899), no. 290, pp. 64-97. Reprinted from Transactions of the Seismological Society of Japan (1888).

27/ Macelwane, J.B.: Reflection and refraction of elastic waves, Introduction to theoretical seismology, Part I, (New York: John Wiley and Sons, 1936), pp. 147-179.

28/ -----: Evidence on the interior of the earth from seismic sources, Physics of the earth---VII, Internal constitution of the earth (edited by B. Gutenberg), (New York: McGraw-Hill Book Co., 1939), chapter 10.

29/ Muskat, Morris: The reflection of longitudinal wave pulses from plane parallel plates, Geophysics, vol. 3(1938), pp. 198-218.

30/ ----- and Meres, M.W.: Reflection and transmission coefficients for plane waves in elastic media, Geophysics, vol. 5(1940), pp. 115-148.

31/ Ott, H.: Reflexion and Brechung von Kugelwellen, Annalen d. Physik (5), vol. 41(1942), pp. 443-466.

32/ Richter, C.F.: An instrumental earthquake magnitude scale, Seis. Soc. Am., Bull., vol. 25(1935), pp. 1-32.

33/ Schmidt, Wilhelm: Nomographische Tafel zur Auswertung von Bebendiagrammen, Gerl. Beitr. Geophys., vol. 12(1913), pp. 114-117, 120. Tafel V.

34/ Wiechert, E.: Theorie der automatischen Seismographen, Imper. Soc. Sci. Göttingen, math.-phys. Kl., new ser., vol. II, no. 1(1903), pp. 1-128.

35/ Zoeppritz, K.: Über Erdbebenwellen VIIB --- Über Reflection und Durchgang seismischer Wellen durch Unstetigkeitsflachen: Nachr. Gesell. Wiss. Göttingen, math.-phys. Kl. (1919), pp. 57-84.

36/ -----, Geiger, L., and Gutenberg, B.: Ueber Erdbebenwellen V, Nachr. Gesell. Wiss. Göttingen, math.-phys. Kl.(1912), pp. 121-206.

THE FAMOUS FLAMING GORGE
View from the northeast with the Green River in the foreground

GEOLOGY OF THE MANILA-LINWOOD AREA

Sweetwater County, Wyoming

and Daggett County, Utah

by

Samuel T. Martner

Submitted as a partial requirement for the Degree of Doctor of Philosophy

California Institute of Technology, Pasadena, Calif.

March, 1948

ACKNOWLEDGMENTS

This thesis is the written results of field work accomplished under the auspices of the Stanolind Oil and Gas Company. The author wishes to thank the supervising and administrative personnel of the Company who authorized the project. Mr. W. S. McCabe, district geologist of the Rocky Mountain area, was in direct charge of this work, and the writer wishes to specially acknowledge his direction and helpful cooperation.

Mr. H. T. Gonsalves was the writer' s field partner, and his loyal assistance contributed largely to the expeditious and successful completion of the project.

The author wishes to express his grateful appreciation to Dr. J. P. Buwalda of the California Institute of Technology for his supervision, help, and inspiration in the preparation of this report.

ABSTRACT

The Manila-Linwood area, so named from the two Utah towns within its boundaries, consists of approximately 200 square miles lying on the Wyoming-Utah state border. It is interesting to the geologist from an historical, stratigraphical, or structural viewpoint.

Historically, this district is one of interest because it contains the famous Flaming Gorge, named by Major John Wesley Powell. It has been a locality for geological investigation by such men as Clarence King, S. F. Emmons, Ferdinand V. Hayden, and many others. A brief review of the records of early geological and geographical explorations is presented.

Stratigraphically, one of the most completely exposed sections, representing a span of geologic time as long as or longer than that seen in any area of comparable size in the United States, characterizes the area. Rocks representing the Archean (?) and Algonkian eras, as well as all the later periods of the geologic time scale, with the possible exception of the Cambrian, Ordivician, Silurian, and Devonian, which are not differentiated into separate units in this report, are present in the district. These sedimentary rocks have been divided into 23 mapping units which are shown on a chart correlating them with the terminology used by previous workers in this area, and giving their tentative correlation with components used in adjacent areas. The character, thickness, age, and correlation of the various rock units are briefly discussed in the text. The only plutonic igneous bodies in the area are those intruded into formations of Archean (?) age. Extrusive accumulations are found at several places in the geologic column but are a very minor part of the section, consisting chiefly of tuffs interbedded in shales and sandstones. None of these igneous rocks were considered important enough to be designated as separate mapping units.

Structurally, the area embraces parts of two divisions of the Rocky Mountain province of the western United States. Its southern portion is a segment of the north flank of the great, east-west-oriented Uinta Mountain arch of northeastern Utah and its northern half is a sector of the Bridger Basin of southwestern Wyoming. Superimposed on the north regional dip are minor, transverse flexures. A part of the much-discussed Uinta fault and other faulting of a rather complex nature are also found in the district. The structure is discussed in a chapter entitled "Structural Geology".

A brief history of the structural geology of the area is presented.

A short chapter on the economic geology of the area, with an emphasis on the oil and gas possibilities is given.

Several problems worthy of further study in this and nearby areas are briefly discussed.

TABLE OF CONTENTS

ILLUSTRATIONS

I. INTRODUCTION

PURPOSE OF THIS REPORT

The search for new petroleum reserves in the Rocky Mountain region has been intensified in recent years; in an effort to find new structures suitable for "wildcat" drilling, a large amount of exploratory work is being conducted in and around the edges of the Tertiary basins of this region. The exploration in the basins is largely by geophysical methods, but geologic work must be done also, especially on the edges of the basins, to provide a basis for interpretation and evaluation of the geophysical results and to map those structures in pre-Tertiary rocks that are more effectively studied by surface geologic mapping than by any geophysical method now known. This report contains the results of one of these geologic surveys.

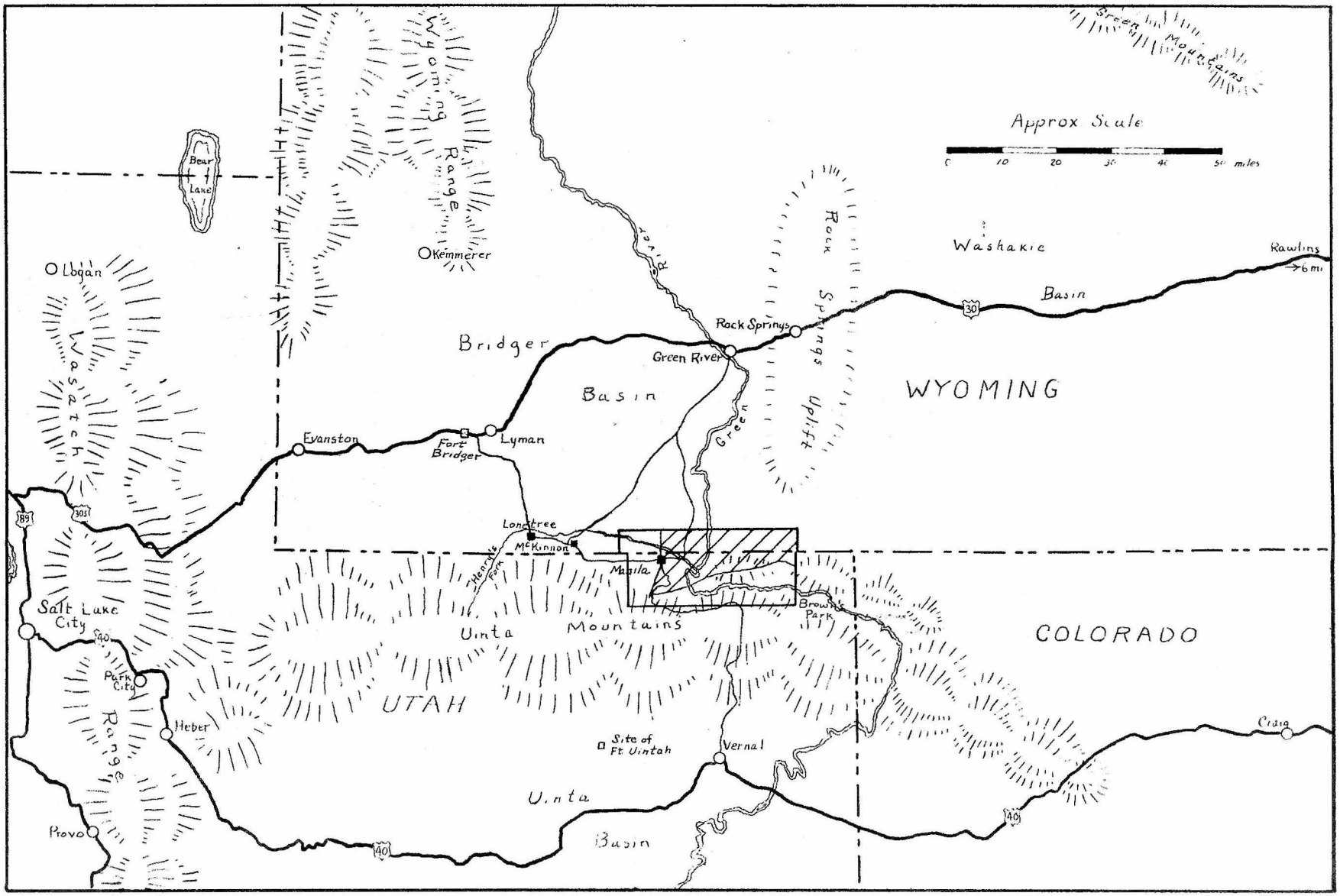

Figure 1.---Index map, showing the location of the area represented on the geologic map (plate I).

LOCATION AND SIZE OF THE AREA

The area under consideration in this report lies in Sweetwater County, southwest Wyoming, and Daggett County, northeast Utah. The crosshatched portion of figure 1 shows the location of the approximately 200 square miles which were mapped. The northern boundary of the area is the north line of Township 12 North, Sixth Principal Meridian. The western boundary is the west line of Range 109 West, Sixth Principal Meridian, thence obliquely across Township 3 North, Range 19 East, Salt Lake Base and Meridian, to and along the gorge of Sheep Creek where it trends SSW in Township 2 North, Range 19 East. The eastern boundary is the east lines of sections 5, 8, 17, and 20 of Range 105 West, Sixth Principal Meridian, and the east line of Range 23 East, Salt Lake Base and Meridian. The southern boundary is the Uinta fault line, which has a sinuous trend from the center of Township 2 North, Range 19 East, Salt Lake Base and Meridian, on the western edge of the area, to approximately two miles south of the north line of Township 3 North at the eastern edge. Some scattered work of rapid reconnaissance nature was done south of the Uinta fault, but the interests and objectives of the project limited work south of this geologic boundary.

AVAILABLE MAPS AND PREVIOUS SURVEYS

Available maps of the area are of several kinds. The southwest portion of the area (south of 41° latitude and west of 109°30' longitude) is covered by the Marsh Peak quadrangle of the United States Geological Survey, (surveyed in 1905-06). The Soil Conservation Service of the United States Department of Agriculture made an aerial survey of the area south of 41° latitude in 1937 and both aerial contact prints and mosaics in the form of 15' quadrangles are available (the mosaics for this area are ALJ 16 and ALJ 17 --- USDA 10801), except for the southwest corner of the area (west of 109°45' longitude). Aero Service Corporation aerially mapped the whole area in the 1940's, but mosaics were made in 15' quadrangles north of 41° latitude only. The two mosaics covering this area are Maxon SW on the east and Twin Buttes SE on the west. All of these aerial mosaics are on a scale of approximately two inches equals one mile.

For roads and an outline of the drainage, Grazing Map No. 36 of the Green River Grazing District 4 was of some use west of the Green River.

The United States Forest Service's map, "Ashley National Forest", is the latest published map available that covers the entire area mapped. It shows the drainage, most of the best roads and trails, the General Land Office land survey net, and the latitude and longitude grid in ten minute intervals.

The General Land Office established the Wyoming-Utah boundary in 1873. Piles of rock were used as markers and only one doubtful state line monument was recovered during the field work for this report, and this was far west of the area mapped. Section lines were resurveyed in Wyoming in 1909 and are marked with brass caps. However, one of these

markers was found ¼ mile from the location shown on the General Land Office map. The northwestern portion of the area in Utah was surveyed prior to 1905. Stone monuments were used and only one was recovered. The southwestern, and also probably the eastern portion of the area in Utah was surveyed after the use of brass caps was begun, but only a few of these in the country south of Manila, Utah, were recovered. The Wyoming-Utah state line is the boundary between land surveys of the Sixth Principal Meridian and the Salt Lake Base and Meridian.

The nature of this report necessitated the use of a base map on which the control was the General Land Office net of sections, townships, and ranges. After investigating the General Land Office maps thoroughly and finding that considerable adjustment was necessary at the Wyoming-Utah boundary, where the two land surveys meet, it was decided that the previously-mentioned map that is issued by the Forest Service would be used as a base. Accordingly the land grid was then enlarged on tracing cloth to a scale of two inches equals one mile by Mr. Clifford Christler, Stanolind Oil and Gas Company. The author here wishes to acknowledge Mr. Christler's accurate work on this project.

This base grid, although it is probably as good as any other that could be made from the General Land Office data, has discrepancies that require an adjustment of the areal geology. This adjustment is essential in order to place the rocks which crop out in a given section on the ground into that same section on the map. The greatest discordance occurs along the Wyoming-Utah state boundary. In the western portion of the area, i.e. north of the town of Manila, the expanse of territory shown by the aerial mosaics agrees with the base grid as well as can be expected with the errors inherent in aerial mapping, especially when the photos are at the edges of the areas where two different surveys meet. However, east of the

Green River, the discordance becomes appreciable. Near the gap made by Spring Creek in the "Devil's Causeway", the north-south distance between the north line of the southernmost section of the 6th principal meridian and the south line of the northernmost section of the Salt Lake base and meridian measures approximately 8000 feet on the aerial mosaics, while the same distance on the base grid measures about 6000 feet. It was necessary to represent the geology in a slightly altered form. This was accomplished by proportionally compressing what would be the true geologic map to conform to the restricted space. Such a method does not change the relationships radically, but the reader is warned not to attempt to make accurate thickness measurements in this portion of the area.

FIELD WORK

The investigations on which the present report is based were made during the summer season of 1947 by a party consisting of the author and Mr. H. T. Gonsalves, both of the Stanolind Oil and Gas Company.

The field work was accomplished in approximately sixty days during July, August, and early September. The limited time available for this field work necessitated the use of reconnaissance mapping practices almost exclusively.

Primary grid control was accomplished by recovering as many section or tract corners as possible during the course of delineating the geology. These points were plotted onto the aerial mosaics and served as "tie-in" points. East of the Green River, where only one tract corner was recovered, a plane table survey was conducted along the road in Lucerne Valley and a number of peaks were established by triangulation.

Elevations west of the Green River were obtained south of 41° latitude from the Marsh Peak quadrangle map; north of this line from stations of a Stanolind Oil and Gas Company gravity party working in this area. A number of U.S.G.S. and U.S.C. and G.S. bench marks are available and those recovered are shown on the geologic map (Plate I).

All of the stratigraphic sections from the bottom of the Weber formation to the top of the Mesaverde group were measured by transit and stadia rod. Thicknesses of the other formations were obtained by less precise methods.

CULTURE AND ROADS

The area under consideration contains two towns, Manila and Linwood, Utah. Both lie in the Lucerne Valley west of the Green River and are trading centers for the farming and ranching activities of this region. Manila is the county seat of Daggett County and has a population of 169. Linwood has a population of six. Both towns have post-offices. With the exception of Lucerne Valley west of the Green River and the valley of Henry's Fork and three residences in the valley of Sheep Creek, the area is uninhabited.

There is a good secondary graded dirt road from Linwood to Green River, a distance of fifty miles. The road from Linwood to Lonetree by way of Manila and McKinnon is a good graded dirt road, gravel surfaced in part. The road from McKinnon to Green River is of the same caliber. The road from Lonetree to Lyman is a poor dirt road most of the way and although passable is not recommended for automobile travel. All of these roads are very difficult and almost impassable during the rainy season. There is a seventy-six mile road from Manila to Vernal. This road is dirt, often single car width, dangerous in wet weather, and impassable for most of the winter. All of the other roads shown on plate I are tertiary or worse, and the best of them are difficult to travel when only slightly wet. The Green River has no vehicular bridge across it, nor is it fordable by automotive equipment. The closest crossing is Briniger's "help yourself" ferry, twenty miles north of Linwood.

The roads in this area were divided by the author into two types for presentation on plate I. Automobiles without special equipment can travel over those shown by two solid lines, while a vehicle with four-wheel drive, an automobile with four-speed transmission, or other special equipment is required to traverse those shown by two dotted lines. Where

roads were washed out to a degree necessitating repair prior to usage, they are marked with a single dotted line. The conditions shown are, of course, applicable for the field season of 1947, and each year wash-outs may obstruct passage on one of these roads. Trails are common in this area and access to any locality by their use is not difficult, so no attempt was made to show them on the map.

If new roads are required to any part of the area, their construction by bulldozer would be a relatively simple matter, except in the bad lands portion of the area east of the Green River and north of the Wasatch-Green River contact.

Lucerne Valley west of the Green River is the center of some grain production but cattle raising predominates. Some lumbering is done just south of the area mapped. The remainder of the area is suitable for grazing during certain months of the year except in some places with bad-land topography.

Rock Springs, which owes its existence to the coal mining industry, is the closest large trading center and has a population of 10,000. Green River is a railroad town with about 2,000 population. Vernal is a farming center with about 4,000 inhabitants. Salt Lake City is 181 miles by U.S. route 30, a paved highway, from Green River.

TOPOGRAPHIC FEATURES, DRAINAGE, AND VEGETATION

The area of this report lies between the east-west trending Uinta Mountains of Utah and the Bridger Basin of Wyoming. The Uinta Mountains are about 130 miles long and 30 miles wide with a relatively flat summit, higher on the western end than on the eastern. The highest point in this range is Kings Peak near the headwaters of Henrys Fork and is 13,498 feet high. From here the summit peaks gradually decrease in elevation to about 10,000 feet south of the area mapped.

The Bridger Basin is a large relatively flat expanse, approximately 100 miles across. The southern portion, which has an elevation of approximately 6500 feet, is dissected into badlands topography, and contains scattered buttes rising from 1000 to 3000 feet above the drainage level.

The area of interest contains portions of both these physiographic features. The northernmost two to four miles is a strip of typical Bridger Basin badlands, the southern edge of which tilts northward. This edge is bounded by a south facing escarpment several hundred feet high of upper Wasatch group sediments. Just south of this is the east-west trending Lucerne Valley, two to four miles wide, cut into the soft shales of the upper Cretaceous and lower Wasatch group. On the east this valley terminates in a saddle in T3N beyond which lies the semi-circular Clay Basin, some seven miles in diameter. Only the westernmost edge of this basin is in the area under discussion. Dividing Lucerne Valley longitudinally, from the western bank of the Green River Valley to the east end saddle, is a thirteen mile long, crescent-shaped, double-crested ridge of Mesaverde sediments, which rises at its center to the elevation of the Bridger Basin escarpment to the north.

West of the Green River the topography south of Lucerne Valley is marked by three successive south facing escarpments with northern dip slopes and narrow intervening valleys. The widest of these valleys is the one eroded into the soft Morrison formation. The southernmost escarpment, capped by the resistant Nugget sandstone, is the north wall of the deep, narrow Sheep Creek valley, and rises 500 to 1000 feet above the valley floor. This escarpment continues to the east across the Green River as Boars Tusk, steep on the north side and practically vertical on the south side, and then continues as a less rugged ridge eastward until it meets flat topped Goslin Mountain.

South of Sheep Creek, the bed of which is about 6000 feet in elevation, the country rises rapidly on a steep dip slope of the Park City formation to a dissected erosion surface of approximately 8000 feet elevation. This erosion surface, which is about six miles wide - north and south - continues eastward across the Green River, forming the flat tops of Bear Mountain and Goslin Mountain. The steep north slope of Goslin Mountain, because of the termination of the Nugget sandstone ridge mentioned previously, forms the southern edge of Lucerne Valley and Clay Basin at the eastern margin of the area. This erosion surface is well dissected by steep sided canyons. Sheep Creek Gorge, over 1000 feet deep, which bounds the area on the west, is one of these canyons.

The Green River, flowing southward through the center of the area, cuts across all of these topographic features with a very sinuous course; but only to a point about half way across the erosion surface, where it turns suddenly and flows eastward longitudinal to the surface through the 1500 feet deep Red Canyon.

All of the drainage of the area flows into the Green River, which is one of the main tributaries of the Colorado River. The drainage may be

divided into several groups. West of the Green River, Lucerne Valley drainage flows into Henrys Fork, one of the main tributaries of the Green River. The area of Tertiary sediments north of Lucerne Valley drains partially into Henrys Fork and partially directly into the Green River by means of minor tributaries. South of the Nugget escarpment, the drainage is principally into Sheep Creek.

East of the Green River and south of the Nugget ridge, the drainage is southward to the Green River, primarily by means of Dutch John Creek. Lucerne Valley drains westward chiefly by way of Spring Creek. East of the divide, the Clay Basin drainage is into Red Creek, which is several miles east of the area mapped.

The vegetation of the area varies greatly in character. On the Tertiary sediments the vegetation is sparse and consists mainly of Artesima. East of the Green River this region has some dwarf cedar. Lucerne Valley is primarily sparse grasslands except for irrigated pasturage and some grain cultivation near Manila and Linwood. The escarpments and erosion surface south of Lucerne Valley have Artesima and dwarf cedar, the former becoming less plentiful and the latter thicker as one proceeds southward. The southern part of the erosion surface, just south of the area mapped, is forested with small diameter pine and aspen. Some of this timber is cut for mine timbers and log structures.

The valleys of Henrys Fork and Sheep Creek have a good growth of cottonwoods and other trees; the Green River Valley has fine grass pasturage, but does not contain many trees.

HISTORICAL REVIEW OF PREVIOUS GEOLOGICAL AND GEOGRAPHICAL EXPLORATION

A complete and comprehensive review of the early explorers who visited the region of southwestern Wyoming and northeastern Utah is beyond the scope of the present paper and will be left for others who are more interested in the romance of early fur trading and exploration in the West. However, a few words concerning some of these early explorers, especially those who crossed the pertinent area, are not without place here as a general background to the reader.

Prior to the nineteenth century, the exploration in the western portion of the United States was primarily restricted to Spanish and French expeditions. Sieur de la Venendrye is reported to have explored as far south as the Wind River in 1743-4. The northernmost exploration of the Spaniards was to the south flank of the Uinta Mountains, Padre Escalante having crossed the Green River east of the present site of Vernal while attempting to find a route from Santa Fe to Monterrey in 1776.

As far as the writer has been able to ascertain, the first white man to actually visit the area encompassed by this report, with the exception of possibly lone and intrepid trappers who left no record, was William Henry Ashley in the year 1825 14/. In 1822, General Ashley and a capable fur trader, Andrew Henry, had joined resources and experience to delve into the risky and lucrative business of fur trading. Up to this time the fur trappers had concentrated their efforts further north in the Columbia, Snake, Yellowstone, Bighorn, and Missouri river basins, ever widening the knowledge of the country which had been opened by Lewis and Clark in 1806. For several years Ashley and Henry operated along the established routes of travel (i.e. the Missouri-Yellowstone-Bighorn river system), with parties working southward into the headwaters of the Green River by 1823. In 1824,

Henry withdrew permanently from the fur trading business. Ashley, in 1825, by using horses instead of the traditional boats, set out with a party to explore and establish a new southern route from St. Louis to southwestern Wyoming by way of the unnavigable South Platte River. He crossed the southern end of the Bighorn Range, and his first sight of the Green River was fifteen miles north of the mouth of the Sandy River, which he named. Here he sent out three parties of men to explore. After building two mackinaw boats, he and the rest of his men embarked on their historic trip down the Green River. On April 25 the party disembarked at Henrys Fork and marked this location as the "General Rendevous" for a later meeting with the other parties. They continued on their voyage on May 2 and arrived at Brown's Park on May 5, after traversing the Flaming Gorge, Horseshoe Canyon, Kingfisher Canyon, Hideout Canyon, and the turbulent Red Canyon. An inscription, ASHLEY 1825, which he painted in Red Canyon, near the falls that now bears his name, was noticed later by Manly in 1849, Powell in 1869, and was still partially visible when Kolb floated down the river in 1911. The party did not reach the mouth of the Grand River, but retraced a portion of their river voyage, turned west, and recrossed the Uinta Mountains by way of the Duchesne River, passed near Bald Peak, and proceeded back to the point of the "General Rendevous" at the junction of Henrys Fork and the Green River.

The Uinta Mountains proved to be a rich source of beaver peltries, and "Brown's Hole" (Brown's Park) became famous as a yearly rendevous for trappers. The last of these regular rendevous was held in 1840.

There is no evidence that Bonneville in the 1830's nor Fremont in the 1840's visited the vicinity of the Flaming Gorge, both men crossing the Green River further to the north. Fremont, however, did visit Brown's Hole while returning from his second expedition in 1844 24/.

In 1849, W. L. Manly with six others followed in Ashley's "footsteps" by floating down the Green River from Black's Fork to the south flank of the Uinta Mountains 50, p. 76-91/.

During the investigation of routes for a transcontinental railroad during the early 1850's, efforts were concentrated in the basins north and south of the Uinta Mountains and the area in the vicinity of the Flaming Gorge was not explored officially. Lieut. E. G. Beckwith, with a party which had Egloffstein as topographer, in 1854 made one reconnaissance southeastward from near Fort Bridger to a high hill south of Henrys Fork, fifteen miles west of the Green River 5/. This was undoubtedly Mount Corson (Phil Pico Peak). He also indicated in his report that a wagon trail existed from Fort Bridger across to and down Henrys Fork, indicating the existence of settlers near the lower end of this stream, although this may have been merely the trail to Brown's Hole by way of Lucerne Valley, Clay Basin, and Red Creek which Hayden later mentioned 30/.

Although Ashley had some knowledge of geology, the first well trained geologist to visit this area was J. W. Powell. On May 24, 1869, he and nine others started down the Green River in four boats from the infant village of Green River on the new Union Pacific Railroad. On May 26, he arrived at the mouth of Henrys Fork and picked up some instruments he had "cached" during a reconnaissance made the preceding summer. While camped here he named the Flaming Gorge and upon resuming his journey named Horseshoe Canyon, Kingfisher Canyon, and Red Canyon. His first written account of this voyage 59/ submitted to the Smithsonian Institution principally included a chronological account of the voyage, the physical features encountered, and the zoology of the region, and has little of specific geologic note except in the field of geomorphology. A year later he published another report on the geology of the Uinta Mountains 60/ which

contains much of geologic interest and will be mentioned later.

In 1870, a year after Powell's first voyage past the Flaming Gorge, Dr. F. V. Hayden conducted a reconnaissance across this area 30/. From Fort Bridger he proceeded south to the summit of Gilbert Peak, thence down Henrys Fork to the Green River, thence across the hills northeast of the Green River to Brown's Hole, and from Brown's Hole through Red Creek Canyon to Clay Basin, westward to Henrys Fork, and northward to Green River Station. By this time Brown's Hole had become a favorite spot to winter cattle and Hayden reported " the day we visited it 2200 head of Texas cattle were driven into it from the east, to remain during the winter, and destined for the California market in the spring". He described the section at the Flaming Gorge below the lower Cretaceous.

The same year Marsh 52/ with a party from Yale University followed approximately the same path to Brown's Hole, then proceeded into the Uinta Basin to Fort Uintah (approximately 20 miles west of the present site of Vernal, Utah), thence northeast over the Uinta Mountains, down Sheep Creek Gorge, across to Henrys Fork, and back to Fort Bridger.

The next geologic visitors were the members of the King Survey. King and his men started in 1867 to do field work that was to take seven seasons and which resulted in the large seven volume publication of the geology of the fortieth parallel 45/. By 1871 Emmons was working in the area under discussion. A deeply scratched inscription reading "KING 1871", found by the writer in a large cave of Nugget sandstone near the Flaming Gorge, seems evidence that the leader of the survey also visited the area during this year. The Flaming Gorge was evidently a region of great interest to this party. Mention is often made of Camp Stevenson on Henrys Fork near its junction with the Green River and the geological formations near here are described in detail. A great amount of paleontological work was done by

Cope and Meek of this survey.

During the rest of the nineteenth century, contributions consisted chiefly of land surveys, paleontological and stratigraphic data concerning the region by Cope, Meek, Marsh, White, Emmons, and many others, and accumulated information concerning the coal bearing horizons, principally further northeast in the Rock Springs uplift. In 1889, White 89/ wrote a paper in which he included a geologic map that included a part of the area here discussed, but most of his work and interest seemed to lie in the Yampa Plateau and Axial Basin to the southeast.

Just after the turn of the century, the United States Geological Survey started its intensive coal investigation program. Gale 25,26/, in 1907, investigated the Henrys Fork coal field, which lies just north of Linwood and within the area described in this report. Schultz made a study of the Rock Springs coal field and in 1920 published a petroleum investigation bulletin 68/ based on his field work in 1907-08 of the southern portion of the area he mapped. The southwest corner of his map encompasses the eastern portion of the district mapped for this report and one of his sections is just east of the Green River in this area.

A few years later the phosphate investigations of the United States Geological Survey again invited the attention of Schultz and six weeks field work in 1914 resulted in a reconnaissance report of the whole Uinta Mountains 67/. This report is restricted in detail to the Park City formation.

Sears and Bradley 72/, from field work conducted during 1921-22, discussed the relation of the Wasatch and Green River formations and their map includes the eastern portion of the area mapped for this report.

Reeside accompanied a party investigating the water power possibilities of the Green River in 1922. His report 61/ for the area in which we are

interested primarily reiterates the earlier work of Schultz.

Forrester, in 1937, published a report 23/, based on reconnaissance work during 1933 and 1934, the primary purpose of which was "to consider, from field evidence, the Uinta Range as a structural unit, in an attempt to find a satisfactory explanation of the origin and peculiar orientation of this range with respect to neighboring Rocky Mountain Ranges".

Bradley 10/,in 1936, reported comprehensively on the geomorphology of the north flank of the Uinta Mountains and his map, of course, covers the area of this report.

Dobbin and Davison, in 1945, issued a map 16/ which includes the eastern-most three miles of this area.

Thomas and Krueger, in 1946, placed in print an article 78/ which includes a stratigraphic section measured in the area of this report from the bottom of the Weber formation to the top of the Curtis formation.

Recently the United States Geological Survey has been conducting field mapping in the oil and gas investigation program, which has resulted in two publications on the geology of portions of the south flank of the Uinta Mountains 36,47/.

II. STRATIGRAPHIC GEOLOGY

INTRODUCTION

This area is so located geographically that it might be termed a stratigraphic "crossroads". Three more or less independent sets of stratigraphic terminology have been developed in the past by geologists working in three different regions, namely: (1) the Grand Canyon and High Plateaus to the south, (2) the Wasatch Mountains and western Wyoming to the west, and (3) central and eastern Wyoming, Colorado, and other areas to the north-east and east. As geologists and geologic knowledge have radiated from these three regions, there naturally has evolved a conflict in the names of the rock units and the upper and lower stratigraphic limits of the formations in the areas where the terminology overlaps. Therefore, there is a choice of names open for a worker in a district such as this. In the following pages, the writer will attempt to explain briefly why he used the terms he did, when such a choice was possible.

The oldest rocks exposed in the area are of pre-Uinta Mountain age, which places them in either the Algonkian or Archean. With the deposition of the Uinta Mountain sediments, there began a long period of deposition that was not disturbed by great orogenic movements until late Cretaceous or early Tertiary time. Some disturbances are noted in this long interval of deposition by a lack of beds found elsewhere in the Rocky Mountain region; but the movements which caused these inter-depositional periods of erosion or non-deposition, as the case may be, were probably of relatively minor intensity, although they may have, and probably did, affect large regions.

The great thicknesses of sediments were folded, faulted, and eroded during the orogeny that started probably in late Cretaceous time and extended certainly into the early Tertiary. Following or concurrent with these movements, a series of land laid fluviatile and lacustrine sediments

were deposited. Culminating the lake deposits was a period of volcanic activity that ended during Eocene time. This terminated the geologic picture of sedimentation which can be read in this area with the exception of some Quaternary terrace deposits.

PRE-CAMBRIAN

Red Creek Quartzite

The Red Creek quartzite is the oldest exposed formation in the Uinta Mountains. It was named by Powell 60/ in 1876 from its type locality in Red Creek about one mile east of the area mapped for this report. Its total recognized distribution is restricted to several rather limited patches in this vicinity. Only the western edge of the largest outcropping of Red Creek quartzite was in the area mapped, with the exception of an exposure never before recognized on published maps, which was found in T3N, R21 and 22E.

Blackwelder 7/ has given a good description of these rocks as "pure white metaquartzite associated with silvery muscovite schist and also garnet-staurolite schist, cut by dikes of amphibolite. The beds are all intensely folded and have been intruded by younger dikes of pegmatite and pink granite." There is some doubt concerning the origin of the amphibolite and some authors contend that it is an amphibole schist derived from sediments interbedded in the quartzite. The new exposure mentioned previously is primarily pink granite and hornblende diorite gneiss with a small amount of quartz.

The relationship between the Red Creek quartzite and the Uinta Mountain group was considered by Powell 60/, King 45/, and Emmons 19/ to be that of an island or headland of Red Creek quartzite during Uinta Mountain time, upon which the overlapping Uinta Mountain sediments were deposited. Weeks 86/ believed it to be a metamorphosed phase of the upper part of the Uinta Mountain group. Van Hise and Leith 81/ reviewed all of the literature prior to 1909, and stated that an unconformable contact can be seen at many places, and he considered it to be of Archean age. Blackwelder 7/ makes tentative

correlation of this occurrence with others in the Rocky Mountain region and states "since none of the intrusives in the Red Creek locality intersect the Uinta [Uinta Mountain] quartzite and since pebbles of granite are found in the basal conglomerate, it is probably safe to conclude that the granitoid rocks of this region are generally older than the late Algonkian or Beltian system". Hinds 33, p.13/, in a paper which reviews the earlier literature, states that "there is no Archean in the Uinta Mountains"; but, in another place in the same report p.91/ when speaking specifically of the Red Creek quartzite, he states that "this section merits further careful study, since exposures of contact between the quartzite series [Uinta Mountain quartzite] and Archean rocks are few, and no other is known in the Uinta region". Forrester 23/ considers the age of the Red Creek quartzite to be Archean.

No published measurement or estimate of the thickness of the Red Creek quartzite metasediments has been made.

As the area mapped had only a small portion of the Red Creek quartzite exposures and the writer had limited opportunities for observations, he has little to add to previous published accounts concerning their lithology or relationship. Although indefinite, the contacts between the Red Creek quartzites and later sediments in the mapped area are all believed to be faults.

Uinta Mountain Group

Name and Distribution---The Uinta Mountain group was named by T. S. Lovering, et al, 49/, in 1935, on a new geologic map of the state of Colorado. The new name was used to replace the term Uinta group (Uinta sandstone, Uinta quartzite) which had been used first by Powell 60/, in 1876. Wood 96, p.244/ had proposed the name Emmons Peak quartzite, in 1934, but this name did not gain favor. Considerable confusion existed as the

name "Uinta" had been used to designate an Eocene formation in the Uinta Basin, just south of the Uinta Mountains.

The Uinta Mountain group makes up the great central core of the Uinta Mountains. In the area of this report it is the only lithologic unit found south of the Uinta fault with the exception of three small exposures of other rock.

Character---This group is composed of a huge thickness of dull reddish-brown sandstones, slightly to moderately quartzitic. They are composed almost entirely of quartz grains, with some black mica and a large amount of ferruginous material that gives them the reddish color. Associated with the sandstones are thin bedded ferruginous shales, usually arenaceous. Also associated with the sandstones, which are usually fine grained, are beds of conglomerate and pebbly sandstones. The pebbles are almost entirely clear glassy quartz, sub-angular to well rounded. Granite pebbles have been reported by Blackwelder 7/ near the unconformable contact with the Red Creek quartzites east of this area. Ripple marks in the series are fairly abundant and rain drop impressions have been reported. The sediments are surprisingly well bedded for sub-aerial deposits.

Although the red color is one of the distinctive features of the bulk of this huge thickness of sediments, there occurs in some places beds of gray to greenish-gray sandstones, containing practically no oxidized ferric compounds.

Thickness---Powell measured the thickness of the Uinta Mountain group in the vicinity of Red Creek to the east of the area mapped for this report. He arrived at a thickness of about 12,500 feet but reported that the bottom of the section was not seen. Eardley and Hatch 17/ measured a partial section in the western end of the Uinta Mountains and arrived at a thickness of approximately 12,000 feet. The writer is aware of no other measurements

of the group, although various opinions of the thickness have been expressed. Forrester 23/ suggests a thickness of at least 15,000 feet.

Age and Correlation---No fossils have ever been reported from this group. There was a considerable difference of opinion among early geologists working in the Uinta Mountains concerning its age. King 45/ erroneously correlated it with the Weber quartzite in the western Uintas and designated it as Carboniferous. Hayden 30/ and Marsh 52/ suggested a Silurian age, and White 88, p.23/, who mapped the group as Weber, was "disposed to agree". Powell 60/ tentatively dated it as Devonian. Emmons 21/, in 1889, was the first to suggest an Algonkian age, by assuming it to be the correlative of the Big Cottonwood quartzite of the Wasatch Mountains. Walcott 84/ assigned a Cambrian age to an unknown thickness, perhaps 2000 feet, of the top of the Big Cottonwood quartzite and referred the remainder to the Algonkian. Berkey 6/ and Butler 11/ considered the group as Cambrian. Weeks 86/ placed it in the pre-Cambrian because of its lack of fossils and its subjacent position to the Lodore shale, believed to be Cambrian. Hintze 34/, in 1934, described what he considered to be the Proterozoic-Paleozoic contact in the Big Cottonwood quartzite. Hinds 33,p.92/ considers that the upper part of the Uinta Mountain group above a similar unconformity is Cambrian in age and is comparable to the Brigham quartzite, while the lower part of the Uinta Mountain group is Uncompahgran in age and is comparable to the Cottonwood quartzite. Eardley and Hatch 17/ have divided the Uinta Mountain group of the western Uinta Mountains into four units. They correlate the upper 1000 feet with the Tintic quartzite and Brigham quartzite, both of which they place in the early middle Cambrian or late early Cambrian. The rest of the group they place in the earlier Cambrian or late Proterozoic. They mention that the unconformity earlier reported by Hintze in the western Uintas could not be found by Schneider, Forrester, nor

themselves; and, if present, must be of a very minor nature.

More detailed work is necessary to fix the exact age of the Uinta Mountain group, although it is probably in large part Algonkian in age.

CAMBRIAN TO LOWER CARBONIFEROUS UNDIFFERENTIATED

In the western part of R3N, T23E, is a small exposure of formations totally different from any other rocks exposed in the area. Lithologically they are composed of contorted hard gray limestones, quartzitic sandstones, and conglomerates with well rounded quartz pebbles up to three or four inches in diameter. Although not measured by precise methods, the thickness of these beds appears to be 2500 feet or more. Time did not permit more than a rapid reconnaissance of this exposure. In one of the limestone beds near the northern edge of this outcrop, the writer found organic remains later identified as a Bryozoan */ of fenestelloid type and probably Devonian or Mississippian in age. The only described formations which might logically correlate with those mapped are the Ogden quartzite and overlying Mississippian (see Weeks 86/).

* Oral communication from Dr. C. R. Stauffer, who identified the specimen.

CARBONIFEROUS

Madison, Brazer(?), and Morgan Formations undifferentiated

Names.---The Madison limestone was named by Peale 57/, in 1893, from its type locality in the Madison Range in central Montana. Since that time the name has found wide usage throughout the Rocky Mountain region. The Brazer limestone was named by Richardson 64/, in 1913, from its exposure in Brazer Canyon in the northern Wasatch Mountains. The Morgan formation was named by Blackwelder 6a/ from a manuscript name applied by F. B. Weeks to a series of beds of red sandstone and shale with intercalated thin limestones exposed near the town of Morgan in the upper canyon of the Weber River in north-central Utah.

These series of formations were mapped in the area in which we are interested by the geologists of the Fortieth Parallel Survey as part of the Upper Coal Measures as they mistook the Uinta Mountain group in this area as Weber quartzite. However, Emmons 19/ in the valley of the Weber River had the Weber overlying the Wasatch limestone, the upper part of which was later determined as Brazer limestone and Madison limestone. Powell 60/ included these formations in his Red Wall and Lower Aubrey groups. Weeks 86/ called these formations collectively the "Mississippian series (upper part Pennsylvanian series)", but differentiated them from the Weber formation. Berkey 6/ and Emmons 22/, in the first decade of the twentieth century, used the name Wasatch for the whole Mississippian and Pennsylvanian limestone section.

In the Wasatch Mountains, many names have been applied to various units of the Mississippian and lower Pennsylvanian rocks, particularly the components of the huge thickness of limestones and other calcareous sediments of the Mississippian. The first attempt, to the writer's knowledge,

to divide the Mississippian and pre-Weber Pennsylvanian in the Uinta Mountains was done by Williams 91/ in 1943. His report includes two sections from the south side of the mountains, one on the Duchesne River and one on Brush Creek. He used the formation names Madison, Brazer, and Morgan, as is done in this report.

Distribution.---In the area under discussion these rocks are found on the north side of, and adjacent to, the Uinta fault in an irregular strip varying greatly in width of outcrop from the western edge of the area to the eastern edge of R19E. One small exposure is also to be found in a fault slice in Sec. 4, T2N, R21E.

Character.---These formations are marked by their calcareous nature in contrast to the overlying Weber sandstone. The upper beds are composed of gray, greenish-gray, and lavender shales and fine grained sandstones interbedded with thin layers of gray limestones. Under these upper layers the rocks assume a reddish color and contain some red sandstones. Below these the sediments become increasingly more calcareous; until, at the lowest part of the exposed series, they are composed almost entirely of massive, gray, cliff-forming limestones. These beds are rather fossiliferous; Brachiopods are predominant in the upper part, and corals were the only fossils which the writer noted in the lower part.

Thickness.---The thickness of these beds is very difficult to ascertain in this area; however, using reconnaissance methods, the writer obtained a thickness subject to some scepticism of 2700 feet.

Age and Correlation.---The ages of the Madison limestone, the Brazer formation, and the Morgan formation have all been fairly well established. However, there seems to be a considerable difference of opinion concerning the age of the sediments between the Weber formation and the Madison formation on the south flank of the Uinta Mountains. J. Stewart Williams 91/,

at his section on Brush Creek, has reported (in descending age):

Weber formation		(upper Des Moines age)
Morgan formation	385 feet	(lower Des Moines age)
Brazer formation	700 feet	(middle Chester age)
Madison formation.		

Thomas, McCann, and Raman 79/, based upon paleontological determinations of J. Steele Williams and L. G. Henbest, have reported the following section at Split Mountain, approximately 22 miles south-east of William's section at Brush Creek:

Weber formation		
Morgan formation (upper member)	710 feet	(lower Des Moines, Lampasas and upper Morrow age)
Morgan formation (middle member)	295 feet	(Morrow age)
Morgan formation (lower member)	280 feet	(Morrow age ?)
Molas (?) formation	65 feet	
Madison limestone.		

This section includes unconformities in the lower member of the Morgan formation and between the Molas and Madison. As will be noticed on inspection the Split Mountain section has 900 feet more of Morgan than the Brush Creek section, and no Brazer as opposed to 700 feet at Brush Creek. This apparent paradox suggests that more further detailed sections are necessary, inasmuch as this amount of apparent thickening and thinning in 22 miles seems somewhat excessive.

In the area of this report, further detailed work is necessary to establish the thicknesses and ages of the formations included in this unit as mapped for this paper. A slight disconfirmity was noted between the Weber and underlying Morgan (?) at Sheep Creek Gorge, the only excellent exposure of this contact in the area, so that the upper part of the Morgan (?) is probably missing. On lithological grounds only it seems that the amount of missing beds is small.

Weber Formation

Name.---The name Weber quartzite was first applied by King 46/, in 1876, to the exposures in Weber Canyon of the Wasatch Range. Powell 60/ considered

it the lower part of the Upper Aubrey group in the eastern Uinta Mountains. However, King, himself, believed the Uinta Mountain group to be Weber, as previously mentioned; and placed the true Weber in the Upper Coal Measures. White 89/ also called the Uinta Mountain group the Weber. Berkey 6/, in 1904, was the first to actually apply this name in the Uinta Mountains to the true Weber as the result of work on the south-western flank of the mountains. Since then the name has been universally applied in its true meaning.

Distribution.---The Weber outcrops in a strip of one and one-half miles width from several miles east of the Green River to and beyond the western edge of the area. The best accessible exposure across the complete section of this formation is in Sheep Creek Gorge, which contains the Manila-Vernal road. Other excellent exposures of most of the section are to be found where the Green River cuts across the northward dipping beds at Horseshoe Canyon and Kingfisher Canyon.

Character.---The Weber formation in this area is entirely composed of one lithologic mapping unit, and consists of tan to light buff to almost white, fine grained sandstone. The sandstone is slightly quartzitic in some places; but, as a whole, it is remarkably friable. It is very well sorted and free from accessory minerals; although it is irregularly calcareous to a slight degree. The bedding is massive and the individual beds are cross laminated in long lines gently sloping from the bedding planes.

The sandstones weather into precipitous bluffs; and, where streams have cut across the dipping beds, deep and almost vertical sided canyons such as those of Sheep Creek and the Green River have been formed. No fossils were found by the writer during this project.

The upper boundary of the formation will be discussed under the Park City formation.

Thickness.---A measured section in Sec. 3, 9, and 10, T2N, R19E, gave a thickness of 1186 feet (see pl.III).

Age and Correlation.---The general lack of fossils in the Weber formation makes exact age correlation somewhat hazardous. It is universally accepted that the lower part of the Weber is of Des Moines age. However, its upper limit is not so well accepted. Thomas, McCann, and Raman 79/ state "it does not seem unlikely, therefore, that the upper part of the Weber may be of Permian age". J. Stewart Williams 91/, at his Brush Creek section, considered the whole Weber section to be Des Moines age. Moore, et al, 54/ do not definitely define its upper limit, but on their chart it appears to include a large part if not all of the Missouri age and possibly some of the Virgil age. However, they do consider that the overlying Park City formation is in part, at least locally, of upper Pennsylvanian.

Moore, et al, 54/ have shown the Weber to be the equivalent of the lower part of the Oquirrh quartzite and the upper part of the Manning Canyon shale in the Wasatch Range; but Baker 2/, at a later date, states "The lithology and the stratigraphic position of the Weber quartzite clearly indicate its equivalence with some part of the Oquirrh formation, but a more precise correlation cannot be made from information now available". Moore, et al, 54/ correlate the Weber with the upper part of the Amsden formation and the Tensleep formation of northern Wyoming; and also with a part of the Wells formation of the northern Wasatch Range and south-east Idaho.

PERMIAN

Park City Formation

Name.---Boutwell 9/, in 1907, first described the Park City formation and named it from Park City in the Wasatch Range. The name Phosphoria was applied by Richards and Mansfield 63/, in 1912, to a formation in southeastern Idaho and was correlated with the two upper members of the Park City formation. The name, Park City, has been used in the area of this report as this same formation continues with discontinuous exposures to the western end of the Uinta Mountains, where it is close to and easy to correlate with the Park City type section.

Prior to the use of the name Park City, other names had been applied in the Uinta Mountains: King 45/ placed the Park City at the top of his Upper Coal Measures of the Carboniferous; Powell 60/ called it the Bellerophon Limestone member of the Upper Aubrey group; and later workers, up to 1907, used these names.

Distribution.---In this area the Park City outcrops in a strip from several miles east of the Green River to and beyond the western edge of the area. The width of the strip varies from several hundred feet to approximately one and one-half miles depending upon the dip and topography.

Character and thickness.---The character and thickness of this formation has been reported by several previous workers in the Uinta Mountains. The presence of phosphates led to an inspection of these beds in 1914 by Schultz 67/. He reviewed the previous literature and gave a detailed description with measured sections at various places on both flanks of the mountains, two of these sections being within and one section about six miles west of the area here mapped. Baker and J. Steele Williams 4/, J. Stewart Williams 90,91/, and Thomas and Krueger 78/ have recently discussed this formation. The first of these papers does not include a discussion

of any part of the Uinta Mountains; and the others are mainly concerned with the south flank, except for one section in the last paper which was measured near the Green River in the area of this report.

The Park City beds consist of dense cherty limestones with calcareous sandstones, phosphatic dark-colored shales, and chert interbedded. This formation can be divided in this area into three general parts: a lower part of sandy limestone interbedded with some dark-colored shales and sandstones, a middle part containing much more dark-colored phosphatic shale with some sandstones and cherty limestones interbedded, and an upper part of gray shales and dense, hard, limestone.

A section was measured in the vicinity of Bennett's Ranch on Sheep Creek as follows (see pl.III):

Cream-colored resistant dense bluff-forming siliceous limestone, the beds near the bottom are massively bedded but bedding is thinner towards top	90 feet
Light gray shales and siltstones, forms talus slope, details obscure	80
Hard dense fossiliferous light gray cherty limestone interbedded with siltstones, some thin-bedded shale breaks and some chert beds	110
Light gray sandstones and siltstones with some thin dark-colored phosphatic shale beds	50
Thin bedded dark-colored phosphatic shale	50
Cream-colored hard massive limestone and hard sandstone	25
Massive cliff forming unit consisting of beds of hard gray sandstones, and dense arenaceous limestone, with some interbedded colored shale beds	110
Total	515 feet

Below this section, Thomas and Krueger 78, p.1293/ place a ten foot brown, massive, cross-laminated sandstone superficially like the Weber which rests on an irregular erosion surface of the Weber. The writer failed to detect this erosion surface without reasonable doubt and further convincing evidence will be necessary before its existence will be verified in his mind. In any event, the bottom of the section detailed above was used as the lower contact of the Park City and proved an admirable marker for mapping.

The Park City topographically forms a distinctive dip slope wherever found in this area. It is the south wall of Sheep Creek Valley west of the Green River and forms the slope of the unnamed valley south of Boar's Tusk east of the river.

The Park City thins from west to east. This was shown by Schultz's work and has been presented recently in more detail for the south flank of the Uinta Mountains by J. Stewart Williams 90/ and Thomas and Krueger 78/. Only one section was measured for this report but rough calculations show an eastern thinning, even in this small area. Time did not permit a detailed investigation of the nature of this change; but previous work has shown that the Triassic (Woodside) interfingers and replaces the Park City on the south flank of the Uinta Mountains 78,90/, and the same interfingering and replacement occurs in central Wyoming between the Phosphoria and Triassic (Chugwater) (see Thomas 38/).

Age and Correlation.---The Park City is considered by most geologists as wholly within the Permian. J. Stewart Williams 90/ reported Pennsylvanian fossils in the lower member of the Park City; but, in a later article 91/, he shows the whole Park City in the Guadalupian age of the Permian. Baker 2/ in the Wasatch Range continued "the previous use of the Park City in this area for a wholly Permian unit".

Faunal evidence indicates that the upper two members of the Park City are equivalents of the Phosphoria as originally indicated by Richards and Mansfield 63/. Baker and J. Steele Williams 4/ show the equivalence of the lower member of the Park City to the Kaibab limestone of southern Utah and Arizona, and express doubts as to the equivalence of this unit to the upper limestone member of the Wells formation in southeastern Idaho.

TRIASSIC

Woodside, Shinarump, and Chinle Formations, Undifferentiated

Names.---In the area of this report the Triassic consists primarily of red beds. These red beds can be logically divided into two main units, but the terminology to be applied to this separation is not very clear. A brief review of the names used in previous reports will be given to acquaint the reader with the present situation. Powell 60/, in 1876, divided the Triassic of this area into two groups, the Vermilion Cliff and the Shinarump. Although his descriptions are rather hazy, it is apparent that he included the lower part of the Nugget formation of this report in the Vermilion Cliff group. His dividing line between the two groups could not be specifically determined by the writer. King 45/, in 1878, did not divide the Triassic into named units. He did, however, present a section at the Flaming Gorge (45, p.260/) from which it is apparent that the first three units are Nugget and the last three are the red beds of the Triassic. His Permo-Carboniferous evidently corresponds to the light gray beds included in the Triassic of this report.

Boutwell 8/, in 1907, divided the Triassic of the Park City district in the Wasatch Range into three formations (in descending order): the Ankareh, Thaynes, and Woodside. Veatch 82/, in the same year, named the Nugget from exposures in southwestern Wyoming. The Ankareh of Boutwell contained the Nugget of Veatch, and the Nugget of Veatch included equivalents of Boutwell's Ankareh. Subsequently the Nugget was restricted to the upper part of Veatch's original Nugget and the Ankareh was restricted to the lower part of Boutwell's Ankareh (see Gale and Richards 27/, Boutwell 9/, Mansfield 51/, Wilmarth 93/). In this report the term Nugget will be used to indicate a restricted Nugget (see Nugget formation of this report),

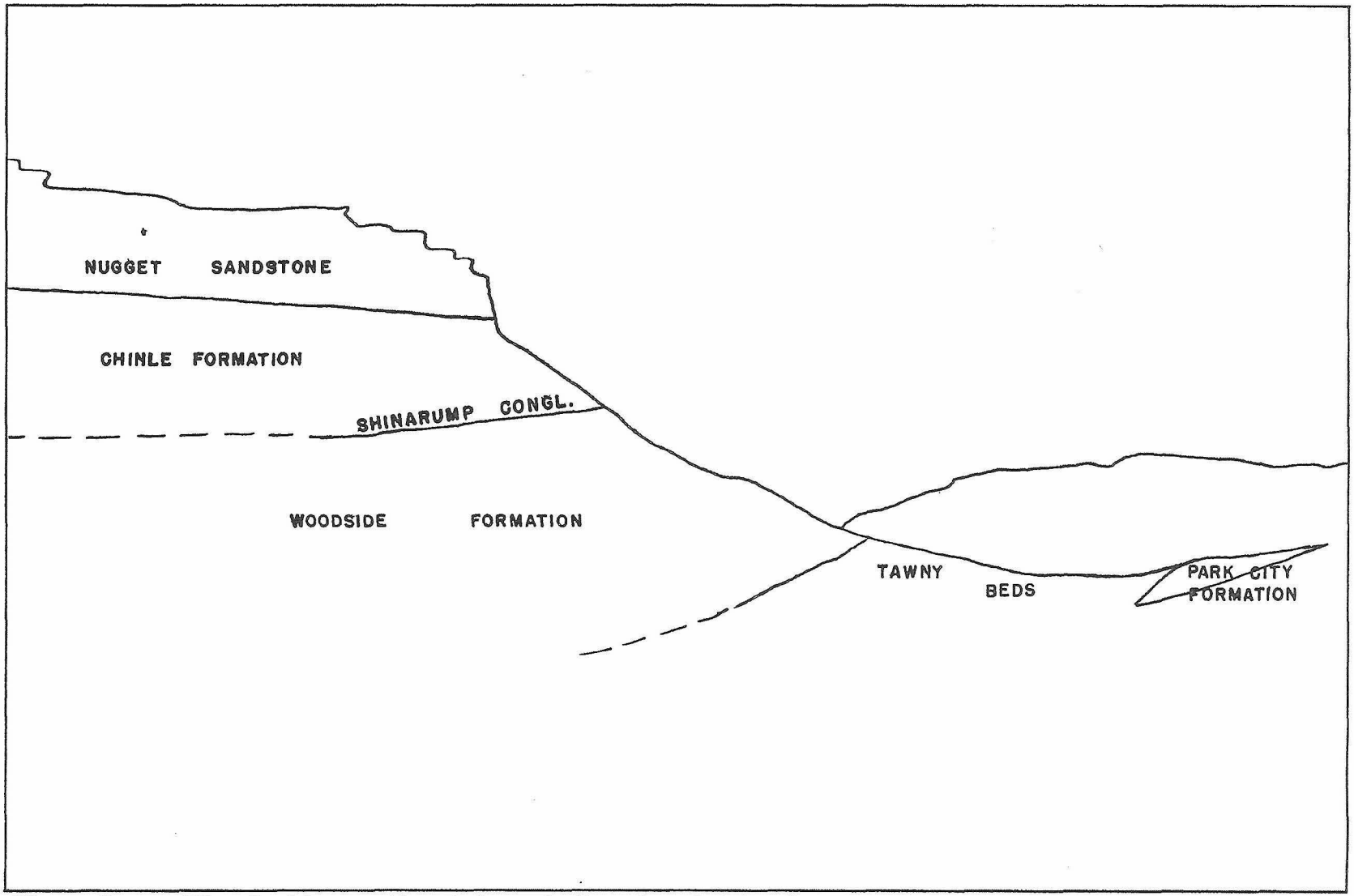

Figure 2. --- View looking northeast towards Nugget and Triassic escarpment. Green River in the foreground. Section 35, T3N, R20E.

and the upper contact of the Ankareh will be considered at the boundary assigned by Schultz 68/, in 1920, when he introduced the terminology of Boutwell into this area, thus dividing the Triassic, as it is distinguished here, into the Ankareh shale, the Thaynes (?) formation, and the Woodside shale. The lower contact of the Ankareh is considered, for the purposes of this report, as the original lower contact as defined by Boutwell in the type area. At the base of the Ankareh he places the only unconformity in this part of his stratigraphic column, which is undoubtedly the unconformity at the base of the Shinarump conglomerate of this report. Reeside 61/, in 1923, used the terminology of Schultz but he placed the lower light gray beds of the Triassic in the Park City formation 61, fig.6, p.40/, which does not agree with Schultz's geologic map. J. Stewart Williams 92/, in 1945, reporting on the south flank of the Uinta Mountains showed that the Thaynes limestone wedged out to the east from the type section in the Wasatch Mountains, and proposed a new name, the Red Wash formation, for the combined Woodside shale and the lower Ankareh shale where the Thaynes limestone is missing. The upper Ankareh shale, which he correlated with the Chinle formation, was separated from his lower Ankareh shale by the Ankareh grit, which he correlated with the Shinarump conglomerate of southern Utah. Thomas and Krueger 78/, in 1947, reported primarily the same results on the south side of the Uinta Mountains as had Williams. However, they thought it best to retain the name Woodside for the combined Woodside-lower Ankareh (where the Thaynes is missing), and they applied to the upper Ankareh, the new name, Stanaker formation, whose basal member was the Gartra grit. Kinney and Rominger 47/, in 1947, used the names (in descending order): Chinle formation, Shinarump conglomerate, and Moenkopi formation for these three divisions. There seems to be little doubt concerning the correlation of the upper part of the Ankareh (that

portion above the unconformity) with the Chinle formation and the Shinarump conglomerate, and this terminology has been used in this report. There seems to be some doubt, however, concerning the equivalence of the so-called Woodside of this area and the Moenkopi (see J. Stewart Williams 92/, Thomas and Krueger 78, p.1269/. The writer has used the Woodside in the same sense as Thomas and Krueger 78/, realizing that it represents in its upper part, the lower part of the Ankareh formation. The lower part of the Woodside as mapped for this report is probably not Triassic, but it has been included under the mapping unit "Triassic, undifferentiated". As mentioned previously (under Park City formation), J. Stewart Williams 90/ and Thomas and Krueger 78/ have shown that the Park City formation and the overlying red beds intertongue, with the Park City thinning and the red beds thickening eastward. The transition zone between the two units has been variously described as "gray shale", "tawny beds", etc. These light gray shales have been included in this report in the Triassic, undifferentiated; they have been considered a part of the Woodside formation, although they are partially, if not wholly equivalent in time to the Park City beds towards the west.

As mapping units, the Woodside (in the sense explained above), the Shinarump, and the Chinle have not been differentiated, but have been mapped together as Triassic, undifferentiated. This term has been used in spite of the fact that a portion of this unit at the bottom is probably Permian.

Character and Thickness.---This mapping unit is principally a red beds sequence of sandstones and shales, with a very minor amount of conglomerate. At the bottom is a vafying thickness of very light gray shales, as has been previously mentioned. On the geologic map, the top of these light beds is shown with a line. Above these light gray beds are some brown shales and gray sandstones, which have a red appearance on exposed surfaces due to

coloring matter furnished from above. The top of the Triassic, undifferentiated, contains green and yellow shales and sandstones, and some beds of shale and sandstone of a lavender color.

An unconformity is present in the section at the base of what has been called Shinarump conglomerate.

A section measured in section 5, T2N, R20E, follows (see pl.IV)

Nugget formation

Chinle formation

Green shale with interbedded sandstone layers	19 feet
Light yellow shales and sandstones in beds two to four feet thick	24
Soft brick red sandstone	9
Hard brick red grit, cliff-former	27
Lavender shale, weathers into nodules from the size of a pea to 18" across, nodules are weathering effects on exposed surfaces and fresh rock is dense hard shale	7
Red and buff shales with thin interbedded sandstones, easily eroded	203
Red fine sandstones and shales as follows: 3' sandstone, 6' shale, 3' sandstone, 4' shale	16
Total thickness of Chinle	305

Shinarump conglomerate

Purple pebbly sandstone containing some 6" shale beds	11

unconformity

Woodside formation

Brick red shales	7
Brick red resistant sandstone, cliff-former	32
Brick red shale	6
Brick red sandstone, resistant	5
Brick red shale	7
Salmon-colored sandstone in beds 4 feet thick with intercalated thin bedded clays and shales, cliff-former	38
Salmon-colored shales	25
Salmon-colored sandstone	10
Salmon-colored shale	11
Gypsiferous dull red shales, easily eroded	178
Salmon-colored, hard, resistant sandstone	29

Gypsiferous dull red shales	146	feet
Red shales, with odd surface coating of salts, which gives a speckled gray appearance to the surface; gypsiferous	16	
Medium-grained gray porous sandstone, giving the impression of intensive leaching	4	
Light salmon-colored thin-bedded sandstones and shales grading downward into brown gypsiferous shales with some gray sandstones	76	
Dark brown shales	15	
Gray micaceous sandstone	28	
Brown micaceous shale	18	
Blue micaceous shale	½	
Dark brown micaceous shale	15	
Fine-grained, resistant, non-continuous grit*	20	
Light gray sandy shales and fine-grained sandstones, easily eroded and a valley former, somewhat calcareous.*	275	
Total thickness of Woodside formation	973	feet
Total thickness of Triassic, undifferentiated	1298	feet

Park City formation

Fossils in the above section are evidently extremely rare. Thomas and Krueger 78/ have reported some obscure molds of pelecypods from the lower part of the column.

Ripple marks are common

Although only one section was measured in detail in this area the lower light gray beds of the Woodside increase in thickness from west to east, and the red beds section of the Woodside decreases in thickness towards the east. This is also indicated by a study of the sections of Sears 70/ at Vermilion Creek, about 35 miles east of the area of this report.

Age and correlation.---The Woodside is generally considered to be of lower Triassic age, with the exception mentioned previously of the probable equivalence of the lower part of the Woodside to the Park City of known Permian age. The Mesozoic-Paleozoic boundary here, as in many places

* Measured in section 3, T2N, R19E (see pl.III)

elsewhere, is in doubt; and the writer has nothing to add towards the solution of this problem. Faunal evidence is scanty for the lower Triassic age of the Woodside. Veatch 82, p.59/ states that "the age of the Ankareh shale, as far as indicated by meager paleontological evidence, is lower Triassic". The fossils on which Veatch bases this determination were obtained from the lower part of the Ankareh, which is probably included in the Woodside of this report.

The age of the Chinle and Shinarump is considered to be of upper Triassic age. Thomas and Krueger 78, p.1274/ favor an upper Triassic age for their Stanaker formation (the Chinle and Shinarump of this report), but mention that other geologists have suggested that its age may be Jurassic. The writer is in accord with the views of Thomas and Krueger.

The lower part of the Woodside probably contains the equivalents of the Dinwoody of Central Wyoming, but the upper part is considered the equivalent of the Chugwater.

The Chinle and Shinarump of this report has a striking lithologic similarity and a stratigraphic position, which indicates its equivalence to the Popo Agie of Central Wyoming, at least in part. Love 40, p.43/ in the southern part of the Absaroka Range, shows a probable unconformity at the base of the Popo Agie, and Richmond 65/, in the Wind River Mountains, has a disconformity at the same contact; however, this is not shown in Love, et al, 43/, in the Wind River Basin of Central Wyoming.

JURASSIC (?)

Nugget Formation

Name.---The Nugget formation was named by Veatch 82/, in 1907, from its exposures near Nugget station in southwestern Wyoming. In his original description of this formation, Veatch included the Ankareh beds; but these have been subsequently divorced from the "restricted Nugget", and the name Nugget is now used in this restricted sense (see a previous discussion of the literature of this restriction under the Triassic of this report). The term Nugget has been used exclusively in this area in recent years, until 1936, when Baker, Dane and Reeside 3/ attempted to show that it was the direct equivalent of the Navajo sandstone of southern Utah. The term Nugget is used in this report as a mapping unit for reasons to be explained below under "correlation".

Distribution.---The Nugget formation extends from the western edge of the area to the western end of Goslin Mountain, in a strip varying from 200 feet to more than 4000 feet wide. In two places east of the Green River, this long exposure is interrupted where the Nugget is faulted out.

Character.---The Nugget is lithologically similar throughout its entire thickness and consists of a cross-bedded, massive sandstone. The color of this unit is primarily light tan, although it shows variations from light gray to buff to light brown with some red streaks in places.

There are some minor differences that can be noted in the section. The lowermost 350 feet is the most massive portion of this unit, with cross-bedding much less distinct than in the overlying portions, and consists of sandstone of smaller grain size (0.1 to 0.2 mm average) than that higher in the section (0.15 to 0.30 mm average). Its color is, as a rule, darker than the upper parts.

Overlying this is about 200 feet of easily erodable and quite friable sandstone that seems lithologically more akin to the topmost portion of the Nugget. It tends to form depressions that give an "amphitheatre" effect, bounded on the south by the dip slope of the lowermost Nugget and on the north by the escarpment of the uppermost Nugget beds. The valleys have floors of loose, shifting sand that make travel difficult. Scattered about in this loose sand are found ventifacts of pearly gray, very fine-grained, dense quartzite, having sharp edges and often resembling artifacts.

The uppermost 200 feet is light gray to buff in color, and is strikingly cross-bedded. Everywhere that the dip is low this unit forms small dissected escarpments.

For mapping purposes the Nugget was not broken down into these three indefinite units, as their boundaries are indistinct and gradational, and it is doubtful that the distinctions are of consequence.

The lower contact of the Nugget is sharp. The upper contact, though not so distinct, was taken as the lowermost gray or reddish shale of the overlying Carmel and can be located within a few feet in almost all places.

Thickness.---The thickness of the Nugget formation was determined as 840 feet (see pl.IV). No east-west thinning of the Nugget was observed but this is due to the fact that its complete thickness is only developed in a limited portion of this area because of faulting, and it may actually thin to the east.

Age and correlation.---The Nugget is considered to be of lower Jurassic(?) age.

Much has been written on the correlation of the Jurassic formations of the Rocky Mountain region, and space does not permit a complete recapitulation of previous literature. For a resume of the literature prior to 1936, the reader is referred to a paper by Baker, Dane, and Reeside 3/,

which gives a correlation between northern Arizona, eastern Utah, western Colorado, and northeastern New Mexico. Heaton 32/ later correlated the Jurassic between southeastern Idaho, the south flank of the Uinta Mountains, and northwestern Colorado.

Baker, Dane and Reeside 3, p.3/ have expressed the belief that the typical Nugget sandstone is the equivalent of the Navajo sandstone. They show ibid p. 14/ the Wingate and the overlying Kayenta, both of which underlie the Navajo sandstone in central Utah, terminating under the Uinta Basin so that their "Navajo" rests directly with unconformable contact on the Ankareh (Chinle) at the south flank of the Uinta Mountains. The writer is somewhat doubtful concerning this interpretation, but cannot offer direct proof to the contrary. The northward thinning Navajo is shown as 205 feet thick south of the Uinta Basin, but the Nugget of the Uinta Mountains is 700 to 900 feet thick on the south flank 47/ and about 850 feet thick in the area mapped for this report. The writer could find no evidence of the unconformity between the Nugget and the Chinle as indicated by Baker, Dane, and Reeside 3, p.14/ and if existant must be of a minor nature. These facts, plus the lithologic changes in the Nugget mentioned previously, have been responsible for the writer's scepticism regarding the equivalence of the Nugget and the Navajo, as he believes that it is possible that the Kayenta only dies out northward under the Uinta Basin, and that the lower part of the Nugget may be in part Wingate. Therefore, the term "Nugget" has been retained in this report in lieu of using the term "Navajo".

At least the upper part of the Nugget sandstone probably is the equivalent of the Nugget of central Wyoming.

JURASSIC

San Rafael Group

Name.---The name San Rafael group was first proposed at a conference 28,93/ of J. Gilluly, J. B. Reeside, H. E. Gregory, and R. C. Moore and derived its name from the San Rafael swell of east central Utah. These men divided the group into four formations (in descending order): Summerville, Curtis, Entrada, and Carmel.

The first use of these terms for the eastern Uinta Mountains was by Baker, Dane, and Reeside 3/, in 1936.

Prior to this time the rocks corresponding to these formations had been designated as follows:

(1) the Carmel and Entrada were included in the upper part of the Nugget sandstone, and

(2) the Curtis (at least the limestone member) was called Twin Creek However, the Carmel was later shown to be the equivalent of the Twin Creek by Heaton 32/, in 1939, while correlating the Jurassic rocks on the south flank of the Uinta Mountains. This correlation was also determined by Thomas and Krueger 78/.

During the course of mapping for this report, the Curtis, Entrada, and Carmel were each used as mapping units. The Summerville was not recognized and to date is not known to exist in the Uinta Mountains.

Distribution.---The San Rafael group occurs aerially in a strip which varies from 600 feet to 6000 feet in width from the western edge of the area to the western slope of Goslin Mountain. The outcrop width is narrowest east of the Green River where the beds are almost vertical. It is widest near the western edge of the area where the dips are less, where the Carmel forms a wide valley, and the Curtis has a wide dip slope on the north.

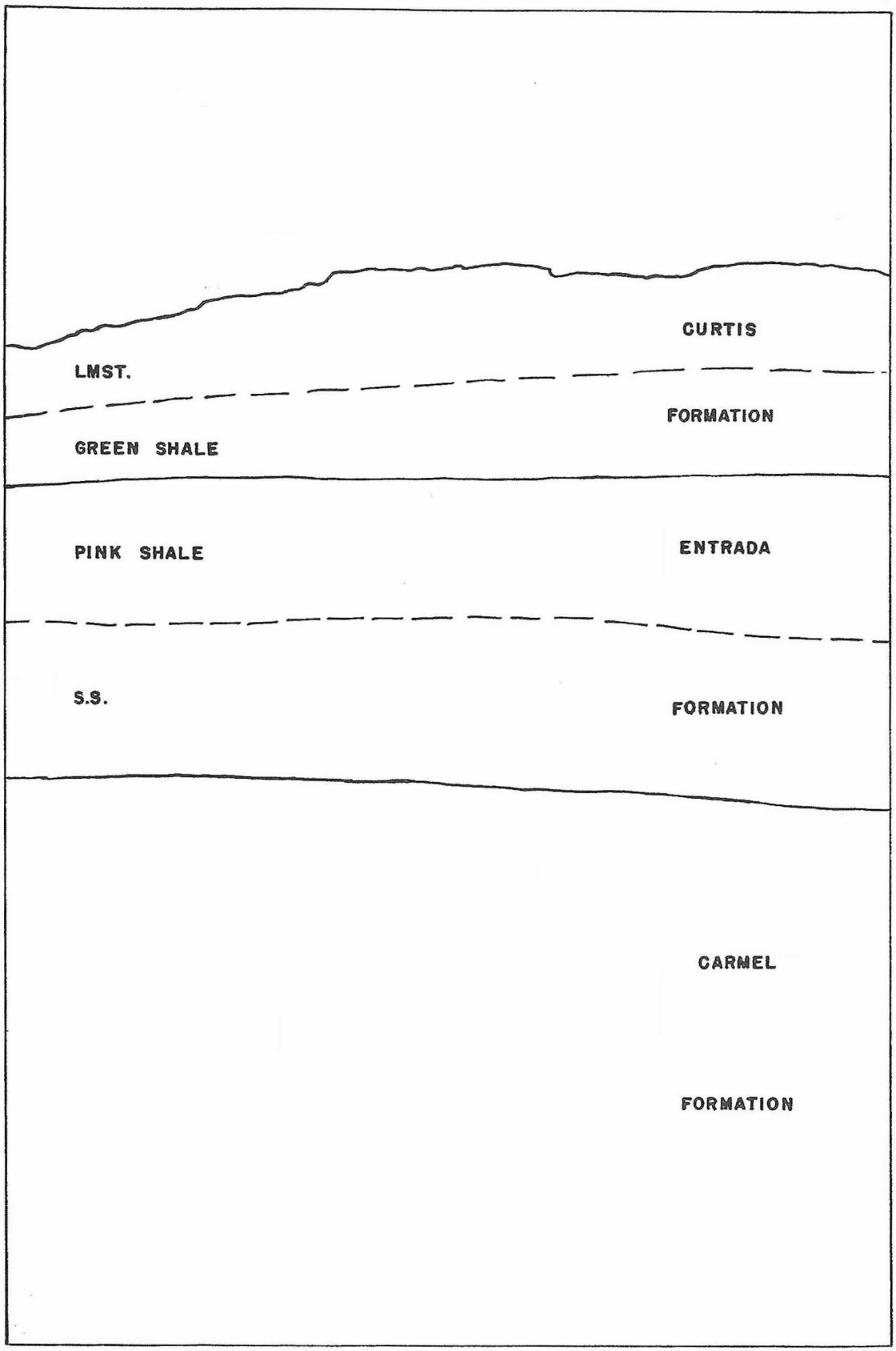

Figure 3. --- View looking north towards Carmel, Entrada, and Curtis outcrop. Section 6, T2N, R20E.

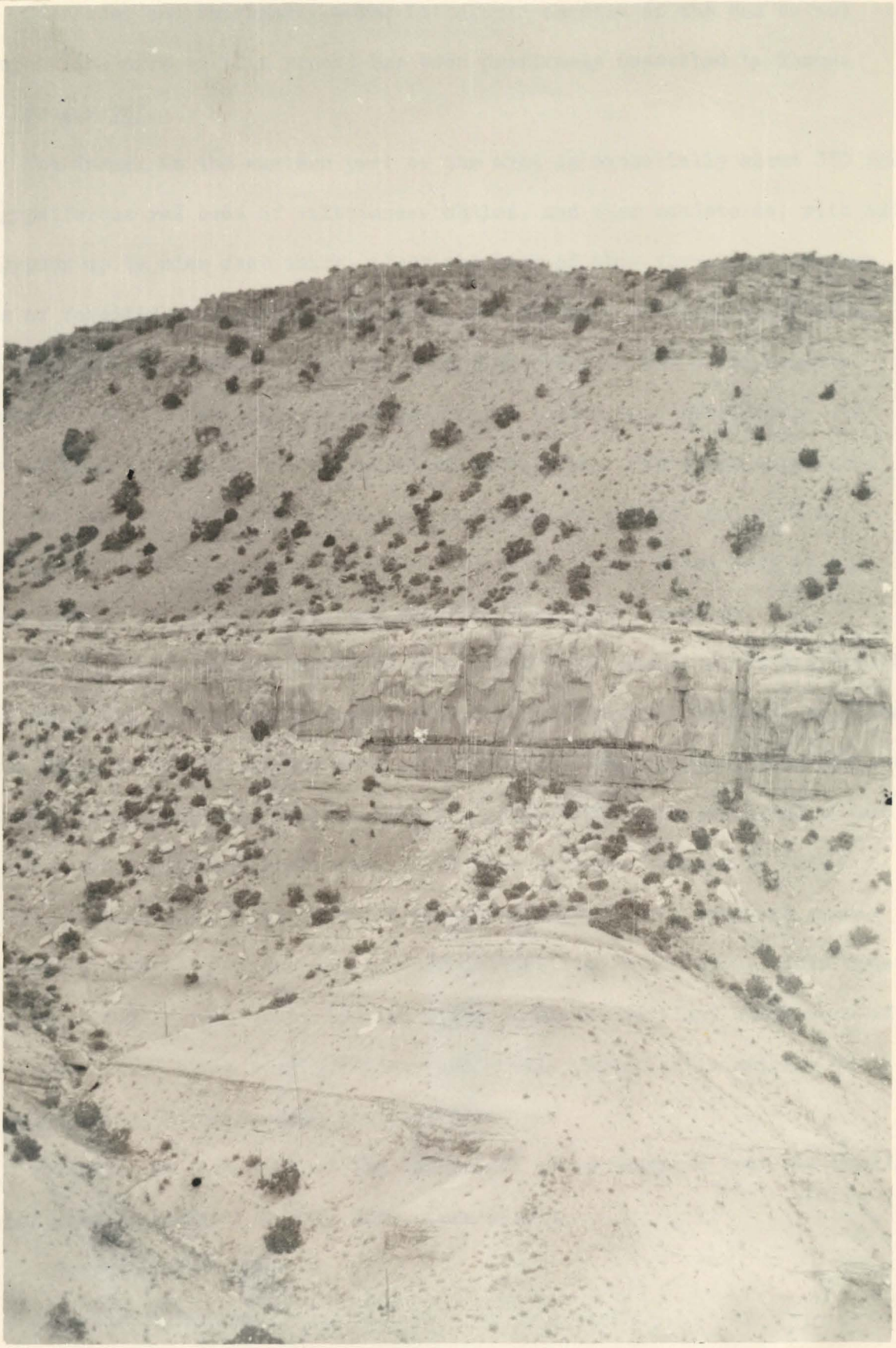

Character and thickness.---The lithologic section of the San Rafael group in the area of this report has been previously described by Thomas and Krueger 78/.

The Carmel in the western part of the area is essentially about 350 feet of gypsiferous red beds of siltstones, shales, and fine sandstones, with beds of gypsum up to nine feet thick. Near the base of this formation are some beds of fossiliferous marine limestones, the thickest of which is 23 feet.

The Entrada consists of 127 feet of pink, yellow, and white massive, slightly cross-bedded, fine-to medium-grained sandstones; overlaid by 118 feet of pink siltstones and fine-grained sandstones. The lower sandstones are resistant to weathering, form bold outcrops and cliffs, and form a prominent, three-mile long, dip slope from three to six miles west of the Green River. No fossils have been reported from this formation.

The Curtis formation has an 83 foot thick basal member of dark greenish gray shale and fine grained sandstone with some thin beds of limestone. The green color is due to an abundance of glauconite. Belimnites densus has been reported from these beds in this area 78, p.1292/ but none was found by the writer. The upper member consists of 67 feet of gray, massive to thin-bedded, hard, dense, crystalline limestone containing very abundant specimens of Kallirynchia myrina and another unidentified brachiopod. This upper limestone is very resistant, forming a sharp, almost vertical cliff west of the Green River, and a very prominent and easily recognizable outcrop east of this stream where the dips are very steep.

Following is a section of the San Rafael group measured near the Manila-Vernal road in section 6, T2N, R20E, (see pl.V):

Morrison formation

Curtis formation

Gray massive to thin-bedded hard dense crystalline limestone	67 feet

Dark greenish-gray glauconitic shale, with some thin beds of limestone	83 feet
Total thickness of Curtis formation	150
Entrada formation	
Pink siltstones and fine-grained sandstones	118
Yellow massive medium-grained sandstone, with minor amount of fine-grained sandstone	80
Pink soft friable massive fine-grained sandstone	20
White massive fine-grained sandstone, stained pink on the surface in spots	27
Total thickness of Entrada formation	245
Carmel formation	
Pink and white variegated shales and siltstones	85
Hard white shale	5
Grayish white shale	32
Gypsum	3
Gypsum with much interbedded shale	20
Greenish gray shale with many gypsum veinlets, green weathering	9
Heavy bedded gypsum	9
Brownish red shale with gypsum veinlets	11
Massive gypsum	1½
Blue green shale	23
Massive gypsum with some interbedded shale	6
Brownish red shale with gypsum	6
Green calcareous shales, punky	12
Green thin-bedded shales	14
Reddish brown shales	5
Green very soft shales, form low dip slope	7
Red shales, soft	6

Thin-bedded greenish blue limestone (8 inches)	
Red shales, soft	6 feet
Hard tan grit with shale intercalations	3
Red shales, soft	26
Hard massive fossiliferous limestone	23
Gray shale, soft, easily eroded	33
Total thickness of Carmel	356

Navajo (gray strikingly cross-bedded sandstone)

Dips of the Entrada pink shale member and the Curtis greenish gray shales indicate that there might be an unconformity between these two members; but if existent it must be of a very minor nature. Although only the one section detailed above was measured by precise methods, it is apparent that the Carmel thins to the east.

Age and correlation.---The San Rafael group in other areas shows paleontological evidence of an upper Jurassic age.

Heaton 32/ was the first, to the writer's knowledge, to show the equivalence of the Twin Creek limestone, Preuss redbeds, and the Stump sandstone, of southeastern Idaho and north central Utah, with the Carmel, Entrada, and Curtis formations, respectively, on the south flank of the Uinta Mountains. Imlay 37/ uses this same general correlation but restricts the Carmel as equivalent only to the upper Twin Creek.

Thomas and Krueger 78/ correlate the Nugget, Carmel, Entrada, and Curtis of the Uinta Mountains with the Nugget, Gypsum Spring, "lower Sundance", and "upper Sundance" of the Wind River basin on the basis of stratigraphic sequence and lithologic similarity. There is little doubt in their minds, nor in the writer's, that the Nugget in the two regions and the Curtis-"upper Sundance" correlations are valid. They do have some question concerning the correlation of the Carmel with the Gypsum Spring and the Entrada

with the "lower Sundance", in spite of the lithologic similarities, as Imlay 37/ has correlated both the Carmel and the Entrada with the "lower Sundance" on paleontological evidence.

Morrison Formation

Name.---The Morrison formation was named by Eldridge 18/, in 1896, from the town of Morrison, Colorado.

Distribution.---The Morrison formation is exposed in a continuous strip from the western edge of the area to the western end of Goslin Mountain. Its width of outcrop varies from 4500 feet near the western end to less than 300 feet in some places.

Character.---The lithology of the Morrison has been intensively studied recently by Stokes 76/, who divided the formation into a number of various units. During the course of this field work, no division into members was made; nor could the writer note the possibility of doing so without extremely detailed and intensive mapping. Certain horizons of sandstone and conglomerate are observed; however, with the exception of one fairly continuous six feet thick sandstone bed, all other possible marker beds by which a subdivision might be made in one locality are discontinuous. In addition to this difficulty, this formation is everywhere poorly exposed due to the softness of the sediments of which it is composed. This fact also causes the tendency for rapid erosion so that the Morrison forms the floors of valleys in most of the area. An exception to this is in section 27, T3N, R22W, where the overlying Dakota has protected it from this type of erosion, and the upper part of the Morrison is well exposed.

Lithologically the Morrison is a series of variegated clay shales and soft siltstones, with lenticular beds of conglomerates, conglomeratic sandstones, and sandstones. The thickest of the conglomeratic beds is about 50 feet. The conglomerate beds are more lenticular than the sand-

stones, but neither can be said to be very persistent. The clay shales are various shades of gray, green, pink, maroon, lavender, and other colors. The conglomerates consist of pebbles of chert and quartzite, with the larger pebbles---up to 2 inches in diameter---being highly polished black chert.

Thickness.---The thickness of the Morrison formation as measured in section 31, T3N, R20E, and section 6, T2N, R20E, is 953 feet (see pl.VI). The formation thins generally towards the east to less than 600 feet in the eastern portion of the area. In some localities the Morrison thins to less than 300 feet. More will be presented concerning this thinning in the chapter on structural geology (see page 95).

Age and correlation.---The Morrison was considered as Cretaceous for many years by some workers; but is now considered upper Jurassic by most geologists. The dinosaur remains taken from this formation in various places, including the famous locality at Dinosaur National Monument east of Vernal on the south flank of the Uinta Mountains, have proven its Jurassic age.

However, included in the unit mapped as Morrison for this report is probably included all but the upper sandstone member of the Cloverly formation as recently designated in the Wind River basin of central Utah (see Love, et al 41/), and which is of lower Cretaceous age.

The Beckwith formation, as used by Schultz in this area, includes the Morrison formation and the Dakota group as mapped in this report; but his use of the Beckwith did not include the Curtis and the Entrada as does the type section of Beckwith.

CRETACEOUS

Dakota Group

Name---Dakota sandstone was first used by Meek and Hayden in the 1850's as the name for their lowest Cretaceous rocks exposed near the town of Dakota, Dakota County, Nebraska. The extension of this Great Plains name to what was believed to be the lowermost Cretaceous of the Uinta Mountains was done by Hayden and King, working independently in the 1870's. Powell, in this same period called the same rocks the Henry's Fork group from exposures in the area of this report. Veatch 82, p.58/, in 1907, objected to the use of the term "Dakota" in the area he worked in southwestern Wyoming, and proposed the name Beckwith, for all of the rocks between the Twin Creek limestone and the bottom of the Bear River formation, which seems to be only locally developed in that area and underlies the Aspen shale. Gale 25,26/, in the area of this report, continued to use the name "Dakota" on his map of 1907; but Schultz 68/, in this same area during the same time, used the term "Beckwith" for all of the rocks between the top of the Curtis (to which he misapplied the name Twin Creek) and the bottom of the Aspen. Reeside 61, p.38/ continued Schultz's use of the Beckwith; but, while discussing the topmost member of the Beckwith formation of Schultz, he stated that "from its lithologic constitution and its position it would be called the Cloverly formation in Wyoming or the Dakota sandstone at many other localities in the Rocky Mountain region." Subsequent workers in the area of the south flank of the Uinta Mountains have called this formation either the Dakota or Dakota(?) formation.

Distribution.---The Dakota crops out generally in a strip from 200 to 1000 feet wide but attains a width of 3500 feet in one locality due to a combination of low dip and topographical conditions. This outcropping

is roughly parallel to, and of the same east-west extent as the Morrison formation.

Character and thickness.---The Dakota sandstone is composed of three members. The lowermost is generally a tan, friable sandstone, conglomeratic in places. However, in some places the sandstone is startlingly white, very clean, and composed almost entirely of quartz grains, with or without a calcareous cementing material. The pebbles, where found, are almost without exception black, white, or brown chert and are very well polished.

The middle member is a dark-colored shale. It is not always present, being replaced very rapidly in some places by tan sandstone, and where present the exposures are poor and details obscure.

The upper member is a tan, medium-grained sandstone. It is fairly well sorted but not so clean as the basal sandstone. There are some thin coal beds up to about one foot in thickness, which are not consistent and obviously sub-commercial.

A section measured in section 31, T3N, R20E, gave the following thicknesses, although nearby the middle shale member was not observed, being replaced by sandstone (see pl. VI):

Aspen formation

Dakota group

Tan medium-grained sandstone, locally pebbly, some coal	107 feet
Dark-colored gray shale	74
Tan or white sandstone, massive, conglomeratic in part	20
Total thickness of Dakota group	201

Morrison formation

Age and correlation:---The use of the name "Dakota" for rocks in the Rocky Mountain region, when the name originated in the Great Plains and the

formations cannot be traced continuously between the two regions, has been a source of argument for many years. No more need be said about this situation here; suffice to say that the name "Dakota" is in active usage at the present time in the Uinta Mountains and contiguous areas by the United States Geological Survey (see Kinney and Rominger47/ and Huddle and McCann 36/), and by many private organizations.

The United States Geological Survey (ibid) considers that the Dakota is the lowest Cretaceous exposed in the Uinta Mountains; however, there is some doubt in the writer's mind concerning the validity of this assumption. The Morrison formation as mapped in this area might very well contain equivalents of the Cloverly formation of the Wind River basin, which has been determined as lower Cretaceous on paleontological evidence (see Love, et al, 41/). It is suggested, based upon stratigraphic position and lithology, that the lower member of the Dakota as here mapped might be the upper sandstone of the Cloverly, and the shale and upper sandstone might be the lower shale and sandstone of the Thermopolis shale of the Wind River basin. More detailed stratigraphic and paleontological work is required on this question.

Aspen Formation

Name.---The Aspen formation was named by Veatch 82/, in 1907, from exposures near Aspen Station, Uinta County, southwest Wyoming.

Distribution.---The Aspen formation in this area is exposed north of and adjacent to the Dakota exposures in a strip from 200 to 1500 feet wide from the western edge of the area to the western end of Goslin Mountain.

Character and thickness.---The Aspen is one of the most recognizable mapping units in the area. It cannot be mistaken for any other rock unit. It consists of black and dark gray, hard, siliceous fissile shales. On weathered exposures this rock assumes a silvery gray to light bluish gray color. Fish scales are exceedingly abundant and other fish remains are not uncommon.

At the base of the above mentioned siliceous shale there is a relatively thin layer of light gray softer shale; but, due to lack of favorable exposures, no differentiation between these two units was made.

The lower contact of the Aspen was drawn at the contact between the shales and underlying tan sandstone of the Dakota. The upper contact was drawn at the top of the dark gray siliceous shale and the overlying softer gray and tan sandy shale of the lower Frontier.

A thickness of the Aspen of 196 feet was measured in section 31, T3N, R20E (see pl.VI)

Age and correlation.---The distinctive lithology of the siliceous, "fish scale" part of the Aspen formation, as here mapped, has been recognized throughout southwestern Wyoming. Veatch 82/ reported a thickness of as much as 2200 feet in that region. Walton 85/ reports a thickness of 79 to 325 feet on the south side of the Uinta Mountains. He differentiated between the two shales here mapped as Aspen, calling the uppermost, Aspen, and the lowermost, the lower shale member of the Mancos shale. He assigns the Aspen to pre-Greenhorn age of the upper Cretaceous, which would make it of Cenomanian age, according to Reeside's age assignment of the Greenhorn 62/.

There is little doubt that the Aspen is the equivalent of the Mowry of central Wyoming, although as here mapped the lowest shale may be equivalent to the upper shale member of the Thermopolis of Love, et al 41/ in the Wind River basin. This would place the Aspen as here mapped in the Cenomanian.

Frontier Formation

Name.---The Frontier formation was named by Knight 48/, in 1902, from exposures near the town of Frontier, in southwestern Wyoming.

Distribution.---The Frontier formation crops out in a strip generally

50 to 1000 feet wide, from the western edge of the area to the western slope of Goslin Mountain. At one locality the exposure reaches a maximum width of 2000 feet, owing to conditions of dip and topography.

Character.---The Frontier, as here mapped, is used in the same sense as designated by Sears 71/ in the Baxter basin gas field, southeast of Rock Springs, Sweetwater County, Wyoming.

Overlying the Aspen shale in this area, there is a gray to tan, sandy shale overlaid by a massive, escarpment forming, fine-to medium-grained sandstone. The shale is not often well exposed as it erodes readily and is generally covered by wash from the overlying sandstones. The sandstone member, buff-colored in a fresh condition, weathers to a darker tan color. The sandstone is fossiliferous, oyster shells being the most common remains found.

A section, measured in section 31, T3N, R20E, resulted in the following thicknesses (see pl. VI):

Hilliard shale

Frontier formation

Buff, fine-to medium-grained, massive fossiliferous sandstone	18 feet
Gray to tan, sandy shale	38
Total thickness of Frontier formation	56

Aspen formation

The sandstone member is quite lenticular, thickening eastward from the above measured section to about 100 feet in section 29, T3N, R22E.

The top of the Frontier can be regarded as a matter of choice of the individual mapping the area. This formation, as originally defined, was to include the coal bearing sandstones between the underlying Aspen shale and the overlying Hilliard shale. In the area mapped, there are sandstones in the section mapped as Hilliard shale. One of these near the base is about

180 feet thick, and contains a coal bed about one foot thick near the top. This sandstone, however, is not persistent and is not found throughout the district. Also color and texture of this fine-grained sandstone resembles more the shales of the Hilliard than the shales and sandstones of the Frontier as mapped for this report. The writer considers that this sandstone at the base of the Hilliard may be a local tongue of the Frontier. This sandstone directly overlies the Frontier in section 30, T3N, R22E, but east and west from this locality there is an intertonguing of shale between the two sandstones. As can be readily seen from the above discussion, the upper contact of the Frontier can be made a matter of individual preference, unless a very detailed mapping program is pursued in which all of the lentils and intertongues of the sandstones and shales, as the case may be, are carefully delineated. The writer has chosen the contact shown because it is a very distinctive horizon, and as far as reconnaissance work is concerned as close to an average contact of the top of the Frontier as is possible to achieve.

Age and correlation.---The Frontier is of lower Cretaceous age. It may be correlated, at least in part, with the Frontier of the type locality in southwestern Wyoming. Forrester 23/, from stratigraphic position and "the fact that, inasmuch as the Cretaceous sediments of this region were all brought in from the west, it is to be expected that the sandy Frontier would be the western equivalent of the more shaly Mancos [Hilliard]". Walton 85/, on faunal evidence, reports the Frontier of the south flank of the Uinta Mountains to be of Greenhorn age, although his Frontier excludes the lower shale of the Frontier of this paper, which he calls "middle shale member of the Mancos". The Frontier of this area is probably the equivalent, in part, of the Frontier of the Wind River basin as delineated by Love, et al 44/; however, Reeside 62/ shows no equivalents of Greenhorn, or even lower Carlile,

age in the region studied by Love.

Hilliard Formation

Name.---The Hilliard formation was named by Knight 48/, in 1902, from exposures near the town of Hilliard, southwest Wyoming.

Distribution.---The Hilliard formation has a very extensive distribution in the area under discussion. The floor of Lucerne Valley is composed of this formation, except where covered by superficial deposits of Quaternary terrace material. The area of this exposure averages approximately 6000 feet wide by about 20 miles long, although the valley is considerably narrower near its eastern end. In the center of T3N, R23E, there is a gap of about one mile between the Hilliard exposures of Lucerne Valley, and what is believed to be the western edge of the Hilliard in the Clay Basin anticlinal nose. The rocks between the Clay Basin fault and the Uinta fault were mapped as Mancos shale (Hilliard) by Dobbin and Davison 16/. The exposures between these two faults in the writer's area are so poor and covered by superficial material that this determination is doubtful. North of the Clay Basin fault the designation of the Hilliard is positive.

Character and thickness.---The Hilliard formation is a large thickness of drab, medium dark shales with a few beds of fine-grained sandstones. The shales weather to a light gray color which is similar to that of the sandstones, which adds to the monotony of color. There is one 56 foot, slabby sandstone unit about 2100 feet below the top of this formation that weathers to a tan color and resembles the Frontier sandstone. The shales are for the most part arenaceous and the sandstones are shaly.

The lower contact of the Hilliard has been discussed under the Frontier formation. The upper contact is also rather indefinite. The writer placed the Hilliard-Mesaverde contact at the base of the 350 feet thick sandstone which caps the south escarpment of the "Devil's Causeway" east of the

Green River. This is the lowest thick sandstone overlying the shale sequence of the Hilliard. This sandstone was believed by Schultz 68, p.37, fig.3/ to be "golden wall" sandstone of his Blair formation which he considered to be equivalent to the uppermost Mancos or Hilliard. Sears 71/ placed the Blair in the Mesaverde group as its lowest formation.

The following section of the Hilliard formation was measured in section 17, 20, and 29, T3N, R22E (see pl. VII):

Mesaverde group

Hilliard formation

Drab gray sandy shale containing some thin shaly sandstone beds, details obscure	1580 feet
Tan thin-bedded sandstone, fine-grained	3
Drab gray arenaceous shale	617
Thin-bedded tan medium-to fine-grained slabby sandstone	56
Drab gray shale	4184
Fine-grained light gray sandstone (tongue of Frontier?)	182
Drab gray sandy shale	126
Total thickness of Hilliard shale	6748

Frontier formation

Age and correlation.---The Hilliard shale is of upper Cretaceous age. Walton 85/ reports the presence of Greenhorn, Carlile, and lower Niobrara fauna at the western end of the Uinta Basin south of the Uinta Mountains, and Greenhorn, Carlile, Niobrara, and post Niobrara fauna near Vernal, Utah, in the eastern part of the Uinta Basin, in his "upper shale member of the Mancos" which is lithologically the equivalent of the Hilliard shale. This change in faunal age of the lower contact of the Mesaverde is not surprising, since regional mapping and stratigraphic studies have indicated that this

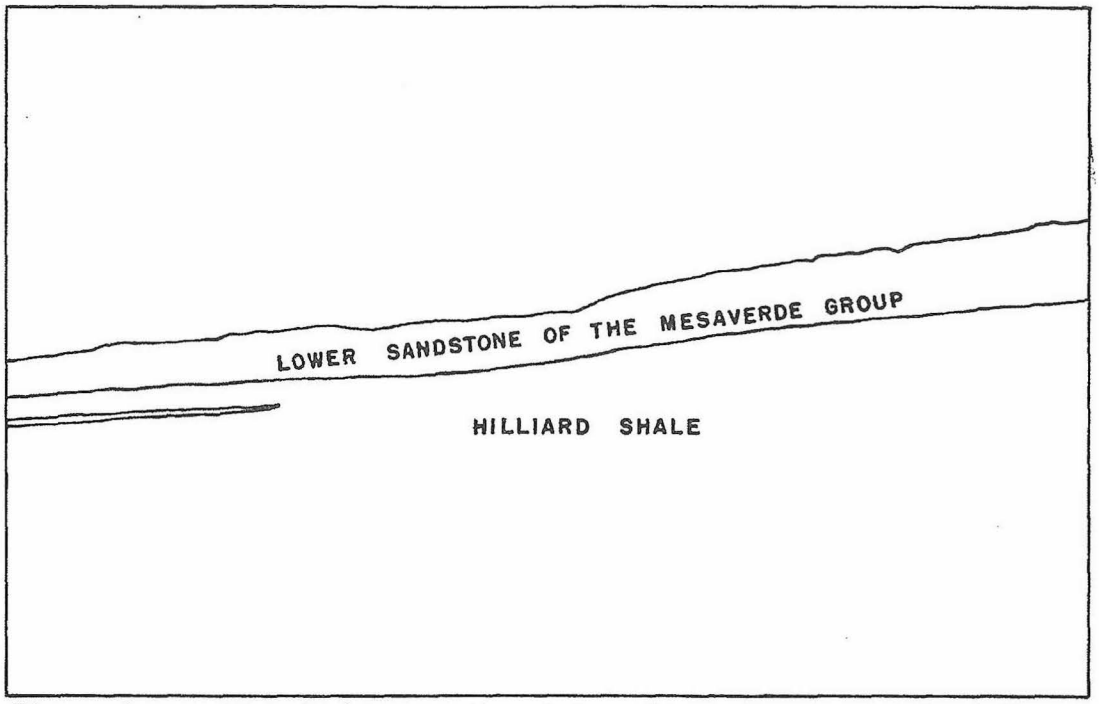

Figure 4. --- View looking northwest towards south escarpment of the "Devil's Causeway". Section 18, T3N, R22E.

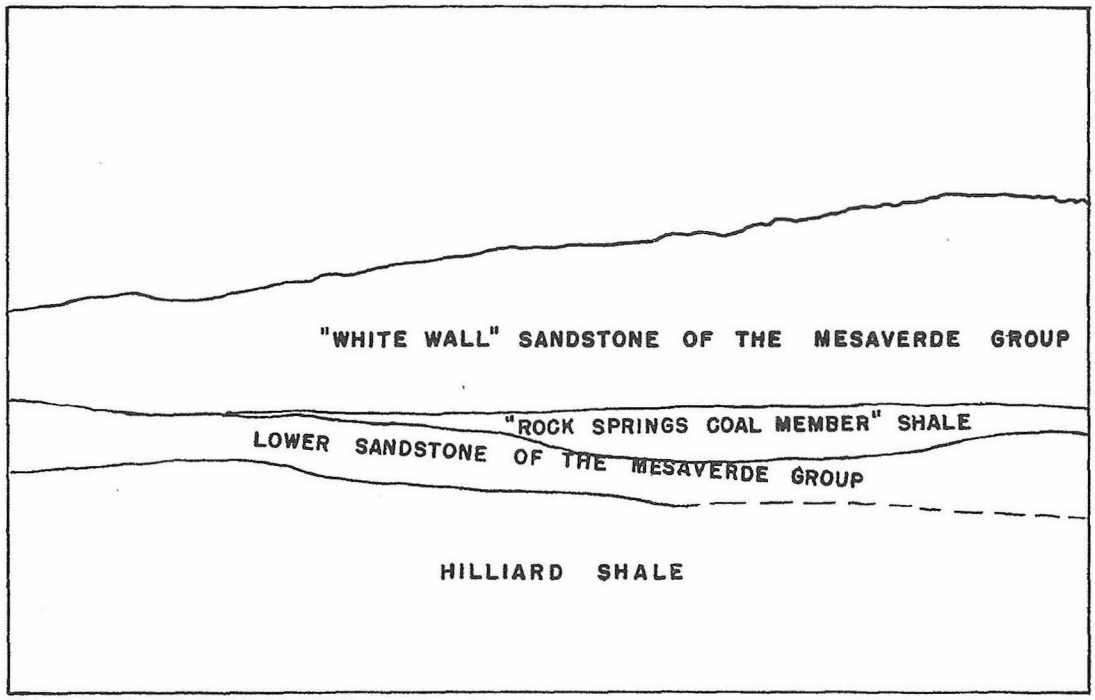

Figure 5. --- View looking north towards north escarpment of the "Devil's Causeway". Section 16, T3N, R22E.

contact transgresses time lines in many regions (see for example Spieker 75/, Sears, Hunt and Hendricks 73/, and Pike 58/).

The Hilliard formation has the stratigraphic position of and a lithologic similarity to the Cody shale of the Mancos group. Its age must be roughly equivalent to that of the Cody, but here again the upper and lower contacts of the two units are probably not at the same faunal level.

Mesaverde Group

Name.---The Mesaverde was named by Holmes 35/, in 1877, from exposures in the valley of the San Juan River in southwest Colorado and northwest New Mexico. Subsequently the name has been applied to the same lithologic sequence as far north as northern Wyoming.

Distribution.---In the area of this report, the Mesaverde crops out from the valley of Henrys Fork in section 23, T12N, R109W, in a discontinuous strip, 700 to 6000 feet wide, to the eastern edge of the area. East of the Green River the sandstone portions of this group form the two escarpments that make up the long, curving, crescent-shaped, double ridge known as the "Devil's Causeway" (named by King of the Fortieth Parallel Survey as Bighorn Ridge).

Character and thickness.---The Mesaverde formation is composed of massive sandstones with some sandy shales. Coal beds are to be found in the thick shale member above the lowermost sandstone east of the Green River, and at a horizon whose position in the formation was not determined north of the town of Linwood, where the formation crops out south of the Manila fault. These occurences have been reported by Gale 25,26/ and mentioned by Schultz 68/.

As mentioned previously, the "Golden Wall" sandstone has been included as the lowermost member of the Mesaverde for this report, although it was

placed in the Hilliard shale by Schultz 68/. The contact between this sandstone and the underlying shales of the Hilliard is an intertongued and interdigitated one as is found to be true in many other localities. A very good exposure of this contact can be seen in the southern escarpment of the "Devil's Causeway". Inspecting from east to west this five mile long, continuous exposure, it is readily apparent that the "Golden Wall" sandstone gradually intertongues into the underlying shales, thickening the Mesaverde section towards the west.

The upper contact of the Mesaverde in this area is extremely obscure. In places, it is definitely in fault contact with the Wasatch group and the contact can be delineated within a "hand span". For the most part, however, where the Mesaverde is overlaid by the Wasatch overlap or by inferred faulting, the contact is obscured either by superficial alluvium, slope wash, or terrace or by the similarity of the lithology of the Mesaverde and the Wasatch. In those localities where the Lewis overlies the Mesaverde, relations are practically as obscure, due to the very poor exposure of the Lewis and the presence of superficial material.

A section of the Mesaverde measured in section 17, T3N, R22E, and section 22, T12N, R107W, resulted in the following thicknesses (see pl.VII):

Lewis shale?

Mesaverde formation

Massively bedded sandstones with some pebbly sandstones; exposures not too good; forms dip slope, some shales	480 feet
A series of massively bedded sandstones with a few thin intercalated shale beds as follows; forms northernmost escarpment of "Devil's Causeway"	770
Drab gray and buff sandstones	202 feet
Conspicuous white sandstone	39
Drab gray and buff sandstones	35
Conspicuous gray sandstone	70
Drab gray and buff sandstones	67
Conspicuous white sandstone	91

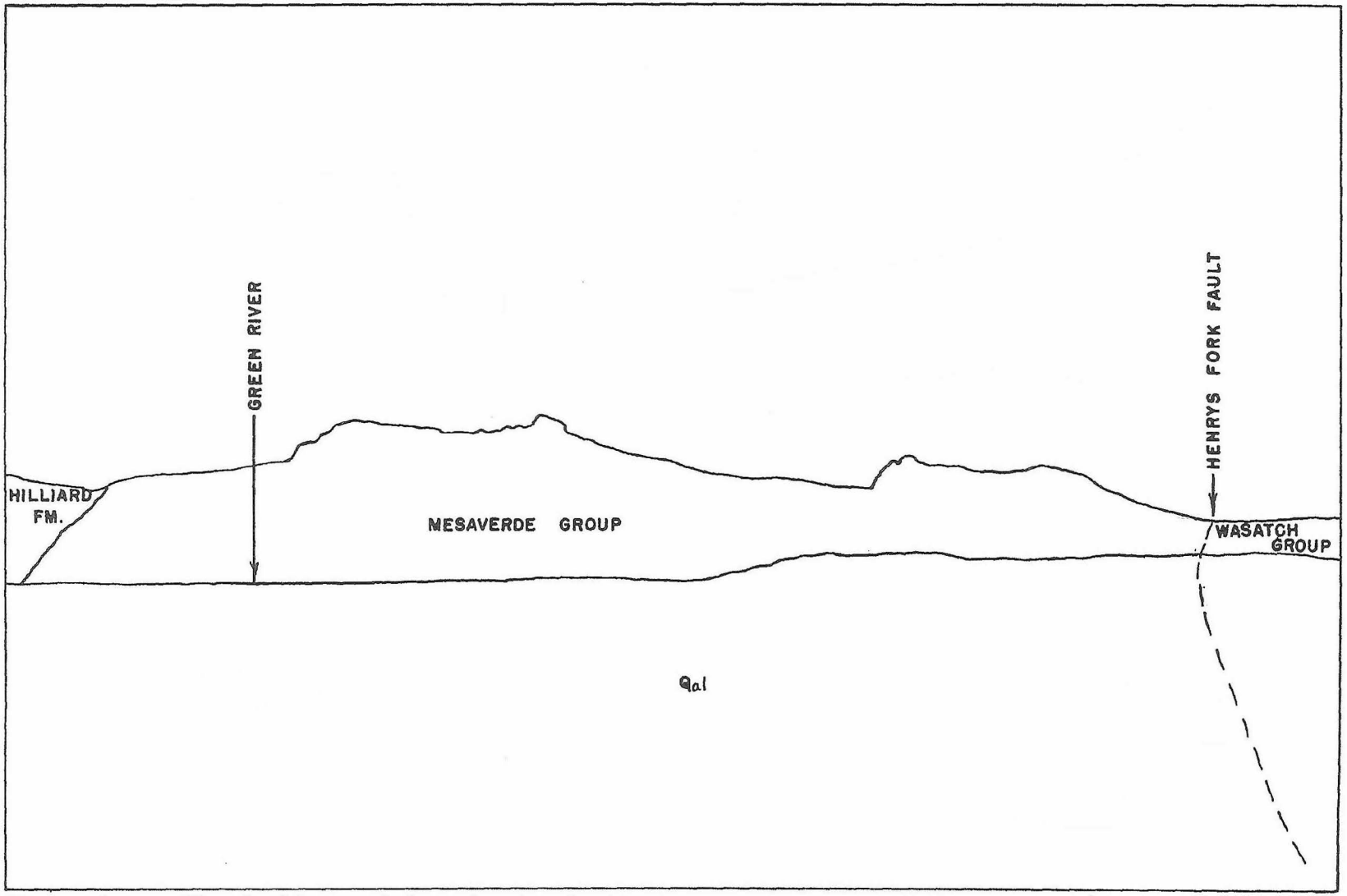

Figure 6. --- View looking west towards steeply dipping Mesaverde west of the Green River. Section 17 and 22, T3N, R21E

Drab gray and buff sandstones	85 feet	
Conspicuous white sandstone	42	
Yellow and tan sandstones	139	
Shales, clays, and sandy shales with some thin-bedded fine-grained sandstones; some coal beds		486 feet
Massive, yellow-tan sandstone, with abundant concretions, especially near the top		347
Total thickness of the Mesaverde group		2083 feet

Hilliard shale

The above four members can be called by the following names, if Schultz's terminology for the Southern Rock Springs coal field 66/ is used:

topmost member --- Almond coal group
next member --- no name; gives rise to the topographic feature known as the "White Wall"
next member --- Rock Springs coal group
lowermost member --- no name; gives rise to the topographic feature known as the "Golden Wall".

Towards the west from the place the above section was measured, the "Rock Springs coal group" becomes more sandy; and near the Green River, the amount of interbedded, massive sandstones in this member is appreciable.

Age and correlation.---The Mesaverde group is upper Cretaceous in age. Walton 85/, based upon identification by J. B. Reeside Jr., has reported fossils of Niobraran age of the Colorado division from the western edge of the south flank of the Uinta Mountains. Reeside, according to Walton ibid./, has indicated that an assemblage of fossils collected from the Mesaverde formation near Vernal, Utah, and identified by Tolmachoff 80/ can be considered only as post-Niobraran in age. Again, this evidence seems to support the idea that the Mesaverde transgresses time lines, being older in the western end of the Uinta Mountains than in the eastern end. Forrester 23, p.64/ has stated that "the sandy Mesaverde formation, which overlies the Mancos on the east, grades imperceptibly, to the west, into the upper part of the Frontier". Spieker 74, p. 2043/, however, has challenged this statement

with "there is certainly no such relationship in the Vernal district, and the strata there mapped in the past as Mesaverde are far above the true Frontier of the west".

Lewis Formation

Name.---The name Lewis shale was first used by Cross and Spencer 13/, in 1899, from its occurrence at Fort Lewis in the La Plata River valley, La Plata County, Colorado. The name has been applied over a fairly extensive area since that time. In the area of this report, Schultz 68/ and Gale 25,26/ both used this terminology for the shales overlying the Mesaverde group.

Distribution.---The Lewis crops out in this area in a few very poor exposures north of the eastern end of the "Devil's Causeway".

Character.---Due to the poor exposures of the Lewis shale, not a great deal may be said of its lithologic character. However, from the little that can be seen it appears to be an easily eroded, dark gray shale which weathers to a lighter drab gray clay. Intercalated in this shale are some beds of sandy shale and some more resistant dark gray to almost black, fine-grained sandstones, containing an abundance of gypsum in minute shiny grains.

Thickness.---For this report, no section of Lewis shale was measured by precise methods, but the thickness by reconnaissance methods was found to be approximately 700 feet at the outcrop in section 18, T3N, R23E. As the Lewis, wherever exposed, is overlaid by the overlapping Wasatch, this thickness may be that of a partial section. In all localities other than the partial exposures north of the "Devil's Causeway" east of Spring Creek gap and west of the gap into Clay Basin north of Goslin Mountain the Lewis is either faulted out, overlapped by younger formations, or covered by superficial material. One small, but excellent, partial exposure of the

Lewis is to be found in the bottom of the gulch cut by Spring Creek north of the "Devil's Causeway" in section 35, T12N, R107W.

Age and correlation.---The Lewis is of upper Cretaceous age, Montana division. Stratigraphically and lithologically, it has the same position as the Meeteetse shale of central Wyoming; but it is doubtful that the two formations have the exact age equivalence. In fact it is doubtful whether the Lewis in various localities has within itself a consistency of age equivalence. Pike 58/ shows in southwestern Colorado and northwestern New Mexico an intertongued contact between the Mesaverde and the Lewis shale, with the Lewis shale thickening and the Mesaverde losing section towards the east. He shows between Cerrillos and Las Vegas, New Mexico, and between Pagosa Springs, Colorado, and Raton, New Mexico, the complete disappearance of the Mesaverde and the merging of the Lewis shale and the Mancos shale to become the Pierre shale. A study of Reeside's paleogeographic maps 62, map 9/ indicates roughly that a similar condition might exist east of the area of this report, although two basins of thicker deposition complicate the picture.

TERTIARY

Wasatch Group

Name.---The name Wasatch group was first applied by Hayden 31/, in 1869, to its occurrences west of Fort Bridger, Wyoming. King 45/, a few years later, used the name Vermilion Creek group to beds which were later determined to be roughly correlative. The name Wasatch survived as the name of this group because of priority and common usage, as all subsequent workers have used this terminology. Veatch 82/, in the Evanston area of southwestern Wyoming, in 1907, divided the group into three formations, namely (in descending order): Knight formation, variegated yellow and red sandy clays with irregularly bedded white and yellow sandstones; Fowkes formation, "white beds" of rhyolitic ash with interbedded limestones containing fresh water shells, fish, and plants; and the Almy formation, yellow and reddish yellow sandy clays with irregularly bedded sandstones, and near the base, conglomerate beds.

In no other area has the attempt been made to divide the Wasatch group into formations, and the Wasatch is called a formation in other localities. However, east of the area of this report, Schultz 68/ divided what he considered to be Green River formation into four members, namely (in descending order): "Tower sandstone" and plant beds of Powell, Laney shale member, Cathedral Bluffs red beds member, and the Tipton shale member. Sears and Bradley 72/ later showed that the Cathedral Bluffs red beds member was actually a tongue of the Wasatch, and they designated it as the Cathedral Bluffs tongue of the Wasatch formation, a term in use where applicable at the present time. Nightingale 54a/, in 1930, applied the name, Hiawatha member, to the Wasatch beds below the Tipton shale member in these areas.

Distribution.---Exposures of the Wasatch are extensive in the area

Figure 7.---- View looking northwest towards typical red beds in the middle part of the Wasatch group. Section 14, T12N, R108W.

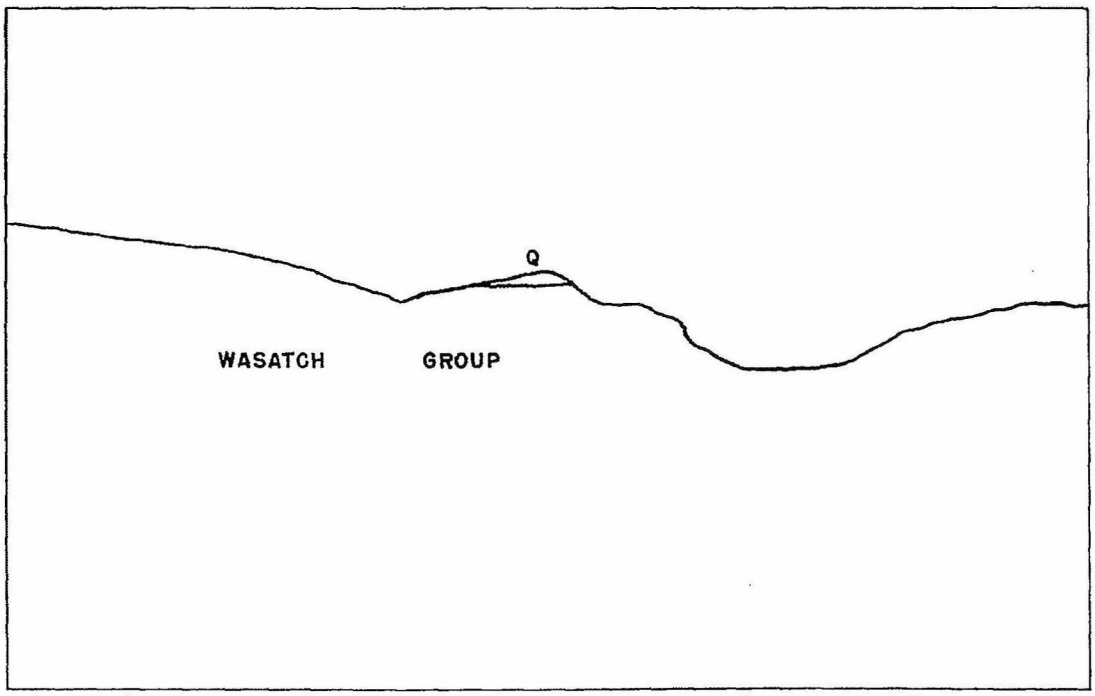

Figure 8. --- View looking east towards typical "white beds" in the lower part of the Wasatch group. Note terrace deposit capping the hill. Section 18, T12N, R107W.

of this report. It occurs in a strip, varying from 600 feet to about 4 miles wide, from the western end to the eastern end of the area and beyond. Most of this strip lies just north of the Utah-Wyoming border, but in the vicinity of Manila, the Green River, and north of Goslin Mountain, it swings into Utah and covers a few square miles.

Character and thickness.---The Wasatch is essentially a thick assemblage of red, brown, yellow, and white sandstones and shales, with several prominant beds of conglomerate in the upper portion of the section. Some coal and carbonaceous shales are present.

The group was not divided into smaller mapping units for this report; although there are some general lithologic differences that are to be noted upon inspection of the section. The lower part is composed of 2100 to 2200 feet of soft, easily eroded beds of yellow, white, and drab gray shales, in some places giving a variegated appearance. Some carbonaceous shales and low grade coal of sub-commercial quality is to be noted. Interbedded with these shales are some thin white and dark tan to brown sandstone beds. North of Goslin Mountain erosion has formed badlands in section 21, T3N, R23E. Here the yellow and light gray shales weather with a peculiar surface covered with many angular pieces of yellow shale, one to two inches across. Although other writers (see Veatch 82/, Schultz 68/) have reported a basal conglomerate in the Wasatch in other areas, the writer detected none in this area. There are some pebbly sandstones, however, near the bottom of the section north of the western end of the "Devil's Causeway" . It is entirely possible that the true base of the Wasatch is not exposed in this area due to overlap, which causes this lack of a basal conglomerate. The contact with the Mesaverde is well exposed near the eastern portion of the area.

The middle portion of the Wasatch consists of approximately 1000 to

1200 feet of red shales interbedded with white and light gray sandstones, quite pebbly in places. Dark brown beds of sandstone are not uncommon. The lithology of this part varies greatly in the proportions of sandstones and shale in various localities. It is readily distinguishable from the above mentioned "white" beds by its deep red or reddish-brown hue, especially when viewed from a distance. This portion of the Wasatch is similar to the typical Wasatch, as exposed in the Red Creek Basin, a few miles northeast of this area. This middle portion changes laterally in the eastern part of the area into a thickness of beds containing a large amount of conglomerate. Richards Peak is composed of this rock type. Powell 60, p.163/ has reported the occurrence of Jurassic fossils in some of the limestone pebbles of these rocks. Limestone pebbles and sandstone pebbles up to a couple of feet in diameter are the predominant constituents of these conglomerates.

The upper part of this group is composed of gray, pink and some red sandstones, pebbly sandstones and conglomerates, with a minor amount of shale. In general, this part can be distinguished from the middle unit by its much softer hue, giving a pink to gray sensation from a distance. Close inspection, however, fails to produce a readily determined contact, as the two units blend into each other by gradation. The upper boundary of the formation is likewise one which is very difficult to determine specifically. It will be discussed under the Green River Formation. The thickness of this unit is variable being approximately 2100 feet north of the "Devil's Causeway", and, although not totally exposed due to faulting, about 3300 feet north of Manila. Near the top of the unit north of the "Devil's Causeway" and approximately 1200 feet from the top north of Manila, are several conglomerate beds that serve as good markers. These conglomerates are found in the Green River formation north of the east end

of the "Devil's Causeway" due to the interdigitation of the Green River-Wasatch contact, which will be further discussed under the heading of Green River formation. These conglomerates are composed of pebbles and boulders, up to three feet in diameter, of white quartzites and sandstones and gray dense limestones, resembling the Carboniferous rocks of this area. As far as is known to the writer, no fossils have been found in these conglomerates, but his observations have confirmed in his own mind the statements of previous geologists (see Sears and Bradley 72/and Powell 60/) that the source of at least a part of these conglomerates was Carboniferous. West of the Green River above the conglomerates the Wasatch is marked by the presence of sandstones containing concretions in abundance.

The total thickness of the Wasatch at any one place in this area is approximately 5400 feet, but to this must be added the 1200 feet previously mentioned at the top of the partially exposed section near Manila, which would give a total thickness of 6600 feet. The upper part of this is the time and depositional equivalent of the lower part of the Green River formation, as will be brought out in later pages.

For additional information regarding the Wasatch group on the north flank of the Uintas with interesting deductions on the source rocks of these beds, the reader is referred to Sears and Bradley 72/.

Age and correlation.---The age of the Wasatch group is well known from faunal evidence and is placed in the Wasatchian stage of the lower Eocene (see Wood, et al 97/).

Green River Formation

Name.---The Green River formation was named by Hayden 31/, in 1869, from exposures along the Green River. To the writer's knowledge, no other name has ever been applied to these rocks. Powell 60/, in 1876, divided the Green River group, as he called it, into the upper Green River (plant

Figure 9. --- Green River shales in section 9, T12N, R106W.

beds and Tower sandstone) and the lower Green River. Schultz 68/, in 1920, divided the Green River formation, as he called it, into four members, namely (in descending order): the "Tower sandstone" and plant beds of Powell, the Laney shale member, the Cathedral Bluffs red beds member, and the Tipton shale member. Sears and Bradley 72/, in 1924, showed that the Cathedral Bluffs red beds member is in reality a tongue of the Wasatch as has been previously discussed. The other member names of Schultz are still used in those areas where applicable, which is to the east of the area mapped. In this report no attempt has been made to break down the Green River into smaller mapping units.

Distribution.---Aerially the Green River formation crops out over a larger part of the area mapped for this report than any other mapping unit. It occurs over the northernmost two miles throughout the length of the area, except in the extreme western and extreme eastern ends.

Character and thickness.---The Green River formation consists primarily of sandstones with abundant shales and minor amounts of limestone. Many of the sandstone and shale beds are calcareous. Oolites are common in both the sandstones and limestones. West of the Green River there is a much higher percentage of sandstone than shale, while in the eastern end of the area shale predominates. In the eastern part there are also several conglomeratic beds, which might correlate with the conglomerates near the top of the Wasatch in the western part. Concretions of limestone are common in this formation; one noted by the writer in section 13, T12N, R109W, being six feet in diameter. The typical fissile, "paper" shales which are so markedly developed in other areas where the Green River formation is found are not abundant in this area as far as the writer was able to determine.

The Green River formation has long been known for its oil shales and

and has been studied intensively as a possible source of petroleum. Winchester 94,95/ was one of the prominent workers in the early exploration of these deposits. He 94, p.168-9/ discusses four occurrences that were sampled along the Green River north of the area of this report in T13N and T14N, R108W. These localities had about three feet of oil shale each, and two of the locations produced 32 to 34 barrels of oil per short ton. Reports of "old-timers" in the region indicate that in earlier days, shales from these general localities were burned as fuel. The only samples of good looking oil shale which the writer saw in the area of this report were in the eastern portion in T12N, R106W.

Fossils are abundant in the Green River formation. Commonest forms are Unio and Turritella-like gastropods.

The lower contact of the Green River formation is difficult to map precisely. In most localities the beds grade upward from the pink and white, commonly concretionary sandstones of the Wasatch group into the white and light yellow-buff, abundantly oolitic sandstones of the Green River formation. It is customary in ascending the section to find beds of pink and light gray Wasatch sandstones overlaid by oolitic sandstones of the Green River formation which are in turn overlaid by pink sandstones typically Wasatch in nature and succeeded again by typical Green River sandstones. This, of course, is to be expected where lacustrine deposits have been laid down on fluviatile deposits of the flood-plain type, with the shoreline oscillatory. From a distance the change in color from Wasatch to Green River is more apparent, the former giving a pinkish gray effect and the latter appearing yellowish buff where overlying ashy white Bridger is present, and banded white and light buff in other localities. As a general rule for mapping, the writer chose the lowest beds containing oolitic sandstones or limestones as the Green River-Wasatch contact. This

contact definitely crosses time lines. In the western part of the area the bottom of the Green River is higher stratigraphically than in the eastern portion. In the upper Wasatch-Green River escarpment in sections 19 and 20, T12N, R108W, and section 24, T12N, R109W, this condition can be noted in a single exposure with the Green River capping only the top of the escarpment in section 24; while, farther to the east in section 20, the Green River is much lower in the escarpment. The contact between the two units can be plainly seen, upon study, to cut across the bedding planes. The degree which this contact crosses the bedding varies, and has its maximum effect in the locality just mentioned. The conclusion to be drawn from this observation is that the lake which deposited the Green River formation encroached upon the Wasatch floodplain later in the western than in the eastern portion of the area.

No measurement of thickness was made by precise methods. Except for the extreme western end of the area, the top of the Green River is not present. Here the Green River would not represent a normal thickness as it does not have its full development due to the interdigitation of the contact mentioned previously. The thickness in the western end of the area is only about 250 feet, while in the eastern edge an incomplete section measures approximately 1400 feet thick.

Age and correlation.---Previous work in the Green River formation has established its age as upper Wasatchian stage and lower Bridgerian stage of the lower Eocene (see Wood, et al, 97/).

Bridger Formation

Name.---The Bridger formation was named by Hayden 31/, in 1869, from exposures near Fort Bridger, Wyoming. Matthew 53/, in 1909, divided this formation into five faunal zones. Wood 96/, in 1934, designated two members for the Bridger; an upper, Twin Buttes member, and a lower, Blacks Fork member, based upon Matthew's faunal divisions. He did not include

the uppermost of Matthew's faunal zones in his Twin Buttes member. During the present field mapping, the Bridger formation was not divided into smaller units.

Distribution.---The Bridger formation crops out over an extent of a few square miles in the northwest corner of the area and extends northerly and westerly from here to become the main surface rock throughout the Bridger Basin.

Character.---This formation is a series of ashy-white, tuffaceous and calcareous shales and fine sandstones. Thin beds of black chert are abundant, although this is not distinctive of the formation since some thin beds of fossiliferous black chert are also to be found in the upper part of what has been mapped as Green River formation in section 16, T12N, R109W.

The Bridger contains an abundant assemblage of invertebrate and vertebrate fauna, although only the former were found during the course of this field work. The abundance of pelecypods and gastropods attests the fact that the Bridger deposits were lacustrine in nature, in part at least.

For further details regarding the character of the Bridger formation the reader is referred to Matthews 53/ or Sears and Bradley 72/.

Thickness.--- Only a thin surface veneer of 100 to 200 feet thickness of Bridger is found in this area, although five miles north at Twin Buttes over a thousand feet of upper Bridger is to be found.

Age and correlation.---According to Matthews 53, p.295-7/ the exposures in this area are in faunal zone C of the Bridger. Faunal zone C falls in the lower upper part of the Bridgerian stage of the middle Eocene.

QUATERNARY

Terrace Déposits

Terrace deposits of unconsolidated conglomerates, sandstones, and clays occur as remnants in Lucerne Valley and the valley of Henrys Fork. The study of these terrace deposits was not considered by the writer to be of prime importance to the successful completion of the project which has resulted in this report, as it would have been if the purpose were a consideration of the late history or geomorphology of the area.

However, a few interesting but incomplete observations will be presented here regarding them. Further additional studies in the future must be made to provide the details for a complete picture.

The terraces more or less conform with the present drainage valleys. East of the Green River this is particularly noticeable. Here the terrace remnants have a profile which clearly shows a negative gradient from the eastern end of the valley to the Green River, and also shows a negative gradient generally from the southern edge of the valley to Spring Creek.

There is a high proportion of conglomerate in the terraces, although some of the terrace exposures, particularly east of the Green River, are only thin veneers of "soil" clay. Although all of the conglomerates contain pebbles of Uinta Mountain quartzite, Carboniferous limestones, and white and gray quartzites not recognized in place in this area; the other pebbles present are more or less distinctive depending upon the locality. For example, in the terrace remnant in section 35, T3N, R19E, there are many pebbles from the Nugget sandstone, and Park City limestone, the Curtis limestone, and the Weber sandstone, while, in the terrace remnants bordering Henrys Fork, there are many pebbles of the fossiliferous black chert and other rocks of the Bridger and Green River formation. Clearly,

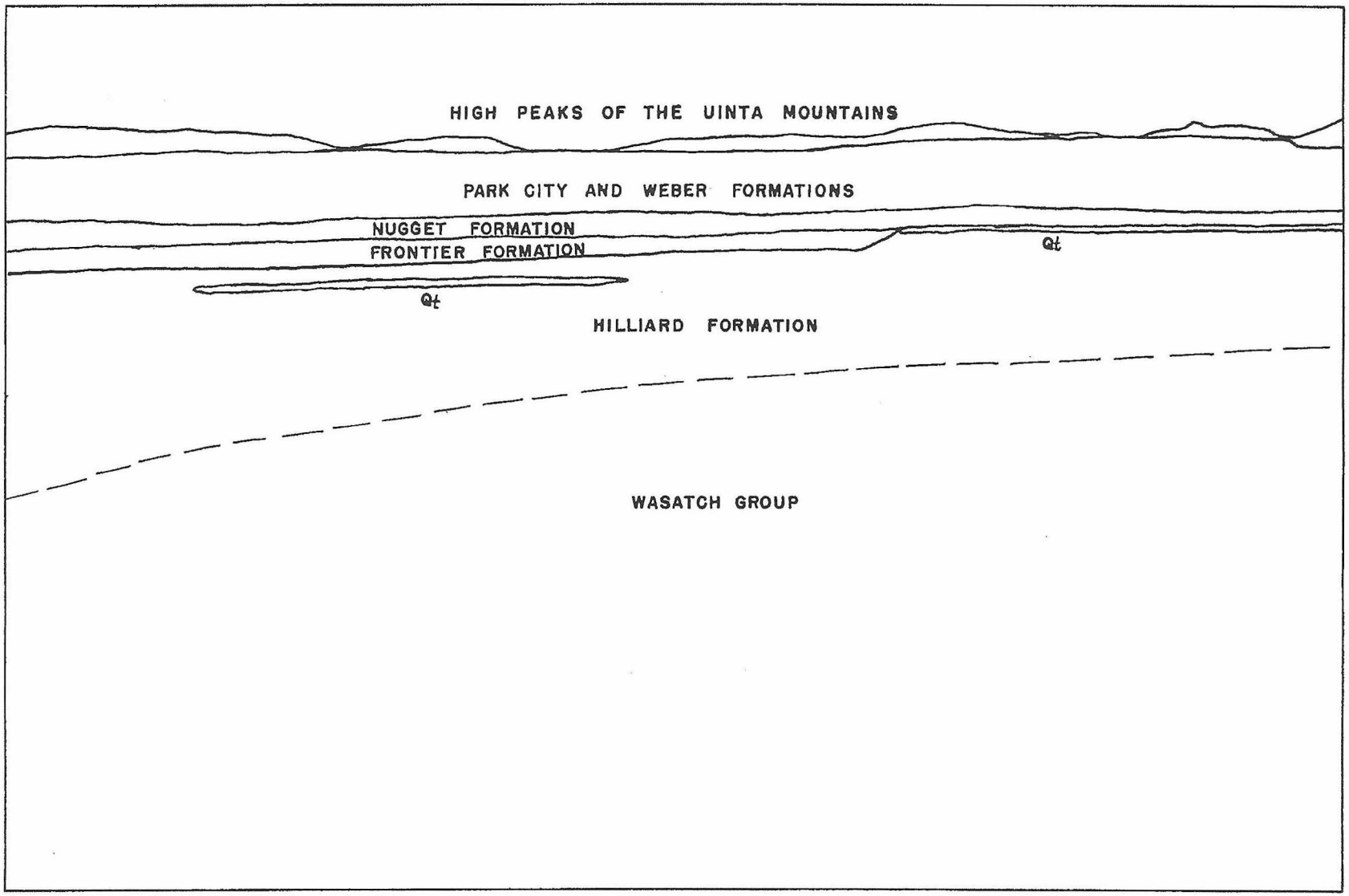

Figure 10. --- View looking west of south, showing Lucerne Valley and town of Manila, with Quaternary terrace remnants in the background.

the pebbles show that the source of much of the material was not too far distant, and the writer from many inspections concluded that the drainage pattern at the time of deposition of the terraces was similar to the drainage pattern of today.

There are several different terrace levels. In the exposure shown on the geologic map in section 19, T3N, R21E, three distinct terrace levels exist. In the valley north of the "Devil's Causeway" at least three terrace levels are evident. No attempt was made during the mapping for this report to differentiate the various levels.

In the strict sense, the Lucerne Valley west of Henrys Fork might be considered a terrace deposit in large part, but the writer hesitated to include such a large area as a terrace deposit, when the purpose of the report was of an entirely different nature from the study of these superficial rocks, and the determination of older formations is apparent under what is probably a thin veneer of soil cover. Lucerne Valley, however, is at a higher level of drainage than Henrys Fork or the Green River. Exposures of rock older than Quaternary are scarce in this portion of the area, and are only exposed where stream cutting has been great.

Alluvium

The alluvium consists of unconsolidated sands, clays, and gravels. The writer has divided it into two types so that the relationships in the eastern part of the area can be more fully understood. Qal has been used to designate all stream deposits at the present level of deposition, while the symbol Qals has been used to represent slope wash that has been deposited in the past or that is being deposited now but is not at the existing level of deposition in the sense that the present streams are cutting headward and removing the material in these deposits. This slope wash is usually at a level higher than the terrace deposits mentioned previously and in places has covered them with debris.

III. STRUCTURAL GEOLOGY

INTRODUCTION

Since the earliest work of geologists in the Uinta Mountains, the general structural features of this range have been known (see Powell 59,60/ and King 45/.

The structure of the Uinta Mountains is a large, gently arched, east-west trending anticline. This arch has been traced from the Wasatch Range on the west, through the main portion of the mountains, eastward through Axial Basin, and thence southeastward into the White River Plateau, which is a part of the Rocky Mountain system proper. The length of this anticline is more than 150 miles and is one of the major uplifts of the Rocky Mountain region. On each side of this great fold lie synclinal basins---the Uinta Basin on the south, and the Green River Basin on the north. Both received huge amounts of early Tertiary sediments. The simple main arch of the Uinta Mountains is complicated by faulting, which on the south flank, although complex and abundant, is relatively unimportant from a broad structural point of view. The faulting on the north flank, however, is of a magnitude that makes it one of the main structural features, and prompted Powell 60, p.17/ to apply the name "Uinta displacement" to this type of anticlinal arch faulted on one flank.

The structure is further complicated by a number of folds trending in a north-south direction, or approximately at right angles to the line of major uplift. Although the structure of the Uinta Mountain group sediments in the "core" of the Uinta Mountains has not as yet been studied in sufficient detail to lead to widespread generalizations, the basins on both sides of the mountains are known to contain these transverse structures.

An example is the Rock Springs uplift, which divides the Green River Basin into two parts - a western portion known as the Bridger Basin and an eastern half called the Washakie Basin. Much reconnaissance work has been done on this feature because of its coal and oil resources and its general structural relationships are well known (see Schultz 66, 67/, and Sears 71/, and Nightingale 55/).

The area under discussion in this report lies on the north flank of the Uinta anticlinal arch, and contains in its northern portion the southeastern corner of the Bridger Basin. Included in the district is the zone of large magnitude faulting that was mentioned previously.

STRUCTURAL TREND

The main structural trend of the Manila-Linwood area is roughly in an east-west direction with a northerly dip that displays considerable variation. In general, the dip of the Paleozoic and Mesozoic rocks, except where they have been subjected to intense fault drag, is roughly fifteen to twenty-five degrees north in most places. East of the Green River in the portion of the area adjacent to the "Devil's Causeway" this dip is steeper and averages from thirty-five to forty-five degrees north. The lower part of the Wasatch group has, in general, approximately this same attitude, but the upper portions decrease in dip radically. The overlying Green River and Bridger formations dips to the northwest at low angles.

This general north-dipping, east-west trending alignment has had superimposed upon it a series of warps whose axes trend in a northerly direction. The anticlinal warps are two in number; the synclinal warps, three. For convenience these subsidiary structures will be designated in this report by the following names reading from west to east: (1) the Bennett syncline, (2) the Linwood anticline, (3) the Williams syncline, (4) the Richards syncline. Each of these will be discussed in detail on following pages.

The structure of this area is further complicated by a number of faults, which can be divided into several groups. The first type consists of the major fractures of the area. They trend generally in an easterly direction, are steep dipping, and have had the greatest influence on the present structure. The Manila and the Uinta fault zones are the two examples of this kind. A second type is the south-dipping, easterly trending thrust exemplified by the Sheep Creek fault. A third type is shown by northwesterly trending, steep-dipping oblique breaks. Lucerne fault, two other mapped, but unnamed, faults east of the Green River, and a number too small to be included in a

mapping project such as this fall in this classification. A fourth type consists of oblique faults that trend in a northeasterly direction. Fifth, and lastly, there is fracturing south of the Uinta Fault zone that was not studied in detail and may or may not be connected genetically with any of the aforementioned types. All of this faulting will be further discussed in succeeding pages.

FOLDS

Linwood Anticline

The Linwood anticline is located as shown on the geologic map accompanying this report, in R20E, R21E, and R109W. It is named from the town of Linwood, which lies on this structure. The best exposure of the structural relationships are shown on the escarpment of the Flaming Gorge and in the ridges just north of this locality.

On the map the term "axis" has been used, as on almost all geologic maps, to indicate a line joining the crests of the various formations exposed at the surface. This line does not coincide with the axis or axial trace since this fold is decidedly asymmetric*, with the southwest flank displaying gentle dips (when the plunge of 25 to 30 degrees is taken into consideration) and the northern flank generally exhibiting very steep dips---in places overturned.

In the vicinity of Horseshoe Canyon and the Flaming Gorge, the determination of the crest is unmistakably definite; and just north of the Wyoming-Utah boundary the exposures are good enough to leave but little doubt concerning its location. However, in the Hilliard shales of the Lucerne Valley between these places the bedrock is so covered by superficial mantle that attitudes cannot be obtained and the location of the crestal trace is conjectural. In fact there is some indication this anticline is double crested; that is, the crest line northwest of the town of Linwood may trend in a more southerly direction and the "axis" at the Flaming Gorge may bear more northerly than shown on the map, with the

---

* In this report the word asymmetric will be used to indicate an anticline or syncline with one flank steeper-dipping than the other. Among some geologists this term is restricted to structures which cannot be divided by a plane that will form "mirror images" on either side, and they might use the term "tilted anticline" where the author uses "asymmetrical anticline". However, among petroleum geologists generally "asymmetrical" is used in the sense of its employment here.

intensity of the folding on these two line diminishing in the incompetant Hilliard shales. This interpretation would occasion two en echelon "axes".

North of the Henrys Fork fault zone, the location of the axis is doubtful due to the superposition of Tertiary sediments. It is believed that the large bend in this fault is significant as an indication of folding that is post-faulting in age.

Causeway Anticline

The Causeway anticline is located east of the Green River, and its axis is located in R22E and R107W. It is named from the "Devil"s Causeway", the double-peaked ridge of Mesaverde group sediments, where it is best exposed.

The crestal trace of Causeway anticline trends in a northerly direction. As is the case of the Linwood anticline, this fold plunges steeply to the north, with an average of approximately 40 degrees in the Mesozoic sediments. This anticline also is asymmetric with the eastern flank showing steeper dips than the western. However, this warp is much broader than the Linwood anticline and the asymmetry is not so marked, so the crestal trace should correspond more closely with the axis than in the other case, although there is no real proof of this in the field.

The crestal trace cannot be followed by reconnaissance methods in the low-dipping Green River formation in the northern edge of the area, but the change in strike of the Wasatch group north of the "Devil's Causeway" gives a fair idea of the crest of the structure in these rocks.

An interesting phenomenon occurs in this flexure just north of the Uinta fault zone. The reader's attention is invited to the relationships in sections 27, 28, 33, and 34, T3N, R22E. Here the Frontier and the Aspen formations show the characteristic convex northward pattern that the strata in a north-plunging anticline should have. However, the steep, northward-

dipping Curtis, Entrada, Carmel, and Nugget formations all are concave northward and show that the anticline has been replaced by a syncline in a distance of about one mile. The Dakota formation west of the axial trace as marked on the map and the Morrison formation east of the axial trace are low-dipping, which accounts for the excessively wide outcrops of these formations. This type of structural relationship is not unique, but it is sufficiently rare to merit mention. The cause of the odd configuration will be discussed later.

Bennett Syncline

The Bennett syncline is to be found on the geologic map at the southwestern corner of the area mapped in R19E and R20E. It is named from its proximity to Bennett's Ranch. It is to be noted that there are two synclinal segments which bound the Linwood anticline on the west---one north of the Sheep Creek fault and one south of this fault. By geometric devices, taking into consideration the dip and strike of the Sheep Creek fault, the dip and strike of the sedimentary strata, and the throw along this fault, it is readily seen that the ends of the two synclinal segments will not join if the fault is removed, if the action along the fault is considered to be simple dip slip. However, these two segments have been considered by the writer to be two parts of the same structure, as they are probably intimately related in their genesis.

From insufficient evidence due to the proximity of this flexure to the edge of the area mapped, it appears that the asymmetry of this syncline is not very great, and does not reach the proportions of that of the Williams syncline to the east.

The plunge of this warp is not as great as those of the structures further to the east, averaging approximately 15 degrees.

Williams Syncline

The Williams syncline is located in R21E and R108W. It is named from the William's Ranch located on the north side of Henrys Fork near its junction with the Green River.

This syncline, whose west flank is the east side of the Linwood anticline and whose east flank is the west side of the Causeway anticline, is, of course, highly asymmetric with a much steeper west flank. The plunge of this structure is somewhat in doubt as all of the good exposures near its axial trace are also near probable or known faulting. It appears, however, that the plunge is approximately 20 to 25 degrees, in general.

This syncline cannot be traced in a northerly direction beyond the Mesaverde-Wasatch contact by reconnaissance methods.

Richards Syncline

Richards syncline is located at the eastern edge of the area mapped in R23E and R106W. It is named from its proximity to Richards Butte.

Richards syncline separates the Causeway anticline and the Clay Basin fold that is east of the area mapped. It is readily recognized in the Mesaverde sediments, but the details of the syncline in the vicinity of the axial trace in this group of rocks are obscured by the tremendous amount of fault drag that has taken place along the Uinta fault.

The syncline is also displayed in the lower Wasatch sediments, although its recognition in the Green River formation by reconnaissance methods is not certain. The plumge of this fold in the Wasatch is approximately nine degrees near the Uinta fault, but the plunge increases to the north to about 15 to 20 degrees. As is true of the other flexures in this area, this syncline is asymmetric with the west flank being the steepest.

FAULTS

Uinta Fault Zone

The Uinta fault zone forms the southern boundary of the area which was mapped for this project. Although other designations have been applied to this feature, the above name has the widest usage. Powell 60, pl.III/ called that portion of the fault west of Goslin Mountain the "Flaming Gorge branch" of the Uinta fault, and used the term Uinta fault in the western part of the area for the fault here mapped as the Henrys Fork fault. Forrester 23/ uses the name "Crest or Uinta Fault" for this feature. Lawson 39, p. 269/ called the Uinta fault by the name "North Flank Fault".

The Uinta fault trends in general in an east-west direction, but it is quite sinuous and the strike of the main fault of the zone (i.e. the fault with the greatest displacement) varies radically. The greatest change in strike can be observed in section 30, T3N, R23E, where the fault abruptly turns at an angle of 45 degrees. Without mapping south of the Uinta fault in more detail, the relationships at this point cannot be stated definitely; but it appears that this radical change in strike can be accounted for most probably by an explanation that is often applied to other high angle faults where the observations are more complete---that of the major displacement in a zone of intense faulting being along two en echelon faults joined by an oblique fault.

Some of the simuosity can be attributed to post-faulting deformation of the fault surface. In sections 33, 34, and 35, T3N, R22E, the southward bulge in the fault trace can be attributed to the post-faulting development of the small synclinal structure that was discussed previously under the Causeway anticline. The southwestward swing of the fault in the eastern part of R21E seems to be more or less in accordance with the general strike of the sedimentary strata north of the fault. The northward bulge in the

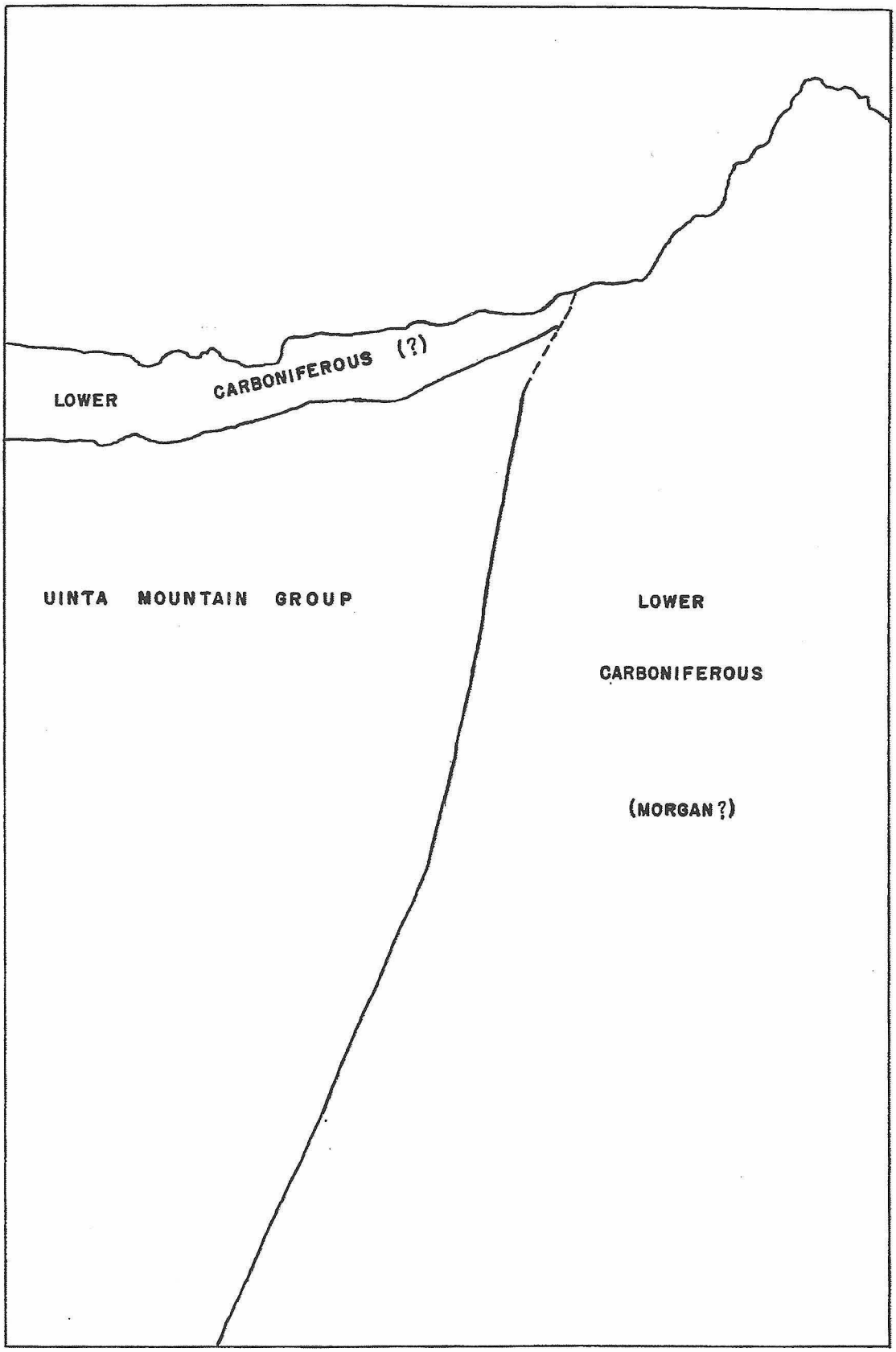

Figure 11. --- View looking west across Sheep Creek gorge along strike of the Uinta Fault. Section 15, T2N, R19E.

western part of R21E appears to coincide with the axis of the Linwood anticline. The southward bulge in R20E also seems to correspond to the bend in the bedding in the Bennett syncline. Of course, these changes in trend may be due to a tendancy to break along weak bedding planes.

However, assuming for the moment that the first part of the movement along the Uinta fault was prior to the folding of the anticlines north of the fault---a sequence that writer will attempt to prove later---so that the minor irregularities in the strike of the fault can be attributed to folding; the fault trace, if reconstructed to a pre-folding condition, would be still remarkably sinuous. This sinuosity, as observed also in other steep-dipping major faults, usually indicates that the fault displacement was dip slip and that the strike slip component, of necessity, must be small.

The discussion as to whether the Uinta fault is a high angle fault or a low-dipping thrust has been a matter of debate for many years. Powell 60/ in his sections indicates that the fault is practically vertical. Schultz 68, p.37/ in a cross-section shows the Uinta fault south of Boars Tusk to be a south-dipping thrust with a dip of 27 degrees. Irwin 38, p.108/, in 1926, on the basis of observations at Clay Basin reports that the Uinta fault is a southward dipping thrust, with a dip of 45 degrees and a displacement of 30,000 feet. Ver Wiebe 83, p.487/, in 1930, makes a statement which is much the same as Irwin's but gives no source for his information. De Lyndon 15/, in 1932, also considered the Uinta fault as a low-dipping thrust based upon Ver Wiebe's statement. In recent years there has been some objection to this idea. Forrester 23, p.646/, in 1937, stated that the dip of the fault is steep (75 degrees) to the south. Bradley 10/, in 1936, indicated on his illustrations that the Uinta fault is a steep-dipping reverse fault. The writer is in agreement with the results of these later workers in this area. There is only one good exposure of the Uinta fault

Figure 12. --- Bedding plane slickensides developed in Nugget sandstone adjacent to the Uinta fault. Section 3, T2N, R21E.

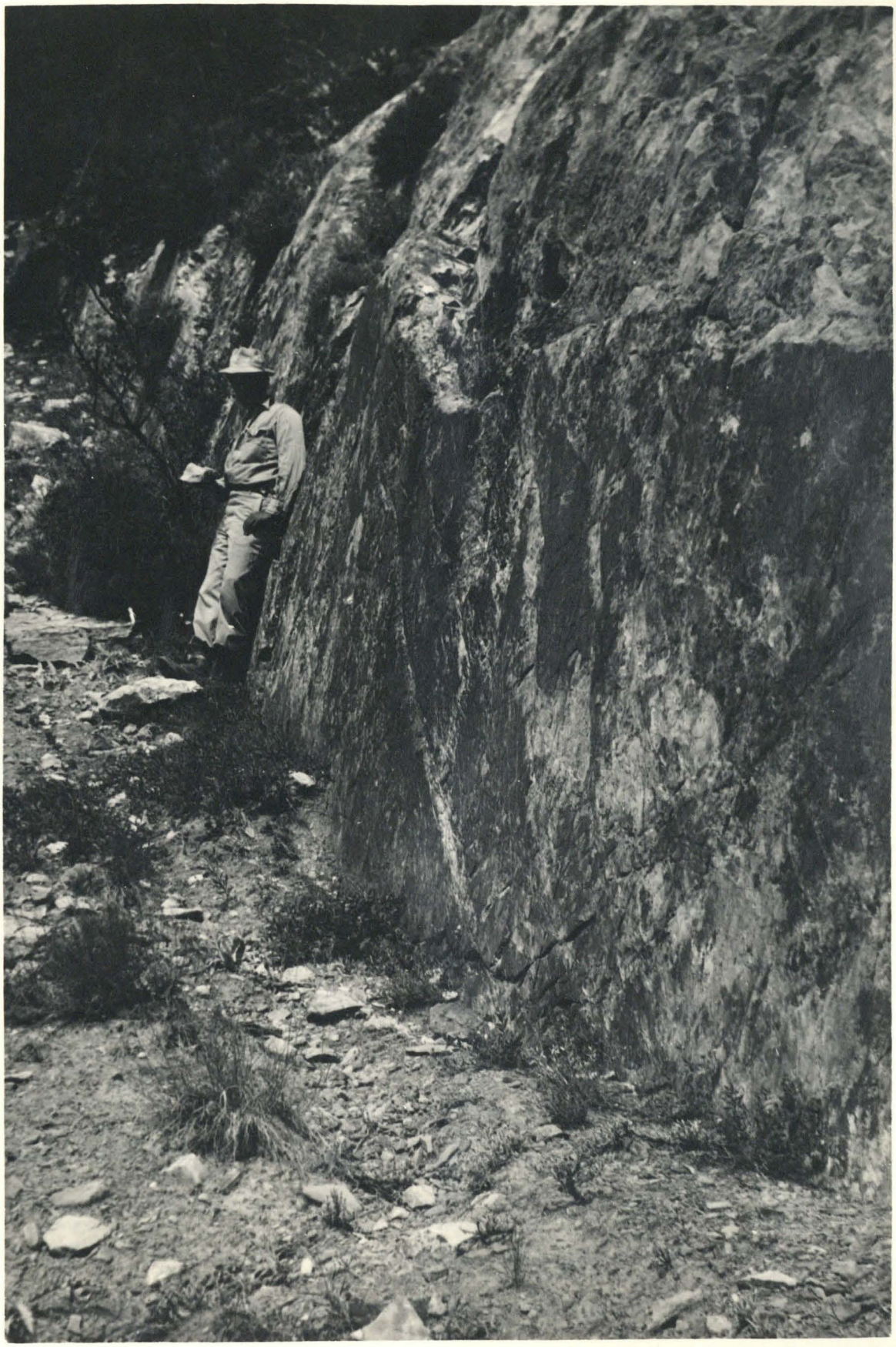

in this area, and this exposure is excellent. It lies in section 16, T2N, R19E, where Sheep Creek crosses the upturned strata of Uinta Mountain quartzite and lower Carboniferous limestones and plunges into the Sheep Creek Gorge. The fault plane can be determined at this locality within a few feet (see fig. 11). The dip of the fault plane at this place is 82 degrees south. This single exposure does not, of course, preclude the possibility of a change so that the fault plane might dip at a lower angle at some other place. Indeed, a study of the dips in the bedding north of and adjacent to the fault shows a large amount of overturning in some places. The maximum degree of overturning was seen by the writer in section 15, T3N, R23E, where the Mesaverde is dipping southward at an angle of 19 degrees (161 degrees of overturn). In many places the strata are overturned to 60 degrees or more. This overturn is difficult to explain on the basis of a steep-dipping reverse fault. However, if the fault were a low-dipping thrust, the fault trace would tend to move northward with an increase in elevation and southward with a decrease. This does not seem to be the case. In spite of large, rapid changes in elevation the fault trace pursues its sinuous path with little regard for the topography. Therefore, the writer has concluded that the Uinta fault is in general a steep-dipping reverse fault. In his opinion the errors of previous workers in assuming the fault to be a low angle thrust were due to the use of erroneous evidence. Schultz, in his report, chose a location for his cross-section where there is a fault slice north of the main Uinta fault (see section 4 and 5, T2N, R21E, of the geologic map). Evidently he mistook the dip of this subsidiary fault as the dip of the main fault. Although the author has not studied the locality (Clay Basin) where Irwin made his determination of a south dip of 45 degrees, he suspects that a southward bend in this sinuous fault coincidental with the rapid decrease in elevation on the east side of

Goslin Mountain may have caused an erroneous interpretation.

Without a more thorough study of the relationships south of the Uinta fault, the amount of throw cannot be determined with precision. However, the minimum stratigraphic separation, or minimum throw, can be calculated with some assurance. North of Goslin Mountain, movement along the Uinta fault zone has brought Red Creek quartzite opposite to Hilliard shale. If the Clay Basin fault is also considered as a part of the Uinta fault zone, the Red Creek quartzite is in close proximity to the low-dipping Mesaverde, and the minimum displacement of the two faults may be considered as the amount of section represented between the Red Creek and the Mesaverde. If the Red Creek south of the fault were assumed to be stratigraphically near the Red Creek - Uinta Mountain contact, the stratigraphic separation would be approximately 28,500 feet. Not far to the west of this locality the Uinta Mountain group is faulted into close proximity to the Mesaverde group.

If it is assumed the former are near the top of the Uinta Mountain section, as a rough tracing of the bedding by air photo from this place to west of the area mapped where the Uinta Mountain is overlaid by later sediments would tentatively indicate, the stratigraphic separation would amount to approximately 16,000 feet. There are two possible explanations concerning this apparently paradoxical situation. The first assumes that the faulting shown on the geologic map between the Uinta Mountain group and the Red Creek quartzite took place at the same time as the major movement on the Uinta fault and there was a large difference in movement in section 22, T3N, R23E, on the portion of the Uinta fault west of the junction with the Red Creek-Uinta Mountain fault and that portion east of this junction. The other possibility is that the Red Creek-Uinta Mountain faulting took place at an earlier date than the Uinta faulting and the later movement on the Uinta

fault is readily seen in section 2, T2N, R21E, where a fault at right angles to the Uinta fault displaces the Uinta Mountain group but does not displace the Uinta fault.

At the western edge of the area, the amount of movement along this fault is much less. Just west of the area mapped, the Uinta Mountain group is overlaid by younger Carboniferous sediments in normal contact according to Bradley 10, Pl.34/, and the writer's observations, though scanty, tend to confirm this relationship. Therefore, the Uinta Mountain group rocks in fault contact with the lower Carboniferous rocks at Sheep Creek Gorge must be near the top of the Uinta Mountain group. This would suggest that the displacement along the Uinta fault at this locality was approximately two thousand feet or less. There is some evidence of faulting a short distance south of this place, which was not studied and might be a part of the general zone of Uinta faulting, but it is believed that the main Uinta fault is the one shown on the geologic map of this report. By tracing the bedding of the Uinta Mountain group on the air photos in a rough way, it is readily determined that the Uinta fault increases in throw towards the east. Thus, the Uinta fault in this area can be regarded as a large scissor fault with a displacement of approximately two thousand feet at the west end and more than sixteen thousand feet at the east end.

The time of faulting will be discussed on later pages.

Henrys Fork Fault Zone

The Henrys Fork fault zone is located near the Wyoming-Utah boundary west of the Green River. One other name has previously been applied to this faulting. Forrester 23/ called it the North Flank fault, but this name had been previously used for faulting in this area by Lawson 39, p.269/ in a different sense. Bradley 10/ first used the name Henrys Fork fault.

This fault is poorly exposed. Almost everywhere it is covered by

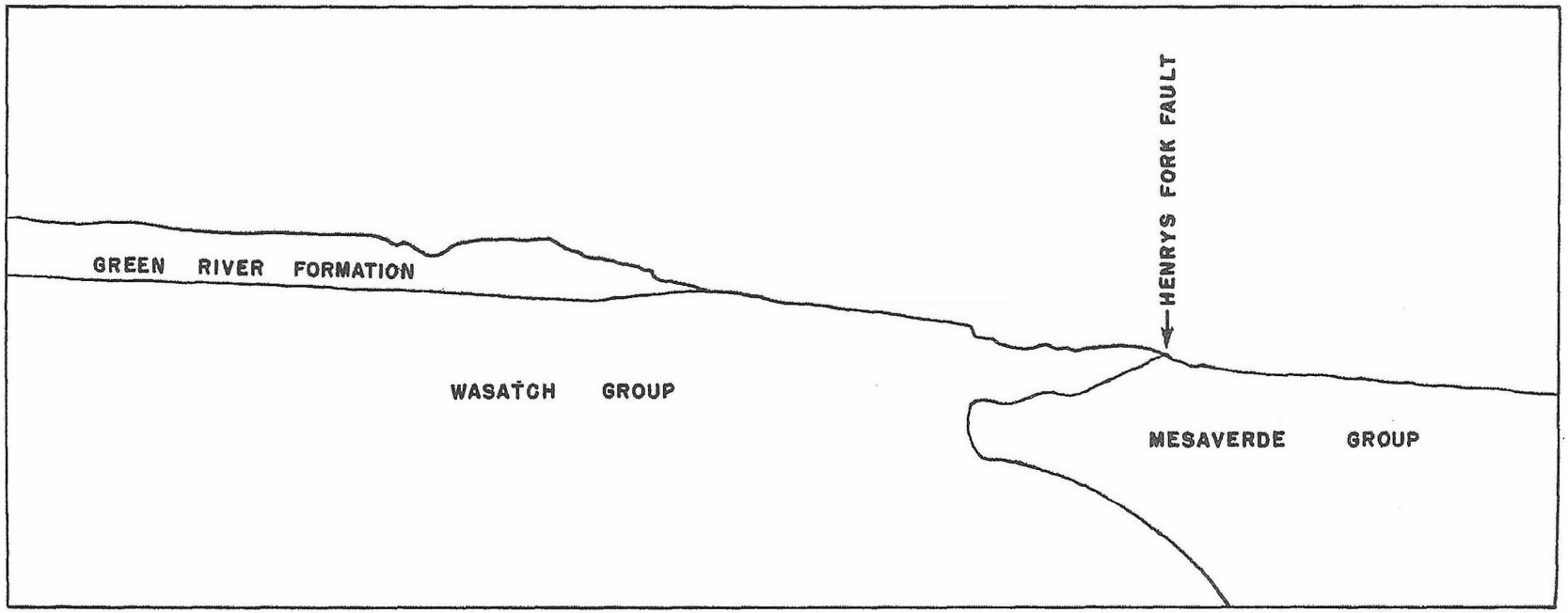

Figure 13. --- View looking east across Linwood-Green River road along strike of the Henrys Fork fault. Section 24, T12N, R109W.

terrace material, soil, or alluvium. The best exposures are found near the Linwood-Green River road, about one mile north of Linwood, and in section 22, T12N, R109W. In the former locality the fault is readily located between beds of Wasatch conglomerate and Mesaverde shales and sandstones overturned to a dip of 72 degrees. In the latter locality, deposition has obscured the Mesaverde and Hilliard shale, but the upturned strata of the Wasatch and the easily recognized subsidiary fault bounding the fault slice shown on the geologic map give evidence of the presence of the main line of faulting. Along the west bank of the valley of Henrys Fork the fault plane is believed to have been located, although the dense growth of vegetation makes this determination somewhat problematical. If this is the true fault plane, it has a dip at this locality of 86 degrees north. With these incomplete observations it appears that the fault plane is practically vertical, but may in places dip southward at a steep angle. The greatest amount of overturning observed in the bedding near the fault was north of Manila, where the strata are overturned to 58 degrees.

The Henrys Fork fault is complex and extremely difficult to map in detail due to the lack of good exposures. The interpretations as set forth herein are therefore rather conjectural. The reasons for mapping the various branches of this fault zone as shown will be presented. Other interpretations also could be given that would be supported by good reasoning.

The main branch of the Henrys Fork fault in R109W is fairly well exposed and the interpretation is considered highly accurate. In the vicinity of Manila in R19E and R20E, four inferred branches of the Henrys Fork fault are shown. The southernmost of these branches is an extension of the fault which divides the Wasatch group from the Hilliard shale. This

fault is everywhere covered by the soil cover of Lucerne Valley. In sections 5 and 6, T3N, R20E, there is a prominent hill of Wasatch sandstones and conglomerate; and the fault, of course, must pass south of this hill. Its inferred extension through the town of Manila in the location shown is made on the basis of a strip of ground through the semi-cultivated fields, that appears to be better watered by underground means than in adjoining properties. This indirect evidence was used as an implication of the existence of faulting.

The other three inferred faults in this vicinity are within the Wasatch sediments. The southernmost of these three is also drawn along a line where the ground is fed by underground springs, but in this case the amount of percolating water is much more abundant. It was found necessary in some property along this line to install tile for drainage purposes and the flow from these ducts is considerable. The next fault to the north is also a conduit for water. A tunnel has been dug into the hillside to intersect this fault and the water which drains from it is used for domestic purposes in the town of Manila. Several other similar tunnels have been excavated along this fault for the same purpose. The shear pattern in these tunnels is complicated, but the main faulting seems to dip northward at a steep angle. The northernmost of these faults was mapped on the basis of a rapid change in dip which overturns the beds to 58 degrees.

East of R109W, exposures along the Henrys Fork fault are again very poor. The main fault trace turns southward very abruptly for a distance of about 1000 feet and then eastward at its former trend. This sudden change in strike may be due to a cross fault, although no evidence of faulting is visible along its trace in the well-exposed Wasatch escarpment to the north, and its southern extension is covered by terrace

Figure 14. --- View looking east showing fault drag in Wasatch sediments north of the Henrys Fork fault. Section 20, T12N, R10SW.

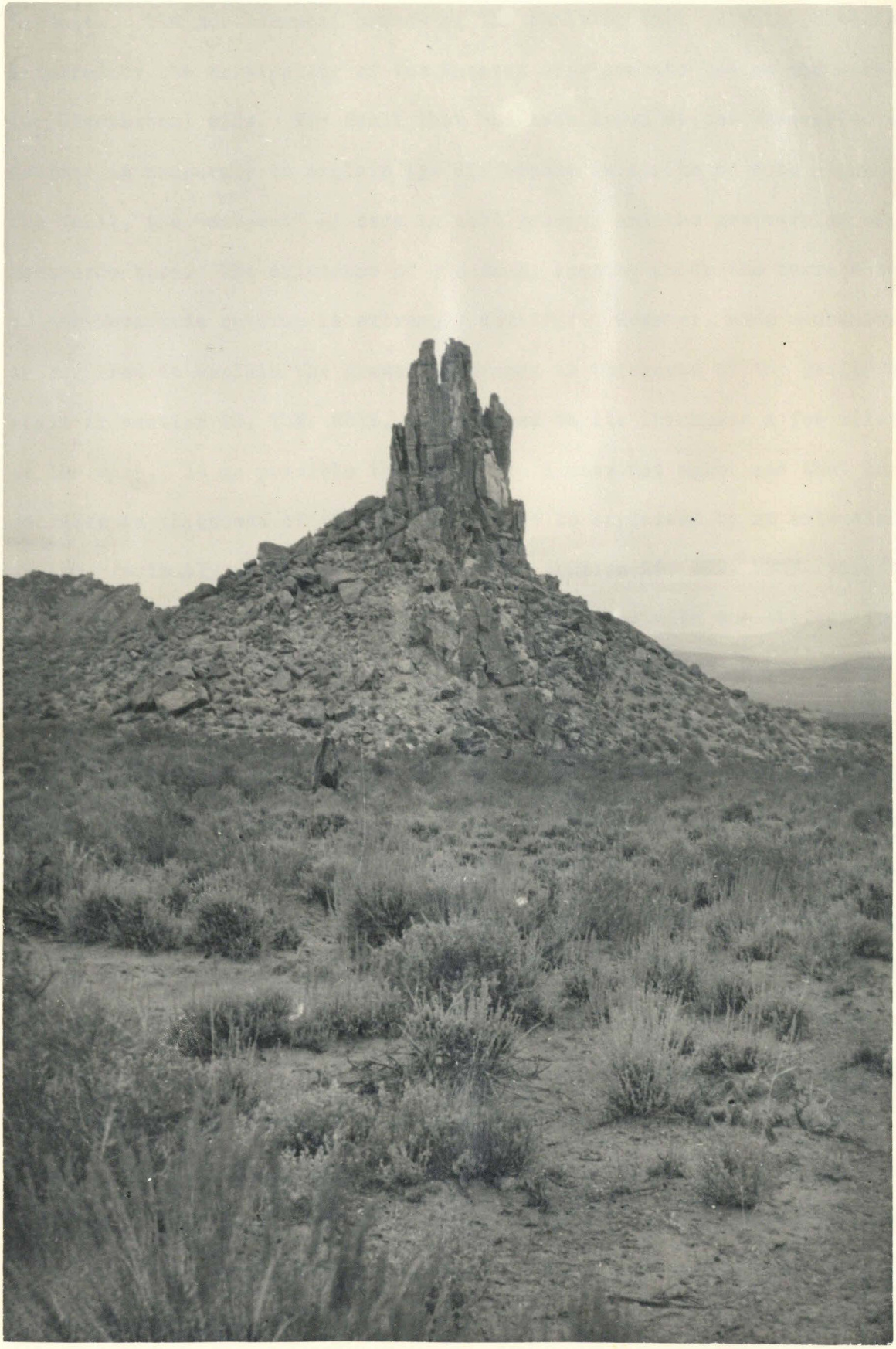

deposits. The northernmost branch of the faulting east of this point is inferred by the verticality of the Wasatch conglomerate bed on the northern (or downthrown) side. The fault that has been drawn at the Mesaverde-Wasatch contact is necessary to explain the difference in strike on both sides of the fault, the "cut-out" of beds in both groups, and the overturning of the Mesaverde beds. The existence of the fault running under the terrace south of the Mesaverde outcrop is extremely doubtful. However, some mechanism is required to explain the great difference in thickness of the Hilliard shale in section 19, T3N, R21E, as compared to its thickness a few miles to the east. It is possible that this fault does not exist and that the decrease in thickness of the Hilliard could be explained by an extension of the previously mentioned fault shown in section 14, T3N, R20E, with the possibility that it even continues onward and joins with the oblique fault at the east end of Boars Tusk. Observations are too obscure because of superficial deposits to reach any definite interpretations.

The fact that the thickness of the Hilliard shale east of the Green River is so much greater than the thickness of equivalent strata in other nearby areas is indicative that there may be additional faulting somewhere in this formation in the eastern part of Lucerne Valley. The total thickness of the Mancos group (Hilliard, Frontier, and Aspen) in sections 17, 20, and 29, T3N, R22E, was measured during this project as approximately 7000 feet. Dobbin and Davison 16/ report a thickness for this group of approximately 6400 feet in the Clay Basin structure, 14 miles to the east. Sears 70/ reports the thickness of the Mancos at Vermilion Creek, forty miles to the east, to be 5367 feet. Nightingale 56/ reports this part of the section to be 5665 feet from drilling observations in the Vermilion Creek Basin. He also reports 55/ about 4000 feet of Mancos at Baxter Basin, about fifty miles to the northeast. The thickness in the area of this report east of

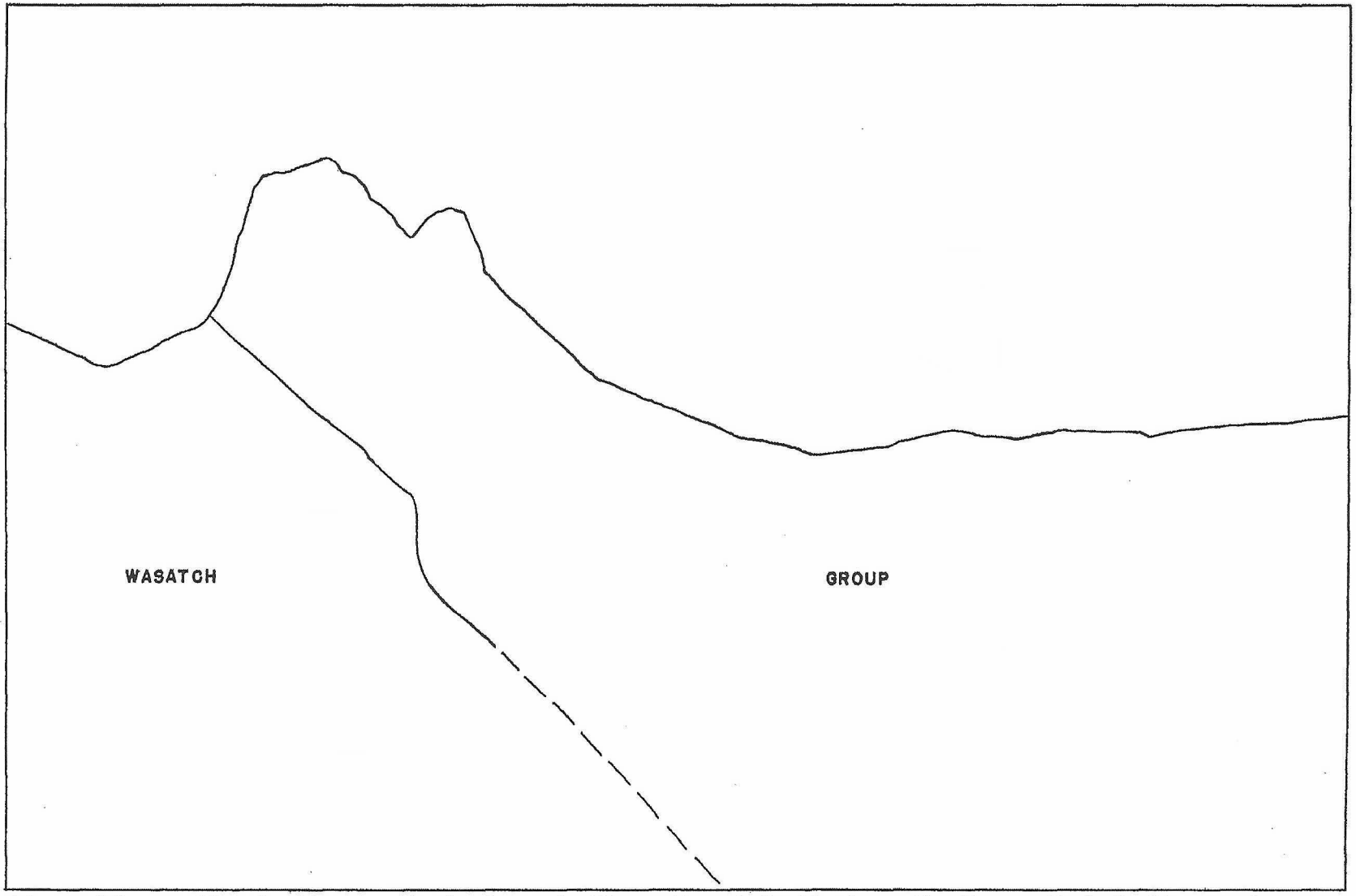

Figure 15. --- View looking north showing subsidiary thrust fault along the Henrys Fork fault, causing fault slice. Section 22, T12N, R109W.

the Green River seems excessive and leads to a suspicion that there is either faulting or a flattening of dip in the formation, The writer was on the alert for such a phenomenon but was unable to detect either. The Hilliard shales, however, as is the case with other incompetent shales, are rather poorly exposed and not readily interpreted at their outcrops.

The displacement on the Henrys Fork fault is greatest at the western edge of the area and decreases towards the east. Because the Wasatch formation is found on the north side of the fault and the amount of Tertiary overlap prior to faulting is not known exactly, no precise determination of the throw on this fault is possible. However, minimum stratigraphic separation can be calculated. In the locality of Henrys Fork , the conglomeratic part of the Wasatch formation is in contact with the Mesaverde group. East of the Green River, the thickness of Wasatch measured below the conglomerate beds is approximately 5400 feet. The amount of Mesaverde missing in the section at Henrys Fork is believed to be approximately 600 feet (?). The Lewis has already been overlapped at the eastern side of the Green River. Therefore, the amount of missing section amounts to about 6000 feet, and the throw of the Manila fault must be at least this much. The throw further to the west appears to be greater as the conglomeratic beds are in contact with the Hilliard shale, but the relationships are not so easily interpreted and conclusions are more indefinite. East of R109W the throw along the faulting decreases decidedly as attested by the incfeasing section between the Frontier formation and any definite horizon chosen in the Wasatch sediments north of the faulting.

Whether by coincidence or by genesis resulting from similar forces, Henrys Fork fault zone loses throw as the Uinta fault zone increases in displacement. This has been noticed previously on the north flank of the Uinta Mountains by Forrester 23, p.647/ who states "These two faults [Uinta

fault and Henrys Fork fault] tend to compensate each other; that is, an algebraic summation of the throw on the two faults remains about the same throughout the central portion of the range". If this area is included in Forrester's definition of the "central portion of the range", the writer is somewhat doubtful about the exactness of obtaining an algebraic sum at points along the two faults that will be constant, but it is certainly true that the increase and decrease in throw on the two is such that they tend to compensate each other.

Clay Basin Fault

The Clay Basin fault is located in the eastern edge of this area in T3N, R23E. It has been mapped eastward from this area through the Clay Basin structure by Dobbin and Davison 16/, who first published the name.

The fault is not well exposed in the area of this report, but its effects, in the form of fault drag, can be seen clearly in the Mesaverde sandstones. The maximum observed dip was 85 degrees to the south or 95 degrees overturned. Exposures of the rock south of the fault are extremely poor due to a cover of detrital material that has been sloughed from the steep northern slope of Goslin Mountain. Dobbin and Davison have mapped these rocks as Mancos shale. They also show that the fault plane dips southward at 80 degrees, a figure probably derived from the drag in the Mesaverde at either end of Clay Basin.

The relationship between the Clay Basin fault and the Uinta fault is effectively obscured by later deposits where these faults come into close proximity. Probably the two faults join, but this is not a certainty. In the western part of T3N, R23E, there is reason to suspect from the fault drag shown by the Mesaverde that there may be a fault trending in the same direction that proceeds westward from this area where the two faults join. This suspicion, however, is dubious, as the exposures in this

locale are practically non-existent.

Sheep Creek Fault

The Sheep Creek fault is located in the northern part of T2N, R19E and R20E. It is named from its proximity to Sheep Creek.

This thrust fault, which dips to the south, is best exposed along the Manila-Vernal road in the gap through the ridge forming the north boundary of Sheep Creek valley. At this location the Nugget sandstone has been thrust over the Entrada, Carmel, and the upper part of the Nugget formations. On the western side of this gap, the fault divides into two branches, with the Carmel formation in the slice. The dip of the fault at this locality is 35 degrees to the south and the stratigraphic separation is approximately 750 feet. This gives a minimum displacement of about 1050 feet.

West from this point the stratigraphic separation is at least as much, if not slightly more. East from the gap the separation decreases rapidly. Where the fault crosses the Triassic-Nugget contact in section 9, T2N, R20E, the stratigraphic separation is only about 60 feet. The eastern end of this fault terminates at the Lucerne fault and no trace of it was found by the writer east of this point.

Adjacent to the fault the Nugget formation is everywhere badly sheared, especially in the ridge between Bennetts Ranch and the gap mentioned previously. This supplementary shearing may total an appreciable amount and give the whole fault zone a greater displacement than shown above. The writer suspects that this is particularly true at the eastern end of the fault, as the displacement along the Lucerne fault appears much larger north of the Sheep Creek fault than south of it.

Lucerne Fault

The Lucerne fault, named from Lucerne Valley, is the largest of several faults in this area that trend in a northwesterly direction. It is located

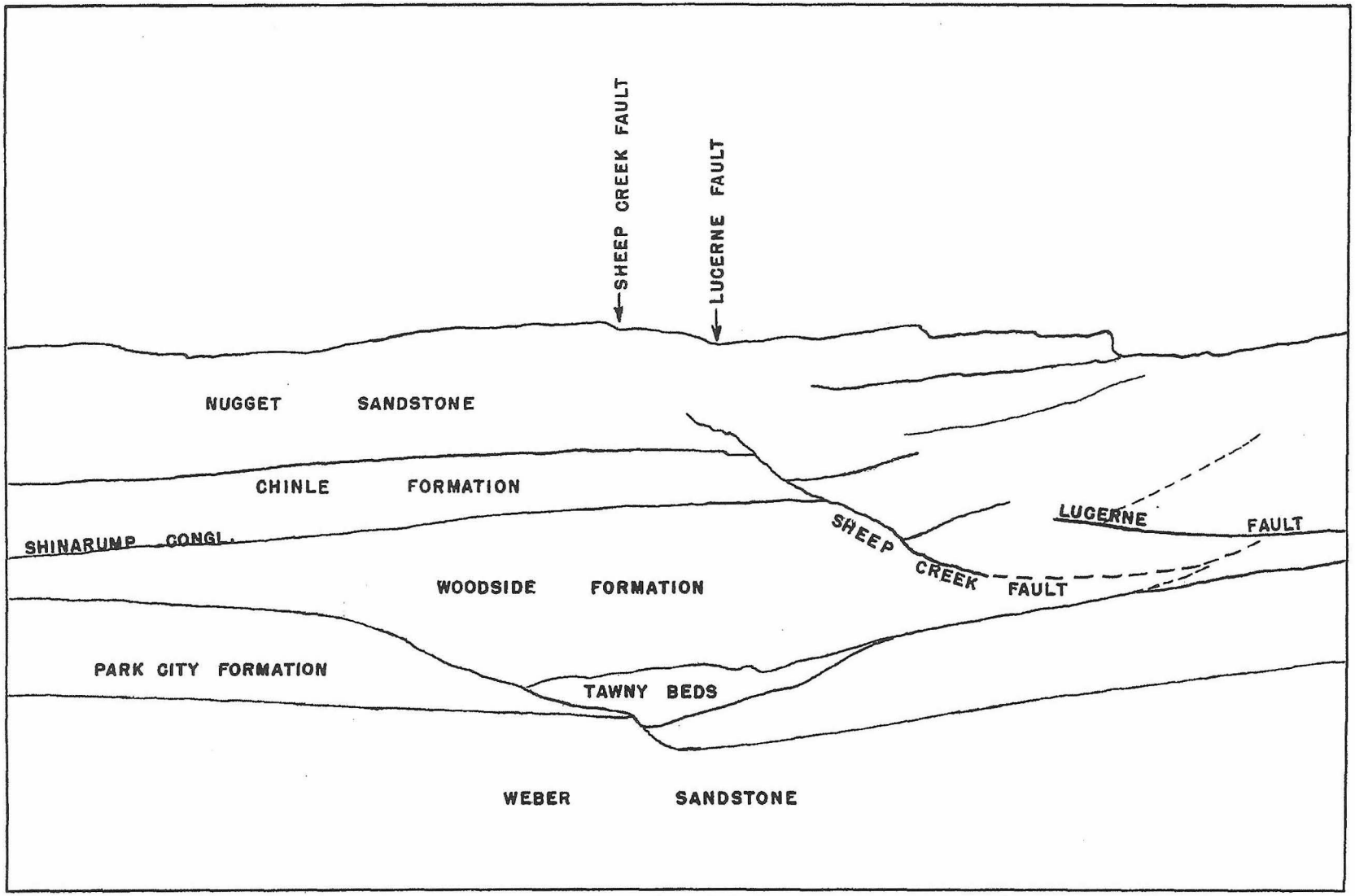

Figure 16. --- View looking northeast towards Nugget and Triassic escarpment, showing relationships near junction of the Lucerne fault and the Sheep Creek fault. Section 9, T2N, R20E.

in the northern part of T2N, R20E, and the southwestern corner of T3N, R19E.

The Lucerne fault is an oblique fault with an apparent upthrow on the northeastern side, but this appearance may be due in great part or entirely by strike-slip movement. The greatest stratigraphic displacement is on the north side of Sheep Creek. From here to the place where the fault disappears under the terrace deposits at its northwestern end, the displacement decreases to only a few feet. Measurements were made in the Triassic just north of Sheep Creek and at the Curtis-Morrison contact. The results were as follows:

At locality in the Woodside, north of Sheep Creek (s. 4-2-20)

Perpendicular separation	542 feet
Vertical separation	554 "
Horizontal separation	2823 "

At Curtis-Morrison contact (s. 5 and 6-2-20)

Perpendicular separation	257 feet
Vertical separation	265 "
Horizontal separation	1054 "

At the southeastern end, this fault appears to terminate against the Uinta fault, but may continue south along the Green River and thence into the Uinta Mountain group sediments. Cursory observation south of the Uinta fault did not reveal an extension of this fault, and time did not permit a thorough examination.

The Lucerne fault everywhere appears to have a vertical or very steep-dipping plane.

Faulting South of the Uinta Fault

The faults south of the Uinta fault were given only a cursory inspection. Evidence of faulting additional to that shown on the geologic map was seen in the Uinta Mountain group; but, as the south border of the area to be investigated for this project had been determined as the Uinta fault line prior to the start of field work, no attempt was made to map the

structures in the Uinta Mountain group.

The unnamed fault in section 31, T3N, R22E, is necessary as a contact between a previously unmapped body of Red Creek quartzite and the Uinta Mountain group, as the Uinta Mountain in this vicinity, as deduced from other considerations, is probably near the top of the stratigraphic column of this group. The location of the trace of this fault was not determined in detail but is roughly as shown on the map.

The fault which forms the contact between the €- Cm and the Uinta Mountain group in sections 21, 22, 28, 29, and 30, T3N, R23E, is necessary to explain the large difference in strike between the two mapping units. A glance at the air photos covering this vicinity shows that the Uinta Mountain group has a strike of approximately N70°W in section 28, T3N, R23E; and, as there is no profound unconformity in the section, faulting is the only possible mechanism. Schultz 68, pl.I/ mapped this as a normal contact. This fault was not traced in detail and the location shown on the map is only approximate. The nature of this faulting is unknown; although a downthrow of the north side of not more than two thousand feet seems quite definite, with the possibility of much less displacement. Its general position indicates that it may have the same general genesis as the Uinta fault, although no possibility of actually dating the fault exists.

The unnamed fault in T3N, R23E, which forms the contact between the Red Creek quartzite and the Uinta Mountain group was first mapped by Schultz 68, pl.I/. Its location on the map is only approximate, being determined by a fairly sharp break on the aerial photos. However, it is unmistakably clear that this contact is a fault because of the trend of the bedding in the Uinta Mountain group and the presence of distortion in the beds adjacent to this contact. The age of this faulting cannot be determined, but the writer suspects that it was prior to intensive

movement along the Uinta fault (see a discussion of this under the "Uinta Fault Zone" earlier in this chapter).

Minor Faulting

Faults of a minor nature were left unnamed. For purposes of identification in the following pages, these faults will be designated by the section, township, and range, in which they may be found on the geologic map. For example, the fault in section 3, T2N, R21E, near the "k" in Boars Tusk will be called the "3-2-21 fault" .

Minor faulting associated with the major east-west reverse faults.--- Both the Uinta and the Henrys Fork faults have supplementary faults that expose small slices at the surface and innumerable smaller faults that constitute part of the shear zone. The former includes such faults as 9-2-21, 2-2-21, 36-3-21, and a horde of small faults in 25-3-22, connected with the Uinta fault; and 22-12-109 connected with the Henrys Fork fault. These faults all bring to the surface older rocks than those exposed to the north of the faults, indicating that the movements have all been in the same sense as the movements of the major faults, and there is no visible evidence of collapse due to tension, reversal of movement on the major faults, or similar phenomenon. Only one of the sympathetic faults has been shown on the map, as they are in general of small displacement and the tracing of these individual shears would be beyond the scope of this reconnaissance report. The one mapped fault of this class is well exposed in Sheep Creek Gorge in section 16, T2N, R19E. It divides Morgan and Weber sediments dipping approximately 20 degrees on the north from Morgan sediments in a vertical or slightly overturned position on the south. Exposures east of this point are too poor for positive identification and the trace is inferred. This shear may increase in throw west of the area mapped for this report and become the major one of the Uinta fault zone.

Other minor faulting associated with the Henrys Fork fault has been

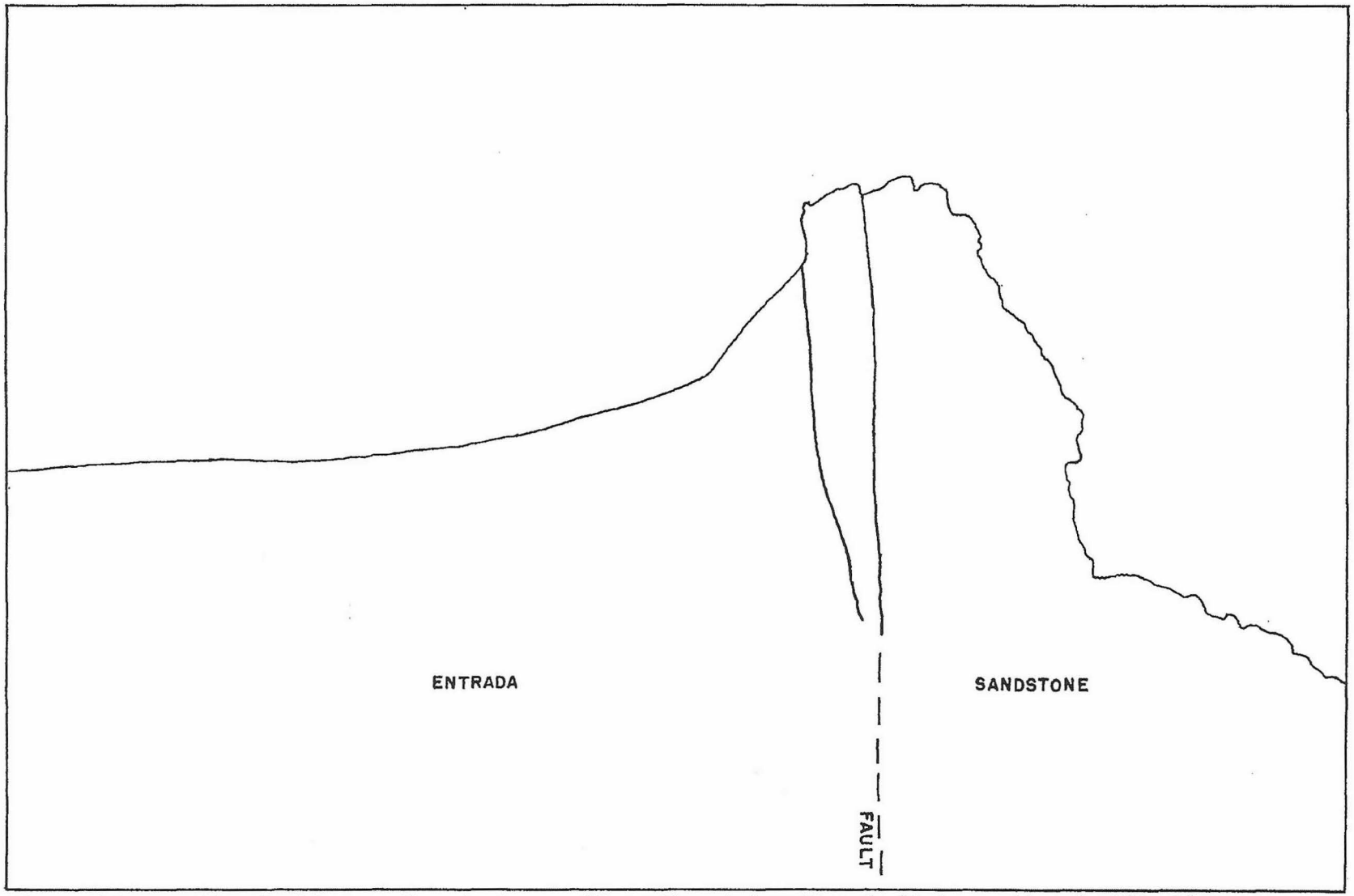

Figure 17. --- View looking northeast at a small northwest trending fault in section 5, T2N, R20E.

previously discussed.

Minor faulting trending in a northwest direction.---Faulting which appears to be associated with the Lucerne fault trend and the direction of most prominent shear pattern in the area is seen in a number of places. Only two of these faults were considered to influence the structure sufficiently to warrant their mapping. Fault 3-2-21 has an apparent upthrow on the east side. It definitely terminates at the Uinta fault on its south end, and appears to die out in the incompetent Morrison clay shales at its northern end. There is a possibility, as mentioned previously in the discussion on the Henrys Fork fault, that this fault extends northwestward and joins with the fault trending southeastward in section 31, T12N, R108W. The intervening territory is so covered by superficial deposits that the relationships cannot be readily interpreted.

Fault 36-3-21 is another of these northwestward trending faults. Its apparent upthrow side is again on the eastern side. It terminates to the south against a fault slice of the Uinta fault zone and on the north against the Dakota sandstone. This last situation is rather interesting, inasmuch as the thickness of the Morrison on the east side of the fault is greatly reduced compared to the west side. This is most readily explained by assuming the existance of faulting between the close of deposition of the Morrison and the deposition of the Dakota. As far as the writer knows there is no other place that faulting has been reported during crustal movements that are post-Morrison and pre-Dakota. Unconformities have been reported in other places between these two formations, however, (see Pike 58, pl.I, p.10/ and Walton 85, p.98/. The possibility exists, of course, that the Morrison is so incompetent that it was able by intra-formational distortion to absorb the movements to which it was subjected by this faulting, in which case the faulting could be post-Dakota. There is also

the possibility that the fault changes strike abruptly and loses itself down-strike in the Morrison. If such is the case the change in strike is extremely rapid.

Minor faulting trending in a northeast direction.---There are a number of small faults and a shear pattern in the area that trends in a northeasterly direction. There were only two faults of this class that were seen during the course of the present project that were worthy of even noting on the geologic map, and no attempt was made to trace them because of their insignificant displacement. Fault 5-2-20 is well exposed in the cliff formed by the Entrada sandstone in the location shown on the geologic map (see fig. 17). This fault has a strike of N31°E, and striae noted on the vertical fault plane dipped 11° E. The total stratigraphic separation on this fault is less than six feet; but, if the striae are accepted as the direction of maximum movement, the total displacement would be in the neighborhood of 30 feet.

Fault 17-12-106 is also a fault that appears to have insignificant displacement, but it is not so well exposed as the other case. Little is known of this fault except that it has a general trend of N55°E.

IV. GEOLOGIC HISTORY

It is beyond the scope of this paper to present a complete and comprehensive geologic history of the area. To attempt such a presentation of the depositional history prior to the Laramide Revolution would involve a discussion of the stratigraphy and paleogeography of an area many times larger than the one mapped, which is but a small part of the great Rocky Mountain geosyncline that remained a basin of deposition throughout most of the Paleozoic and Mesozoic and probably much of the Algonkian. As this is primarily a structural report, the omission of this portion of the history is not considered as a vital part of this paper, since the happenings prior to the Laramide Revolution contributed little to the present structural details. The above statement should not be construed as meaning that the author believes that there may not be a connection between the thicknesses of the Mesozoic, Paleozoic, and possibly the Algonkian sediments, and the uplift of a mountain range such as the Uinta Mountains. This general problem of why the Uinta Mountains are where they are, why they have their peculiar east-west orientation, and the processes causing these phenomena is a problem on which the writer has speculated and for which he has no hypothesis that he would care to put into print at this time. The history of the Rocky Mountain region prior to the Laramide Revolution, of course, must be considered in a problem of so broad a scope. But for all practical purposes, in studying the restricted aspects of the structural evolution of the area mapped, it appears that tectonic history began at the time of the Laramide Revolution. Let it suffice for this report to say that prior to this time there had been a long period of deposition from the Algonkian to at least the late Cretaceous, broken now and then by a period of non-deposition, by times of gentle orogenesis

or epeirogenic movements resulting in minor unconformities, and possibly by a period of post-Algonkian, pre-Carboniferous faulting on a rather large scale.

The exact dating of the Laramide Revolution in this area is not possible by observations made at the surface of the ground, as some of the units of the upper Cretaceous and lower Tertiary, known to exist at other localities in the Rocky Mountain province, do not crop out in this area; and these missing units represent the deposition during the time that is critical for precise dating. However, certain time limitations can be placed upon various events which occurred during this revolution. These limits will be brought out in the following paragraphs. Moreover, there can be deduced from the facts at hand the sequence of tectonic events which deformed the rocks to produce the present structures.

The major movement along the Uinta fault probably occurred after the original main upwarp of the Uinta Mountains was nearly completed. Although evidence in support of this statement is rather incomplete, the factors which can be evaluated in forming an opinion on this subject seem to favor this view. If such were not the case, the northern flank of the Uinta Mountain would not have had its present general northerly dip at the time of faulting, and the Uinta fault originally would of necessity have been a north-dipping normal fault instead of a steep-dipping reverse fault. However, even if one is of the school of thought that the Uinta Mountains were uplifted by upward-directed vertical forces, he cannot preclude the presence of compressional, north-south directed forces, for they are necessary to explain some of the subsidiary warps which trend east-west and are found on both sides of the main uplift. Therefore, in the opinion of the writer, the Uinta fault can be considered as a relief of stresses set up by the main uplift of the Uinta arch and occurring in the late stages of the

main uplift.

The main movement along the Uinta fault preceded the deposition of the lower Wasatch group sediments. This fact can be deduced from a study of the relationship between the Wasatch group and the Mesaverde group in section 21, T3N, R23E. Here the Mesaverde is overturned with an average dip of approximately 60 degrees that reaches 19 degrees maximum. The overlying beds, which are some of the lowest exposed strata of the Wasatch group in the area, dip gently to the north at approximately 9 degrees, steepening to 18 degrees adjacent to the fault. Therefore, the Mesaverde was intensely deformed near the Uinta fault prior to the deposition of the Wasatch beds. The Clay Basin fault could be held responsible for this movement but for the fact that the Clay Basin fault, in both this area and on the east side of Clay Basin (see Dobbin and Davison 16/), cause an overturning of the Mesaverde formation of only 95 to 100 degrees where the influence of the Uinta fault is not present. Therefore, it seems reasonable to infer that both the Clay Basin fault and the Uinta fault had their major movements prior to the deposition of the lower Wasatch. It is also clearly indicated that one or both of these faults moved after the deposition of the Wasatch because the 9 degrees of fault drag in the Wasatch must be accounted for; but this later movement must have been much less severe than the earlier movements.

The upper part of the Wasatch, at least its lower portion, clearly was deformed by the forces which caused the warping of the Causeway anticline. As can be seen from a study of the dips and strikes north of the "Devil's Causeway", the Wasatch beds have attitudes that agree closely enough with those of the Mesaverde and Lewis so that an unconformity would not be suspected using reconnaissance methods over a small area of the Mesozoic-Tertiary contact. From these facts the writer has inferred that the Wasatch was also folded in the movement which formed the Causeway anticline.

The time of the main movement on the Henrys Fork fault is not so apparent as the sequence discussed above. The Henrys Fork fault definitely affects beds near the top of the Wasatch group (i.e. the conglomerate beds discussed under the stratigraphy of this group, and some higher units). But, in addition to this fact, the Henrys Fork fault appears to have been deformed by the movements which produced the Linwood anticline. Its general sinuosity corresponds roughly to this structure and also the Williams syncline. Therefore, the writer infers that the Henrys Fork faulting started after the deposition of the upper Wasatch, at least after the deposition of the conglomeratic beds, and continued concurrently with the movement that formed the north-south trending flexures in this area.

In the last stages of the movements discussed above, a lake was formed; and the Green River formation was deposited. The Green River formation may have been slightly deformed by recurring movements of the type already mentioned. However, by reconnaissance methods, no changes in attitude were detected that would give definite indication of such movements.

In summary, the following sequence of events may be listed: (1) The general uplift that marked the major arching of the Uinta anticline, (2) the major movement on the Uinta fault, probably during the late stages of the movement listed above in 1, (3) the deposition of the major part of the Wasatch group of sediments, (4) the inception of the Henrys Fork faulting, (5) the beginning of the movements that formed the north-south trending flexures in the area, (6) the continuation of the faulting listed in 4, with concurrent continuation of the movements listed in 5, and (7) the formation of a lake and the deposition of the Green River formation over the structures formed during the above sequence.

After the time required for the deposition of the Green River formation, volcanism became active; and a series of ash beds were laid down (represented by the Bridger formation) in the lake beds.

The later history of this area has been recently presented in a very conprehensive manner by Bradley 10/.

The history of the Green River in this and adjacent areas has been a much discussed matter in the past. The reader is referred to Powell 60/, Emmons 20/, Hancock 29/, and Sears 69/.

The forces that caused the various events of the Laramide revolution are of some interest. The direction of application of the stresses which arched the Uinta Mountains is highly speculative. There appear to be two probable explanations, namely: a vertically applied force which acted upward, or a north-south, horizontal compression. The application of a horizontal force alone to raise an arch with the huge dimensions of the Uinta Mountains, would involve stresses so great that they would be many times the crushing strength of the rocks, and the resultant deformation would certainly be visible in the field. Such forces would also probably produce great thrust faults, as exist in other localities in the Rocky Mountaint region. The writer, therefore, leans favorably towards the view that the main active stresses were applied more or less in a vertical direction. However, this is not meant to imply that compressional forces were not also present, as the uplift of the Uinta Mountain arch represents a considerable shortening of the earth's outer crust and there is no evidence of tension in any of the observed faulting. Nor does this belief imply that there may not have been a compression at depth that was responsible for the upward forces.

In the Wasatch Mountains the western end of the Uinta arch has been intruded by igneous bodies (see Calkins and Butler 12, pp.50-53/), but this is the only occurrence of intrusion into this fold in the writer's knowledge.

The forces which caused the uplift of the Uinta arch are probably responsible for the shearing action represented by the Uinta fault. The amount of movement along the Uinta fault apparently is controlled by the localization

of more intensive uplift in certain portions of the arch, a situation that can be easily proved or disproved after detailed mapping of the Uinta Mountain group is completed.

The folding of the north-south flexures in this area probably resulted from the application of east-west directed, compressional forces. How much the Uinta Mountain quartzites that make up the "core" of the Uinta Mountains were affected by these forces is unknown without further detailed mapping of this group. However, it appears, for the amount of warping that the Uinta fault has suffered, that these forces did not warp the "core" of the Uinta Mountains very much. From the appearance of the anticlines formed in the area mapped, the forces acted primarily on the Paleozoic, Mesozoic, and existing Tertiary sediments. This implies that the differential movement between the Uinta Mountain quartzites and the later sediments caused by the flexing, must have been relieved horizontally along the Uinta fault line. A flexing of the Uinta Mountain group in the extreme southwest corner of the area, so that the material of this group near Sheep Creek Gorge were moved eastward, would account for many features now existent. The greater intensity of folding and the northwest trend of the axis of the Linwood anticline would result from such an action. The presence of Sheep Creek fault, with its eastward decrease in throw, and the formation of Lucerne fault, with its southward increase in throw, would also be explained. The change in the southern part of the Causeway anticline from an anticline to a syncline would be the result of warping that was more or less restricted to the later sediments. Therefore, the writer speculatively infers that the formation of the north-south trending anticlines of this area resulted from an east-west applied compressional force that warped the Uinta fault in the southwest portion of the area and caused the Paleozoic and Mesozoic sediments to fold more intensively immediately east of this bend, some of the movement being relieved by the formation of

the Sheep Creek and Lucerne faults and some being alleviated at the southern edge along the Uinta fault.

The genesis of the Henrys Fork fault, at about this same time is probably due to a residual stress left in the area by the previous scissoring action of the Uinta fault, to additional stresses which had accumulated due to the large thickness of early Tertiary sediments that had deposited in the Green River basin to the north, and to the application of the east-west compressional stress discussed above.

In the Wasatch Range, Calkins and Butler 12, pp.50-53, p.61/ have recently discussed the sequence of deformation. The large scale north-south trending overthrusting that they show preceding the main uplife of the Uinta arch, does not seem to exist in the area of this report. However, after the time of the Uinta warping and the accompanying intrusion of stocks, they show another period of east-west compressional movement which caused a tilting of the overthrusts. This second period of east-west directed, compressional movement may correspond to the activity that produced the north-trending warps in the area of this report.

V. ECONOMIC GEOLOGY

PETROLEUM AND NATURAL GAS

One of the main purposes for the project represented by this report was the investigation of the area as a potential producer of petroleum or natural gas. The area that was mapped for this report has never produced either of these substances. In the following pages, a brief presentation of the present production of the region surrounding this area and a statement concerning the writer's views concerning the possibilities of future production will be given.

Present Production of the Region

The nearest production is at the Clay Basin gas field, the center of which lies about three miles east of the area. The westernmost well is in section 19, T3N, R24E, approximately one mile to the east. Dobbin and Davison 16/ published a map in 1945 which shows the structural relationships in this field. The structure consists of an east-west trending dome. During the summer of 1947, the writer was told that there were 9 producing wells in this field. The production is gas from the Dakota sandstone. The top of the Nugget sandstone is the deepest horizon which has been drilled; and, according to Dobbin and Davison, was found to be wet with no gas reported. The depth of the producing sand is approximately 5800 feet at the center of the structure.

The nearest of the Baxter Basin gas fields lies about 20 miles north of the northeast corner of this area. Nightingale 55/, in 1934, wrote a report on these fields that outlined the geology. The fields consist of two faulted domes and a faulted anticlinal nose. Production is gas from the Dakota and Frontier sandstones. A small well, completed in 1945, produces oil from the Entrada sandstone in North Baxter Basin field. Since the time of Nightingale's report, the top of the Madison has been penetrated, but no

deeper production of oil and gas has been reported.

The two Hiawatha gas fields are about 24 miles east of this area. Nightingale 56/, in 1934, reported the geology of these fields. The structures consist of two domes. Production is gas from lenticular sands in the lower part of the Wasatch group.

Powder Wash field is about 50 miles east of this area. Additional reserves were found in 1947 by the discovery of an extension in the Wasatch producing area.

About 60 miles southeast of the area, the Elk Springs oil field, discovered in 1946, produces from the Weber sandstone..

The Church Buttes oil field, discovered in 1946, is producing high gravity oil and gas from the Dakota sandstone at a depth of approximately 12,500 feet. This field, more than any other, has aroused interest in the possibilities for additional future discoveries in the Bridger Basin.

Possibilities of Future Production

In a discussion of the possibilities of future production in any area, the most important factors to consider from a geological point of view are, of course, the presence of source beds, the presence of horizons which are probable reservoir rocks containing oil or gas, and the presence of structural traps suitable for the accumulation of these products. These factors will be discussed in the succeeding paragraphs.

As can be seen from the discussion of near-by production above, there are several horizons that have proved productive in other districts near the area mapped for this report.

The lower portion of the Wasatch group can be considered a producer of both oil and gas in the region east of this area.

The Frontier formation produces gas in the Baxter Basin fields to the north.

The Dakota sandstone is the most productive horizon of the region, producing gas in the Baxter Basin fields and the near-by Clay Basin field, and gas and high gravity oil in prolific amounts in the Church Buttes field to the northwest.

The Entrada formation is a producer of oil in the North Baxter Basin field.

The Weber formation contains prolific sands in the eastern part of the Uinta Basin, south of the Uinta Mountains, and its probable equivalent, the Tensleep, is a prolific producer in central Wyoming; but, to date, despite the test of this formation at several places in the eastern Uinta Mountains and at the south Baxter Basin field, it has proved to be unproductive. However, in the opinion of the writer, the tests in near-by areas have not been conclusive enough to condemn this formation.

Besides the above-mentioned strata, which are now productive in near-by areas, there are several other horizons in the stratigraphic column of this area which are the equivalents of producers in central Wyoming. These are included in the Carmel formation, the Park City formation and the Madison limestone. The sandstone member in the Hilliard shale of this area also may prove to be productive, as it is similar to the Shannon sand of the Steele shale, which is the rough correlative of the Hilliard.

Of the above possible sources of production, the Dakota formation is the most probable. The lower Wasatch, Frontier, and Entrada are considered by the writer as good possibilities. The probability of the Weber is not too good, although it has many beds with high porosity; and because of its prolific production elsewhere, it should not be wholly improbable. Production from the other units mentioned above is not impossible but should be considered as improbable in view of tests to date in adjacent areas.

The two structures in this area which would be the most likely traps for the accumulation of petroleum are the Linwood anticline and the Causeway anticline. Both of these anticlines are mono-plunging, i.e. they are nose-type warps, with no closure on the south ends that would be due to a change in plunge. Therefore, any closure which might be existent must be by faulting, pinch-out, or over-lap.

There is no reason to suspect that the Uinta fault is either a conduit or a seal for the migration of oil and gas. However, if it is a seal, the Uinta fault provides closure on the southern end of both of these anticlines. On the Causeway anticline, closure should be effected on beds of Triassic age or older. On the Linwood anticline, possible closure includes beds of lower Carboniferous (Morgan) or older, with possible closure in some of the sandstone members of the lower Weber. However, since the Uinta faulting probably took place during the late stages of the Uinta uplift, as discussed previously, it is altogether likely that oil and gas which may have existed in some of the possible producing strata had an ample opportunity to migrate updip in the regional tilt produced by the upwarping of the main Uinta flexure prior to the time that the Uinta fault was developed. If such were the case, the oil and gas would have escaped during the post-Laramide-revolution erosion which has removed the Paleozoic and Mesozoic sediments at the crest of the mountains.

The Henrys Fork fault provides structural closure of the Linwood anticline, although this structure is probably made more complex by the existence of one or more northwest trending faults on its east limb. The Henrys Fork fault probably was post-Uinta-faulting in age; and, as is the case of the Uinta fault, the oil and gas which might have been present in the various horizons had a chance to escape prior to the faulting. However, the pre-faulting regional tilt probably did not affect the Wasatch group, and this

fault may provide adequate closure for the lower beds of this group, in which case, an accumulation of oil is likely.

The probability of pinch-outs and overlaps in a formation such as the Wasatch and older, unexposed Tertiary sediments is good, though unpredictable. According to Sears and Bradley 72/, the source of the Wasatch sediments in this area was the highlands formed by the earlier, main Uinta uplift. Assuming this to be the case, the deposition of the Wasatch group must have been the thickest towards the center of the catchment basins to the north, with the coarsest floodplain deposition being near the edges of the basins. This condition of deposition naturally leads to the development of overlaps and pinch-outs. Many fine oil fields have been deposited under similar conditions. However, assuming that an overlap or pinch-out is existent, locating such a trap is a difficult matter. If an overlap or pinch-out is tilted subsequent to deposition, as is the case of the Wasatch of this area, and the warping of the producing member is gentle, the producing member may have its highest structural position in the synclines instead of the anticlines, and the synclines may become the producing areas. In this area, the Linwood anticline, because of its steep east limb is not believed by the writer to be a case of this kind; although, without more work of a detailed nature, the relationships cannot be accurately outlined.

The writer is of the opinion that the Wasatch is a subject worthy of more detailed work in the northern part of the area in the vicinity of the Linwood anticline, although the amount of closure will probably prove to be small. On the Causeway anticline, its closure on the east side is not considered, at this time, to warrant further consideration with the facts at hand.

In regard to the formations older than the Mesaverde, the chances of having a producing trap in this area are considered rather dim. Although not impossible. If, by geophysical or other means, a reversal of the

regional dip, i.e. a south dip such as exists on the south side of the Clay Basin anticline, is found north of this area, the resulting structure would be worthy of test. In the region north of this area, Wasatch production would be at a probable depth of from 4000 to 6000 feet, and Dakota production would be at a depth of at least 12,000 feet and probably more.

There is one portion of this area where the structure is rather doubtful. As has been mentioned previously, the Hilliard formation in the Causeway anticline is thicker than shown in any other near-by area. This thickness may result from faulting not detected during the course of this work or it may be due to a lessening of the northward dip that was not seen. On the other hand, this thickness may be due to a natural increase in the depositional thickness, or it is barely possible that flowage of tremendous proportions in these shales may be the explanation for the phenomenon. The writer is unable to definitely explain this thickening.

OTHER MINERAL RESOURCES

The purpose of this report, as has been already stated, was mainly concerned with the investigation of the petroleum production possibilities of this or adjacent areas. However, certain other mineral products have, in the past, been investigated in this area, and a brief enumeration of these developments will be given.

Coal was known to occur in this area at least as early as the beginning of this century. Gale 25,26/ reported on the Henrys Fork coal field in 1907, and the reader is referred to his reports for additional information on the occurrences. Very little work has been done to develop these properties, although one open cut and several short tunnels have been driven. These properties are now idle, operations having been discontinued prior to World War II.

The Morrison formation contains some manganese mineralization. In several places trenching operations have been carried on and one prospect tunnel was seen in section 35, T3N, R19E. From the location of these operations, it appears that the richest concentration of manganese is related to faulting, as all of the prospecting has been done near the Lucerne fault or the Sheep Creek fault. Evidently the best occurrences are of sub-commercial value, even under war-time conditions.

The presence of oil shale in this area has been previously discussed under the "Green River Formation". To date there has been no attempt to develop these resources, but the region has been inspected by cursory reconnaissance (see Winchester 94/).

The Park City formation has long been known to be a future source of phosphates. No development has been made to date in this area, nor, as far as the writer knows, in any other part of the Uinta Mountains. The reader is referred to Schultz 67/ for further information.

VI. PROBLEMS STILL TO BE INVESTIGATED

There are several problems in this and adjacent areas that the writer, in closing, would like to outline briefly.

The Uinta Mountain quartzite that forms the "core" of the Uinta Mountains is worthy of further, more detailed study. This study might answer some of the unanswered questions, such as those concerning the origin of the present orientation of these mountains, the actual movements that have taken place on the Uinta fault, the existence of additional faulting that is known to be present at the edges of this great bulk and strongly indicated near the center by the drainage patterns and other configurations on the aerial photos, the existence or non-existence of unconformities in this group, and the correlation of this group with stratigraphic sections in other regions. The territory south of the area mapped for this report is fairly accessible.

For the student of geomorphology and Quaternary history, there is a problem that might prove interesting. Although Bradley 10/ has published a recent paper concerning the old erosion surfaces in the higher parts of the range and Atwood 1/, in 1909, reported on the glaciation of the Uinta Mountains, the stream and valley terraces of this and near-by areas have never been studied in detail. The streams on the north flank of the Uinta Mountains show the typical features of maturity, even where the topography is extremely steep, e.g. Sheep Creek valley. The general indications seem to indicate that the load carried by these streams has diminished in rather recent geologic time. Further study would probably reveal some correlations among the terraces, the present maturity of the streams, and differences in climatic conditions, as shown by the change in glacial conditions.

For the student of pre-Cambrian geology, a study of the Red Creek quartzites

would probably prove of interest. Aside from casual remarks in the literature concerning these rocks, no detailed investigation has ever been carried out to the writer's knowledge.

Of course, the matter of broad correlation is an ever-present problem. Further search for fossil evidence in this area might prove beneficial in correlating between the Wyoming and the Colorado Plateau stratigraphic section. Particularly useful would be correlations of the late Paleozoic, Triassic, and lower Jurassic sections.

BIBLIOGRAPHY

1/ Atwood, W. W.: Glaciation of the Uinta and Wasatch mountains, U.S. Geol. Surv., Prof. Paper 61 (1909).

2/ Baker, A. A.: Stratigraphy of the Wasatch Mountains in the vicinity of Provo, Utah, U.S. Geol. Surv., Oil and Gas Invest. Preliminary Chart No. 30 (1947).

3/ -----, Dane, C. H., and Reeside, J. B. Jr.: Correlation of the Jurassic formation of parts of Utah, Arizona, New Mexico, and Colorado, U. S. Geol. Surv., P rof. Paper 183 (1936).

4/ -----, and Williams, J. Steele: Permian in parts of Rocky Mountain and Colorado Plateau regions, Am. Assoc. Petr. Geol., Bull., vol. 24, pp. 617-635, (1940).

5/ Beckwith, Lieut. E. G.: Report of explorations for a route for the Pacific Railroad on the line of the forty-first parallel of north latitude, pp.15-16, in vol. II of Reports of explorations and surveys to ascertain the most practicable and economical route of a railroad from the Mississippi River to the Pacific Ocean, U.S. War Dept. (1855). Also map to accompany this report in vol. XI of the same report.

6/ Berkey, C. P.: Stratigraphy of the Uinta Mountains, Geol. Soc. Am., Bull., vol. 16, pp. 517-530, (1905).

6a/ Blackwelder, E.: New light on the geology of the Wasatch Mountains, Utah, Geol. Soc. Am., Bull., vol. 21, pp. 517-542, (1910).

7/ -----: Summary of the pre-Cambrian rocks of Utah and Wyoming, Utah Acad. Sci., Arts, and Letters, Pr., vol. XII, pp. 153-157, (1935).

8/ Boutwell, J. M.: Stratigraphy and structure of the Park City mining district, Utah, Jour. Geol., vol. 15, pp. 434-458, (1907).

9/ -----: Geology and ore deposits of the Park City district, Utah, U. S. Geol. Surv., Prof. P aper 77 (1912).

10/ Bradley, W. H.: Geomorphology of the north flank of the Uinta Mountains, U. S. Geol. Surv., Prof. Paper 185-i pp. 163-199, (1936).

11/ Butler, B. S.; Loughlin, G. F., Heikes, V. C., et al.: The ore deposits of Utah, U. S. Geol. Surv., Prof. Paper 111 (1920).

12/ Calkins, F. C., and Butler, B. S.: Geology and ore deposits of the Cottonwood-American Fork area, Utah, U. S. Geol. Surv., Prof. Paper 201 (1943).

13/ Cross, W. and Spencer, A. C.: Geologic atlas of the United States --- La Plata folio, U. S. Geol. Surv., Folio 60 (1899).

14/ Dale, H. C.: The Ashley-Smith explorations and the discovery of a central route to the Pacific 1822-1829, (Cleveland: Arthur H. Clark Co., 1918).

15/ de Lyndon, F.: Discussion of "The isostacy of the Uinta Mountains" by Andrew C. Lawson, Jour. Geol., vol. 40, pp. 664-669, (1932).

16/ Dobbin, C. E. and Davison, R.: Geologic and structure map of the Clay Basin gas field and vicinity, Daggett County, Utah and Sweetwater County, Wyoming, U. S. Geol. Surv. (1945).

17/ Eardley, A. J., and Hatch, R. A.: Proterozoic (?) rocks of Utah, Geol. Soc. Am., Bull., vol. 51, pp. 795-844, (1940).

18/ Eldridge, G. H.: Geology of the Denver Basin of Colorado, U. S. Geol. Surv., Mono. 27, pp. 60-62, (1896).

19/ Emmons, S. F.: Descriptive Geology, U. S. Geol. Expl. 40th Par. (King), vol. 2 (1877).

20/ -----: Origin of the Green River, Science, new series, vol. 6, no. 13, pp. 19-21, (1897).

21/ -----: Orographic movements of the Rocky Mountains, Geol. Soc. Am., Bull., vol. 1, pp. 245-286, (1889).

22/ -----: Uinta Mountains, Geol. Soc. Am., Bull., vol. 18, pp. 287-302, (1907).

23/ Forrester, J. D.: Structure of the Uinta Mountains, Geol. Soc. Am., Bull., vol. 48, pp. 631-666, (1937).

24/ Fremont, J. C.: Memoirs of my life, (Chicago: Belford, Clarke and Co., 1887), vol.I, p. 395.

25/ Gale, H. S.: Coal fields of northwestern Colorado and northeastern Utah, U. S. Geol. Surv., Bull. 341-b, pp. 283-315, (1907).

26/ -----: Coal fields of northwestern Colorado and northeastern Utah, U. S. Geol. Surv., Bull. 415 (1910).

27/ ----- and Richards, R. W.: Preliminary report of the phosphate deposits in southeastern Idaho and adjacent parts of Wyoming and Utah, U. S. Geol. Surv., Bull. 430-h, pp. 457-535, (1910).

28/ Gilluly, J., and Reeside, J. B. Jr.: Sedimentary rocks of the San Rafael swell and some adjacent areas in eastern Utah, U. S. Geol. Surv., Prof. Paper 150-d, pp. 61-110, (1928).

29/ Hancock, E. T.: The history of a portion of Yampa River, Colorado, and its possible bearing on that of the Green River, U. S. Geol. Surv., Prof. Paper 90-k, pp. 183-189, (1915).

30/ Hayden, F. V.: Preliminary report of the United States Geological Survey of Wyoming and portion of contiguous territories, U. S. Geol. Surv. of Wyo. and Contig. Terr., 4th Ann. Rept., (1871).

31/ Hayden, F. V.: Preliminary field report of the United States Geological Survey of Colorado and New Mexico, conducted under the authority of Hon. J. D. Cox, Secretary of the Interior, U. S. Geol. Surv. of Colo. and New Mexico, 3rd Ann. Rept. (1869).

32/ Heaton, R. L.: Contributions to Jurassic stratigraphy of Rocky Mountain region, A m. Assoc. Petr. Geol., Bull., vol. 23, pp. 1153-1177, (1939).

33/ Hinds, N. E. A.: Contributions to pre-Cambrian geology of western North America, Carn. Inst. of Wash., Publ. no. 463, p.13, pp.88-92, (1936).

34/ Hintze, F. F.: The Proterozoic-Paleozoic contact in the western Uinta and central Wasatch Mountains, Utah, Utah Acad. Sci.,' Arts, and Letters, Proc., vol. 11, pp. 165-166, (1934).

35/ Holmes, W. H.: Report of William H. Holmes, geologist of the San Juan division, U. S. Geol. and Geog. Surv. of Terr., 9th Ann. Rept. for 1875 pp. 245-257, plate XXXV, (1877).

36/ Huddle, J. W., and McCann, F. T.: Geologic map of Duchesne River area, Wasatch and Duchesne Counties, Utah, U. S. Geol. Surv., Oil and Gas Invest., Prelim. Map 75 (1947).

37/ Imlay, R. W.: Occurrence of middle Jurassic rocks in western interior of the United States, Am. Assoc. Petr. Geol., Bull., vol. 29, pp. 1019-1027, (1945).

38/ Irwin, J. S.: Faulting in the Rocky Mountain region, Am. Assoc. Petr. Geol. Bull., vol. 10, pp. 105-129, (1926).

39/ Lawson, A. C.: The isostacy of the Uinta Mountains, Jour. Geol., vol. 39, pp. 264-276, (1931).

40/ Love, J. D.: Geology along the southern margin of the Absaroka Range, Wyoming, Geol. Soc. Am., Spec. Paper no. 20 (1939).

41/ -----, et al.: Stratigraphic sections and thickness maps of lower Cretaceous and nonmarine Jurassic rocks of central Wyoming, U. S. Geol. Surv., Oil and Gas Invest., Prelim. Chart 13 (1945).

42/ -----, et al.: Stratigraphic sections and thickness maps of Jurassic rocks in central Wyoming, U. S. Geol. Surv., Oil and Gas Invest., Prelim. Chart 14 (1945).

43/ -----, et al.: Stratigraphic sections and thickness maps of Triassic rocks in central Wyoming, U. S. Geol. Surv., Oil and Gas Invest., Prelim. Chart 17 (1945).

44/ -----, et al.: Stratigraphic sections of Mesozoic rocks in central Wyoming, Geol. Surv. of Wyoming, Bull. no. 38, (1947).

45/ King, C., et al.: United States Geological Exploration of the Fortieth Parallel, in 7 vols., Vol. I-Systematic Geology (1878)

Vol. II-Descriptive Geology (1877).

46/ King, C.: Paleozoic subdivisions on the 40th parallel, Am. Jour. Sci., vol. 11, pp. 475-482, (1876). 3rd ser.

47/ Kinney, D. M., and Rominger, J. F.: Geology of the Whiterocks River-Ashley Creek area, Uintah County, Utah, U. S. Geol. Surv., Oil and Gas Invest., Prelim. Map no. 82, (1947).

48/ Knight, W. C.: The petroleum fields of Wyoming-III, the fields of Uinta County, Engin. and Min. Jour., vol. 73, pp. 720-723, (1902).

49/ Lovering, T. S., et al.: Geologic map of state of Colorado, U. S. Geol. Surv. (1935).

50/ Manly, W. L.: Death Valley in '49, (San Jose: Pacific Tree and Vine Co., pp. 76-82, 1894).

51/ M ansfield, G. R.: Geography, geology, and mineral resources of the Fort Hall Indian Reservation, Idaho, U. S. Geol. Surv., Bull. 713 (1920).

52/ Marsh, O. C.: On the geology of the eastern Uinta Mountains, Am. Jour. Sci., 3rd ser., vol. 1, pp. 191-198, (1871).

53/ Matthew, W. D.: The Carnivora and Insectivora of the Bridger Basin, middle Eocene, Am. Mus. Nat. Hist., Memoirs, vol. IX, Pt. VI, pp. 295-297, (1909).

54/ Moore, R. C., et al.: Correlation of Pennsylvanian formations of North America, Geol. Soc. Am., Bull., vol. 55, pp.657-706, (1944).

54a/ Nightingale, W. T.: Geology of Vermilion Creek gas area in southwest Wyoming and northwest Colorado, Am. Assoc. Petr. Geol., Bull., vol. 14, pp. 1013-1040, (1930).

55/ -----: Geology of Baxter Basin gas fields, Sweetwater County, Wyoming, in Geology of natural gas, (Tulsa: Am. Assoc. Petr. Geol., pp. 323-339, 1935).

56/ -----: Geology of Hiawatha gas fields, southwest Wyoming and northwest Colorado, in Geology of natural gas, (Tulsa: A m. Assoc. Petr. Geol. pp. 341-361, 1935).

57/ Peale, A. C.: The Paleozoic section in the vicinity of Three Forks, Montana, U. S. Geol. Surv., Bull. 110 (1893).

58/ Pike, W. S. Jr.: Intertonguing marine and nonmarine upper Cretaceous deposits of New Mexico, Arizona, and southwestern Colorado, Geol. Soc. Am., Memoir 24 (1947).

59/ Powell, J. W. .: Exploration of the Colorado River of the west and its tributaries explored in 1869, 1870, 1871, and 1872, U. S. Govt. Publ. of Smithsonian Inst., Washington, (1875).

60/ Powell, J. W.: Report of the geology of the eastern portion of the Uinta Mountains and a region of country adjacent thereto, U. S. Geol. and Geog. Surv. of Terr., Second Div., Washington (1876).

61/ Reeside, J. B. Jr.: Notes on the geology of Green River valley between Green River, Wyo., and Green River, Utah, U. S. Geol. Surv., Prof. Paper 132-c, pp. 35-50, (1923).

62/ -----: Maps showing thickness and general character of the Cretaceous deposits in the western interior of the United States, U. S. Geol. Surv., Oil and Gas Invest., Prelim. Map 10 (1944).

63/ Richards, R. W., and Mansfield, G. R.: The Bannock overthrust - a major fault in southeastern Idaho and northeastern Utah, Jour. Geol., vol. 20, pp. 681-709, (1912).

64/ Richardson, G. B.: The Paleozoic section in northern Utah, Am. Jour. Sci., 4th se., vol. 36, pp. 406-416, (1910).

65/ Richmond, G. M.: Geology of the northwest end of the Wind River Mountains , Sublette County, Wyoming, U. S. Geol. Surv., Oil and Gas Invest., Prelim. Map 31 (1945).

66/ Schultz, A. R.: The southern part of the Rock Springs coal field, Sweetwater County, Wyo., U. S. Geol. Surv., Bull. 381-b, pp. 214-281, (1908).

67/ -----: A geologic reconnaissance of the Uinta Mountains, northern Utah, with special reference to phosphate, U. S. Geol. Surv., Bull. 690-c, pp. 31-94, (1919).

68/ -----: Oil possibilities in and around Baxter Basin, in the Rock Springs uplift, Sweetwater County, Wyo., U. S. Geol. Surv., Bull. 702 (1920).

69/ Sears, J. D.: Relations of the Brown Park formation and the Bishop conglomerate, and their role in the origin of Green and Yampa Rivers, Geol. Soc. Am., Bull., vol. 35, pp. 279-304, (1924).

70/ -----: Geology and oil and gas prospects of part of Moffat County, Colorado, and southern Sweetwater County, Wyo., U. S. Geol. Surv., Bull. 751-g, pp. 269-319, (1925).

71/ -----: Geology of the Baxter Basin gas field, Sweetwater, County, Wyo., U. S. Geol. Surv., Bull. 781-b, pp. 13-27, (1925).

72/ ----- and Bradley, W. H.: Relations of the Wasatch and Green River formations in northwestern Colorado and southern Wyoming, U. S. Geol. Surv., Prof. Paper 132-f, pp. 93-108, (1924).

73/ -----, Hunt, C. B., and Hendricks, T. A.: Transgressive and regressive Cretaceous deposits in southern San Juan Basin, New Mexico, U. S. Geol. Surv., Prof. Paper 193-f (1941).

74/ Spieker, E. M.: Comment on "Structure of the Uinta Mountains" by J. D. Forrester, Geol. Soc. Am., Bull., vol. 48, pp. 2037-2043, (1937).

75/ -----: Late Mesozoic and early Cenozoic history of central Utah, U. S. Geol. Surv., Prof. Paper 205-d (1946).

76/ Stokes, W. L.: Morrison formation and related deposits in and adjacent to the Colorado plateau, Geol. Soc. Am. Bull., vol. 55, pp. 951-992, (1944).

77/ Thomas, H. D.: Phosphoria and Dinwoody tongues in the lower Chugwater of central and southeastern Wyoming, Am. Assoc. Petr. Geol., Bull., vol. 18, pp. 1655-1697, (1934).

78/ ----- and Krueger, M. L.: Late Paleozoic and early Mesozoic stratigraphy of Uinta Mountains, Utah, Am. Assoc. Petr. Geol., Bull., vol. 30, pp. 1255-1293, (1946).

79/ Thomas, C. R., McCann, F. T., and Raman, N. D.: Mesozoic and Paleozoic stratigraphy in northwestern Colorado and northeastern Utah, U. S. Geol. Surv., Oil and Gas Invest., Prelim. Chart 16, Sht. 2 (1945).

80/ Tolmachoff, I. P.: Upper Cretaceous fauna of the Asphalt Ridge, Utah, Carn. Mus., Ann., vol. 29, pp. 41-60, (1942).

81/ Van Hise, C. R., and Leith, C. K.: Pre-Cambrian geology of North A merica, U. S. Geol. Surv., Bull. 360, pp. 779-782, 789-790,(1909).

82/ Veatch, A. C.: Geography and geology of a portion of southwestern Wyoming, U. S. Geol. Surv., Prof. Paper 56 (1907).

83/ Ver Wiebe, W. A.: Oil fields in the United States, (New York: McGraw-Hill Book Co., Inc., pp. 487, 540, 1930.)

84/ W alcott, C. D.: Correlation papers: Cambrian, U. S. Geol. Surv., Bull. 81, pp. 313-320, (1891).

85/ Walton, P. T.: Geology of the Cretaceous of the Uinta Basin, Utah, Geol. Soc. A m., Bull., vol. 55, pp. 91-130, (1944).

86/ Weeks, F. B.: Stratigraphy and structure of the Uinta Range, Geol. Soc. Am., Bull., vol. 18, pp. 427-448, (1907).

87/ W heeler, G. M.; et al.: Report upon geographical surveys west of the one hundredth meridian, Vol. 1 Geographical report U. S. War Dept. pp. 605-742, (1855)

88/ White, C. A.: Report on the geology of a portion of northwestern Colorado, U. S. Geol. and Geog. Surv. Of Terr., 10th Ann. Rept., pp. 3-60, (1878).

89/ -----: On the geology and physiography of a portion of northwestern Colorado and adjacent parts of Utah and Wyoming, U. S. Geol. Surv.,

9th Ann. Rept., pp. 683-712, (1889).

90/ Williams, J. Stewart: "Park City" beds on the southwest flank of the Uinta Mountains, Am. Assoc. Petr. Geol., Bull., vol. 23, pp. 82-100, (1939).

91/ -----: Carboniferous formations of the Uinta and northern Wasatch Mountains, Utah, Geol. Soc. Am., Bull., vol. 54, pp. 591-624, (1943)

92/ -----: Nomenclature of the Triassic rocks of northern Utah, A m. Jour. Sci., vol. 243, pp. 473-479, (1945).

93/ Wilmarth, M. G.: Lexicon of geologic names of the United States, Ul S. Geol. Surv., Bull. 896 (1938).

94/ Winchester, D. E.: Oil shales in northwestern Colorado and adjacent areas, U. S. Geol. Surv., Bul., 641 pp. 139-198, (1916).

95/ -----: Oil shale in the United States, Econ. Geol., vol. 12, pp. 505-518, (1917).

96/ Wood, H. E.: Revision of the Hyrachyidae, Am. Mus. Nat. Hist., Bull., vol. 67, art. 5, pp. 241-242, (1934).

97/ ----- et al.: Nomenclature and correlation of the North American continental Tertiary, Geol. Soc. Am., Bull., vol. 52, pp. 1-48, (1941).